

## Durham E-Theses

---

*The petrogenesis of the calc-alkaline borrowdale  
volcanic group, Northern England*

John Godfrey Fitton

### How to cite:

---

Fitton, John Godfrey (1971) The petrogenesis of the calc-alkaline borrowdale volcanic group, Northern England. Doctoral thesis, Durham University.

### Use policy

---

The full-text may be used and/or reproduced, and given to third parties in any format or medium, without prior permission or charge, for personal research or study, educational, or not-for-profit purposes provided that:

- a full bibliographic reference is made to the original source
- a <https://etheses.durham.ac.uk/id/eprint/10514/> is made to the metadata record in Durham E-Theses
- the full-text is not changed in any way

The full-text must not be sold in any format or medium without the formal permission of the copyright holders.

Please consult the [full Durham E-Theses policy](#) for further details.

THE PETROGENESIS  
OF THE CALC-ALKALINE BORROWDALE VOLCANIC GROUP,  
NORTHERN ENGLAND

by

John Godfrey Fitton, B.Sc. (Dunelm).

Thesis submitted for the degree of Ph.D.  
at the University of Durham.

Department of Geology,

October 1971.



## ABSTRACT

The Borrowdale Volcanic Group constitutes a major part of the Ordovician succession in the English Lake District. It comprises a suite of lavas, tuffs and ignimbrites with a maximum measured thickness of 5 km. The rocks of the Lake District are folded into a broad anticline which results in the Borrowdale Volcanics being exposed in two main outcrops, one north and the other south of a central core of older Skiddaw Slates. The northern outcrop consists almost entirely of basalts, basaltic andesites and occasional rhyolites, with very few intermediate members. In contrast, the southern outcrop is composed largely of andesites and dacites. Garnet phenocrysts, absent in the northern outcrop, are relatively abundant in the volcanic rocks of the southern outcrop.

Analyses of 229 samples of lavas, ignimbrites and associated intrusives are presented together with electron microprobe analyses of selected garnet and augite phenocrysts. The southern outcrop volcanics are of calc-alkaline affinities, whereas those of the northern outcrop are transitional in character between tholeiitic and calc-alkaline. The use of La/Y ratios is shown to be particularly effective in distinguishing between members of the two suites.

Detailed analytical studies on the garnet phenocrysts, especially La and Y abundances, show that crystal fractionation of garnet phenocrysts is incompatible with the geochemistry of their host rocks. It is concluded that the southern outcrop magmas evolved by some process other than crystal fractionation. A partial-melting hypothesis is proposed as an alternative, the melt being stored at depth (possibly at the crust/mantle interface) long enough for garnet to nucleate, and then transferred rapidly to the surface. In contrast, the northern outcrop lavas are highly porphyritic and present abundant evidence of crystal fractionation. It is suggested that these rocks evolved by the fractionation of a basalt or basaltic andesite parent under relatively dry conditions at shallow depth.

The Borrowdale Volcanics are compared with the volcanic rocks of modern island arcs. In particular the southward transition of magma type from tholeiitic to calc-alkaline compares with similar transitions occurring across modern island arcs. It is concluded that the Borrowdale Volcanics were erupted in an ancient island arc at the margin of a contracting, proto-Atlantic ocean. This hypothesis is consistent with current models for the evolution of the Caledonian/Appalachian orogen.

The Borrowdale magmas were probably derived by the partial melting of basaltic oceanic crust carried down into the mantle on descending lithosphere plates. In the case of the southern outcrop rocks the magma was not affected by subsequent crystal fractionation, whereas the northern outcrop magma has undergone considerable modification by this process.

Finally, the partial melting of oceanic crust is examined in the light of recent experimental studies. It is suggested that island arc tholeiitic magmas are generated at shallow depth by reactions involving amphibole breakdown. Calc-alkaline magmas are produced at greater depths by the partial melting of wet eclogite, and between these two extremes a continuum of transitional magma types could be generated.

## ACKNOWLEDGEMENTS

The author is indebted to Prof. G.M. Brown who supervised this research project and, as former head of the Department, provided research facilities. Thanks are also due to the other members of both academic and technical staff of the Department for assistance during the course of this work. In particular, Dr. A. Peckett provided invaluable assistance with electron-microprobe techniques and Mr. R.C.O. Gill supplied a number of computer programs for processing and plotting analytical data.

During the early stages of this study, helpful advice on the collection of rock samples was provided by Drs. G.H. Mitchell and R.J. Firman. Dr. R.G.J. Strens and Mr. A.J. Wadge allowed the author access to unpublished maps, and Mr. J.L. Knight, Dr. M.J.C. Nutt and Mr. T.J. Shepherd supplied additional rock samples. To these, the author expresses his thanks. The author is also grateful to Mr. J.L. Knight and Mr. F.W. Smith for assistance in the field.

The project was made possible by the financial support of the Natural Environment Research Council.

## CONTENTS

	page
CHAPTER 1      INTRODUCTION.	
(i)      Scope and aims.	1
(ii)     Previous work.	3
(iii)    Lake District geology.	5
(iv)    Collection, preparation and analysis of samples.	12
CHAPTER 2      SOUTHERN OUTCROP.	
(i)      Classification of rock types.	17
(ii)     Distribution of rock types.	18
(iii)    Petrography.	19
(iv)    Mineralogy.	24
(v)     Petrochemistry.	27
(vi)    Intrusions.	38
CHAPTER 3      NORTHERN OUTCROP.	
(i)      Distribution of rock types.	45
(ii)     Petrography.	46
(iii)    Mineralogy.	48
(iv)    Petrochemistry.	53
(v)     Intrusions.	70

	page
CHAPTER 4      GARNETS.	
(i)      Introduction.	81
(ii)     Distribution.	81
(iii)    Petrography.	83
(iv)     Composition.	86
(v)      Origin.	97
(vi)     Petrogenetic implications.	101
CHAPTER 5      CONCLUSIONS.	
(i)      Palaeogeographic implications.	126
(ii)     Genesis of island arc magmas.	128
REFERENCES CITED.	130
APPENDICES.	
1.      The oxidation of ferrous iron in rocks during mechanical grinding (Fitton and Gill, 1970).	140
2.      Trace-element concentrations in U.S.G.S. standards.	141
3.      Analyses of rock samples.	
(a)    Southern outcrop.	142
(b)    Northern outcrop.	160
(c)    Garnetiferous rocks mentioned in text but not plotted.	168
4.      C.I.P.W. Norms.	
(a)    Southern outcrop.	170
(b)    Northern outcrop.	185

	page
5. Electron microprobe analyses.	
(a) Pyroxenes.	192
(b) Garnets.	196
6. Eight-figure National Grid references of sample localities.	209

## LIST OF ILLUSTRATIONS

### FIGURES

	page
1. Location of principal outcrops of British Ordovician volcanic rocks (from Fitton and Hughes, 1970).	2
2. Geological sketch-map of the Lake District (from Mitchell, 1956a).	7
3. Simplified sections of the Borrowdale Volcanic Group (modified after Mitchell, 1956a).	11
4. Location of samples.	13
5. Major-element variation in rocks of the southern outcrop.	28
6. Trace-element variation in rocks of the southern outcrop.	29
7. Plot of total iron against MgO for rocks of the southern outcrop.	33
8. Extent of occurrence of phenocryst phases in rocks of the Borrowdale Volcanic Group.	49
9. Plot of clinopyroxene analyses from rocks of the northern and southern outcrops.	51
10. Major-element variation in rocks of the northern outcrop.	54
11. Trace-element variation in rocks of the northern outcrop.	55

	page
12. Plot of total iron against MgO for rocks of the northern outcrop.	56
13. A.F.M. plot of analysed samples.	59
14. K - Rb relationships in rocks from the southern and northern outcrops.	67
15. Plot of La against Y for the volcanic rocks.	69
16. Compositional variation in garnets from the Borrowdale Volcanics and other rocks.	88
17. Electron microprobe traverses for Fe and Mg across garnet crystal G-302.	92
18. Schematic cooling history of andesite magma generated at a Benioff zone.	107

## PLATES

	page
1. Augite phenocrysts in basalt (LD 148).	41
2. Pseudomorph after olivine in basalt (LD 269).	41
3. Cluster of augite phenocrysts in basaltic andesite (LD 221).	42
4. and 5. Small augite phenocrysts in basaltic andesite (LD 309).	42
6. Perlitic cracks in groundmass of andesite (LD 146)	43
7. Andesite (LD 132).	43
8. Dacitic ignimbrite (LD 303).	44
9. Small sandstone inclusions and augite phenocryst in basalt (LD 275).	44
10. Cluster of augite phenocrysts in basalt (LD 115).	77
11. Polished slab of Eycott type basaltic andesite (LD 73A).	78
12. Berrier type basaltic andesite (LD 85).	78
13. Ignimbrite (LD 102).	79
14. 'Keratophyre' (LD 96).	79
15. Augite phenocrysts in basaltic andesite (LD 86).	80
16. Augite phenocrysts in basaltic andesite (LD 111).	80
17. Garnet phenocrysts in a polished slab of dacitic ignimbrite (LD 175).	116
18. Garnet phenocrysts in andesite (LD 174).	117
19. Garnet phenocrysts in andesite (LD 176).	118
20. Garnet phenocryst in andesite (LD 220).	118
21. Garnet phenocrysts in andesite (LD 274).	119
22. Garnet phenocrysts in andesite (LD 306).	120

	page
23. Large garnet phenocryst in andesite (LD 302).	121
24. Euhedral garnet phenocrysts in ?intrusive dacite (LD 65).	122
25. Garnet phenocryst in dacitic ignimbrite (LD 175).	122
26. Fragment of garnet phenocryst in dacitic ignimbrite (LD 249).	123
27. Garnet phenocrysts (G-316) in ignimbrite from Snowdonia, North Wales.	123
28. Large euhedral garnet phenocryst in dacitic ignimbrite (LD 317).	124
29. Large euhedral garnet phenocryst in hand specimen of dacitic ignimbrite (LD 317).	125

TABLES IN TEXT

	page
1. Average analyses of southern outcrop rocks.	30
2. Average garnet analyses.	94

## CHAPTER I

INTRODUCTION(i) Scope and aims

In recent years one of the major topics of interest in the Earth Sciences has been the genesis of calc-alkaline magmas. An important result of this work was the demonstration by Chayes (1969a) that recently erupted calc-alkaline rocks are confined entirely to the island arc/continental margin environment.

The development of the plate tectonics concept, from the sea-floor spreading hypothesis of Hess (1962), focussed attention on this environment as the site of descending lithosphere plates (Isacks et al., 1968). The resulting implication of a genetic connection between the descent of these plates and the generation of calc-alkaline magmas has now received strong support from a wide variety of sources.

A natural extension of the work on recent calc-alkaline rocks is a study of ancient members of the suite. If present day calc-alkaline volcanoes are restricted in occurrence to the world's tectonically active zones of lithosphere destruction then it is reasonable to suppose that the same may have held true in the past. Consequently the location of ancient calc-alkaline volcanic rocks may have important implications in the fields of palaeogeography and continental drift.

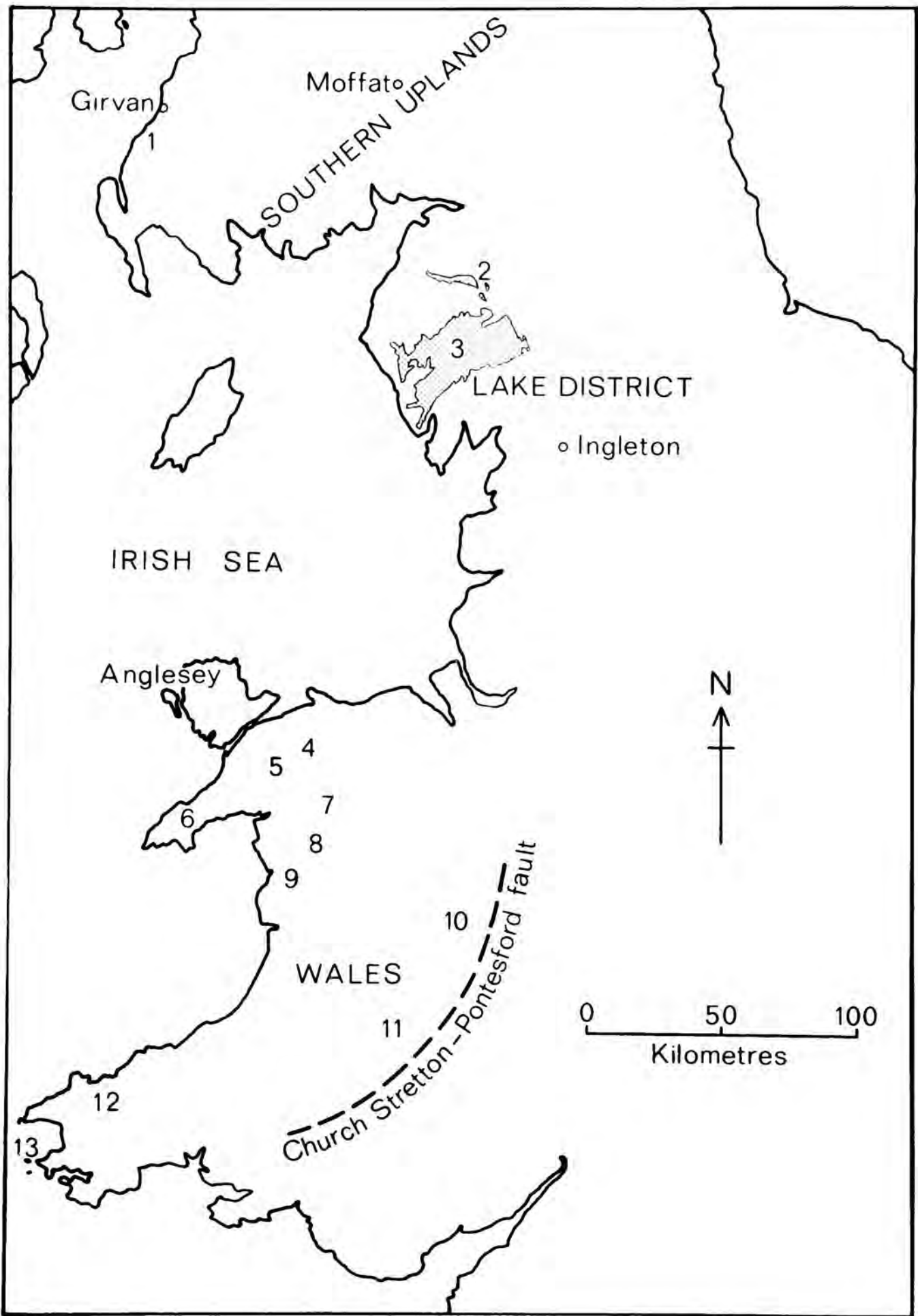
Fig. 1

Location of principal outcrops of British Ordovician volcanic rocks.

1. Ballantrae      2. northern      and      3. southern outcrops  
of Borrowdale Volcanics      4. Capel Curig      5. Snowdonia  
6. Lleyn Peninsula      7. Arenig Mountains      8. Rhobell Fawr  
9. Cader Idris      10. Shelve area      11. Builth Wells      12. north  
Pembrokeshire      13. Skomer Island.

Outcrop of Borrowdale Volcanics shown stippled. The Church Stretton  
- Pontesford fault system forms the south-eastern margin of the Welsh  
Basin.

From Fitton and Hughes (1970).



One such volcanic pile is represented by the Ordovician Borrowdale Volcanic Group of the English Lake District (Fig. 1). This comprises a slightly deformed and well-exposed group of lavas and tuffs with a maximum measured thickness of 5 kilometres. The reasons for undertaking a detailed study of these volcanic rocks were threefold. First, the geochemistry and mineralogy of the rocks could provide information relevant to the genesis of calc-alkaline rocks in general. Second, the Borrowdale Volcanics are unusual in that they contain almandine-pyrope garnet as an abundant primary phenocryst phase (Oliver, 1956). In view of the rarity of garnets in igneous rocks and their possible relevance to the problem of the genesis of calc-alkaline magmas (Green and Ringwood, 1968a) a special study of these garnets was viewed as a worthwhile project. Thirdly, a petrochemical study of the Borrowdale Volcanics could provide valuable information about Ordovician palaeogeography.

(ii) Previous work

The Lake District has a history of geological research stretching back well over a century although the structure and stratigraphy of the area are not yet fully understood. The more recent publications on the

area have been reviewed by Mitchell (1956a) whose paper also includes an extensive bibliography. Consequently, only work directly relevant to the present study will be mentioned here.

Surprisingly little geochemical or petrological work has been published on the Borrowdale Volcanics. The first attempt at elucidating the petrochemical evolution of the volcanic rocks was that of Oliver (1961) who demonstrated the calc-alkaline nature of the lavas in the Scafell area. This was later supported by Strens (1962) in the Borrowdale - Honister region. Detailed petrographic descriptions of rocks from a sequence of Borrowdale Volcanics in the northern part of the Lake District have been given by K. C. Dunham and J. Plemister (in Eastwood et al., 1968).

Garnets have long been recognised in the igneous rocks of the Lake District although opinion on their origin has varied considerably. The most recent work on the garnets (Oliver, 1956) suggested that they crystallised directly from the magmas.

A prominent feature of the Borrowdale Volcanics is the abundance of acidic volcanic rocks which were sometimes described as tuffs and at other times as rhyolite flows. The recognition by Oliver (1954) that many of these rocks are ignimbrites represents an important contribution to the geology of the Lake District.

(iii) Lake District geology

a. Tectonic setting

Structurally, the Lake District occupies a position in the non-metamorphic zone of the British Caledonides between the Irish Sea geanticline and the Moffat geosyncline (George, 1963). The area is thus within the Appalachian/Caledonian orogen in a position adjacent to the Precambrian south-east foreland.

The sedimentary rocks of the area have suffered severe polyphase deformation although the more competent volcanic rocks are relatively undeformed. Many of the lavas are very fresh considering their age although, in others, the development of secondary albite, epidote and chlorite suggest lower greenschist-facies metamorphism.

b. Stratigraphic succession

The oldest exposed rocks in the area are the Skiddaw Slates which comprise a group of highly deformed shales, sandstones and grits. These are overlain by the Borrowdale Volcanic Group. The nature of the junction is the subject of a controversy at present although it is now generally agreed that the Skiddaw Slates were folded, or at least uplifted, and eroded before the eruption of the Borrowdale Volcanics. The youngest

beds in the Skiddaw Slates yield an Upper Llanvirnian, Didymograptus murchisoni fauna (Wadge et al., 1969) which places an upper limit on the age of the volcanic rocks.

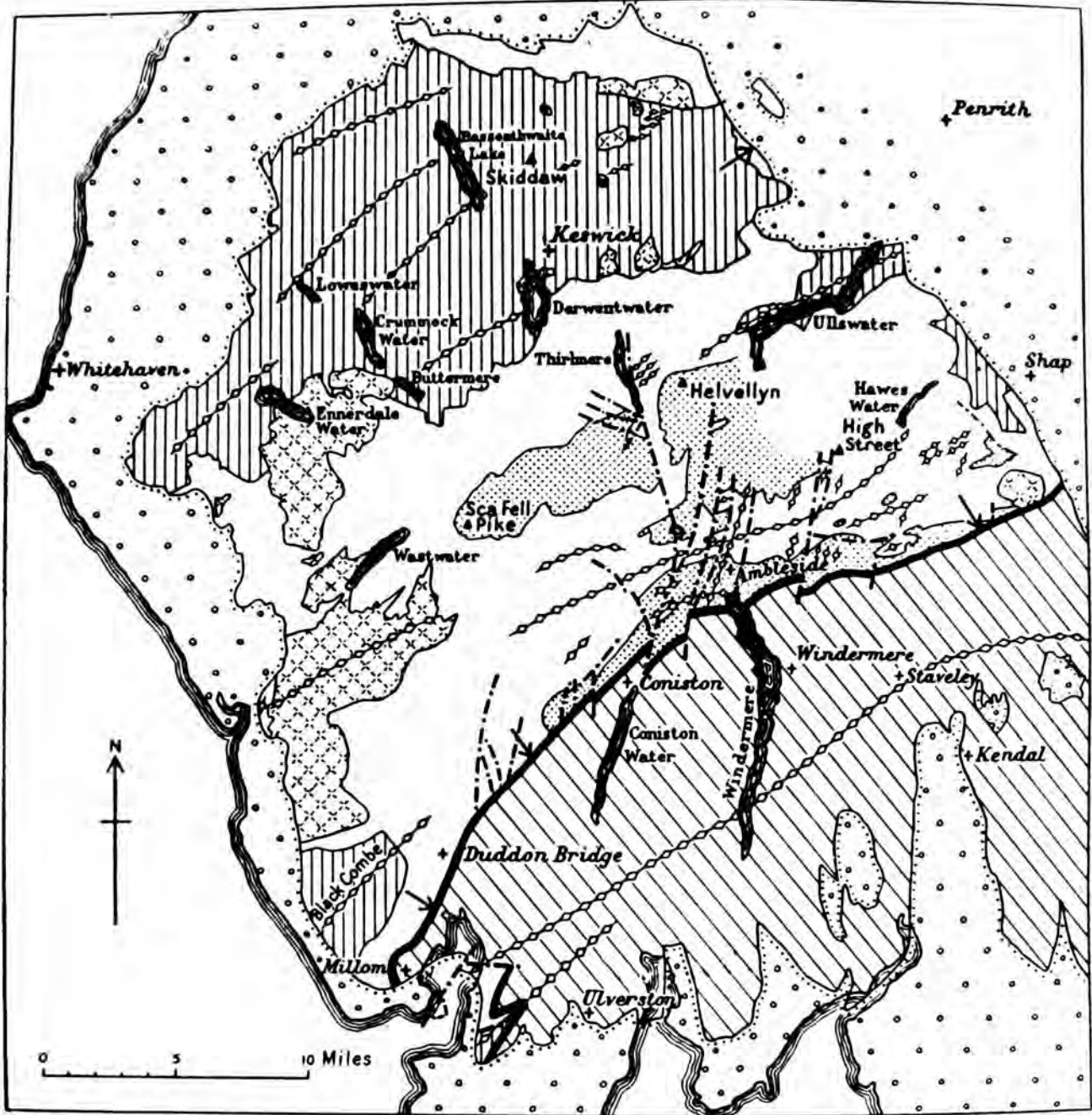
Coarse conglomerates occur towards the base of the volcanic group in the Keswick, Ullswater and Bampton areas (A. J. Wadge, in preparation). These are beautifully exposed in the new Manchester Corporation Waterworks tunnel between Heltondale and Ullswater where they contain rounded and weathered blocks of volcanic material and microgranite. The succession in the Borrowdale Volcanics will be discussed in later chapters but is summarised in diagrammatic sections (Fig. 3).

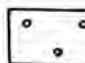

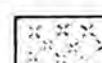


The Borrowdale Volcanics are overlain unconformably by limestones and shales of Caradocian (Longvillian) age (Dean, 1963) and so the top of the volcanic succession is not seen. Consequently the age of the volcanics cannot be determined more precisely than as post-Didymograptus murchisoni Zone and pre-Longvillian.

The distribution of the various stratigraphic units in the Lake District is shown in the geological map (Fig.2).

Fig. 2

Geological sketch-map of the Lake District. From Mitchell (1956a).



- |   |  |   |
|---|--|---|
|  <p>New Red Sandstone and Carboniferous<br/>UNCONFORMITY AT BASE OF BOTH</p> |  <p>Borrowdale Volcanic Series<br/>(Yowdale Breccia and higher beds stippled)</p> |  <p>Intrusions</p> |
|  <p>Silurian<br/>Coniston Limestone Group<br/>UNCONFORMITY</p>               |  <p>Skiddaw Slates</p>  | <p>↙ General dip of strata</p> <p>◊-◊-◊ Anticline</p> <p>- - - - - Fault</p>                            |

### c. Intrusions

In addition to the considerable igneous activity represented by the volcanic rocks the Lake District contains a large number of intrusions. Most prominent among these are the granites which probably also underlie a large part of the area (M. H. P. Bott, personal communication, 1970). Radiometric dating by Brown et al. (1964) gives a Devonian age for the exposed granite bodies.

None of the smaller intrusions has been reliably dated and some of these have been suggested as feeders for the volcanic rocks. These will be discussed individually later. The smaller intrusions range in composition from olivine-bearing mafic rocks to granophyres.

### d. Distribution of volcanic outcrops

The main structural feature of the Lake District is a broad anticline with its axis running south-west to north-east through Skiddaw and plunging to the north-east. It is this anticline which accounts for the Skiddaw Slates now being exposed by erosion. Flanking the Skiddaw Slates to the north and south-east are the two main outcrops of the Borrowdale Volcanics (Fig. 2). Henceforth these will be referred to as the northern and southern outcrops respectively.

The southern outcrop, which is by far the larger of the two, is responsible for the rugged scenery of the central Lake District mountains. The main rock types are tuffs, andesite lavas and dacitic ignimbrites. Basalts and rhyolites are comparatively rare.

The main part of the northern outcrop stretches in a narrow belt from the village of Bothel in the west to the River Caldew in the east. Also included in the northern outcrop are the small inliers of Greystoke Park and Eycott Hill. In marked contrast to the southern outcrop the rocks are predominantly basalts and basaltic andesites. Acid and intermediate types are very rare and tuffs are confined largely to the base of the succession. Peculiar to the northern outcrop are the big-feldspar basalts (Eycott type lavas) which are well developed over much of the area. The difference in character between rocks of the two outcrops is apparent even in hand specimens, with the porphyritic, dark-coloured basaltic andesites of the north contrasting strongly with the pale, sparsely porphyritic andesites of the south.

East of the Vale of Eden, in the Cross Fell area, an elongate body of Lower Palaeozoic rocks is exposed along the Pennine fault-escarpment. These rocks form the Cross Fell inlier and include volcanic rocks

belonging to the Borrowdale Volcanic Group. The volcanic rocks are mainly tuffs, andesites and ignimbrites and can be equated with the volcanics of the Lake District southern outcrop. At the extreme northern tip of the inlier, however, a single small outcrop of big-feldspar basalt is exposed near the village of Melmerby. This rock is identical with the Eycott type basalts of the northern Lake District and will be considered as a genetic associate of the northern outcrop.

Further east, in Teesdale, a small outcrop of Skiddaw Slates occurs as an inlier in the Carboniferous limestone. The drift around this locality contains boulders of volcanic material which may be of Borrowdale age. Since these volcanic rocks have not been found in place, however, they were not considered in the present study.

The dissimilarity of rock types in the northern and southern outcrops has prevented correlation of volcanic units across the Skiddaw anticline. Correlations within each outcrop have, however, been proposed and are summarised in Fig. 3. The correlations are essentially those proposed by Mitchell (1956a) although they have been modified slightly by the writer to allow the inclusion of recent work around Ullswater, Haweswater and Borrowdale.

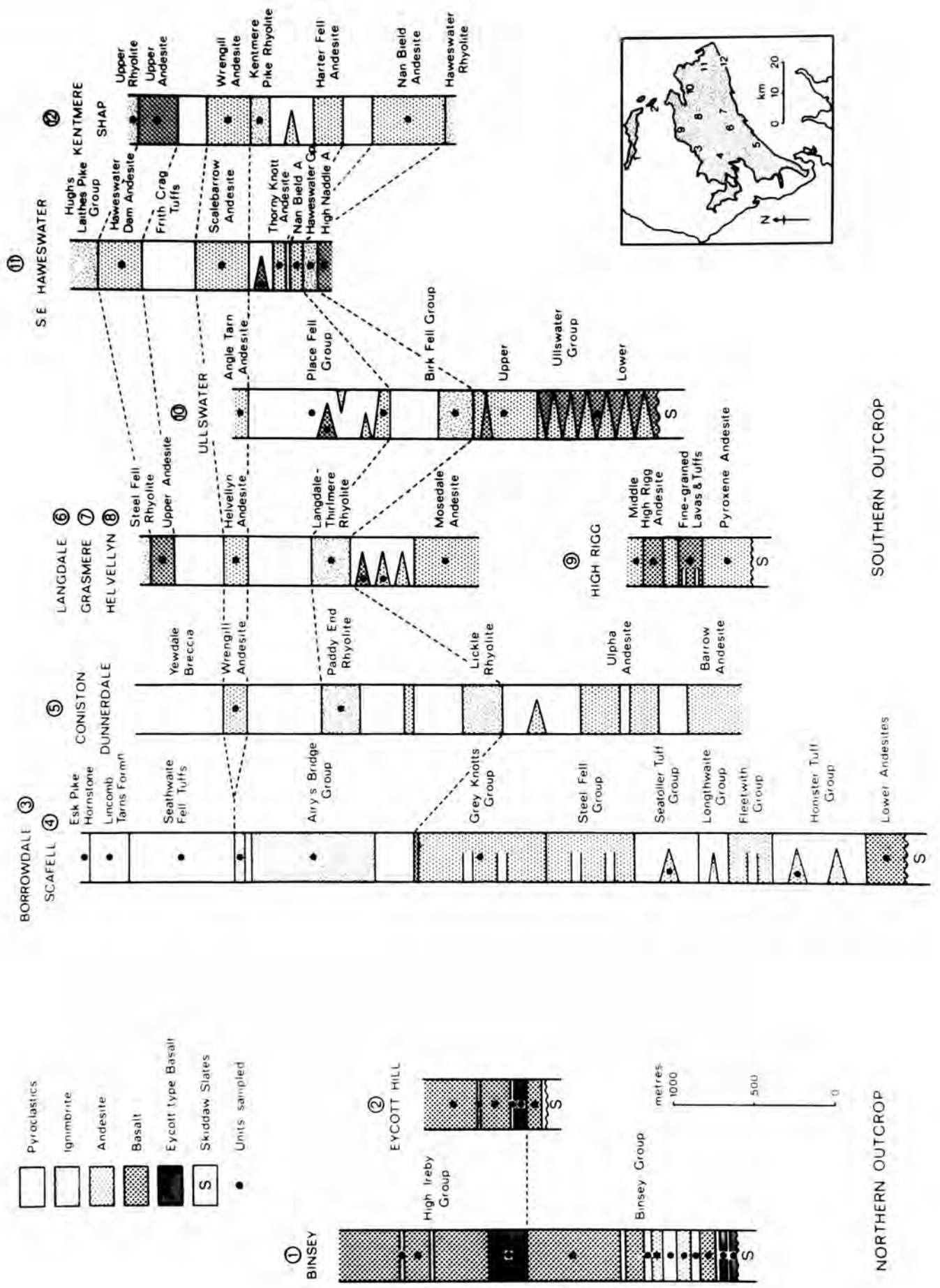
Fig. 3

Simplified sections of the Borrowdale Volcanic Group.

Sources of information:-

1 and 2	Eastwood <u>et al.</u> , (1968)
3	Strens (1962)
4	Oliver (1961)
5	Mitchell (1940, 1956b, 1963)
6	Hartley (1932)
7	Hartley (1925)
8	Hartley (1942)
9	Hadfield and Whiteside (1936)
10	Moseley (1960, 1964)
11	Nutt (1970)
12	Mitchell (1929, 1934)

Modified after Mitchell (1956a)



SOUTHERN OUTCROP

NORTHERN OUTCROP

In view of the dissimilarity of the two outcrops it is convenient to describe them separately in the following chapters.

(iv) Collection, preparation and analysis of samples

Collecting the samples presented certain problems. The age and deformation of the rocks has resulted in their being invariably altered to some degree and in many parts of the area the intrusion of granites has added to this alteration. Sampling is further complicated by the variable quality of available geological maps. However, most of the area is well exposed and, by avoiding the vicinity of granites and belts of obvious deformation, it was possible to assemble a representative collection of 338 samples. Analyses of 229 of these rocks are presented here. The remainder included 61 samples of agglomerate, tuff and conglomerate, 32 of granite and lamprophyre, and 12 samples which were rejected on account of excessive alteration. Most of the tuffs were analysed but the analyses were not used. The granites and lamprophyres were collected as part of a geochemical study of Caledonian granites which is not yet complete. The areal distribution of these samples is shown on Fig. 4. Representative samples are included from most of the volcanic units in the area (Fig.3).

Fig. 4

Location of samples:- extrusive (x) and intrusive (+) rocks.

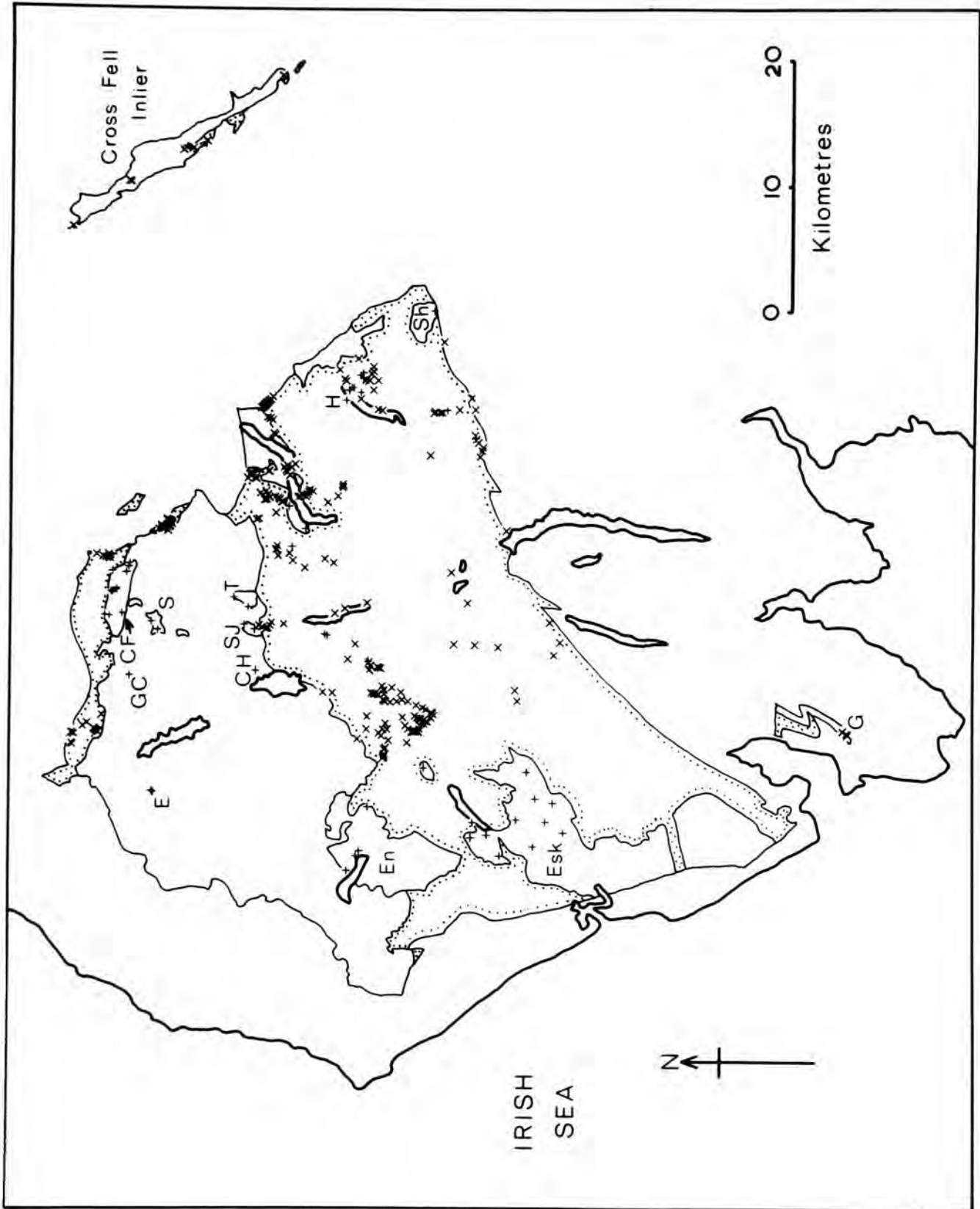
Granites:-

Esk: Eskdale      En: Ennerdale      S: Skiddaw      SJ: St. John's  
T: Threlkeld      Sh: Shap

Other intrusions:-

CF: Carrock Fell      GC: Great Cockup 'picrite'      E: Embleton  
microdiorite      CH: Castle Head dolerite      H: Haweswater complex  
G: Greenscoe vent

Dotted boundaries enclose the Borrowdale Volcanic Group.



Prior to analysis the rocks were ground to a fine powder using a jaw-crusher and a disc mill. Extensive tests were carried out to assess the effects of milling on the ferrous oxide content of the samples. The results showed considerable oxidation in samples ground for more than 30 seconds (Fitton and Gill 1970). Accordingly, sample rock chips were ground for 30 seconds, a small sample removed for the FeO determination and the remainder ground for a further  $2\frac{1}{2}$  minutes. Oxidation ratios determined on a number of the "unoxidised" samples (less than 30 seconds grinding) showed wide variation, presumably due to the altered and oxidised nature of the original rocks. Consequently for the purpose of norm calculations a constant ferric:ferrous ratio (by weight) of 0.808 (Chayes, 1969b) was used. For all other purposes total iron (usually expressed as  $\text{Fe}_2\text{O}_3$ ) was employed.

Analyses were performed on pressed powder briquettes using a Philips PW 1212 X-ray fluorescence spectrometer. For major elements the U.S.G.S. international standards W-1, G-1, G-2, BCR-1, AGV-1 and GSP-1, and the C.A.A.S. standard S-1 were used for calibration. Mass absorption corrections were applied using the method of Reeves (1971).

Ba, Nb, Zr, Y, Sr, Rb, Zn, Cu, Ni, and Cr were determined using a series of Pilkington synthetic glass standards (Brown et al., 1970) for calibration. U.S.G.S. standards were used for V and La. Mass absorption corrections were found to be unnecessary for La but were applied to V and Cr using the coefficients of Heinrich (1966). For all other trace elements approximate correction for absorption difference was made using scattered white radiation as internal standard (Andermann and Kemp, 1958). Corrections were also applied for  $K_{\beta}$  interference on Nb, Zr, Y, Cr and V. In the case of vanadium an iterative procedure developed by D. J. Hughes, G. C. Brown and J. Esson (paper in preparation) was used to correct for the interference of Ti  $K_{\beta}$ .

Garnets and pyroxenes were analysed using a Cambridge "Geoscan" electron probe microanalyser. The analytical technique and method of data processing employed were those described by Sweatman and Long (1969). For trace element determinations on garnets, the mineral was separated using a combination of magnetic and heavy liquid techniques. Analyses were performed by the same methods used for trace element determinations on rocks except that artificially prepared standards of

garnet composition were used for La, Y and Sc. These standards were prepared by mixing "Specpure" oxides (Johnson, Matthey & Co.) to produce a "garnet" matrix which was then spiked with "Specpure" La, Y and Sc oxides. Corrections were applied for the interference effects of Ca  $K_{\beta}$  on Sc  $K_{\alpha}$ .

## CHAPTER 2

SOUTHERN OUTCROP(i) Classification of rock types

The southern outcrop comprises a suite of rocks ranging in composition from basalt to rhyolite. Between these extremes is a continuum of rock types which renders any classification more or less arbitrary. Most conventional classifications of volcanic rocks are based on normative or modal feldspar composition or in some way involve the alkali metals. These cannot be applied to the Borrowdale Volcanics as the feldspars are usually altered and the possibility of alkali migration cannot be ruled out. Of all the other possibilities the silica content of the rocks suffers from the fewest objections and will be used here as a basis for classification. The divisions in this classification have been chosen to coincide closely with changes in the phenocryst phases whilst being consistent with modern usage. The classification is as follows:-

	wt. % SiO <sub>2</sub>
Basalt	< 53
Basaltic andesite	53 - 58
Andesite	58 - 64
Dacite	64 - 70
Rhyolite	> 70

(ii) Distribution of rock types

The stratigraphic distribution of the main rock types in the area is shown diagrammatically in Fig. 3. For the purposes of this diagram, basaltic andesites with silica contents less than 55% have been included with the basalts, the remainder being assigned to the andesites. Correlation of volcanic units is complicated by frequent and rapid lateral variations in rock type but despite this it is possible to make a few generalisations about the succession.

The lowest units, where they are exposed, comprise basalts, basaltic andesites and andesites. These are particularly well exposed around Ullswater where they form the Ullswater Group although they may be seen along most of the northern margin of the southern outcrop. Throughout much of the southern outcrop these lavas are overlain by a thick and persistent group of ignimbrites which are well developed around Scafell (Airy's Bridge Group) and in Langdale (Langdale 'Rhyolite'). Together, the lower lavas and the ignimbrites may be regarded as a volcanic cycle. After the cessation of ignimbrite activity the widespread eruption of the Wrengill Andesites and their lateral equivalents marks the beginning of a second, smaller cycle. This cycle culminated in the eruption of a

sequence of ignimbrites now exposed along the southern margin of the outcrop. These include the Upper 'Rhyolites' of Kentmere and the Hugh's Laithes Pike Ignimbrite Group to the south-east of Haweswater.

Pyroclastic rocks are well developed in the southern outcrop and show the same range in composition as the lavas (i.e. basaltic to rhyolitic). They occur sporadically throughout the succession.

The lavas and ignimbrites form a chemically coherent suite with no significant compositional gaps. Though the rock type is repeated cyclically upwards through the succession (i.e. with time) the essential character of the magma suite remained unchanged since rocks of the first cycle are similar in composition to their counterparts in the second cycle. The suggestion by Hadfield and Whiteside (1936) that the basalt and andesite lavas were progressively enriched in titanium and phosphorus during the volcanic episode was not supported by the present work.

### (iii) Petrography

#### a. Basalts

The basalts of the southern outcrop are typically dark green, aphyric to sparsely porphyritic rocks. Augite is the predominant phenocryst phase (Plate 1) and crystals of the mineral often occur in clusters up to 4mm in

diameter. Orthopyroxene is a subordinate phenocryst phase and is always completely altered to chlorite. It is recognised by its crystal shape, prismatic crystals with square cross-sections. Olivine occurs very rarely in the more basic basalts as characteristic pseudomorphs composed of a fine-grained aggregate of calcite, chlorite and serpentine with haematite developed along cracks (Plate 2). These are quite distinct in shape and composition from the chlorite pseudomorphs after orthopyroxene. The relationship between olivine and orthopyroxene is obscured by alteration. Plagioclase phenocrysts are typically absent although they are found in some specimens of basalt.

The groundmass is composed of a fine-grained intergrowth of plagioclase, augite, chlorite and magnetite. The magnetite occurs as fine octahedral granules and rarely as larger crystals which may be regarded as microphenocrysts.

The value of 53%  $\text{SiO}_2$  taken as the upper limit for the basalts is that used by Taylor et al. (1969a). In the basalts considered here it corresponds approximately with the appearance of plagioclase as a prominent phenocryst (liquidus) phase.

b. Basaltic andesites

With increasing silica content the proportion of augite phenocrysts decreases while orthopyroxene (altered to chlorite) increases although there is no obvious reaction relationship between the two pyroxenes. Plagioclase feldspar becomes the dominant phenocryst phase. The final disappearance of phenocryst augite occurs at about 58% SiO<sub>2</sub> and this is used to define the upper limit of the basaltic andesites. Consequently all rocks with silica contents between 53 and 58% are classified here as basaltic andesites although not all contain the characteristic phenocryst phase assemblage: plagioclase-orthopyroxene-clinopyroxene. At the lower end of the range the augite occurs as large clusters of crystals (Plate 3) as in the basalts but at the upper end it is seen only rarely as small isolated crystals (Plate 4) or as tiny clusters (Plate 5). Microphenocrysts of magnetite are abundant throughout the range.

As in the basalts the groundmass is a fine-grained intergrowth of plagioclase, augite, chlorite and magnetite although in the more silica-rich members the groundmass becomes very fine-grained and even glassy. The glass is completely devitrified but the presence of perlitic cracks in the groundmasses of some of the rocks suggests an originally glassy nature.

### c. Andesite

The disappearance of phenocryst augite is followed closely by the appearance of garnet phenocrysts. The andesites are thus characterised by the unusual phenocryst assemblage: plagioclase-orthopyroxene-garnet. Again, magnetite is abundant as microphenocrysts.

The groundmass is always fine-grained or glassy. Perlitic cracks are commonly seen in the andesites (Plate 6) although in some the groundmass is composed of a felted mass of very small plagioclase laths and minute grains of magnetite. A photomicrograph of a typical andesite is presented in Plate 7.

The upper limit for the silica content of andesites (set here at 64%) corresponds very closely with a drastic change in rock type. Nearly all the rocks analysed which have silica contents greater than this have textures typical of ignimbrites. It is therefore convenient to place the division between andesites and dacites at 64%  $\text{SiO}_2$ .

### d. Dacites

Distinguishing between dacite lavas and ignimbrites is complicated by the complete devitrification of the glassy component of the rocks. However, the presence of broken crystals, pumice fragments and

devitrified glass shards, together with the marked eutaxitic texture of most of the acid rocks studied, suggests that these are ignimbrites (Plate 8). The wide areal extent of some of the dacitic units supports this conclusion.

Garnet and plagioclase are the major phenocryst phases with occasional microphenocrysts of magnetite. The groundmass is composed of a very fine-grained intergrowth of quartz, albite and potash feldspar (Oliver, 1961) which probably represents devitrified glass. Small euhedral, prismatic crystals of zircon and apatite are present as accessories.

The division between dacites and rhyolites is placed, rather arbitrarily, at 70%  $\text{SiO}_2$ . At this level of silica content the CaO in the rocks is usually too low for significant quantities of anorthite to appear in the norm. Rhyolite is thus a more appropriate term for these rocks. Petrographically the rhyolites do not differ significantly from the dacites except that garnet is less abundant in the former. Consequently they will not be discussed further here.

#### c. Inclusions and xenoliths

Cognate xenoliths representing crystal cumulates are of common

occurrence in calc-alkaline rocks and may be locally abundant, as in the West Indies (Wager, 1962; R. J. Arculus, personal communication, 1971). It is noteworthy, therefore, that such xenoliths were not found in the present study. Fragments of pre-existing volcanic material, however, are common in some of the lava flows.

In the lower units of the succession quartz xenocrysts and small fragments of sandstone (Plate 9) and slate are sometimes found in the lavas. These are presumably derived from the underlying Skiddaw Group.

#### (iv) Mineralogy

Only the garnet and clinopyroxene phenocrysts were fresh enough for analysis by electron microprobe. The other phenocryst and groundmass phases were all altered to some extent so that analyses of these would be of questionable value. Garnet will be dealt with in detail in Chapter 4 and so will not be discussed here.

##### a. Pyroxenes

Clinopyroxene phenocrysts in three samples were analysed. The rocks were a basalt (LD 148) and two basaltic andesites; one from the basic end of the group (LD 221) and one from the silica-rich end (LD 309). These clinopyroxenes are magnesium-rich augites with mean compositions of  $\text{Ca}_{42} \text{Fe}_{15} \text{Mg}_{43}$ ,  $\text{Ca}_{38} \text{Fe}_{15} \text{Mg}_{47}$  and  $\text{Ca}_{42} \text{Fe}_{13} \text{Mg}_{45}$  respectively and are plotted

in Fig. 9 (Chapter 3). Complete analyses are listed in the Appendix.

The lack of systematic variation in composition is noteworthy. Only PX-221\* shows any sign of optical zoning and this pyroxene is the only one to show significant, though very slight, compositional zoning. This zoning is in the 'normal' sense (i.e. with enrichment of iron towards the margin).

Phenocryst augite is confined to the more basic rocks of the area. Orthopyroxene phenocrysts, on the other hand, are rare in these rocks but become abundant in the andesites. The presence of chlorite pseudomorphs in some of the ignimbrites may indicate that orthopyroxene phenocrysts were originally present in the dacite magma. Unlike many calc-alkaline areas (e.g. the West Indies) primary amphibole is completely absent from the volcanic rocks of the Lake District. The significance of this will be discussed later.

---

\* In this and succeeding chapters analysed minerals will be referred to by the number of the host rock preceded by a suitable prefix, viz. PX = Augite, G = Garnet.

### b. Feldspars

Approximate compositions of plagioclase feldspars were determined optically on some of the less-altered phenocrysts using the Michel-Lévy method. The results show a variation in composition from about An<sub>65</sub> in the basaltic andesites to almost pure albite in some of the dacites. Zoning is poorly developed with individual crystals showing only a narrow range of composition; the rims being slightly more sodic than the cores (Oliver, 1961). Plagioclase is the dominant phenocryst phase in all the rocks except the basalts.

Orthoclase is seen only in the devitrified glass groundmasses of the andesites, dacites and rhyolites where its presence was demonstrated by Oliver (1961) using sodium cobaltinitrite staining techniques.

### c. Iron - titanium oxides

Titanomagnetite occurs both as a groundmass phase and as microphenocrysts in the basalts, basaltic andesites and andesites of the southern outcrop. Ilmenite, however, was not seen as discrete grains in any of the rocks studied although it occurs occasionally as exsolution lamellae in the magnetite. The absence of ilmenite has been noted by Lowder (1970) as a widespread feature of calc-alkaline rocks. In the dacites and

rhyolites the iron oxide minerals are usually completely altered to limonite and leucoxene.

(v) Petrochemistry

The chemical variation, with silica content, of the rocks of the southern outcrop is shown in Figs. 5 and 6. Since the silica percentage of the rocks has been used as a basis for classification it is convenient to use this parameter as an index of fractionation. Average analyses of the various rock types are given in Table 1 and individual analyses are listed in the Appendix.

The continuity of plotted points in the variation diagrams suggests that the rocks are genetically linked by some process of chemical fractionation. Opinion on the nature of this fractionation process in calc-alkaline rocks in general is divided. Hypotheses involving the contamination of basaltic magma, the mixing of magmas or partial melting of sialic crustal rocks have now been largely discredited. The only viable alternatives are crystal fractionation of a basaltic parent (e.g. Osborn, 1959) and partial melting of basaltic material at depth (e.g. Green and Ringwood, 1968b). The geochemistry of the southern outcrop rocks will be discussed in the light of these two hypotheses.

Fig. 5

Major-element variation in rocks of the southern outcrop.

- Lavas
- Ignimbrites
- △ Intrusive rocks from Haweswater Complex
- Castle Head dolerite
- ▽ Minor intrusions associated with volcanics

The broken lines on the plot of  $\text{Na}_2\text{O} + \text{K}_2\text{O}$  against  $\text{SiO}_2$  enclose the field of Japanese calc-alkaline rocks as defined by Kuno (1966).

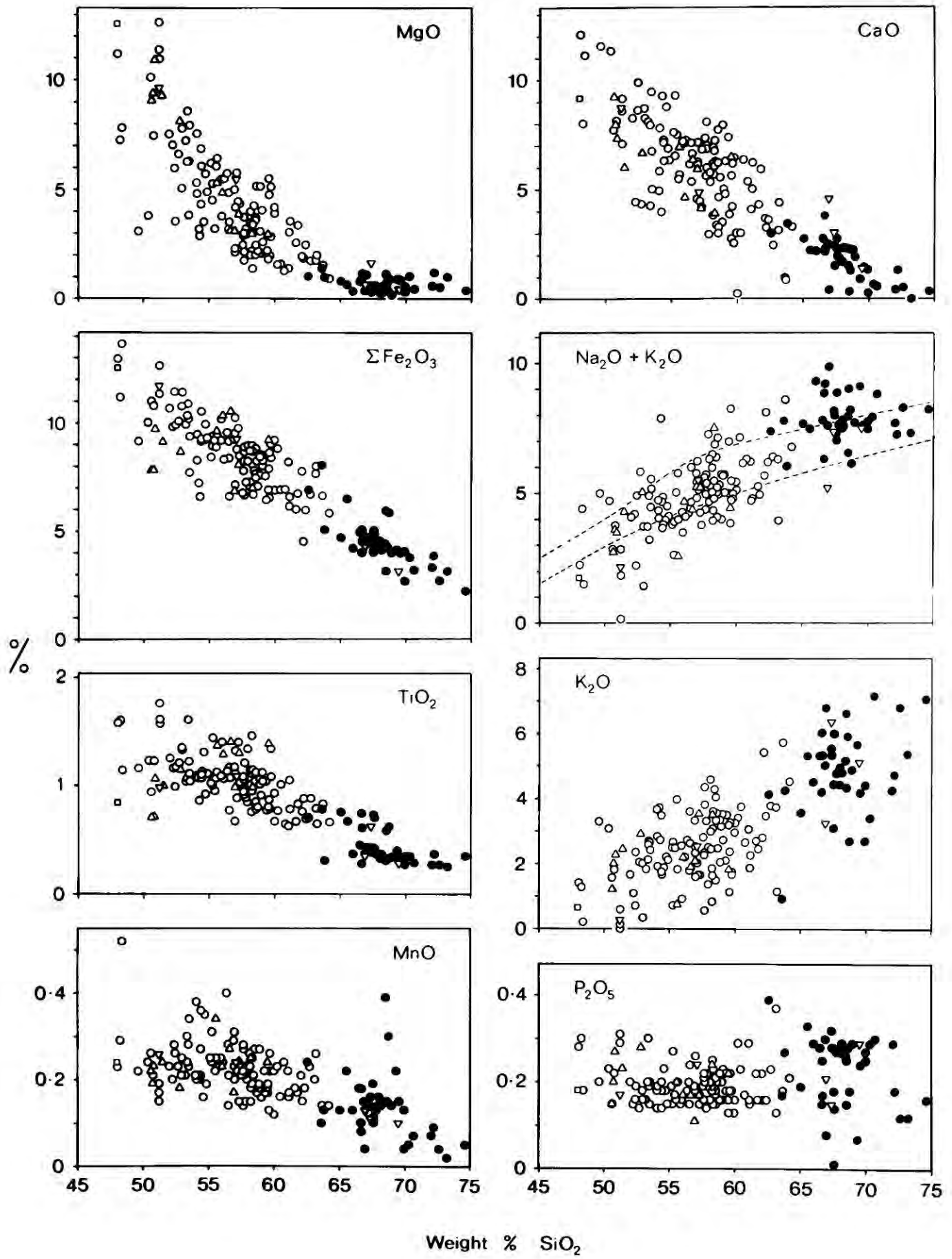


Fig .6

Trace-element variation in rocks of the southern outcrop.

Symbols as in Fig. 5.

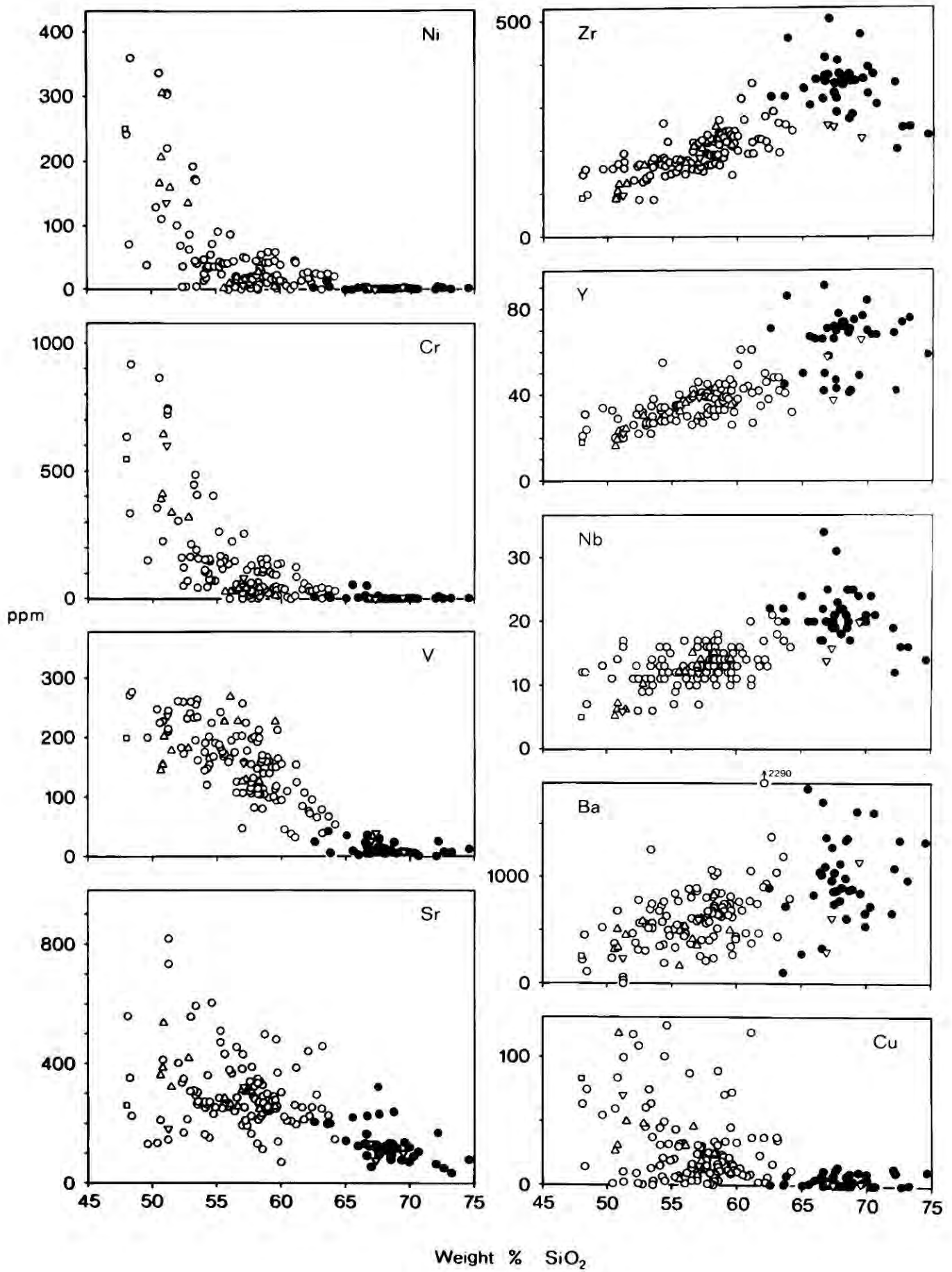


Table 1 - Average analyses of southern outcrop rocks

	Basalts	Basaltic andesite	Andesite	Dacite	Rhyolite
No. of analyses	18	46	46	32	7
Percent					
SiO <sub>2</sub>	51.04	55.74	59.98	67.38	72.21
Al <sub>2</sub> O <sub>3</sub>	16.26	17.81	17.76	16.55	14.72
Fe <sub>2</sub> O <sub>3</sub>	11.11	8.84	7.54	4.66	3.17
MgO	7.73	4.63	2.83	0.69	0.75
CaO	8.68	6.53	4.75	1.96	0.58
Na <sub>2</sub> O	1.88	2.32	2.67	3.09	2.36
K <sub>2</sub> O	1.33	2.42	2.97	4.71	5.55
TiO <sub>2</sub>	1.29	1.09	0.91	0.46	0.31
MnO	0.24	0.24	0.20	0.15	0.06
S	0.20	0.16	0.16	0.10	0.08
P <sub>2</sub> O <sub>5</sub>	0.21	0.19	0.19	0.23	0.21
p.p.m.					
Ba	349	586	747	954	1096
Nb	11	12	14	22	17
Zr	141	179	227	357	282
Y	27	34	40	65	65
Sr	346	310	270	142	85
Rb	49	97	124	211	237
Zn	104	101	93	69	43
Cu	48	26	23	4	5
Ni	145	38	22	2	2
Cr	410	123	62	6	3
V	231	171	119	13	8
La	19	22	35	54	46
CIPW Norms *					
Quartz	5.4	11.0	17.8	25.9	34.9
Corundum	-	-	2.0	3.4	4.3
Orthoclase	7.9	14.4	17.6	27.9	32.9
Albite	16.0	19.7	22.7	26.2	20.0
Anorthite	32.2	31.2	22.4	8.2	1.5
Diopside	7.8	0.1	-	-	-
Hypersthene	20.5	15.3	10.3	3.9	3.3
Magnetite	6.8	5.4	4.6	2.9	1.9
Ilmenite	2.5	2.1	1.7	0.9	0.6
Apatite	0.5	0.5	0.5	0.5	0.5
Pyrite	0.4	0.3	0.3	0.2	0.2
D.I. **	29.4	45.1	58.2	80.0	87.8

\* Fe<sub>2</sub>O<sub>3</sub> / FeO taken as 0.808 (by weight)

\*\* D.I. = Thornton-Tuttle Differentiation Index (Normative  
Qz + Ab + Or)

In the Osborn (op. cit.) model basaltic magma fractionates under conditions of constant oxygen fugacity to precipitate magnetite, olivine, pyroxene and possibly plagioclase. The products are andesite liquid and gabbro or peridotite cumulates. Early precipitation of magnetite prevents the enrichment of iron shown by tholeiitic magmas and is an essential feature of the model. There are, however, many opponents to this idea. Carmichael (1967) has objected on the grounds that the iron-titanium oxides of certain acid calc-alkaline rocks indicate that  $f_{O_2}$  is not constant with falling temperatures but decreases - thus reducing the efficiency of the model. Taylor et al. (1969b) suggested that the abundances of Cr, Co, Ni, Sc and V in calc-alkaline rocks are incompatible with Osborn's model although these objections have been refuted by Osborn (1969) and Hedge (1971).

In the basalts of the southern outcrop the suppression of plagioclase as a liquidus phase is consistent with crystallisation under conditions of moderately high  $P_{H_2O}$  (Yoder and Tilley, 1962, Fig. 28). The abundance of pyroclastic rocks and ignimbrites support this conclusion. This high water pressure would be capable of maintaining the  $f_{O_2}$  at a higher level (external buffer) than would obtain in a relatively dry magma where the

$f_{O_2}$  would be buffered by the crystalline phases (internal buffer). The magnesian nature of the clinopyroxenes and their lack of iron-enrichment in the more silica-rich rocks (cf. Carmichael and Nicholls, 1967) provide evidence for the operation of such an external buffer. The magmas which produced the southern outcrop lavas were thus potentially capable of fractionating in the manner proposed by Osborn (1959).

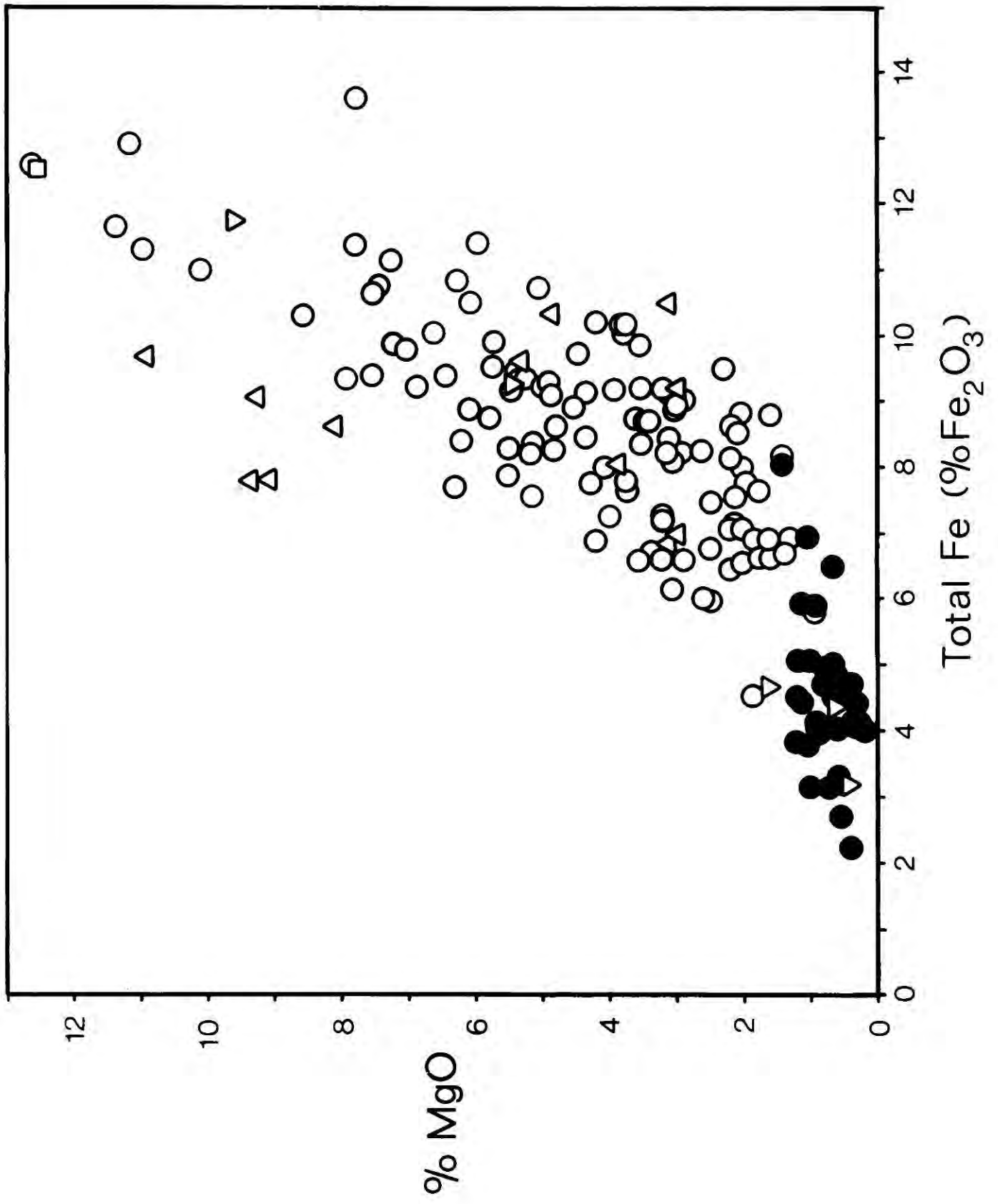
The geochemistry of the lavas is quite consistent with this model. Thus the exponential decline in Mg, Ni and Cr with increasing silica can be explained by the preferential incorporation of these elements in early-formed magnesian olivines and pyroxenes (Burns and Fyfe, 1964). The linear decline in Fe, Ti and V is similarly consistent with their incorporation in magnetite which is seen to occur as phenocrysts throughout the fractionation sequence. Precipitation of plagioclase would, likewise, deplete the magma in Ca and Sr (Philpotts and Schnetzler, 1970). Most of the other elements determined (K, Rb, Ba, Zr, Y, La and Nb) do not enter easily into the lattices of the precipitating phases and are therefore enriched in the later fractionates.

The variation of iron relative to magnesium is shown in Fig. 7. The absence of absolute iron enrichment is typical of calc-alkaline rocks and

Fig. 7

Plot of total iron (expressed as  $\text{Fe}_2\text{O}_3$ ) against MgO for rocks of the southern outcrop.

Symbols as in Fig. 5.



is consistent with early separation of iron oxide minerals and magnesium-rich silicates from the magma. It should be noted, however, that the Fe/Mg ratio increases steadily from the basalts to the rhyolites - presumably indicating that silicates, rather than oxides, are dominant in controlling the fractionation (cf. Brown and Schairer, 1968).

Plots involving the alkali metals (Figs. 5 and 6) show a wide scatter of points, probably due to the mobility of these elements during alteration of the rocks. Despite this, most of the points on the plot of  $\text{Na}_2\text{O} + \text{K}_2\text{O}$  against  $\text{SiO}_2$  fall within, or very close to, the field of Japanese calc-alkaline rocks defined by Kuno (1966).

The application of Osborn's (1959) model to the present study suffers a number of objections. To obtain the large volumes of andesite and dacite observed it would be necessary to fractionate a vast quantity of basalt. Basalts are rare in the southern outcrop and so there would seem to be a volume problem. The relative abundance of rock types appearing at the surface, however, need not reflect abundances at depth since andesite and dacite magmas are more likely to reach the surface than are the denser basalts.

A more serious objection is the scarcity of olivine in the rocks. The production of large quantities of siliceous differentiates requires the fractional crystallisation of silica-poor phases. Magnetite alone is not sufficient since the separation of this phase would remove all the iron from the magma before silica had been enriched very much. Other possible minerals are olivine, garnet and hornblende, although primary hornblende is never seen in the volcanic rocks. The possibility of garnet fractionation will be discussed in Chapter 4. The rapid decline in nickel content with increasing silica suggests that separation of olivine, with a high crystal/liquid partition coefficient for nickel (Häkli and Wright, 1967), is a controlling factor in the fractionation process. None of the other possible mineral phases has a partition coefficient large enough to allow the efficient removal of nickel from the system. Olivine, however, is confined to the most basic of the basalts and all but one of the rocks is quartz-normative so that extensive olivine precipitation seems unlikely. It is possible, though that olivine was fractionating at depth. Work by Kushiro (1969) on the forsterite-diopside-silica system has shown that with increasing  $P_{H_2O}$ , the primary phase field of forsterite is extended towards the silica apex.

Consequently, at high pressures (c. 20kb) a wet basaltic magma could fractionate olivine to produce intermediate and acid liquids. On their ascent to the surface the olivine-phyric liquids would cease to be in equilibrium with olivine and so their phenocrysts would be resorbed. A similar argument could be applied to hornblende and garnet. The survival of garnet phenocrysts in the andesites, however, casts doubt on any models involving resorption of the other two phases.

In the alternative model (Green and Ringwood, 1968b), solid olivine tholeiite is taken down into the mantle and partially melted at depths greater than 30 km. The plate tectonics concept provides a mechanism for this since lithosphere plates descending beneath continental margins would necessarily carry basaltic oceanic crust with them. Given similar conditions of water pressure and total pressure, either partial melting or crystal fractionation of the same basalt composition could yield essentially the same products. Partial melting would, of course, produce its derivative liquids in reverse order to crystal fractionation. Thus a small degree of melting would yield acid magmas whilst it would require extensive melting to produce basaltic magma. The demonstration by Green and Ringwood (op. cit.) that the andesite liquidus lies in a low-temperature

trough at 30 kb makes it possible to derive large volumes of andesitic and dacitic magmas, accompanied by relatively trivial amounts of basaltic and rhyolitic magmas, by this partial melting process. The resulting distribution of rock types would be similar to that observed in the Lake District southern outcrop, so there is no volume problem associated with this model. Moreover, the model is not jeopardised by the absence of olivine phenocrysts. Equilibration of wet, silica-saturated liquids with residual olivine crystals (as required by the distribution of nickel in the rocks) could take place at depth at the site of partial melting (Kushiro, 1969). At lower pressures the contraction of the primary phase field of forsterite (Kushiro, op. cit.) would favour the crystallisation of orthopyroxene, rather than olivine, as a phenocryst phase in the ascending magma.

On balance, the geochemistry of the rocks favours an origin by partial melting rather than fractional crystallisation although the latter possibility is by no means eliminated. The absence of cognate xenoliths and the scarcity of accumulative porphyritic rocks is consistent with this conclusion. Further evidence relevant to the genesis of the rocks of the southern outcrop is provided by the garnet phenocrysts. This will be discussed in Chapter 4.

(vi) Intrusions

The possibility that some of the igneous intrusions of the Lake District represent the remains of the volcanoes from which the Borrowdale Volcanics were erupted was mentioned in Chapter 1. Two such intrusions were sampled and analysed in the present study. One of these, the Castle Head dolerite (near Keswick), has long been suggested as a feeder pipe to the lavas (Ward, 1876). The intrusion has the form of a plug and is intruded into the Skiddaw Slates. It is composed of a fine-grained dolerite containing abundant augite phenocrysts. These are usually present as clusters of crystals resembling the augite clusters typical of the southern outcrop basalts. Chemically, the rock (LD 283) is very similar to these basalts (Figs. 5 and 6).

The other intrusion is the Haweswater Complex described by Hancox (1934) and recently, in greater detail, by Nutt (1970). The latter author considered the intrusion to be a feeder to the volcanics on the basis of structural evidence. It is essentially gabbroic with fine-grained dolerite occurring at the margin. The gabbro is typically composed of plagioclase, chlorite pseudomorphs after orthopyroxene, large ophitic plates of augite and irregular grains of opaque oxides.

Analyses of representative samples taken from the intrusion are plotted in Figs. 5 and 6. They fall within the scatter of points for the lavas for all the elements determined except that some of the gabbro samples have slightly higher MgO/total Fe<sub>2</sub>O<sub>3</sub> ratios. This is probably due to accumulation of pyroxene crystals in the gabbro.

The geochemistry of these two intrusions is quite compatible with their being feeder pipes to the lavas though such evidence cannot be conclusive. Both intrusions, however, have suffered similar degrees of deformation, cleavage and alteration to the effusive rocks so that it is quite probable that they represent the core-remnants of two of the eroded ancient volcanoes.

Within the volcanic pile are numerous small intrusions which are petrographically very similar to the associated lavas. Five such intrusions were sampled in the present study. These comprised two small intrusions on the north-west side of Ullswater (LD 152 and LD 153) described by Moseley (1964); a 'porphyrite' (LD 24) and 'garnetiferous biotite-quartz-porphyry' (LD 65) from the Scafell area (Oliver, 1961) and a quartz-porphyry (LD 289) from Kentmere (Mitchell, 1929). Chemically, the two samples from Ullswater are dacitic and basaltic respectively and

the 'porphyrite' from Scafell is a basaltic andesite. The 'garnetiferous biotite-quartz-porphyry' has the form of a sill although its intrusive character has been questioned by Strens (1962) who considers it to be an ignimbrite flow. Mitchell's (op. cit) quartz-porphyry is closely associated with ignimbrites to which it may have been a feeder.

Analyses of these five samples, indicated on Figs. 5 and 6 by inverted triangles, are very similar to analyses of the associated effusive rocks. There can be little doubt that these small intrusions represent the same magma series as did the effusive rocks.

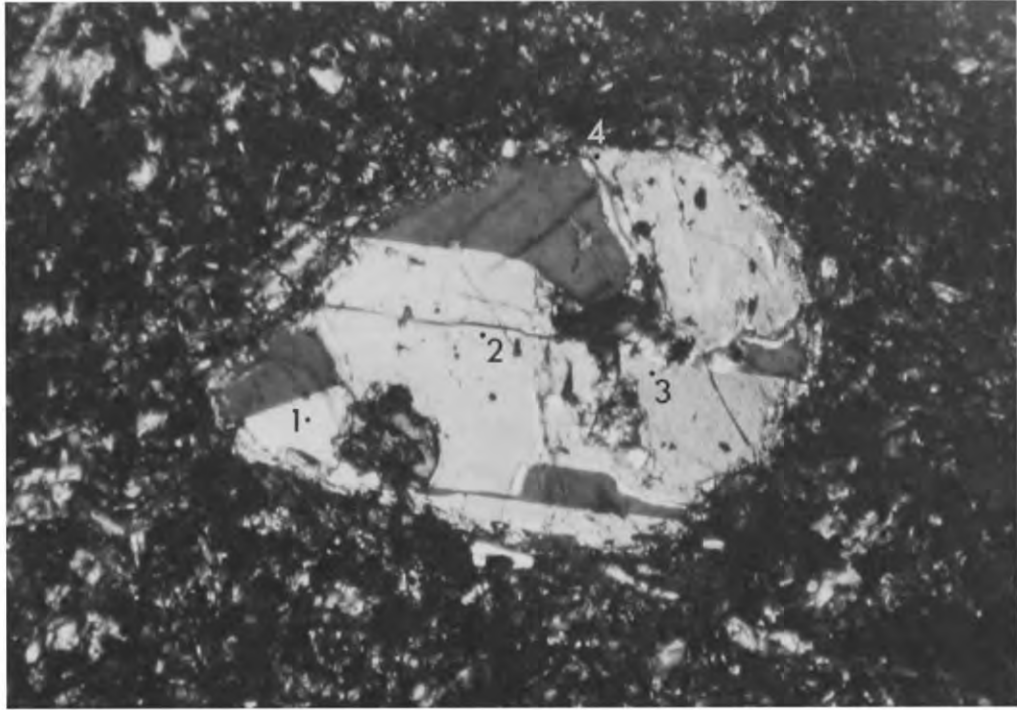


Plate 1. Augite phenocryst in basalt (LD 148)

Crossed polars, x 70.

In this and subsequent photomicrographs the numbers indicate the location of probe-analysed points. Analyses are listed in the Appendix.

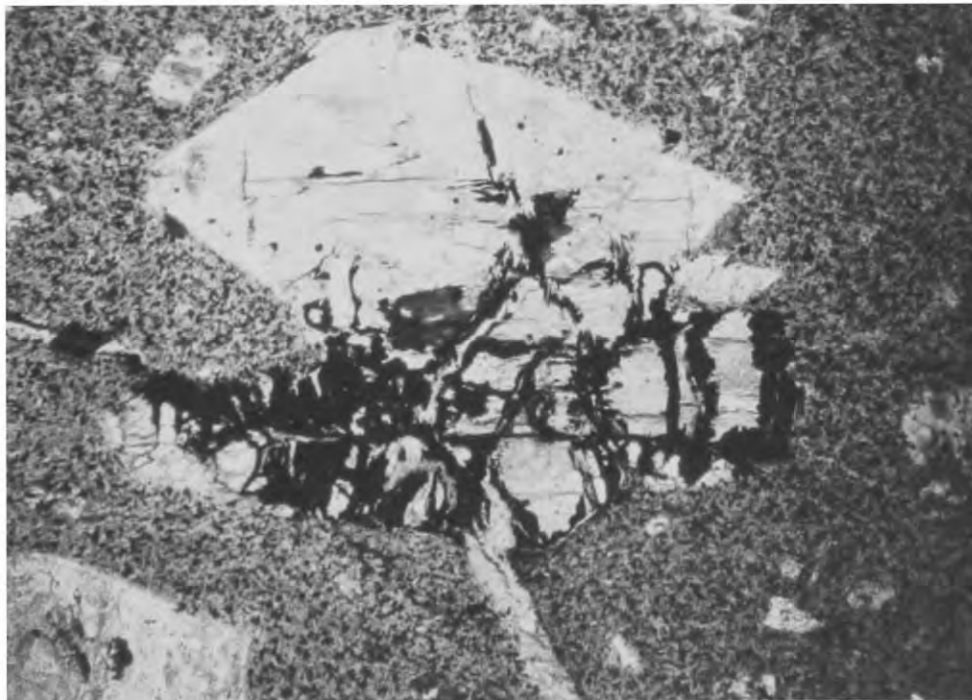


Plate 2. Pseudomorph after olivine in basalt (LD 269)

Plane polarised light, x 32.

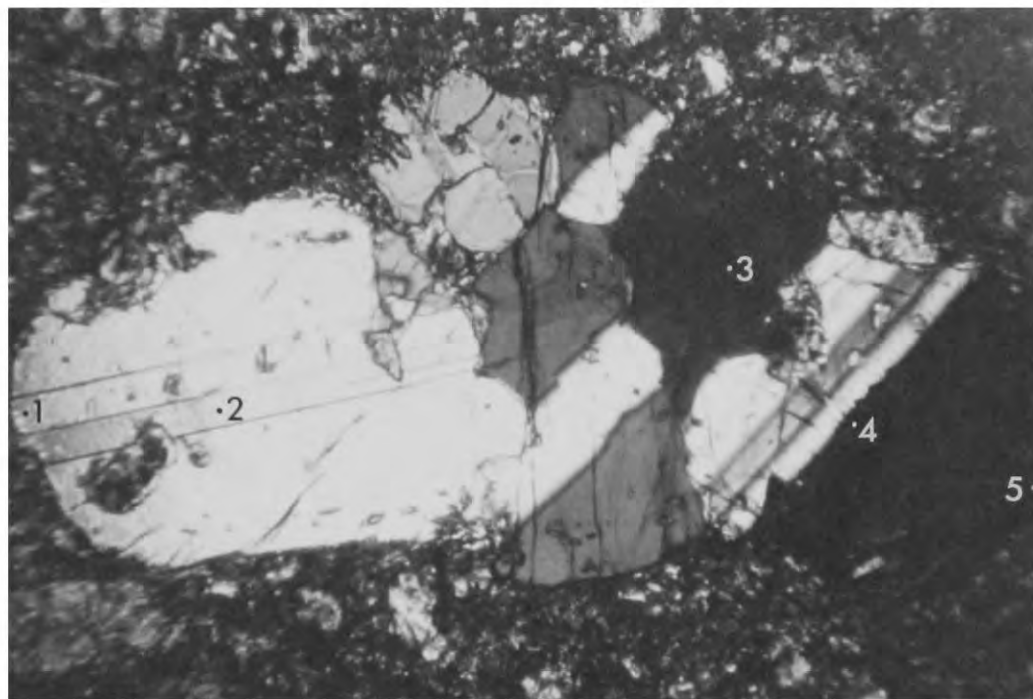


Plate 3. Cluster of augite phenocrysts in basaltic andesite (LD 221)  
Crossed polars, x 54

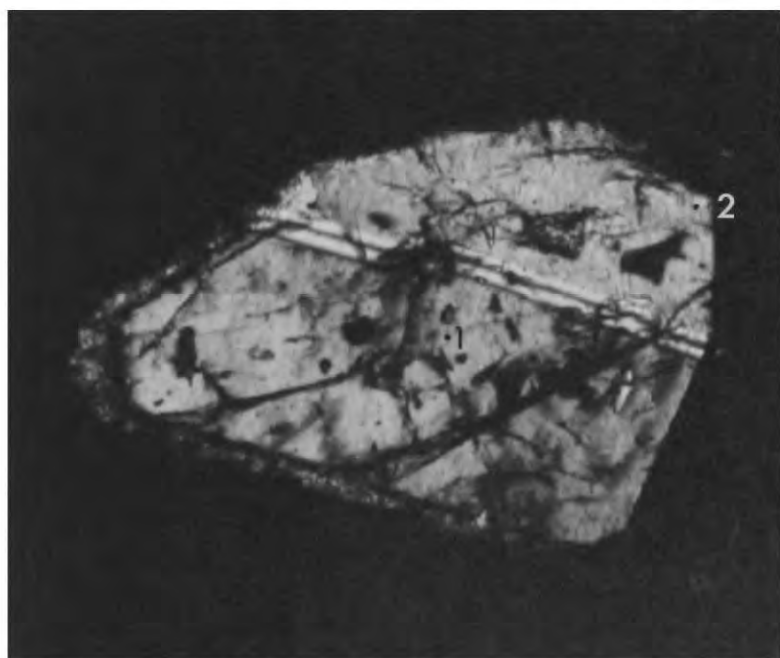


Plate 4

Small augite phenocrysts in basaltic andesite (LD 309)  
Crossed polars, x 165

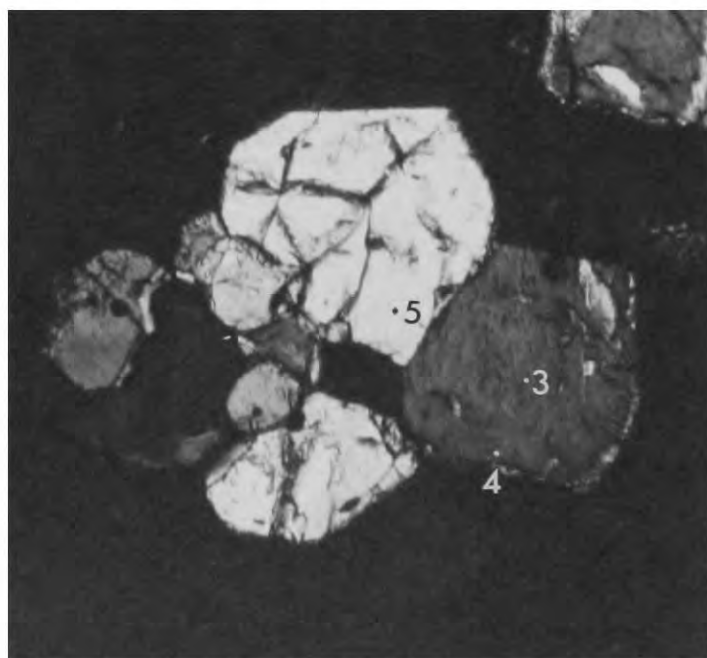


Plate 5

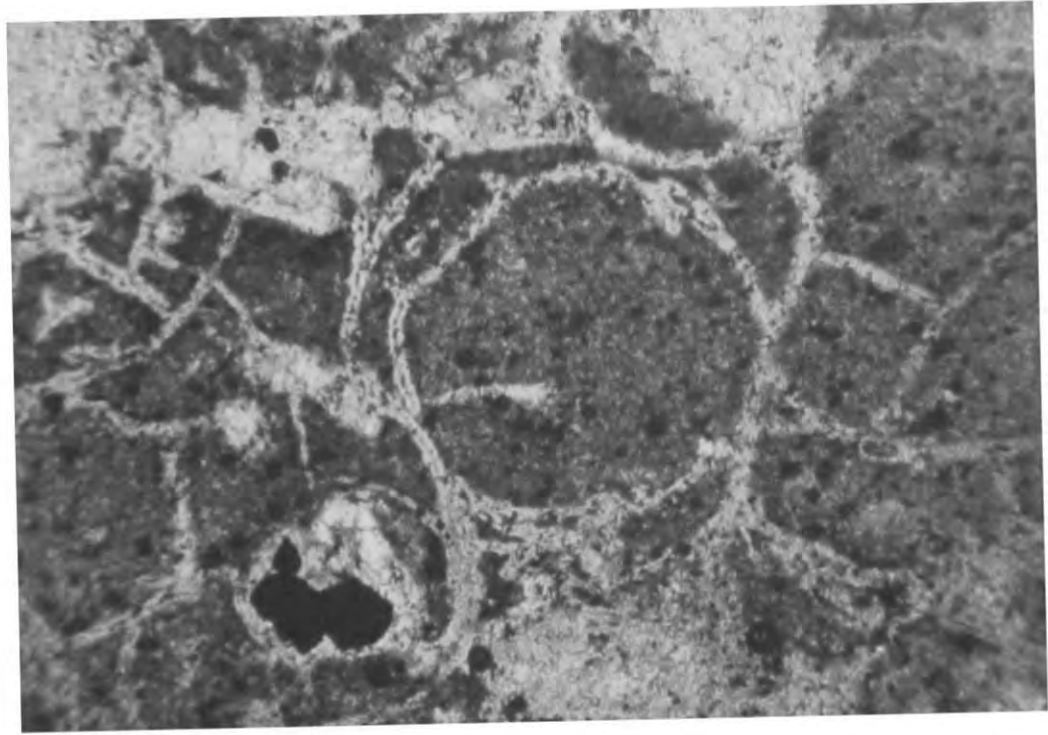


Plate 6. Perlitic cracks in groundmass of andesite (LD 146)  
Plane polarised light, x 54.

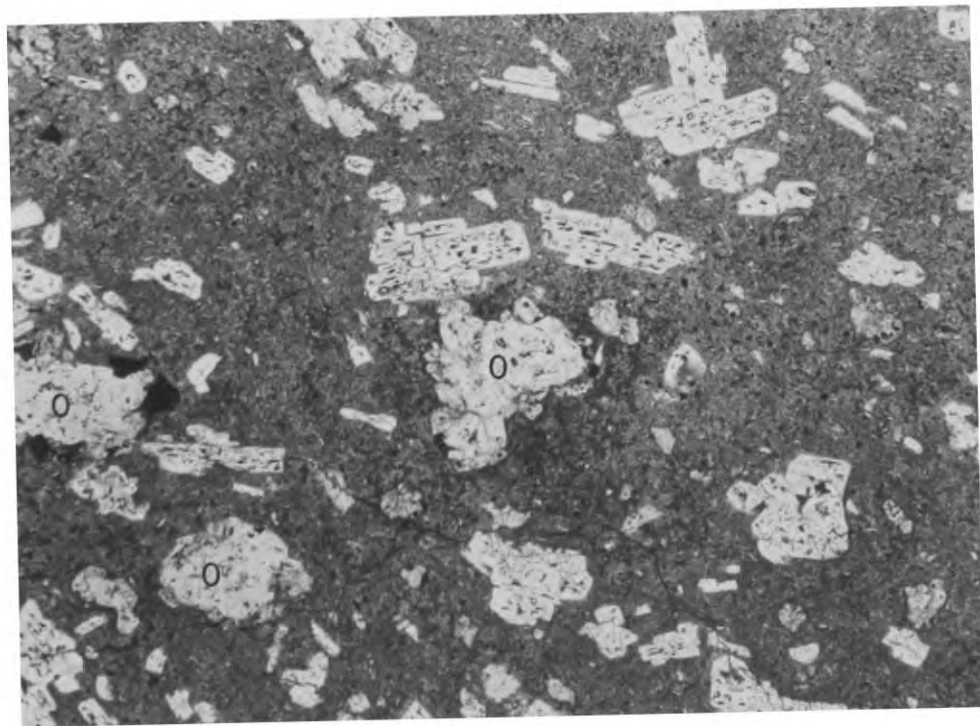


Plate 7. Andesite (LD 132) with phenocrysts of orthopyroxene (O,  
altered to chlorite), plagioclase and magnetite.  
Plane polarised light, x 12.

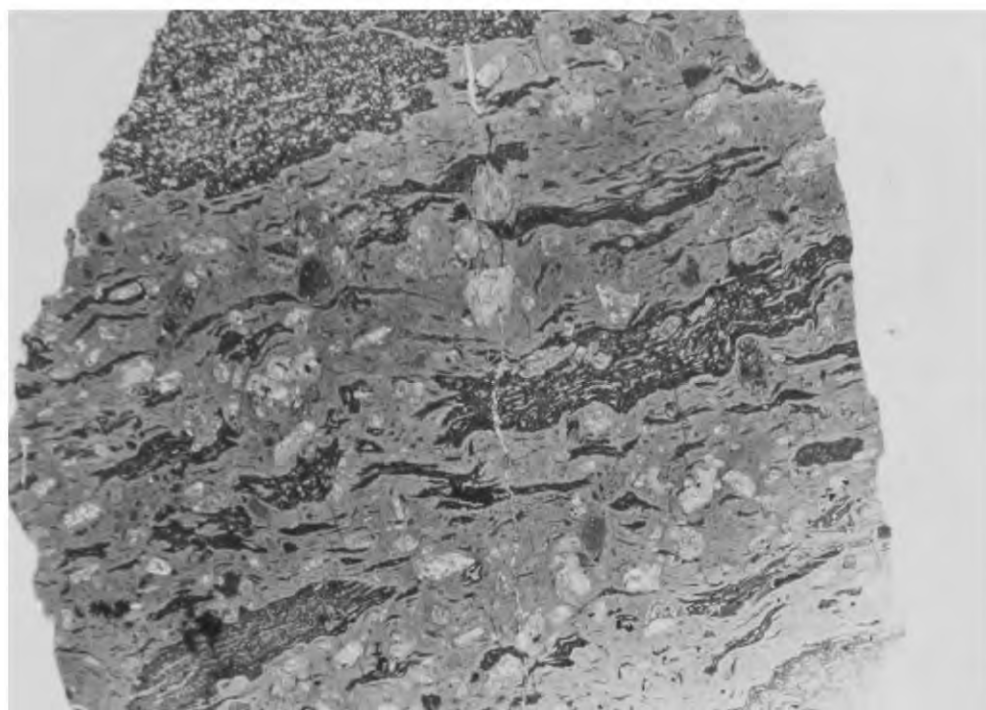


Plate 8. Dacitic ignimbrite (LD 303) containing pumice fragments and showing typical eutaxitic texture.  
Plane polarised light, x 4.4

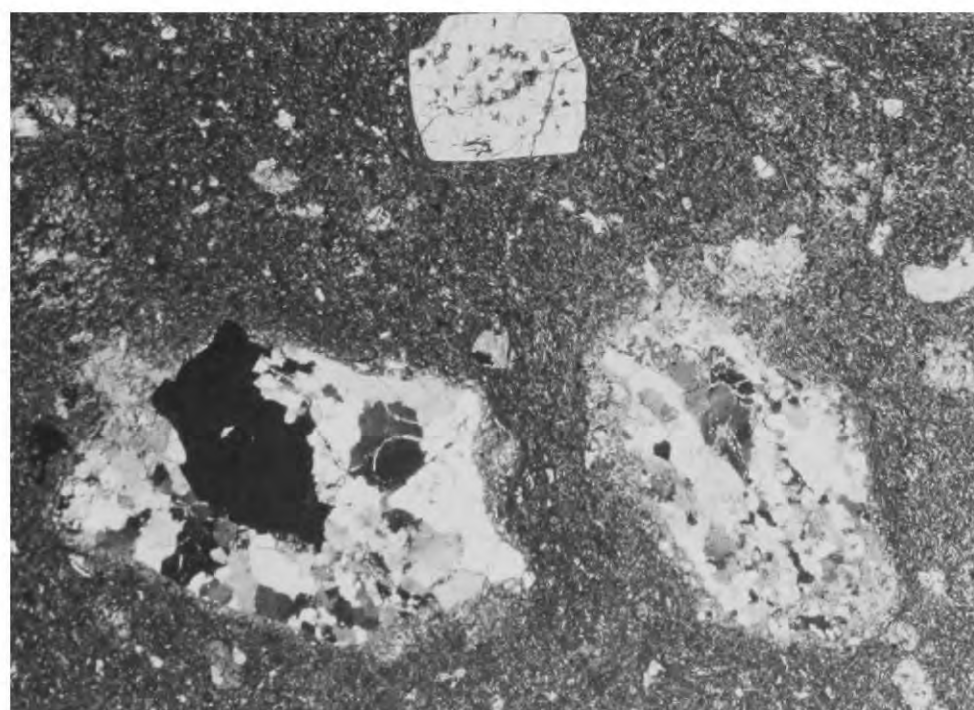


Plate 9. Small sandstone inclusions and augite phenocryst in basalt (LD 275)  
Crossed polars, x 12.

NORTHERN OUTCROP(i) Distribution of rock types

A striking feature of the lavas of the northern outcrop is the abundance of basic porphyritic types. On the classification scheme used for the southern outcrop most of the lavas are basaltic andesites with a predominance of rocks towards the basic end of this group (less than 55% SiO<sub>2</sub>). Consequently in Fig. 3 most of the lavas in the northern outcrop are classified as 'basalts'. Acid types are rare and probably account for less than 1% of the total thickness (c. 2½km.) of the exposed volcanic succession.

Eastwood et al. (1968) have divided the succession into a lower (Binsey) and an upper (High Ireby) group. The basal flows of each group are composed of distinctive, highly porphyritic lava (Eycott type) containing phenocrysts of plagioclase up to 3cm. across. Much of the remainder of the succession is made up of less spectacular, but still highly porphyritic, lavas (Berrier type) containing smaller phenocrysts of plagioclase. Most of the less basic (>55% SiO<sub>2</sub>) basaltic andesites and nearly all the pyroclastic rocks in the succession appear to be confined to the Binsey group (Fig. 3). Acid lavas and ignimbrites are seen occasionally in both groups.

(ii) Petrography

The petrography of the lavas of the northern outcrop has been described in detail by K. C. Dunham and J. Phemister in the I.G.S. Memoir of the Cockermouth area (Eastwood et al., 1968). Consequently only a brief description of the rocks will be given here with emphasis on the points of contrast between the northern and the southern outcrops. The classification scheme described in Chapter 2 will be used for naming the rock types.

Truly basaltic lavas are not very common. They are usually porphyritic with phenocrysts of plagioclase, augite and orthopyroxene (altered to chlorite). The augite frequently occurs as clusters of crystals (Plate 10). Pseudomorphs after olivine have been recorded in some of the basalts by Dunham and Phemister (op. cit.) but were not seen in any of the rocks examined here. Magnetite is abundant in the groundmass but, unlike the basalts of the southern outcrop, it is not seen as phenocrysts.

By far the most abundant rocks are the basaltic andesites which were classified by Dunham and Phemister (op. cit.) into three types. Two of these, the Eycott and Berrier types, have been mentioned already.

Examples of these two are illustrated in Plates 11 and 12 respectively. The third type is represented by the relatively rare flows of aphyric lava. These rocks are very similar in appearance, both in hand-specimen and thin section, to the groundmasses of the porphyritic types.

Plagioclase forms the dominant phenocryst phase in the basaltic andesites although phenocrysts of orthopyroxene (altered to chlorite) and augite are commonly present. In the more basic lavas magnetite is confined to the groundmass although it appears as a phenocryst phase in the more siliceous of the basaltic andesites. This appearance of phenocryst magnetite occurs at about 55%  $\text{SiO}_2$ . The magnetite phenocrysts are accompanied by occasional discrete crystals of ilmenite.

In general the groundmasses of the basaltic andesites are more coarse-grained than are those from similar rocks in the southern outcrop. Magnetite is abundant as small octahedral crystals and is responsible for the dark colour of the rocks. Other groundmass phases are plagioclase, augite and, more rarely, pigeonite.

Andesites seem to be absent from the northern outcrop and the rocks collected included only one dacite (LD 102). This rock has the textural features of an ignimbrite (Plate 13) and is composed of a compact mass

of devitrified glass shards enclosing phenocrysts of albite, chlorite pseudomorphs after orthopyroxene, quartz and magnetite. The remaining acid rocks collected were rhyolitic. One of these (LD 96), described by Dunham and Plemister (in Eastwood et al., 1968) as 'keratophyre', is clearly a lava and is composed of a relatively coarse-grained ( $>0.1\text{mm}$ ) matrix of alkali feldspar and quartz with phenocrysts of albite, quartz and magnetite (Plate 14). The other two acid rocks are very fine-grained and difficult to classify as either lavas or ignimbrites. On rather slender textural evidence they are regarded here as ignimbrites.

### (iii) Mineralogy

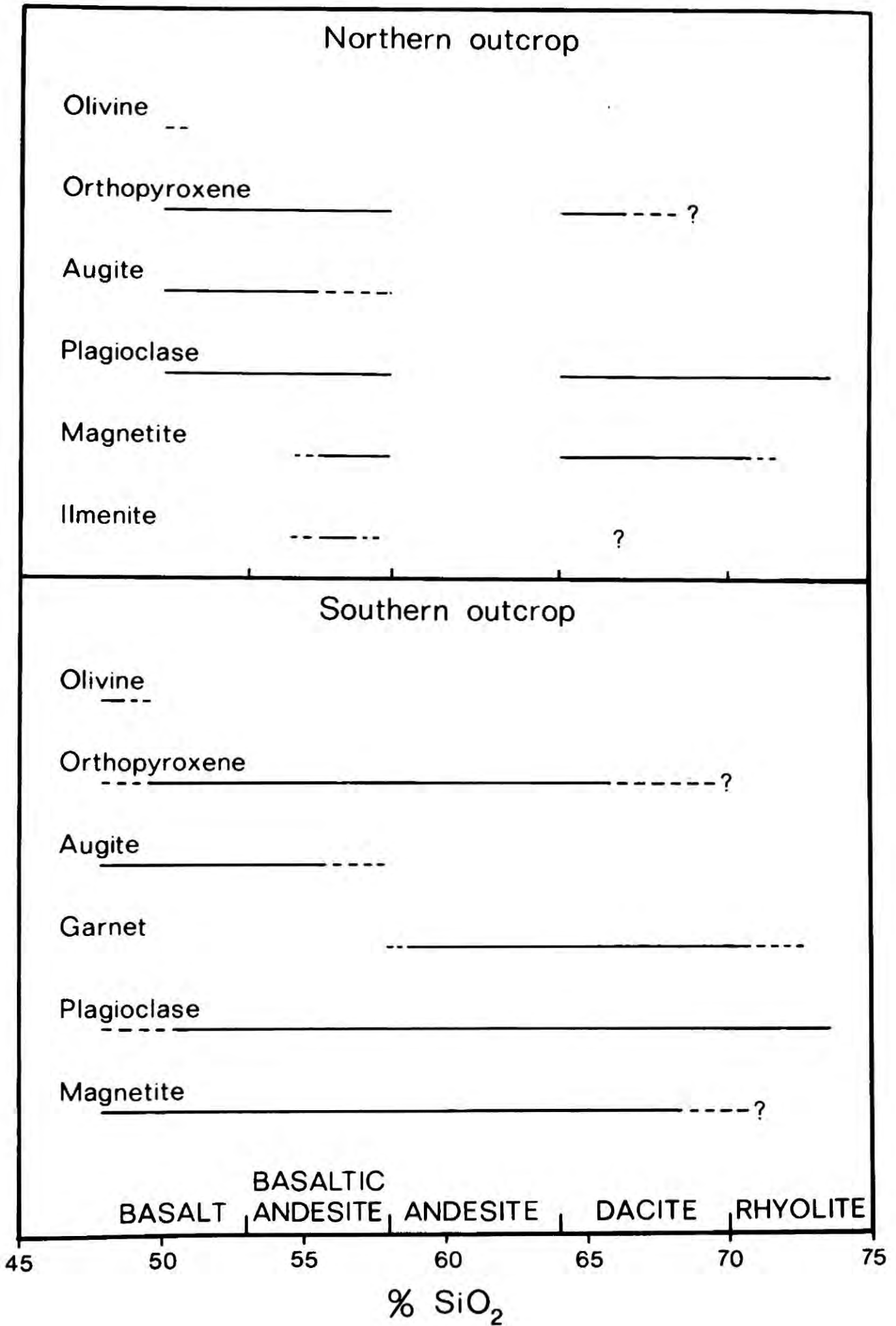
The extent of occurrence of phenocryst phases in rocks of the northern and southern outcrops is summarised diagrammatically in Fig. 8. A number of important differences between the two outcrops are apparent. Garnet is not seen in the northern outcrop although this may be due to the scarcity of intermediate and acid rocks. A thorough search of heavy mineral residues (using bromoform for separation) from the dacite and a rhyolite, however, failed to reveal any traces of garnet. Treatment of similar rocks from the southern outcrop in this way usually reveals a number of small garnet fragments.

Fig. 8

---

Extent of occurrence of phenocryst phases in rocks of the Borrowdale  
Volcanic Group.

Broken lines indicate that the phase is seen only rarely.



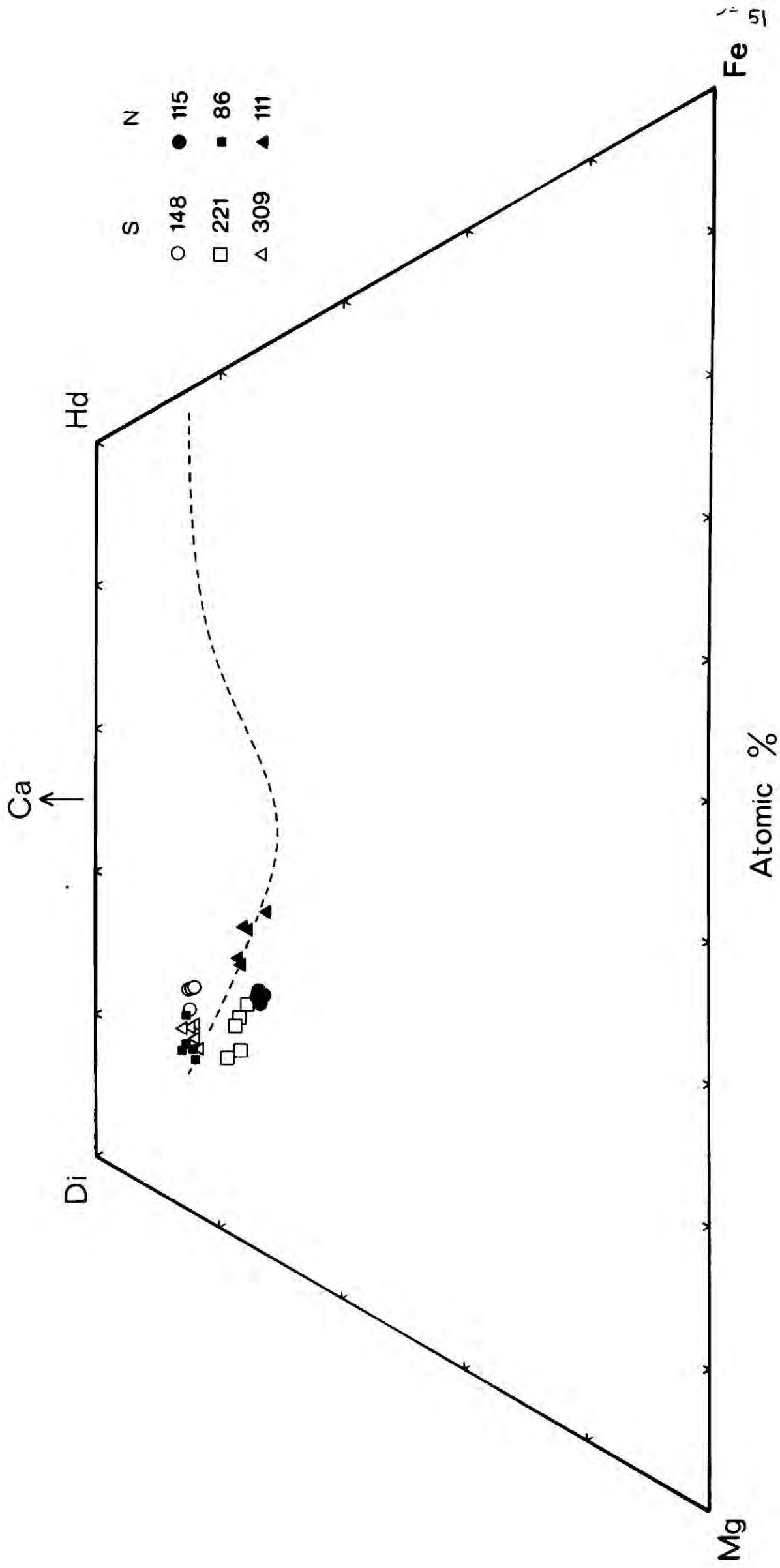
In the lavas of the northern outcrop, magnetite phenocrysts are only seen in the more silica-rich members ( $>55\% \text{SiO}_2$ ) where they are accompanied by phenocrysts of ilmenite. This is in marked contrast to the rocks of the southern outcrop which contain magnetite (but no ilmenite) throughout the range of compositions. The iron-titanium oxide minerals are invariably altered to some degree and attempts to analyse magnetite-ilmenite pairs were not successful.

Pyroxene phenocrysts occur in a similar range of rocks as do those of the southern outcrop. Thus, with increasing silica content, orthopyroxene becomes dominant over augite until, in the most acid of the basaltic andesites, augite phenocrysts become very scarce. The orthopyroxene is invariably replaced by chlorite although augite is usually fresh enough for analysis by electron microprobe. Phenocrysts of augite from three rocks, a basalt (LD 115) and two basaltic andesites (LD 86 and LD 111), were analysed. Photomicrographs of these phenocrysts showing the positions of analysed points are presented in Plates 10, 15 and 16 respectively. End-member compositions of the pyroxenes are plotted on Fig. 9 and complete analyses listed in the Appendix. All the analyses plot close to the early part of the Skaergaard clinopyroxene trend

Fig. 9

Plot of clinopyroxene analyses from rocks of the northern (solid symbols) and southern (open symbols) outcrops. Sample numbers are indicated in the key.

The Skaergaard clinopyroxene trend (Brown and Vincent, 1963), shown as a broken line, is included for comparison.



(Brown and Vincent, 1963). PX-111 (from the more silica-rich of the two basaltic andesites) is enriched in iron relative to the other analysed pyroxenes. Curiously, this pyroxene shows reversed zoning (Mg-rich rim) which may be the result of the co-precipitation of magnetite depleting the magma in iron as it cooled. The presence of minute parallel, rod-like inclusions of an opaque mineral (probably magnetite) in a zone around the core of the crystal (Plate 16) could indicate oxidation of early-formed, iron-rich pyroxene while later, more magnesian, parts were crystallising. The other two pyroxenes show no significant zoning and are similar in composition to the southern outcrop pyroxenes (Fig. 9).

Augite is the predominant groundmass pyroxene in the basalts and basaltic andesites although pigeonite has been recognised optically in some of the latter. None of the groundmass phases, however, was analysed in the present study.

Optical determination of plagioclase compositions gives values of about  $An_{65}$  for the large phenocrysts in the basaltic andesites and almost pure albite for the phenocrysts of dacites and rhyolites. In this respect the rocks of the northern outcrop are similar to those of the south.

(iv) Petrochemistry

The highly porphyritic nature and restricted range of composition of most of the northern outcrop lavas makes the construction of variation diagrams rather difficult. Only the ignimbrites and aphyric lavas represent liquids and these have been plotted as solid symbols on the variation diagrams (Figs. 10 and 11). In addition to these the groundmasses of four samples of Eycott type lava have been separated, using heavy-liquid techniques. Analyses of these are plotted as solid inverted triangles joined by tie-lines to points representing the bulk composition of the respective porphyritic rocks. Together, these solid symbols represent the chemical variation of the northern outcrop magma. The variation of iron with magnesium is shown in Fig. 12.

In contrast with the southern outcrop there is abundant evidence to suggest that crystal fractionation was important in the evolution of the northern outcrop magmas. The feldspar phenocrysts in the Eycott type basaltic andesites are certainly accumulative and in some samples may account for over 50% of the volume of the rock. The small volume of acid rocks could easily be derived by this process as was demonstrated numerically by Lowder and Carmichael (1970) for the lavas of Talasea,

Fig. 10

Major-element variation in rocks of the northern outcrop.

- Porphyritic lavas
- ▲ Aphyric lavas
- ▼ Separated groundmasses from Eycott type lavas
- Ignimbrites
  
- Embleton microdiorite

Carrock Fell Complex:-

- △ Gabbros and granophyres (L-leucogabbro)
- ▽ Harestones felsite

The open circle at c. 70% SiO<sub>2</sub> represents the 'keratophyre' lava (LD 96) from Eycott Hill.

The broken lines in the plot of Na<sub>2</sub>O + K<sub>2</sub>O against SiO<sub>2</sub> enclose the field of Japanese calc-alkaline rocks as in Fig. 5. Tholeiitic rocks plot below the lower of the two lines.

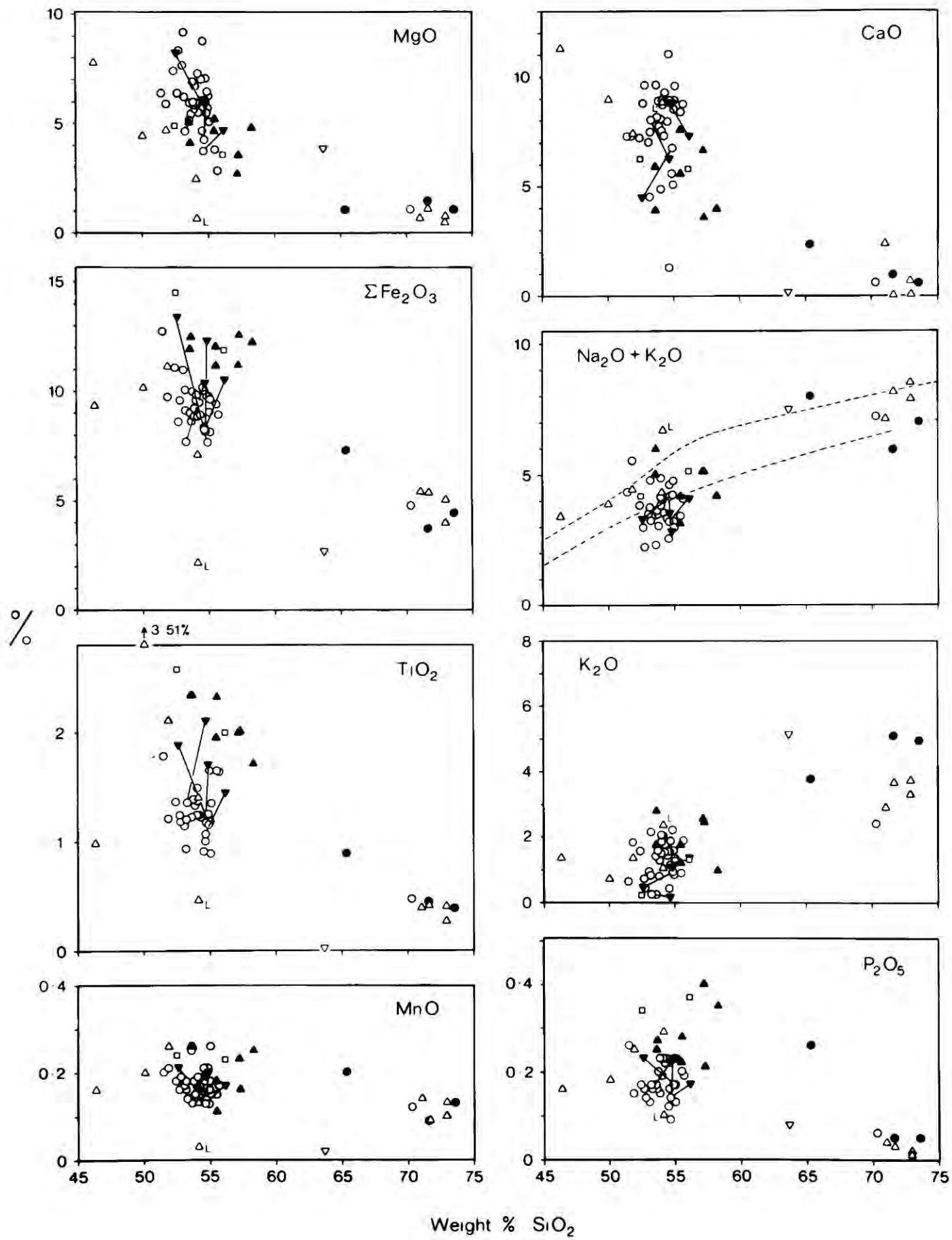


Fig. 11

---

Trace-element variation in rocks of the northern outcrop. Symbols as in Fig. 10.

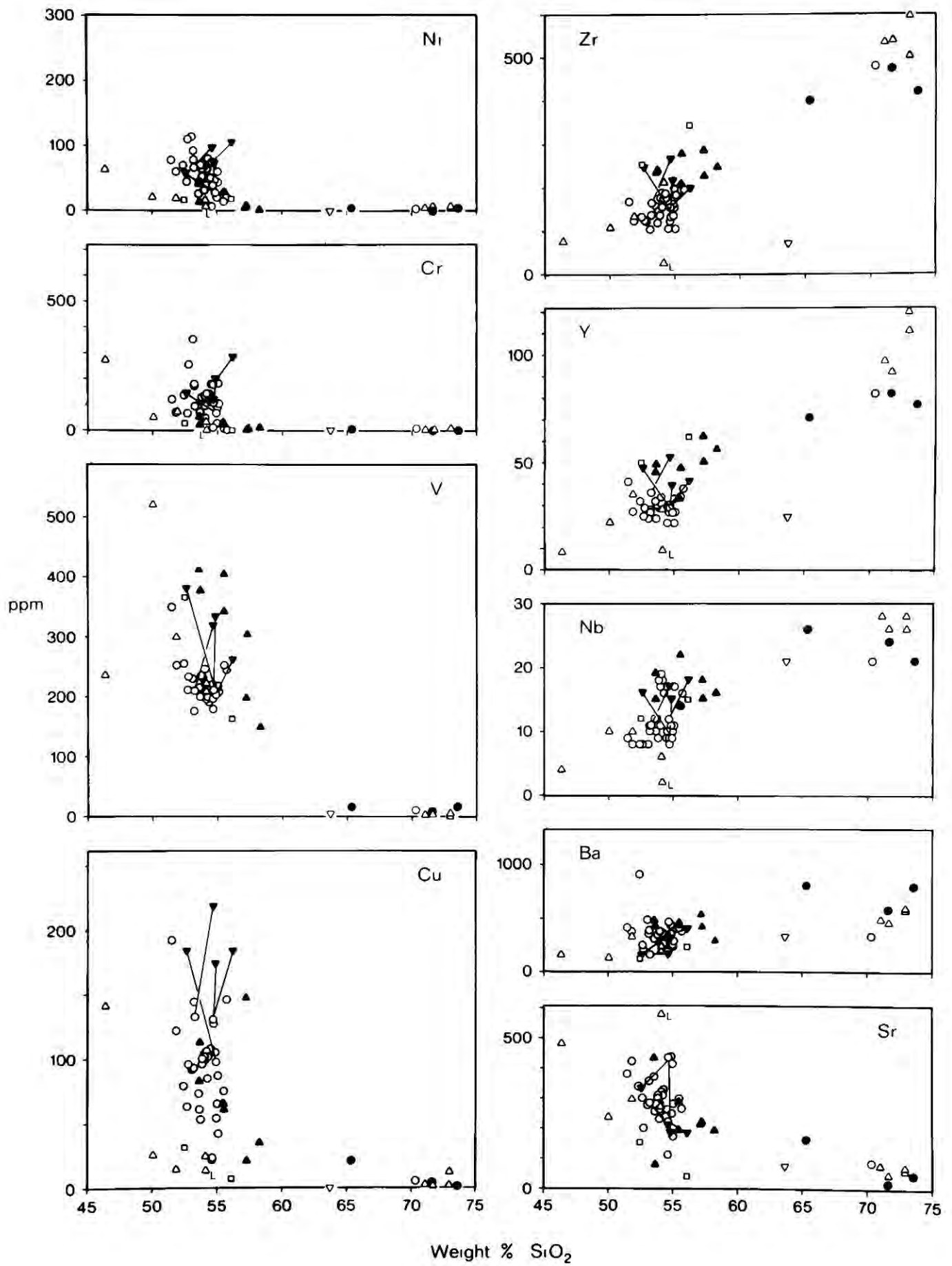
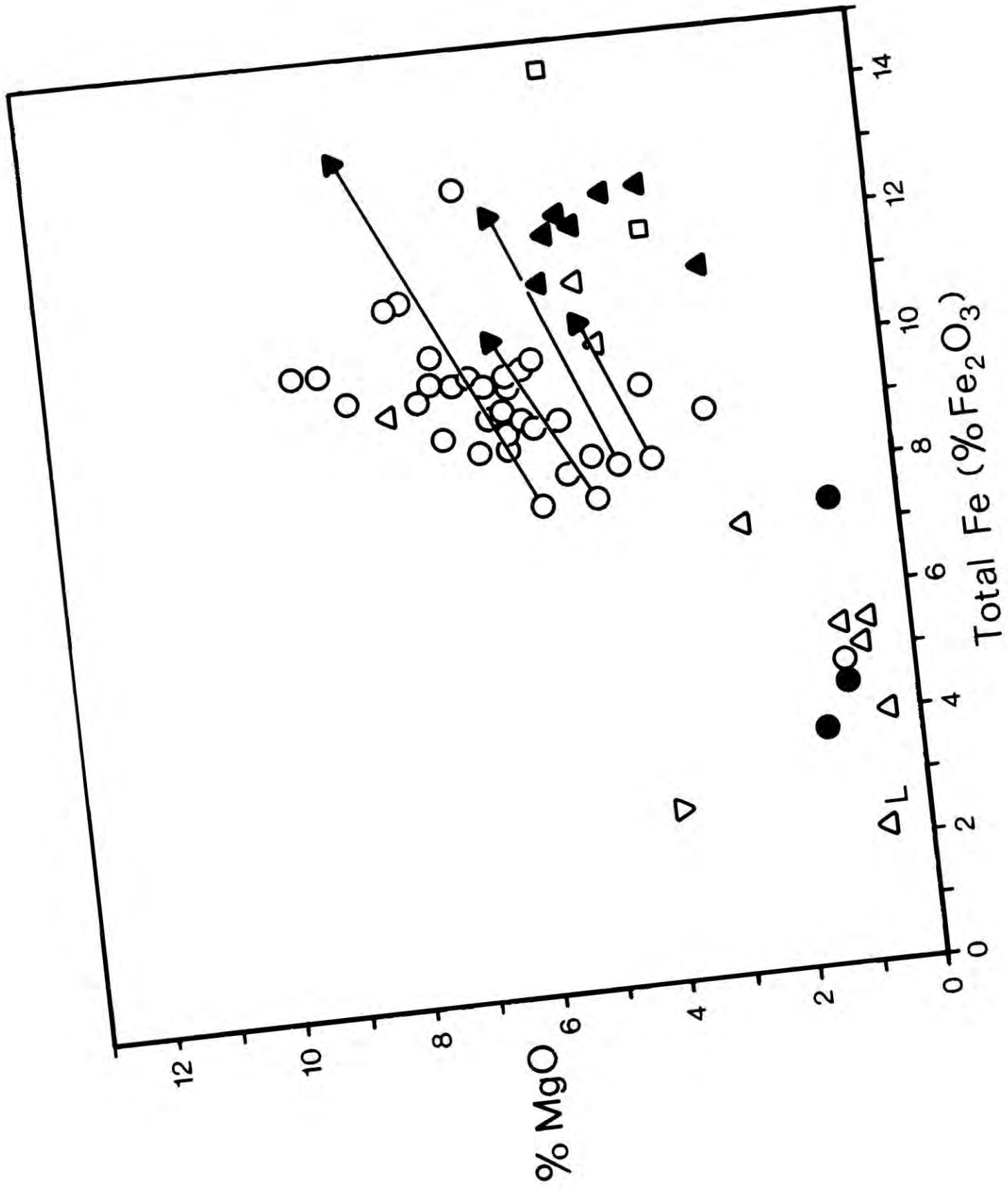


Fig. 12

Plot of total iron (expressed as  $\text{Fe}_2\text{O}_3$ ) against MgO for rocks of the northern outcrop.

Symbols as in Fig. 10.



New Britain. Using a least-squares method, these authors showed that crystal fractionation of the phenocrysts could account for the observed liquid line of descent of the lavas. By analogy with the Talasea lavas the subtraction of plagioclase, two pyroxenes and magnetite from a basaltic andesite magma could yield the small volume of acid rocks observed in the northern outcrop. The absence of rocks of intermediate composition, reminiscent of the 'Daly Gap' in rocks from oceanic islands (Chayes, 1963), is not a serious objection to a crystal fractionation model. Wyllie (1963) has shown that the presence of thermal shelves in the system diopside-anorthite-albite, such that small changes in temperature could cause large changes in liquid composition, may account for the absence of intermediate rocks in basalt-rhyolite associations.

In addition to the petrographic differences, the rocks of the two outcrops show a number of important petrochemical differences. The northern outcrop 'magma' (as represented by solid symbols in Figs. 10, 11 and 12) is richer in iron, titanium, vanadium and copper than that of the southern outcrop. For iron, the relative difference is of the order of 25% but for the other three elements differences of 100% are seen in the basic rocks. The northern outcrop 'magma' is also signifi-

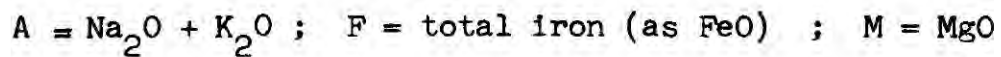
cantly, though less obviously, richer in Zr, Y and Nb and slightly poorer in K and Ba. The distribution of phosphorus also reveals differences in the rocks and the two outcrops. In rocks from the south the element remains at a constant level of about 0.2% throughout the fractionation sequence (Fig. 5). In the north, however, it appears to increase with increasing silica in the basaltic andesites reaching a maximum of 0.4%. Thereafter it declines in abundance, dropping to about 0.05% in the rhyolites (Fig. 10). This rise and fall in phosphorus content is similar to that inferred for the Skaergaard liquids (Wager and Brown, 1967).

The relative iron-enrichment in the northern outcrop lavas is shown on an A.F.M. diagram (Fig. 13). On this basis these rocks appear to be transitional in character between calc-alkaline and tholeiitic. Their transitional nature is also suggested on the plot of total alkalis against silica (Fig. 10). Whether or not the northern outcrop series shows absolute iron enrichment cannot be established from the data available as all the sampled basalts were porphyritic. It seems likely, however, that fractionation of a southern outcrop-type basalt magma involving the extensive precipitation and removal of plagioclase and augite together with the removal of a small amount of olivine could yield the observed iron-rich

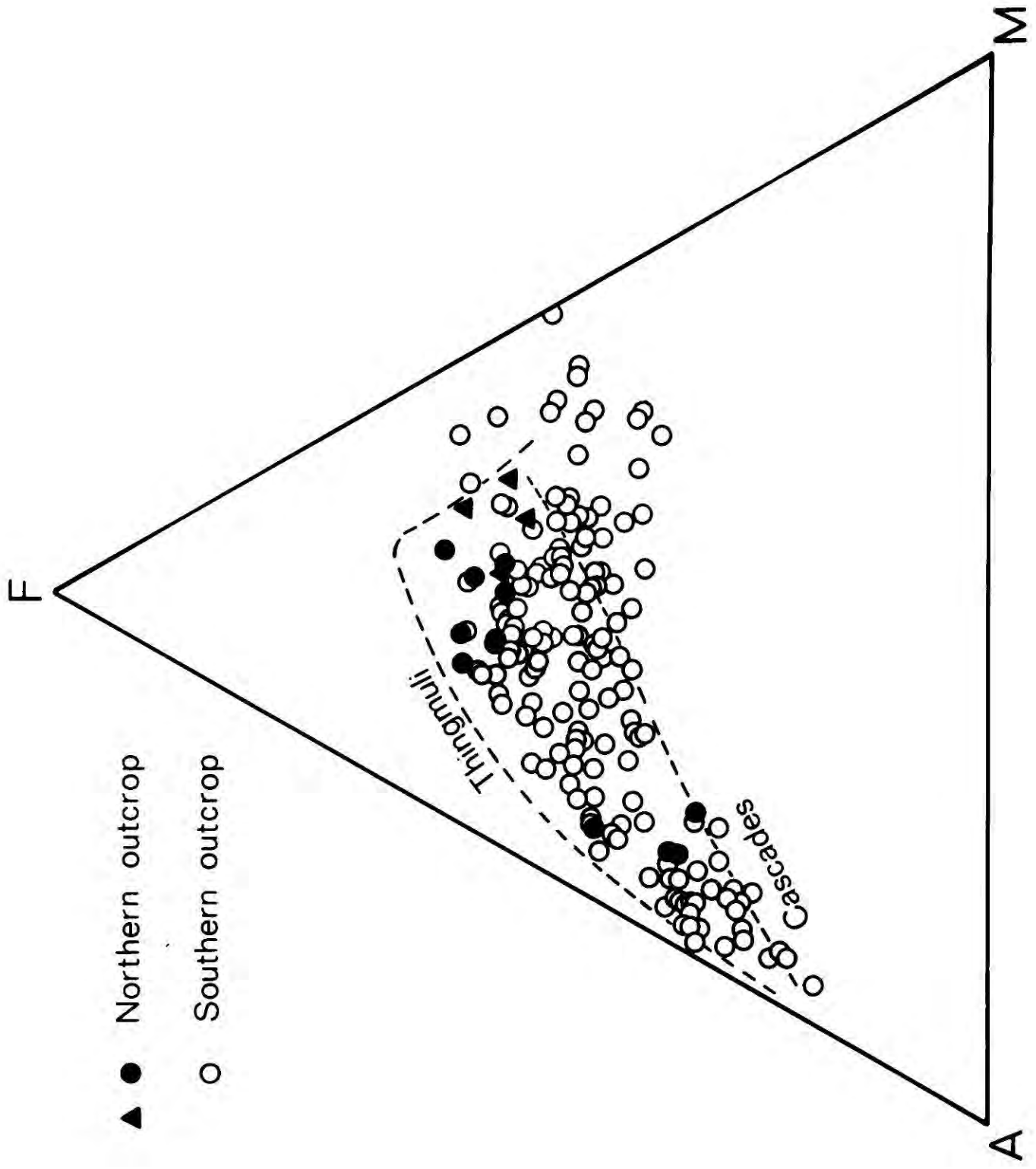
Fig. 13

---

A.F.M. (weight %) plot of analysed samples from the northern (solid symbols) and southern (open circles) outcrops. The solid circles represent aphyric lavas and acid rocks of the northern outcrop. Solid triangles represent groundmasses separated from Eycott type lavas.



Typical tholeiitic (Thingmuli) and calc-alkaline (Cascades) trends, both from Carmichael (1964), are included for comparison.



basaltic andesite liquids. Suppression of magnetite precipitation in the more basic liquids (as observed petrographically) would be essential for the process to operate efficiently. The greater enrichment in Ti and V relative to Fe in the basaltic andesite liquid can be accounted for by the presence of iron, and scarcity of the other two elements, in the pyroxenes. The appearance of magnetite as a phenocryst phase in the more silica-rich basaltic andesites is consistent with the rapid decline in Fe, Ti and V observed in the later differentiates (Figs. 10 and 11). Copper falls off exponentially with increasing silica suggesting that the separation of a sulphide phase is involved in the fractionation. The occurrence of minute blebs of chalcopyrite in some of the rocks supports this hypothesis.

The only objection to this model of crystal fractionation of a basaltic parent is the scarcity of basalts and apparent lack of the more basic basalts seen in the southern outcrop. This is best illustrated by comparing the Mg, Ni and Cr distributions of the two outcrops (Figs, 5, 6, 10 and 11). Rocks rich in these elements are lacking in the northern outcrop. Crystal fractionation has undoubtedly taken place in the northern outcrop liquids but the nature of the parent magma is obscure.

On the evidence of the rocks exposed at the surface a basaltic andesite magma would seem to be a more realistic parent. Large volumes of this magma, accompanied by small amounts of basaltic magma, may have been derived by the partial melting process envisaged for the magmas of the southern outcrop. Iron-enrichment may be an original feature of this magma but it is more likely the result of extensive crystal fractionation.

If crystal fractionation was responsible for the chemical variation in the northern outcrop magmas, what were the physico-chemical factors responsible for this fractionation and for the differences between rocks of the two outcrops? For crystal fractionation to take place a body of magma must be stored for long periods of time and allowed to cool. This condition is more likely to obtain in relatively dry magmas than in magmas with a high  $P_{H_2O}$ . In the latter case the drop in pressure as the liquid rises from its source region would lower the solubility of water in the magma (Hamilton et al., 1964) and lead to water saturation. The escape of excess water would favour explosive volcanism and reduce the efficiency of crystal fractionation in any but the most deep-seated magma chambers.

Such explosive eruption of water-rich magma is suggested by the rocks of the southern outcrop (eg. the abundance of pyroclastics and ignimbrites). However, there are several lines of evidence to suggest that the northern outcrop magmas were relatively dry. Pyroclastic rocks are much less abundant and the rare ignimbrites are accompanied by acid lavas - a feature not seen in the south. The extensive precipitation of plagioclase could suggest a dry magma since high  $P_{H_2O}$  tends to suppress plagioclase crystallisation in basic magmas (Yoder and Tilley, 1962). Finally, the absence of magnetite phenocrysts in the more basic rocks of northern outcrop suggests that the magma crystallised under conditions of lower  $f_{O_2}$  (and lower  $P_{H_2O}$ ) than the southern outcrop magmas (Osborn, 1959).

In Osborn's (1959) original model for the evolution of calc-alkaline magmas he distinguished two contrasted types of basaltic fractionation. In one, the total composition of the system remains constant, oxygen fugacity falls with falling temperature and the residual liquids are enriched in iron resulting in a tholeiitic fractionation sequence. In the other, water enters the system from an external source and maintains the  $f_{O_2}$  at a constant level as fractionation proceeds; iron-enrichment is prevented and a suite of

calc-alkaline liquids is produced. Carmichael and Nicholls (1967) have suggested that this concept could be stated in a more realistic way. They consider Osborn's (op. cit.) two fractionation types as extremes in a continuous series with the oxygen fugacity of the magma controlled by the crystalline phases (internally buffered) and the volatile component (externally buffered) respectively. Fractional crystallisation of a magma will result in the residual liquids becoming enriched in volatiles so that at some stage in the fractionation sequence the oxygen fugacity of an internally buffered system will cease to be controlled by the crystalline phases and instead be externally buffered by the volatiles. Carmichael and Nicholls (op. cit.) consider that the point in the fractionation sequence at which this 'crossover' stage is reached will be critical in establishing the character of the sequence. In a water-rich system this will occur early and, if fractionation occurs, the residual liquids will follow a calc-alkaline trend. In a dry system (eg. the Skaergaard intrusion), however, it will occur in the latest stages of crystallisation by which time a sequence of iron-enriched, tholeiitic liquids will have resulted.

In the magma sequence represented by the northern outcrop lavas the 'crossover' stage seems to have been reached at about 55% SiO<sub>2</sub>. Up to this point fractionation of plagioclase and pyroxene resulted in iron-enrichment in the residual liquids. The appearance of magnetite as a phenocryst phase then depleted the succeeding liquids in iron. The reversed zoning in a clinopyroxene phenocryst in sample LD 111 (with 57.2% SiO<sub>2</sub>) provides evidence for the operation of an external buffer during the crystallisation of these later liquids (cf. Carmichael, 1967; Carmichael and Nicholls, 1967).

On the basis of the petrochemistry the rocks of the northern outcrop may be regarded as transitional in character between calc-alkaline and tholeiitic. The development of mild iron-enrichment in the basaltic andesites together with the occurrence of pigeonite in the groundmasses of these rocks are typical tholeiitic characters (Kuno, 1968). Lavas of the tholeiitic suite commonly occur in association with calc-alkaline volcanics in modern island arcs. Where both magma types are represented in an island arc, the tholeiitic lavas always occur on the oceanward side of the arc (Kuno, 1966). It is tempting, therefore, to draw an analogy between the Borrowdale Volcanics and a modern island arc.

This analogy receives support from other lines of evidence. In a comparison between the tholeiitic volcanics of the South Sandwich Islands and the calc-alkaline volcanics of the Lesser Antilles, Baker (1968a) pointed to the predominance of basalts and scarcity of pyroclastics in the former relative to the latter. The eruption of intermediate and acid rocks in the Lesser Antilles arc is characterised by violently explosive activity whereas the basalts and basaltic andesites of the South Sandwich Islands seem to have been erupted much more quietly. The rocks of these two island arcs are comparable, in these features, with the Borrowdale volcanic rocks of the southern and northern outcrops respectively. The predominance of basaltic rocks over intermediate and acid members seems to be a general feature of the island arc tholeiitic suite (Jakeš and Gill, 1970).

The question remains whether the observed differences between the rocks of the two outcrops reflect a fundamental difference in magma type or whether they are simply the result of fractionation under different conditions of  $P_{H_2O}$ . To answer this one must look at the more subtle features of the geochemistry of the rocks.

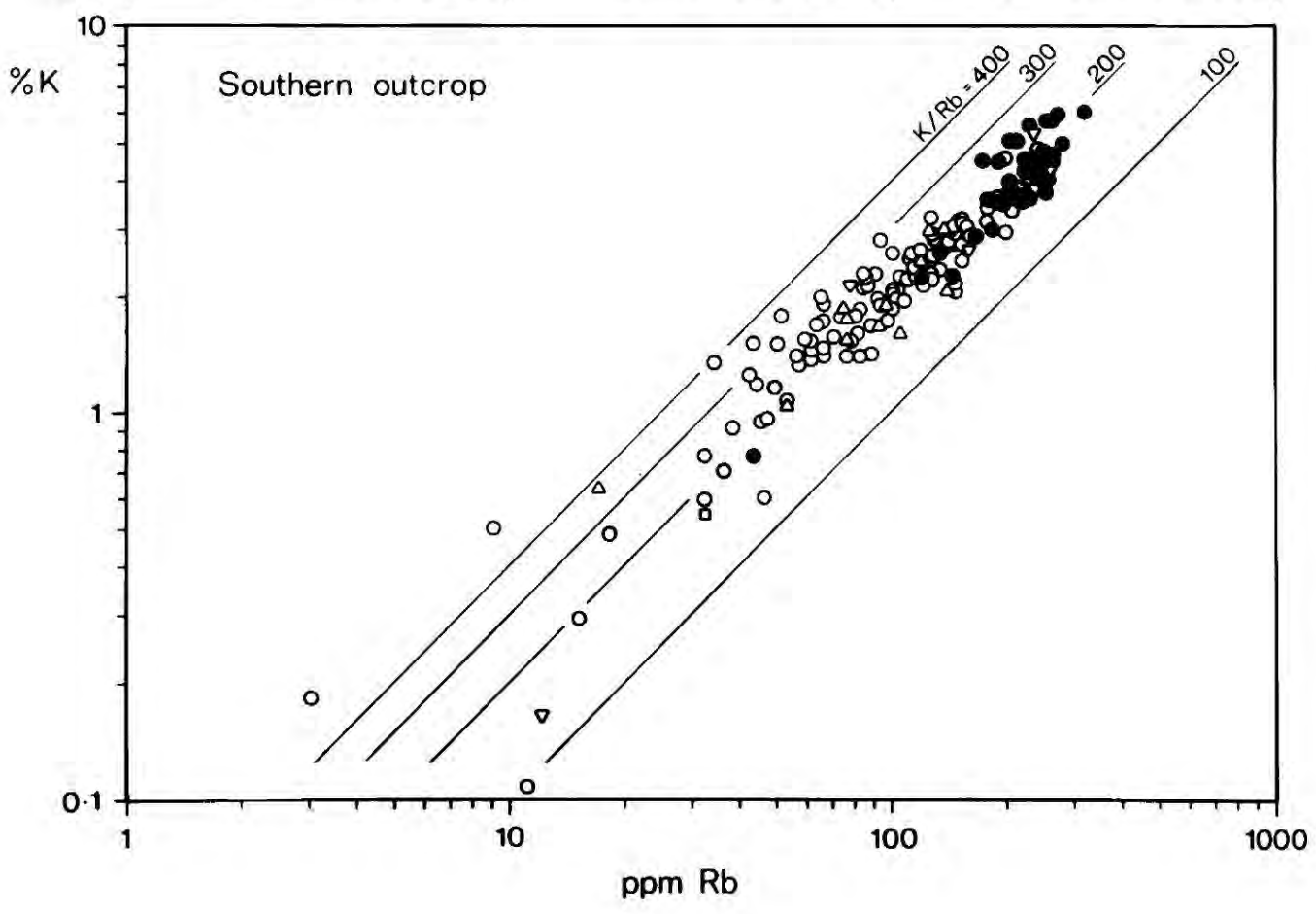
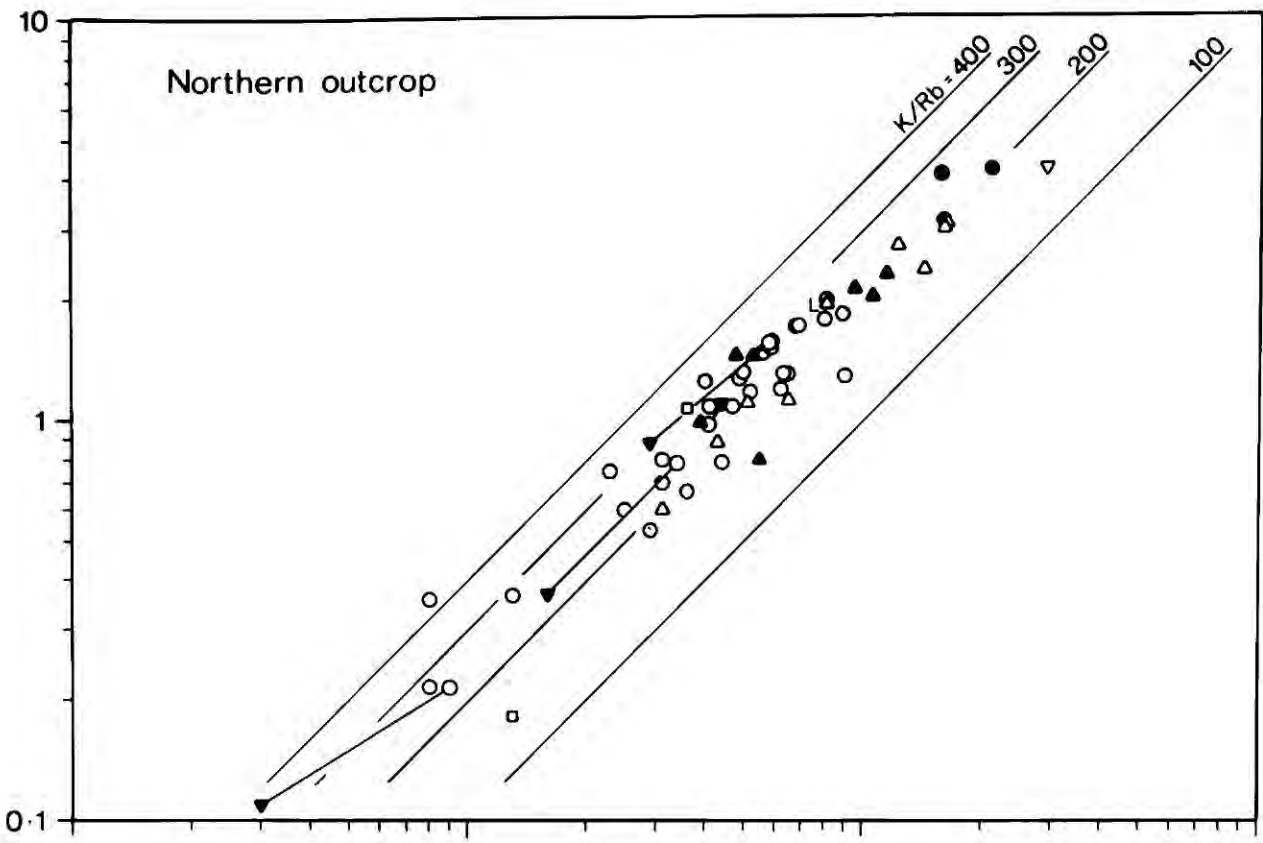
Jakeš and White (1970) have shown that the increase in the potassium content of lavas across island arcs in a direction away from the ocean, as demonstrated by Dickinson and Hatherton (1967) is accompanied by a decrease in the K/Rb ratios. Jakeš and White (op. cit.) ascribe these differences to differences in the phases undergoing partial melting at depth. In the Borrowdale Volcanics, however, the K/Rb ratios for the rocks of the two outcrops are not significantly different. Both groups of rocks give ratios of around 200, falling slightly with increasing potassium (Fig. 14). This ratio is very close to Shaw's (1968) 'main trend' for igneous rocks which has an average value of 230. The lack of a significant difference between the rocks of the two outcrops is not surprising in view of the small difference in potassium content.

Perhaps a more significant difference between island arc tholeiites and calc-alkaline rocks in general lies in the distribution of the rare-earth elements. Jakeš and Gill (1970), in a study of the rare-earth element abundances in rocks from a number of modern and ancient island arcs, have shown that the two magma types are characterised by different distribution patterns for these elements. Members of the island arc tholeiitic series have flat chondrite-normalised distribution patterns (as do oceanic tholeiites) whereas calc-alkaline rocks are always

Fig. 14

---

K - Rb relationships in rocks from the southern and northern outcrops.  
Symbols as in Figs. 5 and 10 respectively.



enriched in the light rare earths (La - Eu) relative to the heavy rare earths (Gd - Lu). Analytical limitations imposed by the available equipment made the determination of the heavy (and least abundant) rare earths impractical. These heavy rare earths, however, are chemically very similar to yttrium and, together with this element, form a geochemically coherent group known as the 'yttrium earths' (Goldschmidt, 1954, p. 310). It should be possible, therefore, to obtain a qualitative estimate of the relative shape of the chondrite-normalised rare earth distribution pattern from the La/Y ratio of the rocks. Both these elements can be determined precisely by X.R.F. techniques.

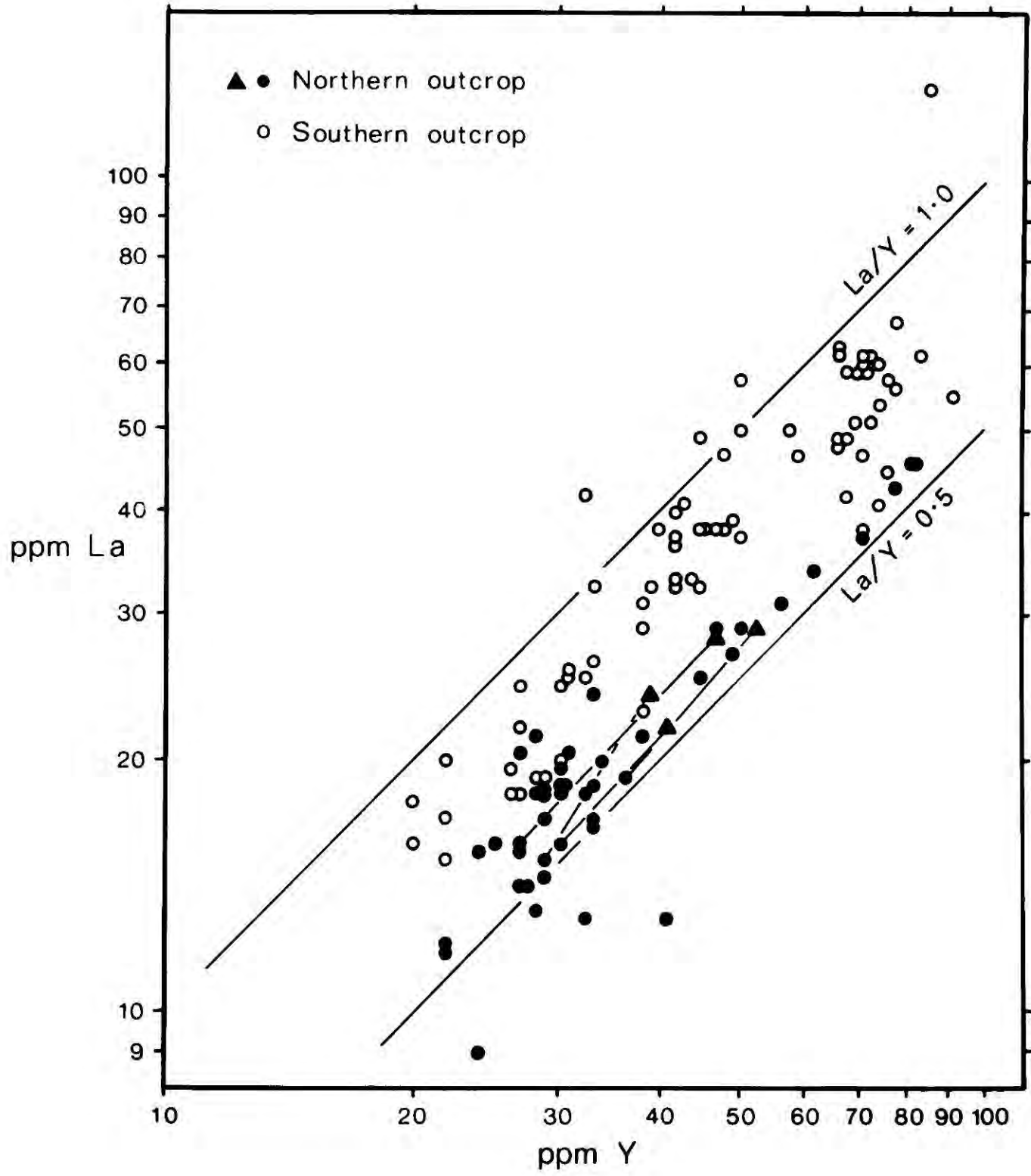
If the rocks from the northern outcrop are akin to the island arc tholeiites they should have lower La/Y ratios than the calc-alkaline rocks from the southern outcrop. Yttrium has been determined for all the rocks studied, and all the northern outcrop samples plus a representative selection of rocks from the southern outcrop were analysed for lanthanum. A logarithmic plot of La against Y (Fig. 15) shows that rocks from the northern and southern outcrops form two distinct, parallel trends with La/Y ratios of 0.55 and 0.78 respectively. This distinction applies throughout the range of rock types from basalts to rhyolites and is,

Fig. 15

---

Plot of lanthanum against yttrium for the volcanic rocks of the northern (solid symbols) and southern (open circles) outcrops.

The solid circles represent all the analysed samples (lavas and ignimbrites) from the northern outcrop. Solid triangles represent groundmasses separated from Eycott type lavas.



therefore, a fundamental character of the two magma suites and not the result of a crystal fractionation relationship between them. In comparison, La/Y ratios calculated from analytical data presented by Gill (1970) for volcanic rocks from Viti Levu, Fiji, have mean values of 0.14 for island arc tholeiites and 0.50 for calc-alkaline rocks.

It must be concluded that the Borrowdale Volcanics represent two distinct magma types and that they may have been erupted in an ancient island arc. The palaeogeographic implications of this island arc hypothesis will be discussed in Chapter 5. Little has been said so far concerning the genesis of the two magma types. The discussion of this problem will also be reserved for the concluding chapter.

#### (v) Intrusions

Like the southern outcrop, the northern part of the Lake District contains a number of intrusions which may be related to the volcanic rocks. The largest of these, the Carrock Fell Complex, forms an elongate intrusion (6km. long by 1.5km. wide) and, excepting the granites, is the largest intrusion in the Lake District. Many of the adjacent minor intrusions are associated with this complex. Of the remaining minor intrusions two groups are particularly prominent and will be discussed

here. These are the microdiorite and dolerite bodies of the Embleton area and the so-called 'picrite' of Great Cockup.

(a) Carrock Fell Complex

This intrusion has been the subject of many investigations since the classic study of Harker (1895). The most recent is the extensive work carried out by the I.G.S. and published in the Cocker-mouth Memoir (Eastwood et al. 1968). This memoir includes a detailed petrographic description of the complex by K. C. Dunham.

The complex is a composite intrusion largely composed of gabbro and granophyre. The gabbros are layered (Eastwood et al. op cit., Plate IV B) and range from melagabbro, rich in pyroxene, magnetite and ilmenite, to leucogabbro composed almost entirely of plagioclase. The granophyres are typically composed of a micrographic intergrowth of quartz and alkali feldspar enclosing small phenocrysts of sodic plagioclase and occasionally an iron-rich clinopyroxene. A third rock type is represented by the Harestones felsite. This intrusive body is important in establishing the age of the complex as it encloses a large, elongate mass of Caradocian Drygill Shales (Dean, 1963) measuring about 1km. in its longest dimension. The felsite is a devitrified glassy rock

containing small phenocrysts of perthitic alkali feldspar and quartz.

The age of the complex has not been established with any certainty. It intrudes the lower part of the northern Borrowdale Volcanics succession (Binsey Group) and contains blocks of Eycott type lava which probably came from the base of the High Ireby Group. Parts of the complex have been thermally metamorphosed by the intrusion of the nearby Skiddaw Granite of Lower Devonian age (Miller, 1962). If the Harestones felsite was intruded at the same time as the remainder of the complex then the age of the intrusion must be post-Caradocian and pre-Lower Devonian. However, Hollingworth (in Eastwood et al., 1968) suggests that the Harestones felsite may be genetically related to the Skiddaw granite and not to the remainder of the Carrock Fell Complex. He also suggests that the gabbro was intruded into its present position at a late stage in its crystallisation history, as a crystal mush. Consequently, if one can discount the evidence provided by the Harestones felsite, it is quite possible that the complex was genetically related to the northern Borrowdale Volcanics. This possibility was examined in the present study.

Ten samples (5 of gabbro, 4 of granophyre and 1 sample of Harestones felsite) were collected and their analyses are plotted in Figs. 10 and 11. In all the elements determined the granophyres are very similar to the acid

effusive rocks of the northern outcrop and are particularly similar to the sample of 'keratophyre' (LD 96) which they resemble petrographically. The chemical relationship between the gabbros and the basic lavas is more complex. It is tempting, however, to regard the layered gabbros as cumulates resulting from the crystal fractionation of the lava magmas. In particular the leucogabbro (CN-16, marked 'L' on Figs. 10 and 11) and the ilmenite-melagabbro (CN-7) would fit easily into the crystal fractionation scheme proposed for the northern outcrop lavas. The Harestones felsite analysis (LD 285, plotted with an inverted open triangle), which must approximate the composition of the liquid from which it crystallised, falls a long way off the liquid line of descent of the lavas and is clearly different from the granophyres. It is much more similar in chemical composition to the Lake District granite samples so far analysed by the writer (work in progress).

The Carrock Fell Complex is therefore similar, chemically, to the nearby lavas of the northern outcrop. The polarity of rock types in the complex (gabbro-granophyre) is reflected by a similar polarity in the lavas (basaltic andesite-rhyolite). The high titanium and vanadium contents in both the gabbros and the basic lavas and the close similarity between

the granophyres and the rhyolites could be purely coincidental but are more likely to reflect a genetic connection between the intrusion and the volcanics. On the results of this reconnaissance study, then, it is proposed that the Carrock Fell Complex may represent the remains of one of the magma chambers which supplied the northern Borrowdale Volcanics. The complex would certainly repay more detailed geochemical and mineralogical investigation.

(b) The Embleton Intrusions

Around the village of Embleton, east of Cockermouth, are a number of sill-like bodies of microdiorite intruded into the Skiddaw Slates. The intrusive rock is composed of crystals of plagioclase (andesine to oligoclase) with chlorite pseudomorphs, probably after orthopyroxene. Augite is present in some samples of the rock. Quartz and alkali feldspar are commonly present as an interstitial intergrowth with a micrographic texture. An opaque mineral, probably titanomagnetite, is typically abundant in the rock as large skeletal crystals.

Two samples of the rock were collected for analysis from one of the intrusions at Close Quarry. One (LD 266) was taken from the centre of the intrusion and the other (LD 267) from the chilled margin. Analyses of these samples are plotted on the variation diagrams (Figs. 10 and 11)

as open squares; the more basic of the two is the analysis of the chilled margin. Both samples fall on or close to the liquid line of descent of the northern outcrop volcanic rocks for all the elements plotted. The high iron, titanium and vanadium contents of the two samples is particularly noteworthy. On the basis of the chemistry of these two samples it is possible that the Embleton intrusions are related to the northern Borrowdale Volcanics. Unlike the cumulates of Carrock Fell, however, these intrusive rocks represent chilled liquids.

(c) Great Cockup 'Picrite'

This intrusion is one of three small sill-like bodies outcropping in the fells to the east of Bassenthwaite. They are composed of an ultramafic rock classed by Bonney (1885) as picrite. The rock is a hornblende-rich cumulate containing interstitial aggregates of plagioclase. The hornblende forms large (up to 1cm.) crystals which sometimes enclose pseudomorphs after olivine and orthopyroxene. Detailed petrographic descriptions of these intrusions have been given by Plemister. (in Eastwood et al., 1968).

From its appearance in thin section the hornblende in these rocks seems to be primary. It is therefore unlikely that the rocks are related to the Borrowdale volcanics because primary hornblende phenocrysts are

never seen in the latter. Dunham (in Eastwood et al., op cit.) classes the rocks with the spessartites and considers them to form a consanguineous group with the Embleton intrusions and the lamprophyres in the area. If this is so then the rocks of this group are probably genetically allied to the Lake District granites and not to the volcanic rocks. Whether or not the Embleton intrusions should be placed in this group is, as shown above, debatable.

An analysis of a sample from the Great Cockup intrusion (LD 72) is listed in the Appendix although this analysis has not been plotted on the variation diagrams.

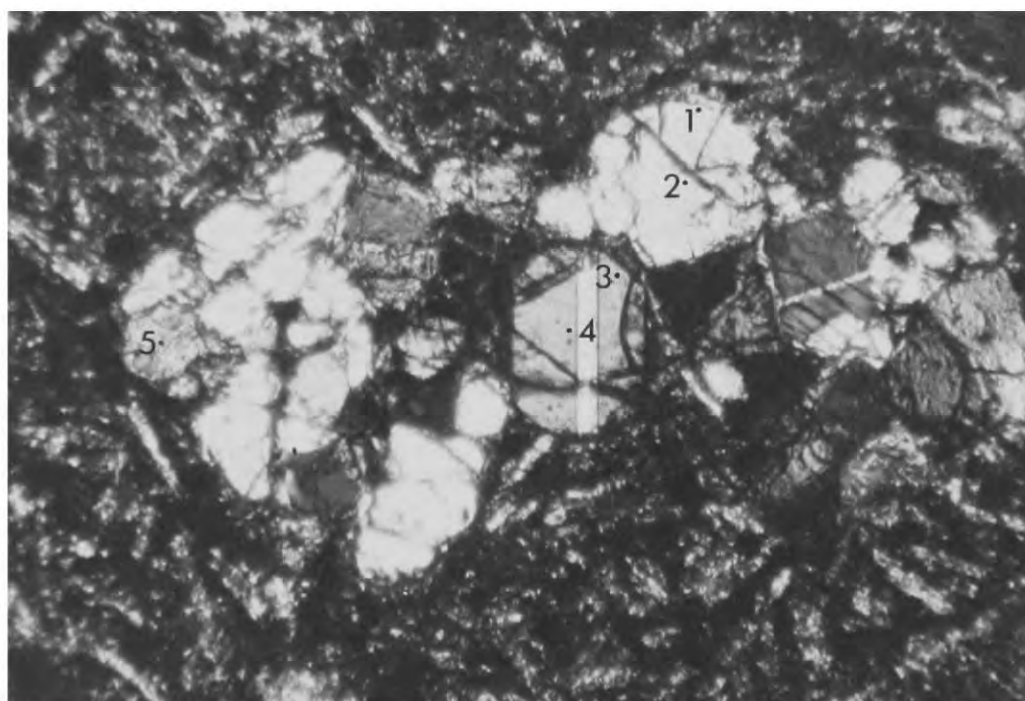


Plate 10 Cluster of augite phenocrysts in basalt (LD 115)  
Crossed polars, x 73

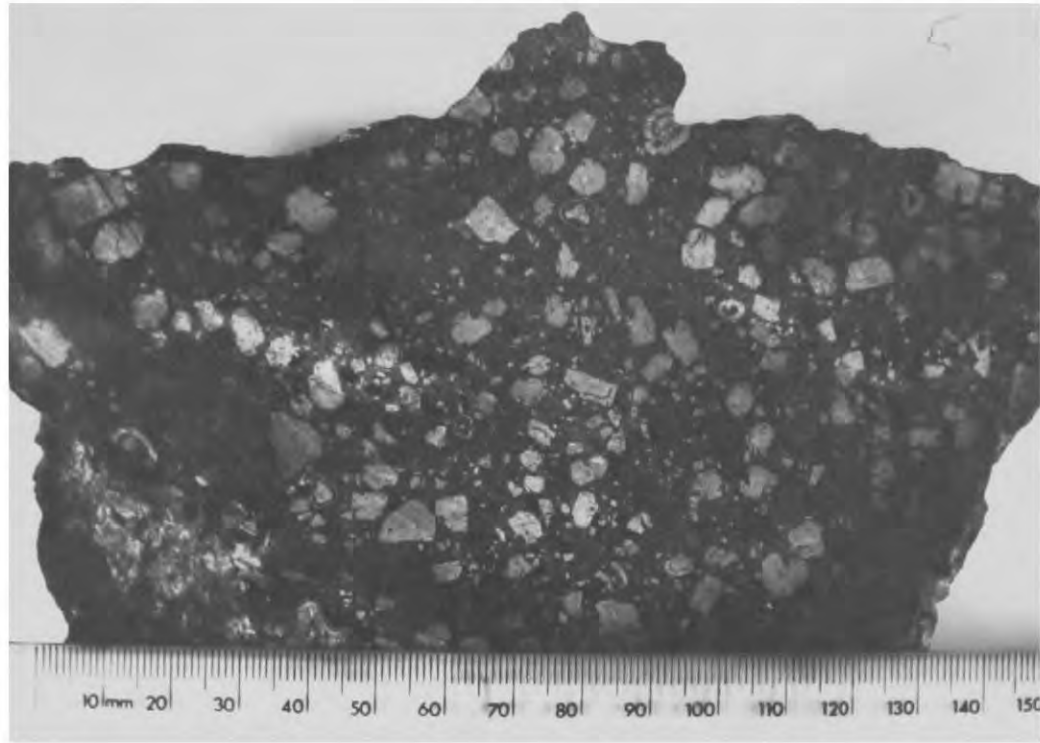


Plate 11 Polished slab of Eycott type basaltic andesite (LD 73A)  
The surface has been etched with hydrofluoric acid to  
accentuate the plagioclase phenocrysts

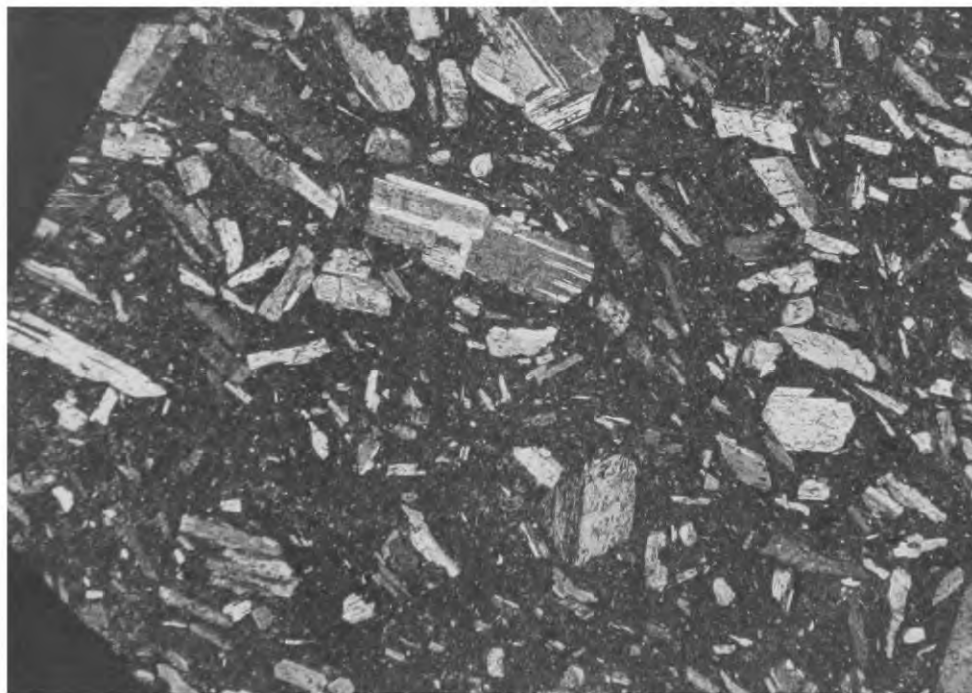


Plate 12 Berrier type basaltic andesite (LD 85). In this sample the  
phenocrysts are almost exclusively of plagioclase.  
Crossed polars, x 4.4

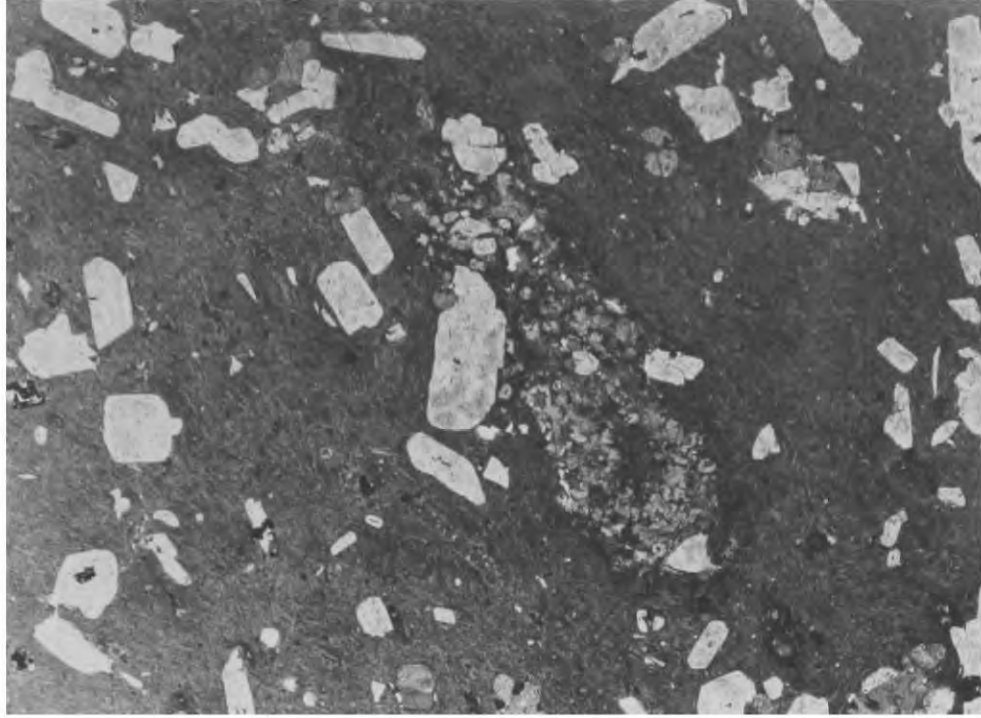


Plate 13 Ignimbrite (LD 102) with rounded phenocrysts of albite  
Plane polarised light, x 11



Plate 14 'Keratophyre' (LD 96) with phenocrysts of albite  
Crossed polars, x 15

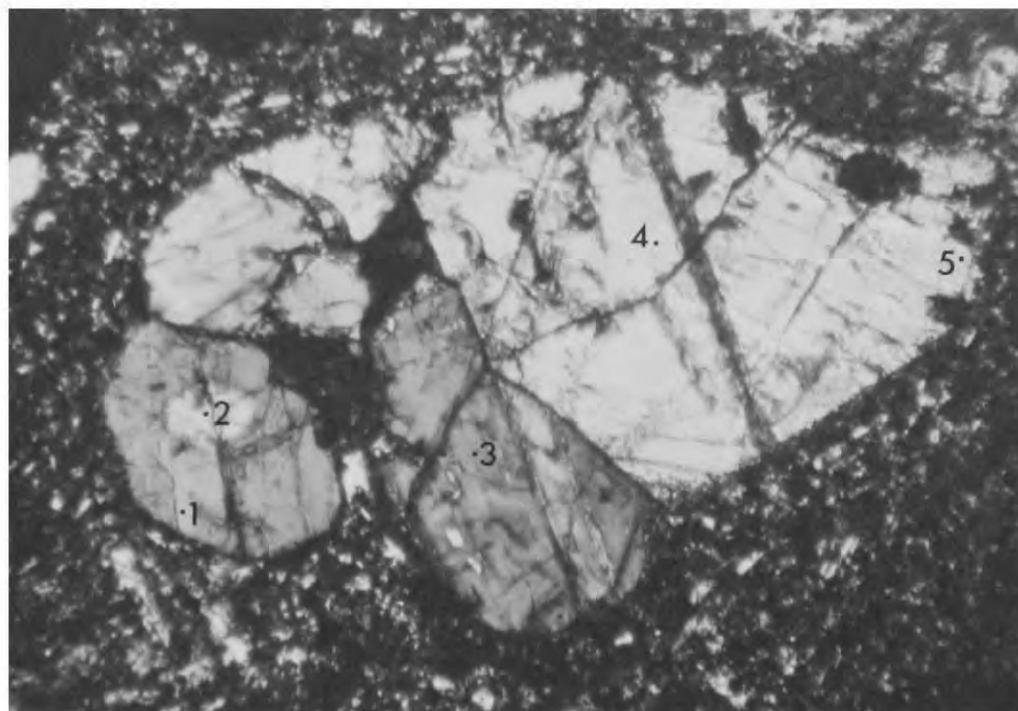


Plate 15 Augite phenocrysts in basaltic andesite (LD 86)  
Crossed polars, x 73

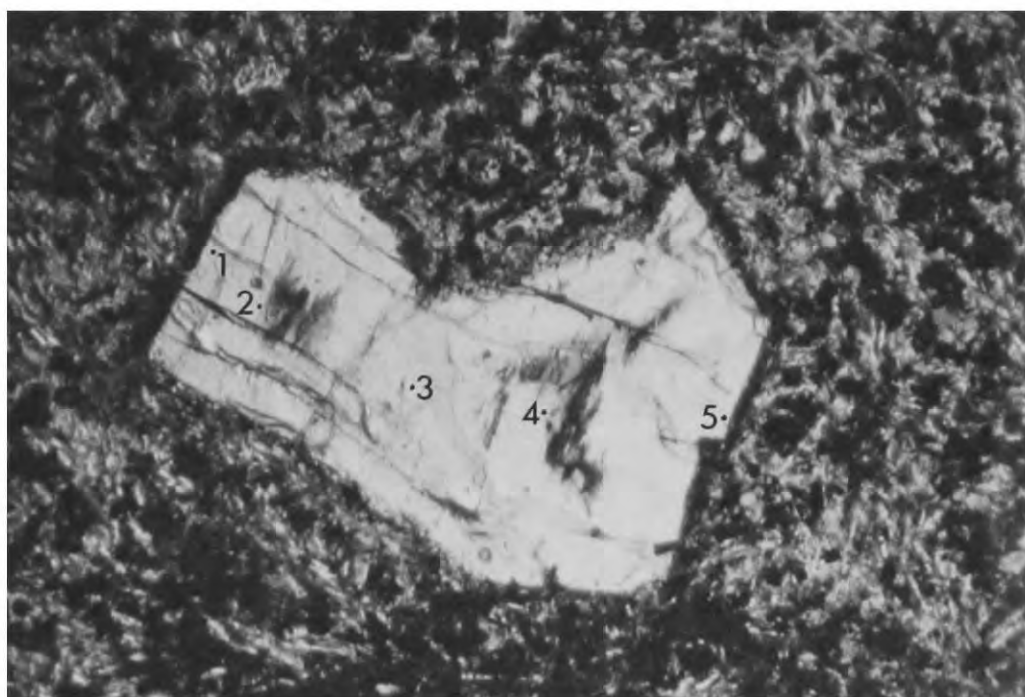


Plate 16 Augite phenocryst in basaltic andesite (LD 111)  
Plane polarised light, x 73  
Note exsolution of an opaque mineral in core of crystal.

GARNETS(i) Introduction

In general, garnets occur very rarely in igneous rocks and so their abundance in the Borrowdale Volcanics deserves special attention. Their presence in these rocks has been noted since the earliest days of geological research in the Lake District. A review of previous work on the garnets and of the diverse opinions on their origin has been given by Oliver (1956). In the present study an attempt was made to assess the distribution and compositional range of the garnets and to establish their mode of origin and petrogenetic significance. The study is therefore an extension of the investigation carried out by Oliver (op. cit.).

(ii) Distribution

The apparent restriction of garnets to the rocks of the southern outcrop has been noted in the previous chapter. Within the volcanic succession of this outcrop, garnetiferous rocks are largely restricted to units below the horizon of the Wrengill Andesites (see Fig. 3). Garnets are abundant in the Airy's Bridge Group and its lateral equivalents and it was from this group that most of the samples used in Oliver's (op. cit.) study were obtained. Garnetiferous horizons are also found in the underlying andesites, and Moseley (1960) cites several occurrences of

garnet-rich andesite flows in the Ullswater Group.

In the upper units of the succession garnets are extremely rare. Garnet fragments are sometimes seen in the tuffs of the Lincomb Tarns Formation in the Scafell area (Oliver, 1961) and a single garnet crystal (G-302) has been found by the writer in the Wrengill Andesite near Ambleside. The mineral has not been recorded from any of the other andesite or dacite units in the upper part of the succession.

In addition to this stratigraphic restriction garnets are also restricted to certain rock types. They are abundant in andesites and dacites and are sometimes seen in rhyolites but have never been recorded from the more basic rocks. Moseley (1960) has described garnet-bearing 'basalts' from Ullswater but analyses of these rocks show them to be andesites. Garnet occurs sporadically in the andesites and dacites of the lower part of the succession. In some units it is apparently absent although in others it becomes very abundant (Plate 17).

Garnets are not confined to the extrusive rocks of the Lake District. Many of the associated minor intrusions contain garnet as do some of the larger intrusions (e.g. the Haweswater complex; Hancox, 1934). They also occur in some of the granites (e.g. St. John's and Threlkeld microgranites)

and in their associated dykes (e.g. Armboth dyke). Hadfield and Whiteside (1936), however, consider the garnets in the St. John's and Threlkeld intrusions to be xenocrysts derived from the Borrowdale Volcanics. The Armboth dyke may also have acquired its garnets in this way.

(iii) Petrography

In the andesites of the southern outcrop garnet appears to replace augite as a phenocryst phase. Augite phenocrysts are usually present in the basaltic andesites and their disappearance in the more silicic rocks is followed closely by the appearance of garnet. None of the rocks examined in the present study contain both phenocryst phases and so there is no evidence of any reaction relationship between them.

The garnets vary a great deal in size. The largest crystal observed in the present study (G-302, Plate 23) is almost a centimetre in diameter although such large crystals are rare. Most of the garnets are between one and two millimetres in diameter.

The garnet phenocrysts in the andesites invariably show some signs of resorption. This varies from a rounding of the crystal outline (e.g. Plate 20) to almost complete breakdown, leaving only a few small detached fragments (e.g. Plate 18 B). In some samples, circular patches of break-

down products suggest the original presence of garnet which is now totally resorbed.

The breakdown products of garnets in the andesites comprise fine aggregates of a pale green, chlorite-like material, sometimes accompanied by the separation of magnetite grains. They often form a corona around a core of unaltered garnet (Plate 21 A). The andesite garnets are usually traversed by a network of cracks which facilitate breakdown and resorption. Not all partially resorbed garnets are accompanied by breakdown products, however. In many cases the garnets appear to have been dissolving in the magma before it solidified and possess only a narrow reaction rim (e.g. Plates 19 and 23).

Many of the andesite tuffs and coarser pyroclastic rocks of the southern outcrop contain garnets. In these rocks the garnets are usually present as crystal fragments.

The dacitic and rhyolitic ignimbrites of the southern outcrop also contain garnets. These are seldom resorbed to the same extent as those from the andesites and frequently possess sharp crystal outlines (e.g. Plates 24 and 28). Unlike the andesite garnets they are relatively free from cracks. Where these garnets do show resorption they are often

surrounded by clusters of plagioclase crystals (Oliver, 1956). In these cases it appears that the resorbed garnet has tended to nucleate the plagioclase.

Many of the ignimbrites possess a prominent flow-banded texture resulting from the alignment of glass shards. These flow-lines are often seen to swirl around any garnets present in the rock, as in Plate 24. This feature, together with the common occurrence of definite crystal fragments of garnet in the ignimbrites (Plate 26), provides strong evidence that the garnets crystallised from the magma before it solidified (Oliver, 1956).

The garnets in both the andesites and the dacites frequently contain inclusions. Titanomagnetite crystals and minute spherical blebs of a sulphide phase (probably pyrite) are the most abundant inclusions in the andesite garnets. In the dacite garnets, apatite needles and tiny euhedral crystals of zircon are frequently seen and are occasionally abundant as in G-317 (Plate 28). Magnetite inclusions sometimes occur in these garnets though apatite and zircon inclusions are only rarely seen in the andesite garnets.

(iv) Composition

Garnets from 14 samples were analysed for major elements using the electron microprobe. Of these, 11 were prepared as polished thin sections so that zoning and variation between individual phenocrysts could be assessed. The samples prepared in this way comprised 6 andesites, 4 dacitic ignimbrites and a sample of garnetiferous ignimbrite from Snowdonia in North Wales. The use of polished thin sections for the other three samples was impracticable on account of the scarcity of garnet in them. Consequently the garnet was separated from crushed rock samples with bromoform and mounted in plastic as grain-mounts. The rocks treated in this way comprised a sample of silicic tuff from the Lincomb Tarns Formation (LD 21) and representative samples of the Threlkeld microgranite (LD 204) and Armbboth dyke (LD 277). In all, 69 analyses were obtained from these 14 rocks, each representing the average of at least six probe analyses per analysed point. The location of these analyses are indicated on the photomicrographs presented in Plates 18 - 28. The three analyses obtained from grain mounts represent average analyses of several grains and no significant variation between the grains in each mount was found. All the individual analyses are listed in the Appendix.

The analyses were recalculated into end-member molecules according to the scheme proposed by Rickwood (1968) and the three major components (almandine, pyrope, and spessartine) plotted on a ternary diagram (Fig. 16). The garnets are all almandine-rich and their analyses plot along a clearly defined trend. Garnets from the dacites (solid symbols in Fig. 16) are consistently richer in almandine and spessartine than are those from the andesites (open symbols). The grossular component varies irregularly from about 3 to almost 9 molecular per cent although it is generally lower in the dacite garnets (average c. 3.5%) than in those from the andesites (average c. 4.6%).

The garnets from the Welsh ignimbrite (G-316, Fig. 16) are clearly different, compositionally, from the Lake District garnets. They are essentially of almandine-spessartine composition with only minor amounts of pyrope and grossular. Surprisingly, the garnets from the Threlkeld microgranite and the Armbboth dyke are quite different in composition from each other; the former plots with the andesite garnets while the latter plots with the dacite garnets.

No significant differences in composition were found between phenocrysts in the same polished section where more than one phenocryst was

Fig. 16

Compositional variation in garnets from the Borrowdale Volcanics  
(southern outcrop) and other rocks.

**Borrowdale Volcanics:-**

**Andesites**

○ LD 174

◇ LD 176

□ LD 220

△ LD 274

▽ LD 306

△ LD 302

**Dacites**

▲ LD 65

■ LD 175

▼ LD 249

● LD 317

Tuff from Lincomb Tarns Form<sup>n</sup>.

◆ LD 21

**Threlkeld microgranite:-**

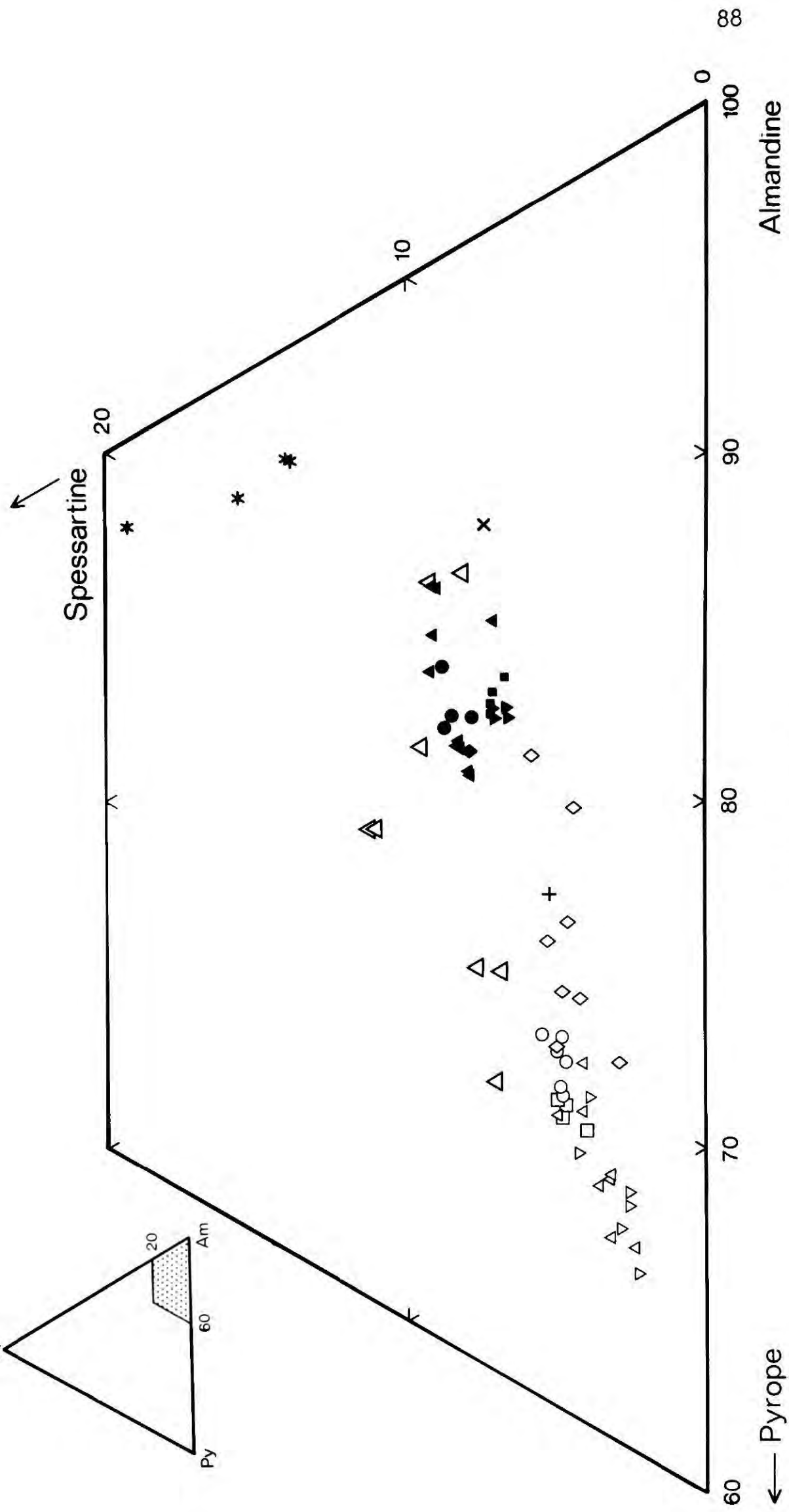
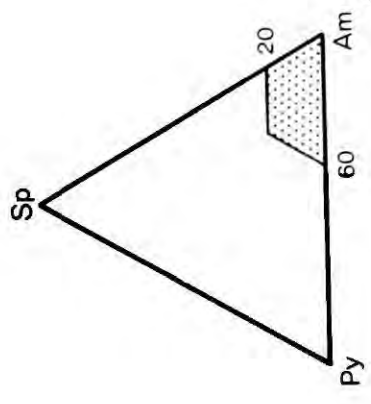
+ LD 204

**Armboth dyke:-**

X LD 277

**Ignimbrite from Snowdonia, North Wales:-**

\* 316



Molecular %

88

100

90

80

70

60

← Pyrope

Almandine

Spessartine

20

10

20

Am

60

Py

Sp

analysed (G-174, G-176, G-274 and G-306). Of the ten Lake District garnets analysed in polished section, five (G-176, G-274, G-302, G-306 and G-317) show significant compositional zoning and in all five this zoning is in the reverse direction with the crystal becoming progressively enriched in the pyrope component towards the margin. In these garnets the spessartine content generally varies sympathetically with almandine (i.e. decreases towards the margin) although in one example (G-317) it varies in an oscillatory fashion. This reversed zoning is seen in garnets from both the andesites and the dacites. The Welsh garnet (G-316) is also zoned with a progressive decline in spessartine content away from the centre.

Green and Ringwood (1968a) have analysed a number of garnet phenocrysts in silicic calc-alkaline volcanic rocks from Victoria. These are "quite uniform in composition except for a marginal zone 10 - 40  $\mu$  wide which is slightly richer in almandine-spessartine and poorer in pyrope than the rest of the crystal." This tendency towards normal zoning was looked for in a large zoned garnet (G-317) with well-developed crystal faces. The pyrope content of this garnet, however, continues to increase to within a few microns of the margin and no sign of normal zoning could

be found. In other respects the Australian garnets are similar in composition to those from the Lake District.

One of the Lake District garnets (G-302) shows very well developed compositional zoning and is worthy of special mention. This garnet was found in the Wrengill Andesite and is, therefore, from the highest garnet-bearing lava flow in the succession. It is also the largest garnet recorded from the Borrowdale Volcanics (c. 1 cm in diameter) although some of the Australian garnets described by Green and Ringwood (1968a) reach a size of 2 cm. The crystal is relatively free from inclusions except in the centre where a core, 2mm in diameter, contains numerous tiny apatite needles and a few small crystals of zircon. This core is just discernible in the photomicrograph (Plate 23).

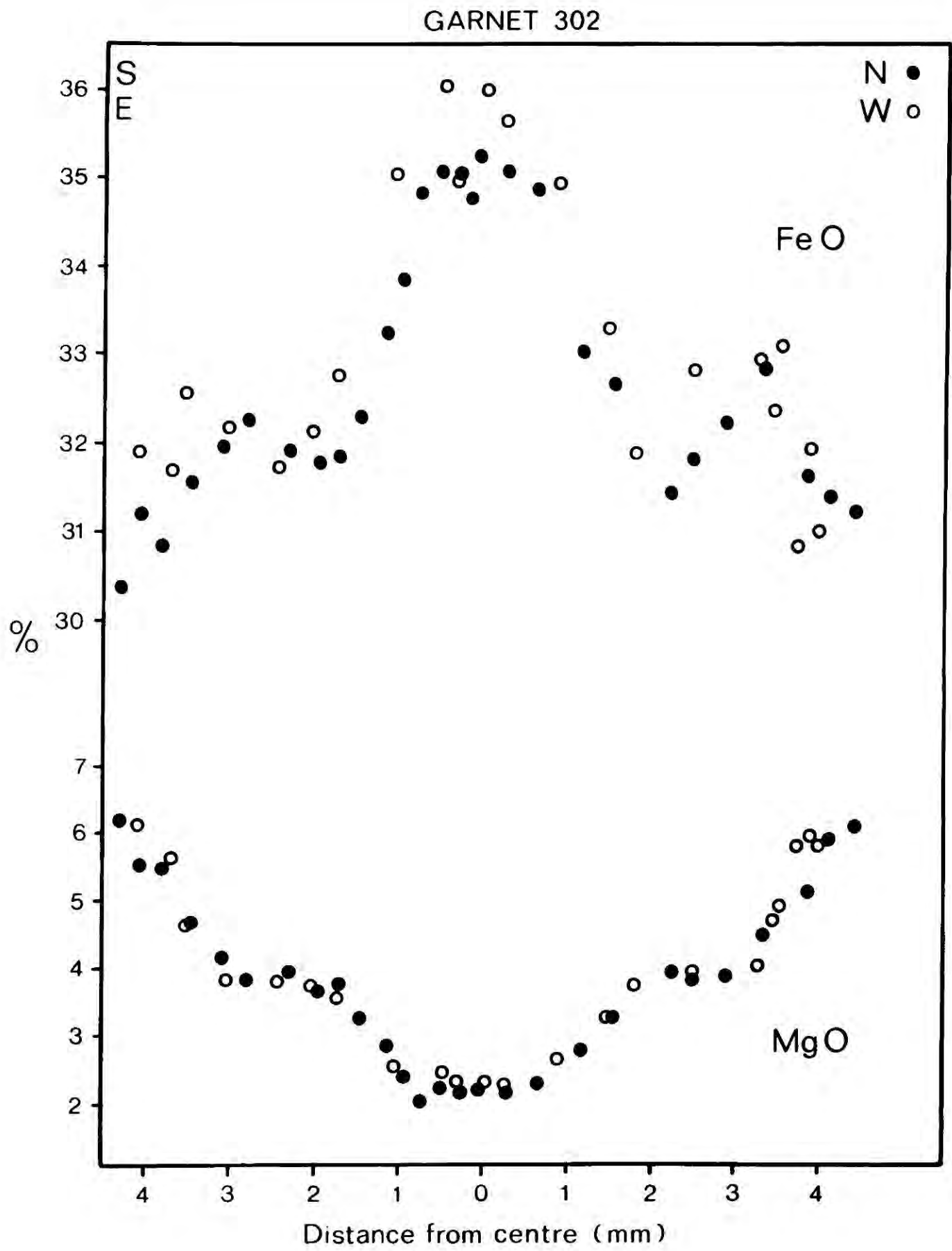
Electron microprobe analyses made at several points across the crystal (Plate 23) are plotted in Fig. 16 as large open triangles. The garnet is seen to be richer in the spessartine molecule than the other Lake District garnets but, more significantly, the analyses from the core of the crystal plot with the dacite garnets whilst those nearer the margin plot close to the field of andesite garnets.

To examine the zoning in more detail, a large number of closely spaced points were analysed for iron and magnesium in two traverses running north-south and east-west across the crystal as seen in Plate 23. The data from these two traverses are plotted against distance from the crystal centre in Fig. 17 as solid and open circles respectively. The radial symmetry of the reversed zoning is indicated by the similarity of the two traverses. Also noteworthy is the sharp break between the iron-rich core and the more magnesian outer zone. The abundance of apatite and zircon inclusions in the core of G-302 and the compositional similarity between this core and the dacite garnets suggests that the crystal was initially derived, in some way, from a dacite and later overgrown with andesite-type garnet. The significance of this will be discussed later.

In order to determine the abundance of trace elements in the garnets, the mineral was separated from seven rock samples (5 andesites and 2 dacites). Using standard magnetic and heavy liquid techniques it was possible to separate the garnets to a high degree of purity (>99%). The only visible impurity was a small amount of chlorite adhering to some of the grains. In the dacite garnets, the presence of zircon

Fig. 17

North-south (solid circles) and east-west (open circles) electron microprobe traverses for Fe and Mg across garnet crystal G-302. The locations of the traverses are indicated on Plate 23.



inclusions initially presented a problem. Repeated centrifuging of the finely ground garnet with Clerici's solution, however, removed all visible traces of zircon. The separated garnet was finally washed in hot distilled water to remove Clerici's solution, digested in hot hydrochloric acid for several minutes to dissolve any remaining traces of apatite and then washed in distilled water once more and dried. Small quantities of the garnet separates (1 gram) were then ground to a fine powder in an agate mortar, pressed into boric acid-backed briquettes and analysed by x-ray fluorescence techniques.

The concentrations of Y, La, Sc, V and Cr in the seven garnet samples are listed in Table 2 together with averages of the probe analyses (listed in the Appendix) for the major elements. Other elements (Ba, Nb, Sr, Rb and Ni) were looked for but not found. The most notable feature of these analyses is the abundance of Sc and Y which was first noted by Oliver (1956). The scandium content of the host rocks could not be determined reliably because of calcium-scandium interference effects although a number of approximate determinations were made. These suggest that, for the southern outcrop rocks, the scandium content falls steadily with increasing silica from about 45 p.p.m. in the basalts to a value below the detection limit (c. 10 p.p.m.) in the dacites and

TABLE 2. AVERAGE GARNET ANALYSES

ROCK TYPE	G-174 A	G-176 A	G-220 A	G-274 A	G-306 A	G-175 D	G-249 D
PERCENT							
SiO <sub>2</sub>	38.26	38.18	38.62	38.46	38.74	36.97	37.62
Al <sub>2</sub> O <sub>3</sub>	21.17	21.79	21.07	20.99	22.27	21.44	21.74
FeO	32.65	32.29	31.78	31.49	31.20	34.80	35.46
MnO	2.08	1.95	1.94	1.51	1.35	2.97	2.92
MgO	6.01	5.24	6.36	6.80	7.37	3.22	3.42
CaO	1.57	2.16	1.58	1.61	1.65	1.26	1.31
TOTAL	102.74	101.61	101.35	100.86	102.58	100.66	102.47
MOL. PERCENT							
ALMANDINE	66.88	69.15	65.58	64.57	64.12	76.58	76.15
PYROPE	23.92	20.44	25.47	27.33	28.36	12.98	13.53
SPESSARTINE	4.71	4.34	4.40	3.45	2.95	6.80	6.58
GROSSULAR	4.49	6.07	4.55	4.65	4.57	3.64	3.74
PPM							
Y	730	375	742	350	378	1723	1715
LA	1	14	5	11	15	32	44
SC	145	105	155	100	110	660	655
V	209	233	202	227	228	16	12
CR	210	207	199	209	206	0	5

A = ANDESITE  
D = DACITE

rhyolites. These values are comparable with those determined by Oliver (1961) for the Borrowdale volcanic rocks in the Scafell area and also with those for other calc-alkaline regions (Norman and Haskin, 1968; Baker, 1968b, Taylor et al. 1968a, b). It is surprising, therefore, that the scandium contents of the dacite garnets (c. 660 p.p.m.) are more than four times as high as those of the andesite garnets (100 - 155 p.p.m.). Manganese behaves in a similar fashion, being enriched in garnets from the dacites relative to those from the andesites although the andesites themselves contain more manganese than do the dacites. Almandine-spessartine garnets containing about 3600 p.p.m. of scandium have been reported by Frondel (1970) from a rhyolite containing only 4 p.p.m. of the element. These, however, are of hydrothermal origin and are not strictly comparable with the Lake District garnets.

The geochemistry of scandium is complex and it seems to obey no simple direct substitution laws for any single major element (Norman and Haskin, 1970). It is possible, therefore, that the behaviour of scandium in the garnets is governed more by their physical conditions of formation than by their crystal chemistry. This will be discussed later.

Of the other trace elements determined, yttrium, vanadium and chromium all enter the garnet lattice freely and may show complete substitution for the more common elements (Rickwood, 1968). These trace elements are all enriched in the garnets relative to their host rocks; yttrium being particularly noteworthy in this respect. The calculation of phenocryst/matrix partition coefficients for these garnets is complicated by the fact that their host rocks are all particularly garnet-rich (chosen to facilitate separation) and are almost certainly cumulative. Estimates of these partition coefficients can best be made by ratioing the average contents for the andesite and dacite garnets to the average values for all the andesite and dacite rocks (from Table 1, Chapter 2), many of the rocks being garnet-free. This procedure is still far from ideal but is adequate for the present purposes. Calculated in this way, the partition coefficients for yttrium for the garnets from the andesites and dacites are 13 and 26 respectively. Unlike yttrium, lanthanum is depleted in the garnets relative to their host rocks. For this element the corresponding partition coefficients are 0.26 and 0.70. The figures for the dacite garnets compare well with rare-earth partition coefficients determined by Schnetzler and Philpotts (1970) for garnets in a Japanese dacite. As

with the Lake District garnets, the Japanese garnets are strongly enriched in the heavy rare earths and depleted in the light rare earths relative to their host rocks.

Since small amounts of zircon impurities could seriously affect the apparent rare-earth contents of the garnets it was important to obviate this possibility. To test the efficiency of the separation techniques employed, the garnet samples were all analysed for zirconium. The largest concentration found was 225 p.p.m. (G-249) which sets the maximum possible zircon contamination at 0.045% since some of the zirconium may be present in the garnet itself. If the rare-earth data presented by Nagasawa (1970) for zircons from two Japanese dacites may be taken as typical then the effects of such small amounts of zircon contamination should have a negligible effect on the apparent rare-earth content of the garnets.

(v) Origin

So far it has been assumed that the garnets are primary phenocrysts which crystallised from the magma. This view was held long ago by Sorby (1880) who considered garnet to be an original constituent of the Lake District tuffs. Many later workers in the Lake District, however, have

argued strongly against such an origin and three alternative hypotheses have been proposed. These are:-

1. The garnets are metamorphic (e.g. K. C. Dunham, in discussion of Oliver, 1961).
2. The garnets were formed at a late stage in the formation of the volcanic pile as a result of solfataric activity and are therefore of metasomatic or hydrothermal origin (Green, 1915).
3. The garnets are xenocrysts derived from a hypothetical metamorphic basement (Firman, 1956).

Outside the thermal aureoles of the major intrusions the rocks of the Lake District appear to have suffered only the slightest of metamorphic effects. Consequently an in situ metamorphic origin for the garnets is unlikely. Moreover, there is abundant evidence to suggest that the garnets were present in the magma prior to eruption. The occurrence of detached crystal fragments in the tuffs and ignimbrites (e.g. Plate 26), the occasional development of flow-lines around the crystals (e.g. Plate 24) and the partially resorbed nature of some of the garnets

(e.g. Plates 19 and 23) may all be cited in this respect. Oliver (1956) has used similar lines of evidence in support of a magmatic origin for the garnets.

The same evidence can be used to argue against a metasomatic or hydrothermal origin although an analogy between the dacite garnets and the hydrothermal, scandium-rich garnets described by Frondel (1970) may be drawn. This analogy, however, is only superficial. Miyashiro (1955) has emphasised the difference between garnet phenocrysts and those, probably hydrothermal, garnets occurring in cavities in lavas. The former are poorer in manganese than the latter and are compositionally similar to the Lake District garnets (Miyashiro, op. cit. Fig. 1).

The only non-magmatic origin consistent with the petrographic evidence is that the garnets are xenocrysts (Firman, 1956). If the garnets were derived from a metamorphic basement, however, it is hard to see why they are confined entirely to certain rock types. Also, one would expect the large number of garnet 'xenocrysts' observed to be accompanied occasionally by fragments of this hypothetical metamorphic basement. No such metamorphic xenoliths, however, have been reported from the Borrowdale Volcanics. Many of the garnets in the dacites are perfectly euhedral with

well developed crystal faces (Plate 29). It is impossible to reconcile this fact with the harsh physical removal of these garnets from a host metamorphic rock as proposed by Pirman (1956). Perhaps the most convincing evidence against a xenocrystal origin, however, is provided by the composition of the garnets themselves. With the exception of G-302, the garnets from the andesites and the dacites fall into two completely separate groups (Fig. 16). If the garnets were foreign to the magma there should not be any correlation between their composition and that of the host rock. This evidence also militates against an origin of the garnets involving the metamorphism or metasomatism of the volcanic pile.

All this evidence supports Oliver's conclusion (1956) that the garnets crystallised from the magma as phenocrysts. Further support has recently been provided by the experimental work of Green and Ringwood (1968a, b) which showed that garnet is a liquidus - or near-liquidus phase in rocks of andesitic and dacitic composition at the pressures expected to obtain in the upper mantle and lower crust.

The difference in composition between the analysed garnets in the Threlkeld microgranite and the Armbboth dyke are surprising in view of the

similarity in composition of their respective host rocks (Hadfield and Whiteside, 1936; see also analyses in Appendix). This may be taken as evidence that these garnets were derived from the Borrowdale Volcanics (Hadfield and Whiteside, op. cit.) although analyses of many more garnets would be needed for this to be convincing. The generally ragged appearance of the garnets in these two intrusions, however, is consistent with a xenocrystal origin.

No definite conclusions can be drawn regarding the origin of the Welsh garnets (Plate 27). There is textural evidence to suggest that the garnets were originally present in the magma (flow-lines swirling around the crystals) though it is not clear whether they are phenocrysts or xenocrysts. They are certainly different, in composition, to the Lake District garnets (Fig. 16) and are more similar to garnets occurring in granites (Miyashiro, 1955; G. C. Brown, personal communication, 1971).

(vi) Petrogenetic implications

Garnet phenocrysts are seldom seen in volcanic rocks and so they rarely feature in petrogenetic schemes. However, the demonstration by Green and Ringwood (1968a) that, at elevated pressures, garnet is a liquidus phase in intermediate and acid calc-alkaline rocks suggests that

garnet may be more important in the evolution of these rocks than would be implied by its scant occurrence. The scarcity of garnet in volcanic rocks may well be due to its resorption at low pressure or to its high density leading to its settling out of the magma rapidly, rather than its general rarity as a crystallising phase. Consequently the garnets in the Borrowdale Volcanics probably represent only a fraction of those which were crystallising at depth. These garnets have an important bearing upon the origin and subsequent cooling history of the Borrowdale Volcanics magma.

From its occurrence as phenocrysts (relatively free from inclusions) it would seem that garnet was a liquidus - or near-liquidus phase in the andesite and dacite magmas of the southern outcrop. Consequently, if the dacites were derived from the andesites by a process of crystal fractionation then garnet must have been a fractionating phase and must have exerted some control over the composition of the residual liquids. Since the compositions of the garnets and the host andesites and dacites are known in some detail it should be possible to assess the consequences of such a control.

Perhaps the most notable feature of the garnets considered here is their capacity for fractionating the rare earth elements. The heavy rare earths (as exemplified by yttrium) are strongly concentrated in the garnets whilst the light rare earths (e.g. lanthanum) are less abundant in the garnets than in the magma from which they crystallised. Therefore, the removal of garnet during crystal fractionation would result in a marked increase in the La/Y ratio of the residual liquids. If only one gram of average andesite-type garnet (Table 2) was subtracted from 100 grams of average andesite (Table 1) the La/Y ratio of the residue would be increased by about 14%. The La/Y ratio of the southern outcrop rocks, however, remains essentially constant throughout the range of composition (Fig. 15) implying that garnet fractionation was not involved in the evolution of these rocks. This in turn implies that the andesites and dacites are not linked by any process of crystal fractionation but were derived by some other process such as partial melting.

This conclusion receives further support from the major element composition and zoning of the garnets. In any large body of magma undergoing crystal fractionation the composition of successive generations of a precipitating phase will change in response to changes in the liquid

composition (Wager and Brown, 1967). When individual crystals are zoned the zoning will, in general, reflect the change in bulk composition of the phase with time. Applying this principle to the Lake District garnets, one would expect the zoning in the andesite garnets to reflect the change in garnet composition in later differentiates. Since this zoning is in the reversed sense, the dacite garnets should be more magnesian than those from the andesites. The data in Fig. 16, however, show that this is not the case; the dacite garnets are consistently more iron-rich than their counterparts in the andesites. This suggests that liquids of andesite to dacite composition were already in existence before garnet began to crystallise and so supports the partial melting hypothesis.

These two lines of evidence eliminate the possibility that the dacites of the southern outcrop were derived from the andesites by a crystal fractionation process involving the removal of the observed phenocryst phases. They do not, however, eliminate the possibility that the andesites were derived from more basic liquids by this process. It is unlikely, though, that crystal fractionation would proceed as far as andesite and then stop. Consequently, when the evidence from the garnets is considered together with the petrochemical evidence presented in

Chapter 2 it must be concluded that a crystal fractionation hypothesis for the evolution of the southern outcrop rocks is untenable. The partial melting hypothesis of Green and Ringwood (1968b) provides a much more satisfactory explanation.

In order to understand the compositional variation and zoning of the garnets we must consider the cooling history of the southern outcrop magma. We will assume that the magma suite as a whole (basalt to rhyolite) was generated by some process of partial melting of a plate of oceanic crust thrust beneath the Lake District (cf. Green and Ringwood, 1968b). The mechanics of this process will be discussed in the next chapter.

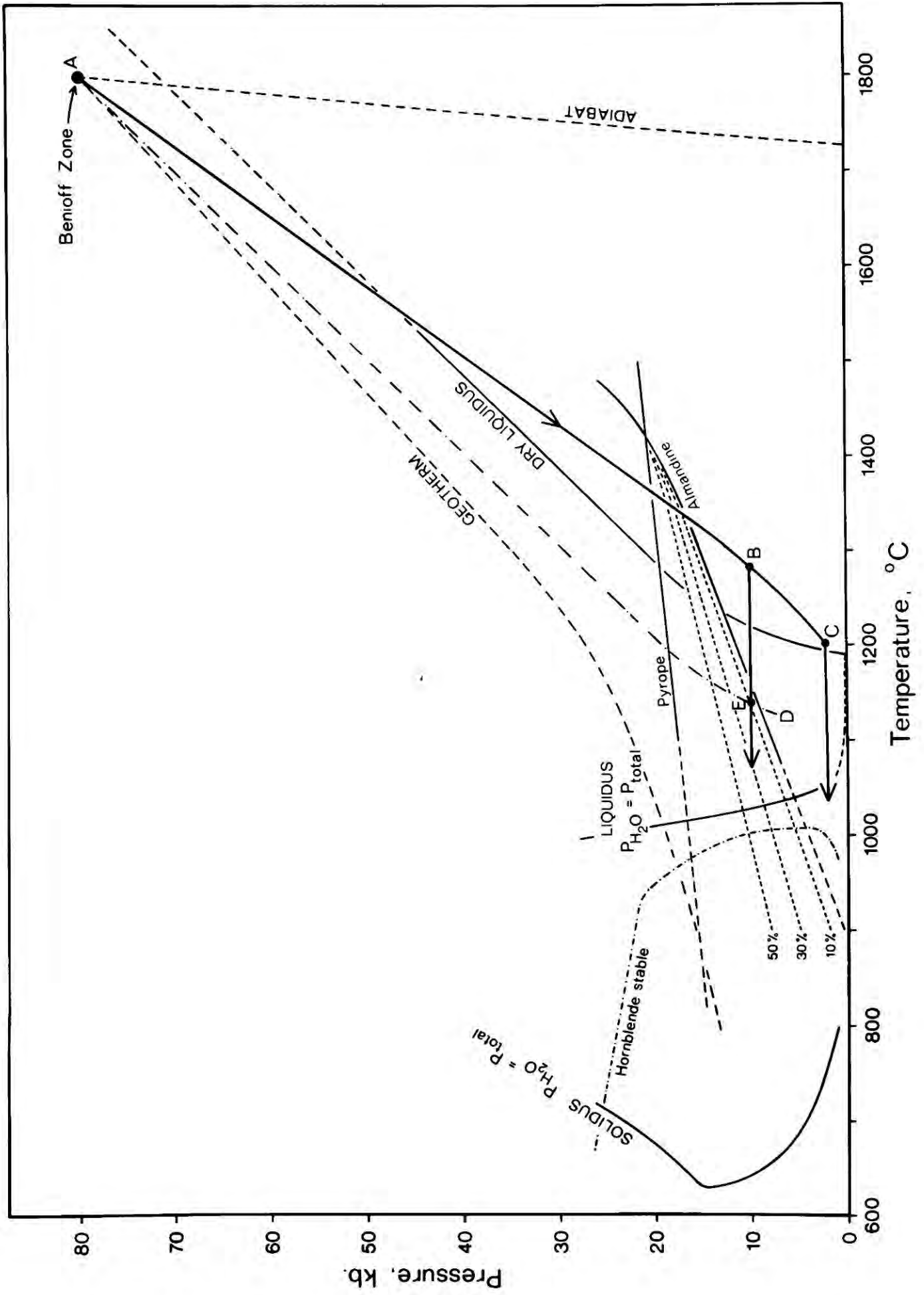
In modern island arcs it is possible to estimate the depth to the site of partial melting and magma generation (Benioff zone) from seismic evidence (Isacks et al. 1968). This is, of course, impossible in an ancient island arc and a more indirect method must be employed. Hatherton and Dickinson (1969) have gathered together a large volume of seismic and chemical data for modern island arcs and have shown that a good correlation exists between the  $K_2O$  content of lavas erupted from an andesite volcano and the depth to the Benioff zone beneath the volcano. They have produced

two curves relating these parameters for  $K_2O$  contents at 55 and 60%  $SiO_2$  respectively (Hatherton and Dickinson, op. cit. Fig. 6). Applying these curves to the  $K_2O$  contents of the southern outcrop rocks, a depth to the palaeo-Benioff zone of 250 km is obtained. Since the earth's mantle may have been depleted in potassium since the Ordovician (Taylor and White, 1965) this value must be regarded as an upper limit.

The cooling history of a mass of andesite magma rising to the surface from a depth of 250 km is illustrated schematically in Fig. 18. The temperature distribution in the mantle above a Benioff zone is not known with any certainty and so a calculated geotherm (Minear and Toksöz, 1970, Fig. 11) for a 180 km-thick plate descending at 8 cm/year has been assumed. Magma generated at the Benioff zone (A in Fig. 18) will be in thermal equilibrium with its surroundings and will, therefore, begin its ascent to the surface at a temperature of around  $1800^{\circ}C$ . This temperature is below the extrapolated liquidus temperature for dry andesite (from Green and Ringwood, 1968b) and is consistent with the presence of water in the magma. A hypothetical water-undersaturated liquidus curve for this magma has been constructed parallel to the dry curve and is indicated by a dash-dot line (AD) in Fig. 18. The water-saturated liquidus

Fig. 18

Schematic cooling history of andesite magma generated at a Benioff zone  
(A). See text for explanation.



has been constructed from data presented by Brown and Schairer (1968) for andesite, and Piwinski (1968) and Lambert and Wyllie (1970) for tonalite. The water-saturated solidus curve and the curve for hornblended stability in magmas of intermediate composition are taken from Lambert and Wyllie (1970).

As the magma rises towards the surface it will tend to lose heat to the surrounding mantle. It will travel along a P - T path somewhere in the area bounded by the adiabatic curve (calculated by Jeffreys, 1929) and the geotherm in Fig. 18. Magmas seldom arrive at the surface at temperatures much in excess of 1200°C and so the curve AC is probably a reasonable estimate of this path. This curve will be critically dependent upon the rate of ascent of the magma and will vary considerably in practice. Variations at the lower end of the curve of 100°C or so will not affect the conclusions drawn here, however.

The field of garnet stability in calc-alkaline liquids has not been established beyond reconnaissance experiments of Green and Ringwood (1968ab) in which the oxygen fugacity was uncontrolled. Yoder (1955) has determined the stability curve for pure almandine experimentally using a CO/CO<sub>2</sub> buffer to control  $f_{O_2}$ , at pressures up to about 10 kb. In Green and Ring-

wood's experiments the appearance of garnet was confined within the field bounded by an extrapolation of Yoder's stability curve. Hsu (1968) has examined the effects of oxygen fugacity on the stability of almandine at up to 3 kb  $P_{H_2O}$  and has shown that lowering the  $f_{O_2}$  causes the stability field to expand. More recently, Keesmann et al. (1971) have extended Hsu's curves up to about 25 kb using metallic iron as an oxygen buffer. Although the resulting  $f_{O_2}$  was lower than would obtain in natural liquids the resulting stability curve is probably more realistic than the original curve defined by Yoder's (1955) experiments. Consequently the curve established by Keesmann et al. (1971) has been used in Fig. 18.

The garnets occurring in the Borrowdale Volcanics are not pure almandine but contain up to 30 molecular per cent of pyrope. In order to examine the crystallisation history of these garnets, therefore, the effects of the pyrope component must be considered. In Fig. 18 the stability curve for pure pyrope is that determined experimentally by Boyd and England (1959). Almandine and pyrope garnets are stable above (at higher pressure than) their respective stability curves. It is probable that the garnets considered here crystallised somewhere in the wedge-shaped area between these two curves, where almandine-pyrope solid solutions should be stable.

The extent of solid solution within this area has been examined theoretically and experimentally by Yoder and Chinner (1960). They showed that there is an approximately linear relationship between molar volume and composition within the almandine-pyrope series and suggested that the same may hold true for the breakdown products. From this, they argued, it should be possible to calculate limits of solid solution, as a first approximation, by simple linear interpolation between the stability curves of the end-members. This has been done using the data in Fig. 18 and limits of solid solution for 10, 30 and 50 molecular per cent of pyrope are indicated by broken lines. Thus, a garnet crystallising on the line marked '30%' could incorporate the pyrope molecule up to a maximum of 30 molecular per cent. This simple model is, of course, only a crude approximation and its implications cannot be taken literally. It is nonetheless adequate for the present purposes.

Consider now a body of andesite magma rising to the surface as depicted in the semi-quantitative model (Fig. 18). If the magma is stored in a relatively deep-seated magma chamber at B and allowed to cool then garnet might be expected as a liquidus phase at E. This crystallisation path may be similar to that along which the southern outcrop

magmas cooled. If the magma had risen to shallower levels before being stored (e.g. C in Fig. 18) then garnet would not be a liquidus phase. Heat losses from such a magma chamber would be large because of the low temperature of the surrounding rock, and the magma would cool rapidly enough to undergo extensive crystal fractionation. The cooler residual liquids from such a system would probably enter the hornblende stability field where hornblende would crystallise instead of garnet. If the fractionating magma were erupted from these shallow chambers they would produce a lava sequence comparable with that seen in the West Indies calc-alkaline suite. In the deeper magma chambers (at B) the potential for heat loss will be less so the liquids will cool more slowly. Crystal fractionation will be less likely to take place here and the magma may remain too hot to enter the hornblende stability field. This may account for the absence of hornblende in the Borrowdale Volcanics.

From these considerations it would appear that cooling at depth is a prerequisite for the crystallisation of garnet. In Fig. 18 the path B - E is at a pressure (10 kb) corresponding to a depth of about 30 kilometres. The storage of the magma at the crust/mantle interface provides a plausible explanation for this and could imply the existence of a thick crust beneath

the postulated Lake District island arc. This thickness of crust (30 km) is similar to that beneath Japan (Kanamori, 1963) and it is perhaps significant that garnet phenocrysts have been observed in volcanic rocks from Japan (Miyashiro, 1955). The apparent absence of garnet from the northern outcrop can be accounted for if the magma was stored in relatively shallow chambers. This could also explain the crystal fractionation which seems to have taken place in that magma.

As a magma body cools at constant pressure beyond E on the path B - E in Fig. 18 the capacity for incorporating the pyrope molecule in the precipitating garnet crystals is progressively increased. Consequently if the magma is sufficiently rich in magnesium, the garnet phenocrysts would be expected to show a progressive enrichment in pyrope from core to rim. Such reversed zoning is a prominent feature of garnets from the Borrowdale Volcanics. Of the garnet crystals studied, G-176 shows the most well-developed zoning (Fig. 16). This amounts to an increase in pyrope content of almost 10 molecular per cent from core to rim within a single crystal. From the data in Fig. 18 this zoning could be produced by a fall in temperature of only 30°C. The same effect could, of course, result from the garnet sinking in the magma although the crystal would need to sink

about 2.5 kilometres to produce the zoning seen in G-176. A third explanation could be that the reversed zoning is a result of crystallisation under the influence of an external oxygen buffer (cf. Carmichael and Nicholls, 1967). The general rarity of reversed zoning in the ferromagnesian silicates of calc-alkaline rocks (Carmichael, 1967), however, casts doubt on the efficiency of this mechanism. Of these three possibilities the cooling hypothesis provides the best explanation for the observed zoning.

The consistently higher almandine content in the dacite garnets relative to those from the andesites (Fig. 16) probably results from the Fe/Mg ratio in the dacites being higher than in the andesites (Fig. 7). The increase in the Mn/Fe ratio in the garnets with increasing almandine content (Fig. 16) is also noteworthy. Hsu (1968) has shown that almandine becomes unstable under oxidising conditions although spessartine is unaffected. Consequently garnet will tend to be stabilised during growth by the presence of spessartine under such conditions. Under the influence of an external oxygen buffer dacite magmas will probably be more oxidised than andesite magmas although the absolute value of  $f_{O_2}$  may be lower in the former relative to the latter (cf. Lowder, 1970, Fig. 3). The

operation of such an external buffer in the southern outcrop magmas may thus explain the distribution of spessartine in the garnets. It is possible that the oxidation state of the magma may control the scandium content of the garnets in a similar manner.

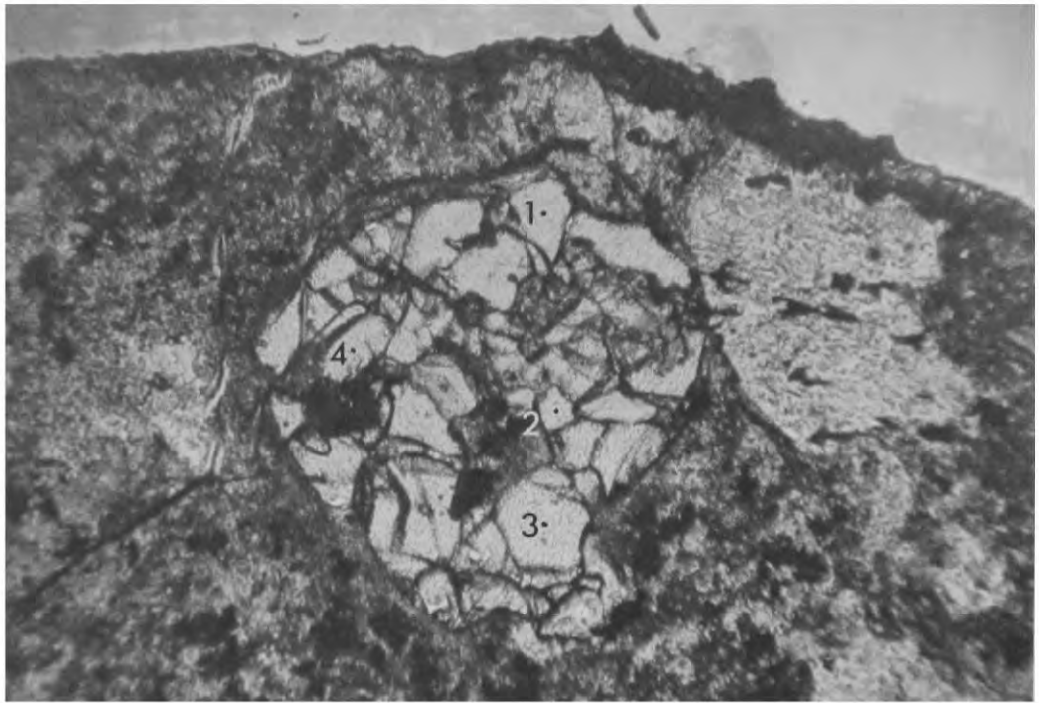
The remarkable zoning in G-302 has been described earlier and may have some petrogenetic significance. This garnet appears to have started crystallising from a dacite magma (?Langdale 'Rhyolite'; Fig. 3) but was later incorporated in andesitic magma (Wrengill Andesite) where it continued to grow. The dacite-type core of the crystal may have been derived from a chilled veneer of dacite lining some deep-seated conduit through which andesite magma later passed. Alternatively it could have settled through the interface between immiscible dacite and andesite liquids. If the latter possibility was the case then this garnet would lend some support to Yoder's (1971) suggestion that andesite and rhyolite liquids may be derived separately from a common mafic parent by partial melting and maintain their respective identities through an immiscibility relationship. The sharp compositional break between andesite lavas and dacitic ignimbrites, together with the possibility of a composition gap between garnets from the two rock types (Fig. 16) also supports this hypothesis.

In conclusion it is proposed that the preservation of garnets in volcanic rocks requires that the magma be stored temporarily in deep-seated magma chambers, possibly at the crust/mantle boundary, and then brought rapidly to the surface. If the magma ascends slowly any garnet phenocrysts will be resorbed. The remarkable state of preservation of some of the garnets from the ignimbrites (e.g. Plate 29) may be ascribed to their rapid transport to the surface. In addition to their considerable petrogenetic significance, garnet phenocrysts are potentially very sensitive geobarometers. Further experimental work on natural calc-alkaline rocks will be needed before this can be applied rigorously however. The semi-quantitative approach adopted here to the occurrence and composition of garnet phenocrysts leaves many questions unanswered. Why, for example, are garnets confined to intermediate and acid volcanic rocks and what is their relationship, if any, to other phenocryst phases (e.g. augite)? The answers to these and other questions may well emerge from experimental studies.

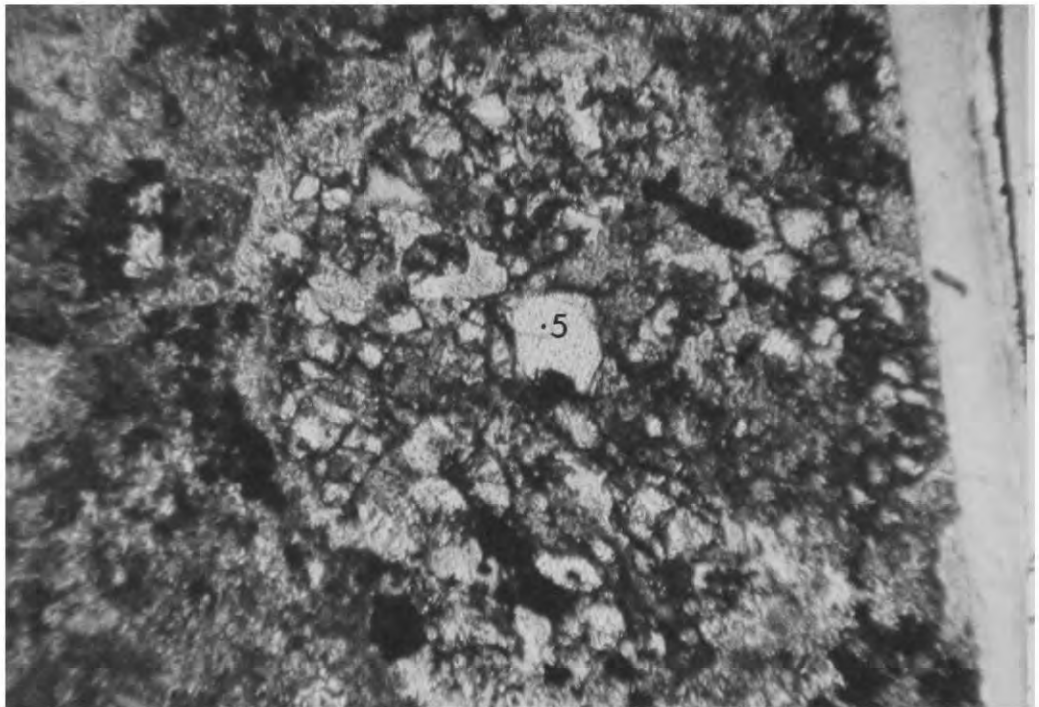


Plate 17      Garnet phenocrysts (red) in a polished slab of dacitic ignimbrite (LD 175) from the Birk Fell Group, Ullswater. The specimen is 12 cm. long.

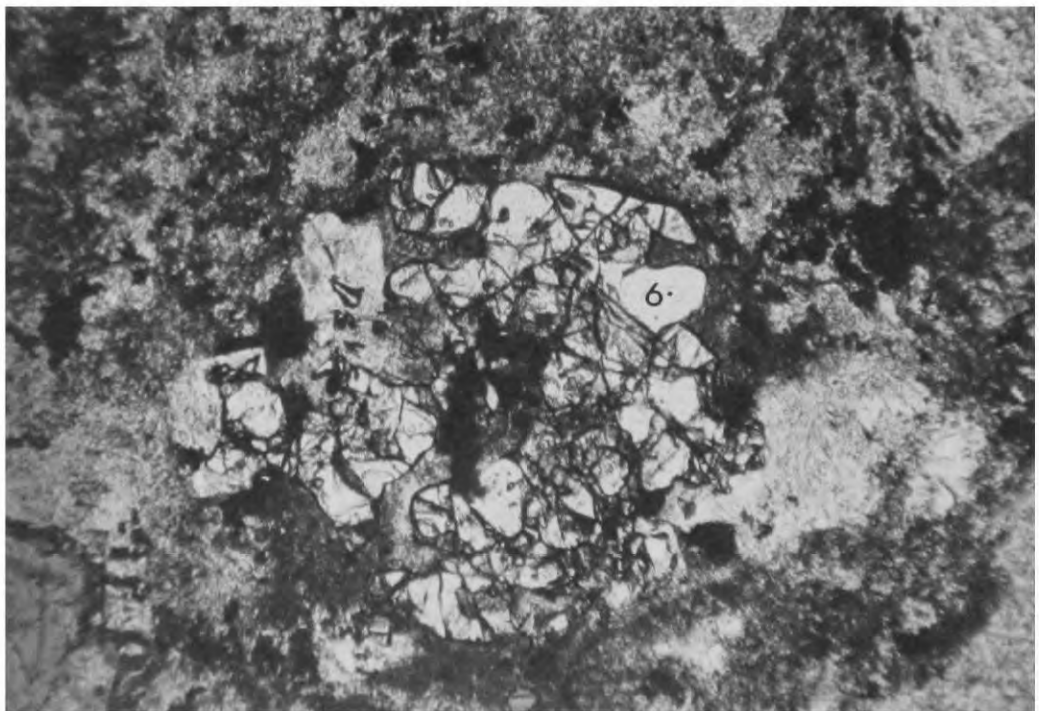
A.



B.



C.



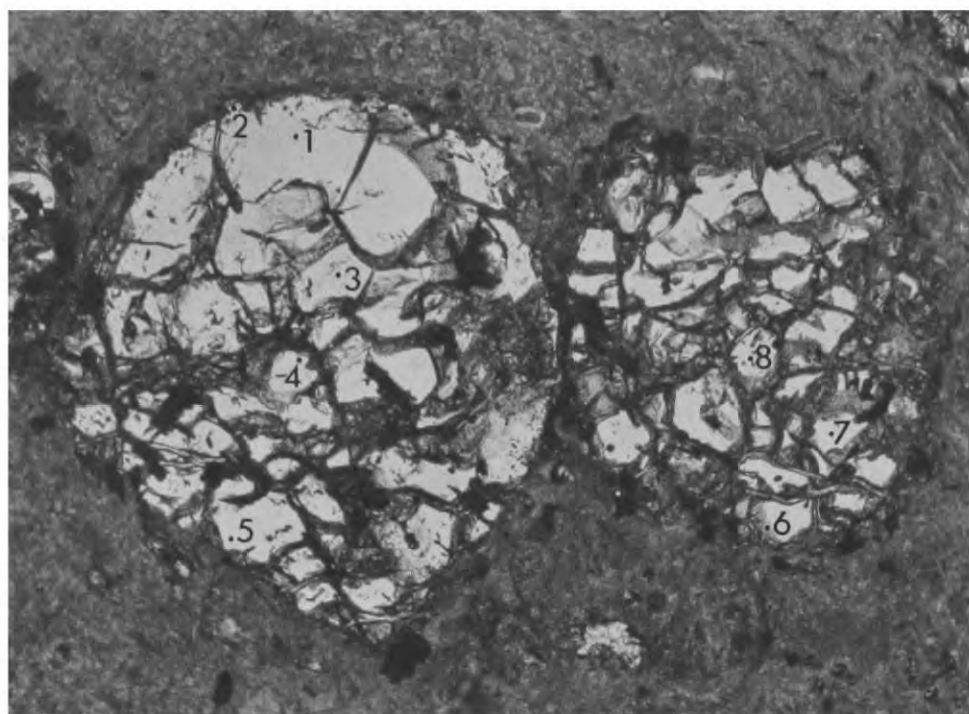


Plate 19 Garnet phenocrysts in andesite (LD 176) from the Ullswater Group.

Plane polarised light, x 27.

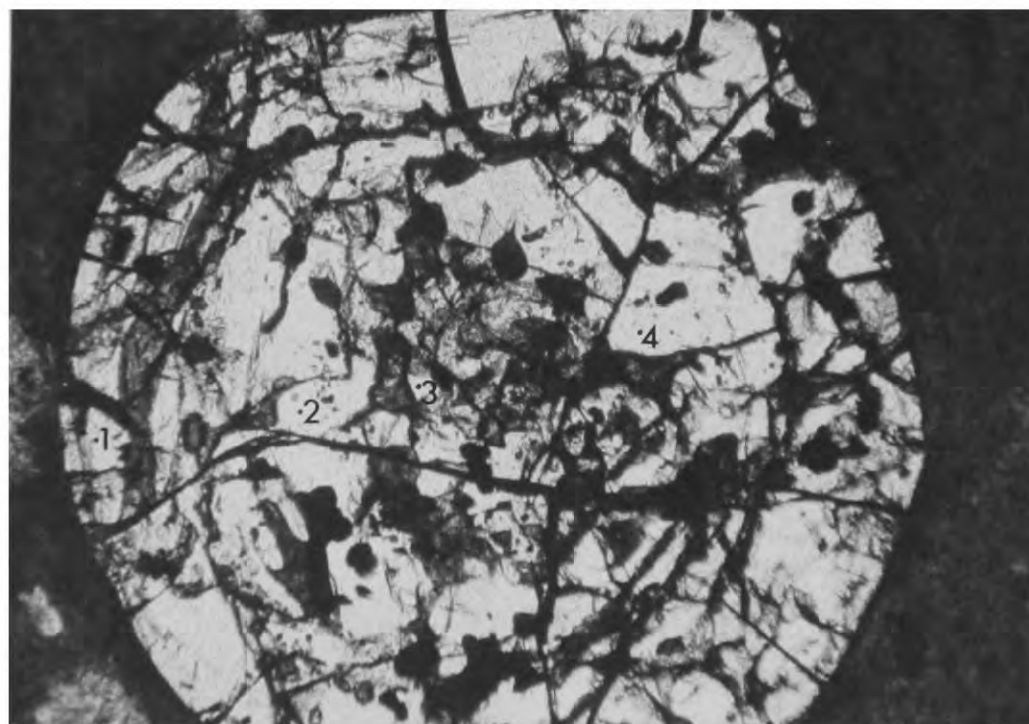
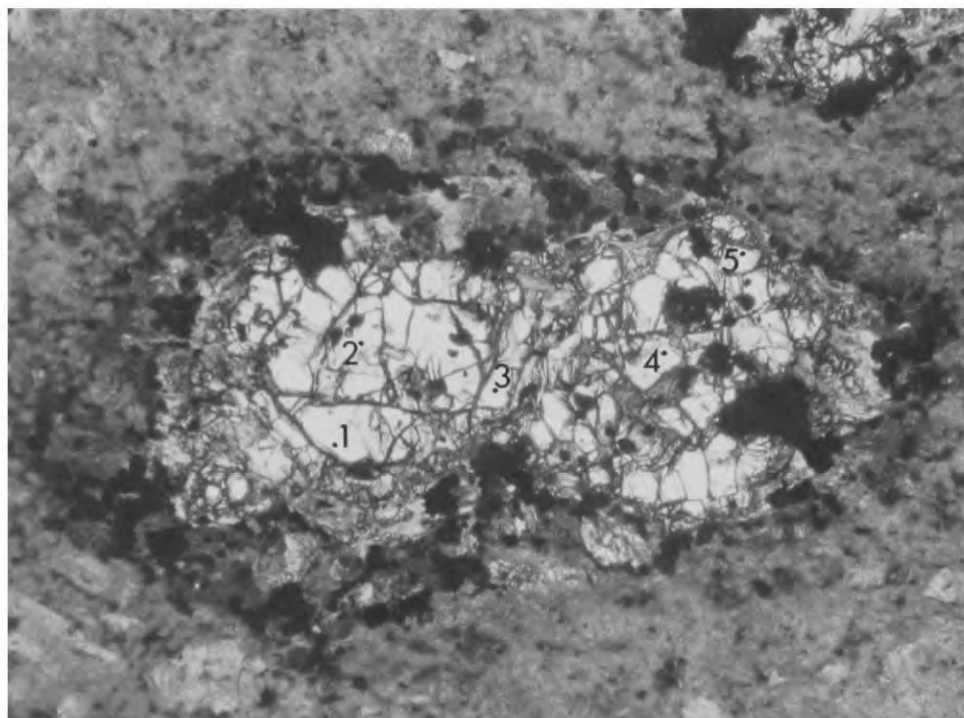
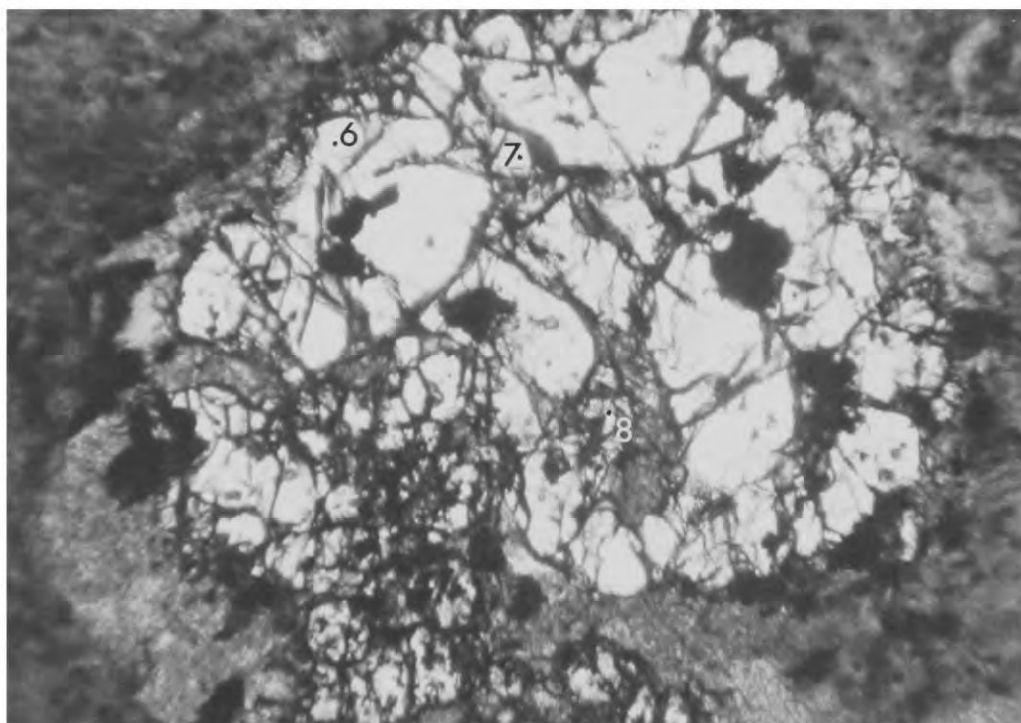


Plate 20 Garnet phenocryst in andesite (LD 220) from the Ullswater Group.

Plane polarised light, x 56.

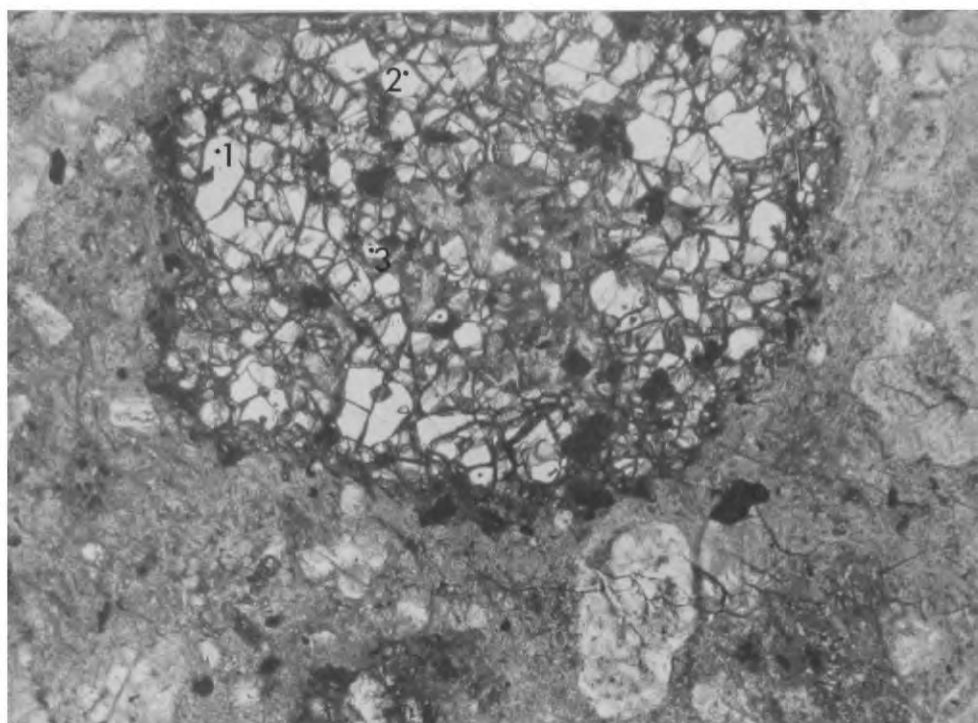


A. x 27

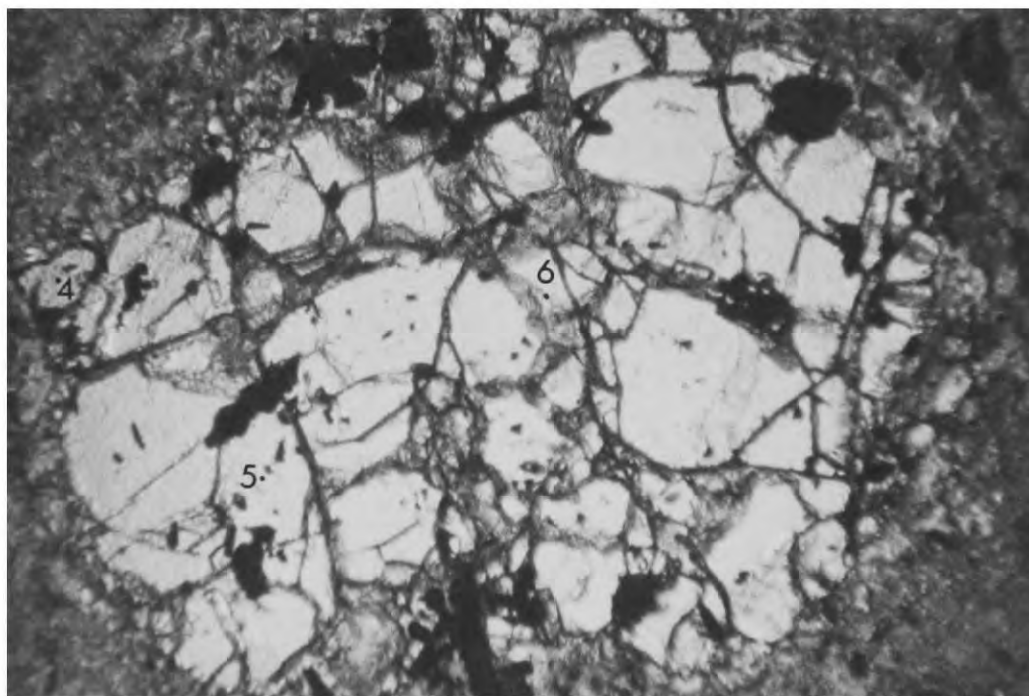


B. x 56

Plate 21      Garnet phenocrysts in andesite (LD 274) from the Grey Knotts  
Group, Borrowdale.  
Plane polarised light.



A. x 28



B. x 56

Plate 22 Garnet phenocrysts in andesite (LD 306) from the Mosedale  
Andesite, Wrynose Bottom.

Plane polarised light.

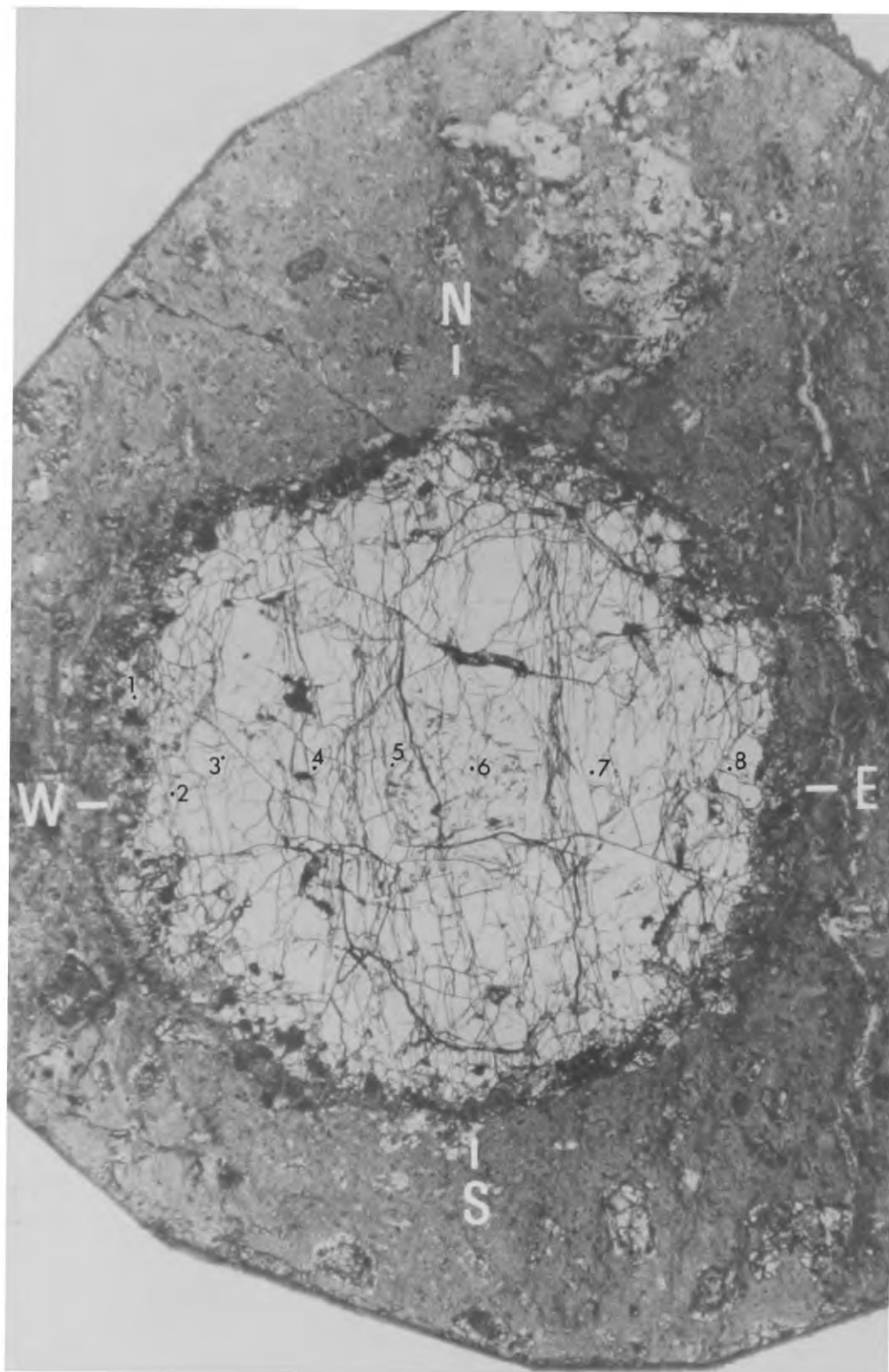


Plate 23 Large garnet phenocryst in andesite (LD 302) from the Wrengill Andesite, Ambleside. Note the inclusion-rich core.

Ordinary transmitted light, x 9.6

The location of east-west and north-south microprobe traverses (see Fig. 17) are shown.

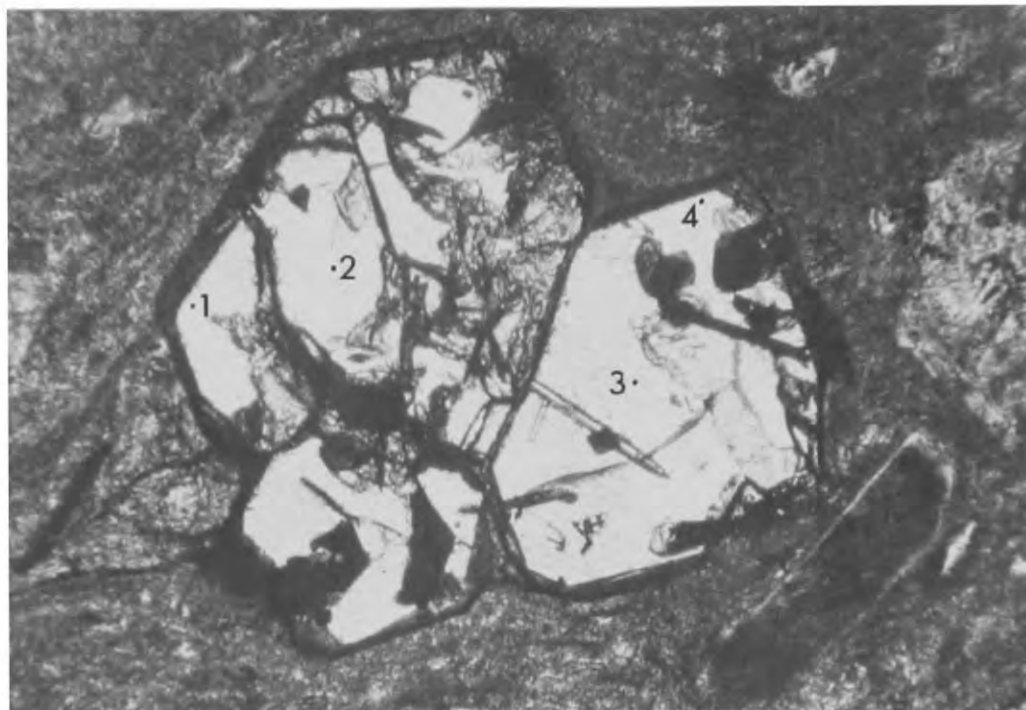


Plate 24 Euhedral garnet phenocrysts in ?intrusive dacite (LD 65 from Borrowdale.

Plane polarised light, x 55.

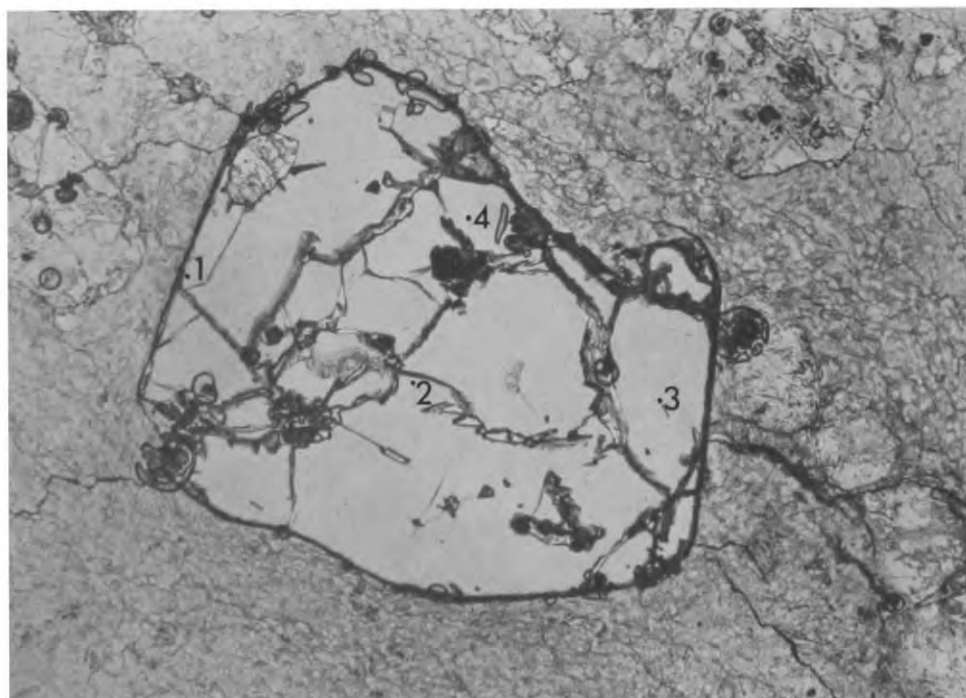


Plate 25 Garnet phenocryst in dacitic ignimbrite (LD 175) from the Birk Fell Group, Ullswater. See also Plate 17.

Plane polarised light, x 28.

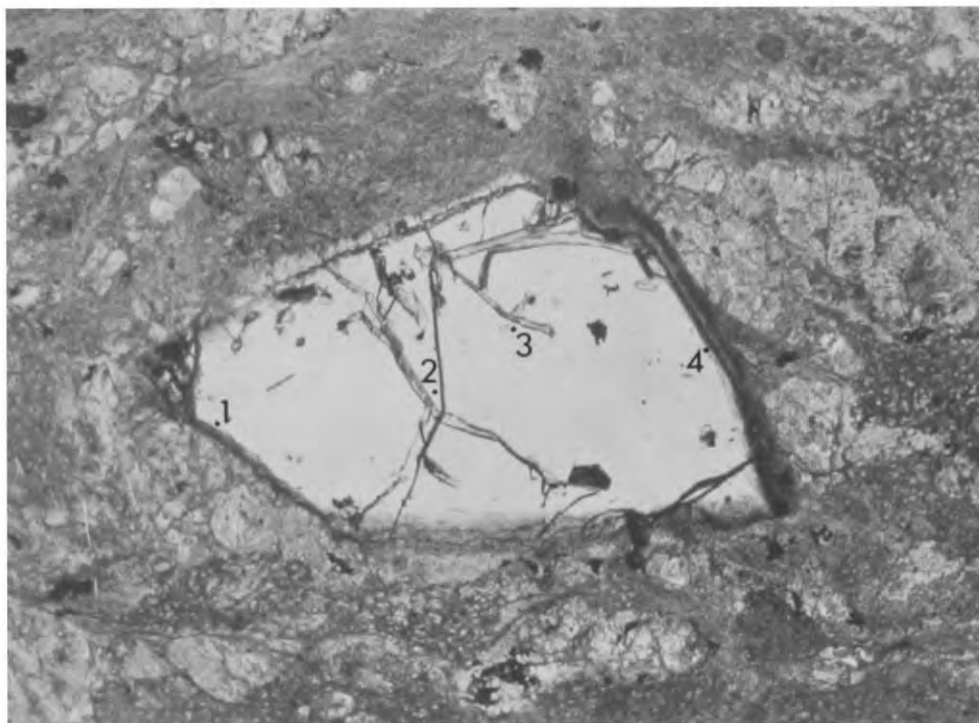


Plate 26      Fragment of garnet phenocryst in dacitic ignimbrite (LD 249)  
 from the Haweswater Ignimbrite Group.  
 Plane polarised light, x 17.



Plate 27      Garnet phenocrysts (G-316) in ignimbrite from Snowdonia,  
 North Wales (grid ref; SH 6776 6149).  
 Plane polarised light, x 15.5.

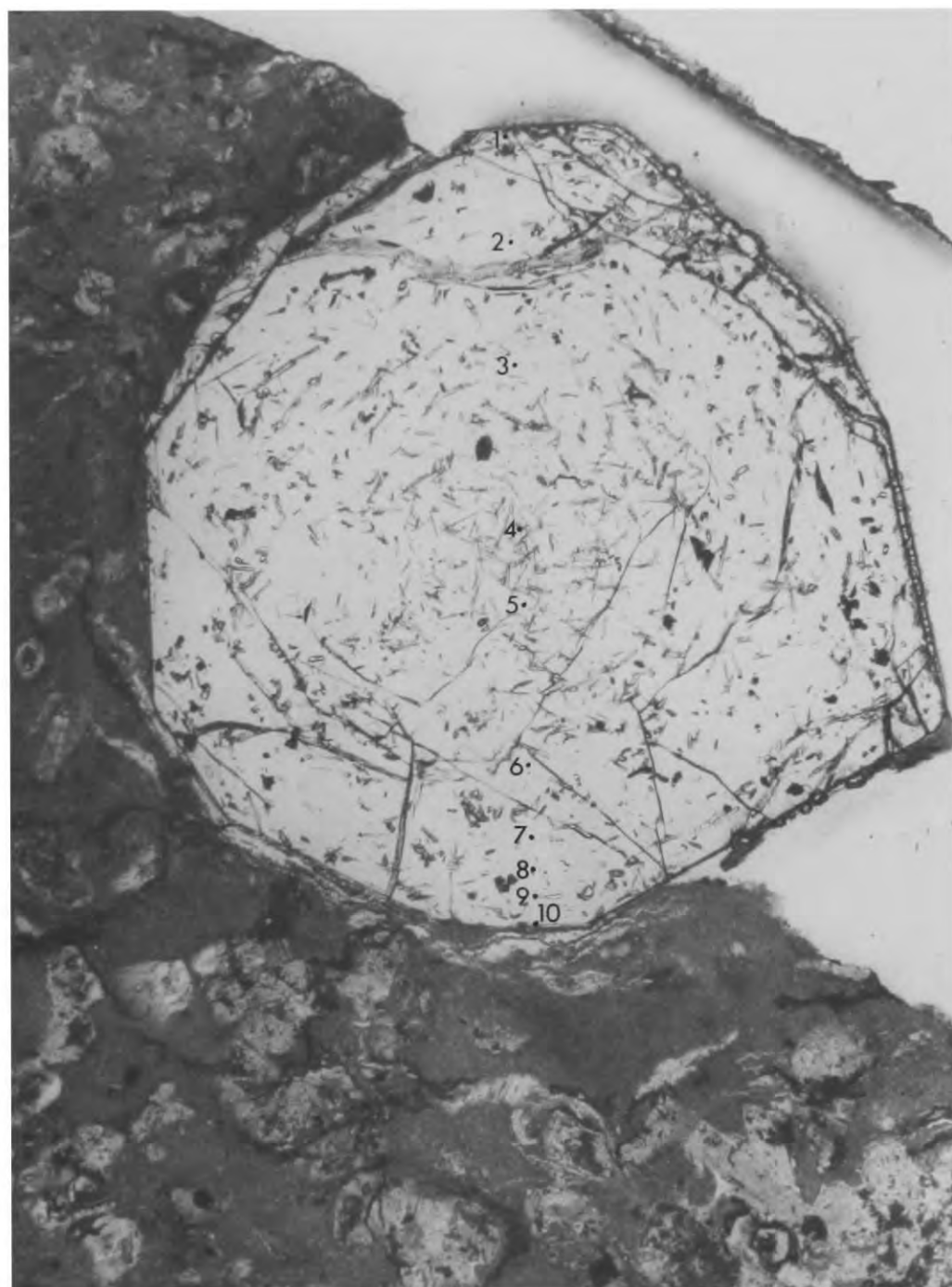


Plate 28 Large euhedral garnet phenocryst in dacitic ignimbrite (LD 317) from the Airy's Bridge Group, Borrowdale.  
Note the abundance of acicular apatite inclusions.  
Plane polarised light, x 20.



Plate 29      Large euhedral garnet phenocryst in hand specimen of dacitic ignimbrite (LD 317). See also Plate 28. x 14.

## CONCLUSIONS

### (1) Palaeogeographic implications

The petrochemical data presented in Chapters 2 and 3 suggest analogies between the Borrowdale Volcanics and the volcanic rocks of modern island arcs and continental margins. It was concluded that the Borrowdale Volcanics may have been erupted in such an environment. Further support for this hypothesis is forthcoming from other areas in Great Britain where Ordovician volcanic rocks are exposed (Fig. 1). The distribution and development of these rocks have been reviewed by Mitchell (1957).

In Wales, definite alkali-olivine basalts have been found amongst the Upper Ordovician volcanic rocks of Snowdonia (D. J. Hughes, personal communication, 1971). Further south, in Pembrokeshire, a sequence of alkali basalts and their differentiates has been described from the area around Skomer Island (13 in Fig. 1) by Thomas (1911). These volcanic rocks have recently been dated, palaeontologically, by Ziegler *et al.* (1969) who consider them to lie on or about the Ordovician/Silurian boundary.

If the Lake District formed part of an island arc in Ordovician times then Wales would have been situated on the landward side of the arc. Volcanic rocks erupted on the landward sides of modern island arcs frequently show alkaline affinities (Kuno, 1966). The presence of alkaline volcanic

rocks in Wales, therefore, strengthens the island arc hypothesis.

Along the east and south-east coasts of Ireland are a series of outcrops of Caradocian and Ashgillian volcanic rocks. These all lie to the north-west of the Irish Sea geanticline and are thus situated in a tectonically similar position to the Borrowdale Volcanics. A number of samples of these volcanics have been collected by Dr. C. J. Stillman and analysed by the writer. Work on these rocks is still in progress but the results so far seem to indicate a transition northwards from calc-alkaline to more tholeiitic magma types. The analogy with the Borrowdale Volcanics is obvious. It is proposed, tentatively, that these volcanic rocks formed part of the Lake District arc and represent a shift in the site of active volcanism south-westwards along the arc in Upper Ordovician times.

The suggestion that England, Wales and most of Ireland were situated on or near a continental margin in the Ordovician has important implications in the field of palaeogeography. These have been discussed by Fitton and Hughes (1970) and this paper will form the remainder of this section.

## VOLCANISM AND PLATE TECTONICS IN THE BRITISH ORDOVICIAN

J.G.FITTON

*Department of Geology, University of Durham, England*

and

D.J.HUGHES

*Department of Geology, University of Manchester, England*

Received 25 February 1970

Examination of petrochemical data on Ordovician igneous rocks from the English Lake District and Wales suggests that they were formed in an island arc/continental margin environment. The tectonic and palaeogeographic implications are discussed.

### 1. Introduction

Volcanic rocks form a significant proportion of the British Ordovician strata. They are well developed in southern Scotland (Ballantrae volcanics), the English Lake District (Borrowdale volcanics) and around many centres in Wales. The development and distribution of these volcanic rocks has been reviewed by Mitchell [1].

From a consideration of faunal evidence Wilson [2] has proposed the existence, in Lower Palaeozoic times, of a proto-Atlantic Ocean which separated the north-western and southeastern forelands of the Caledonian/Appalachian 'geosyncline'. As this ocean closed, volcanic island arcs developed around its margins. More recently Dewey [3] has elaborated Wilson's theory in terms of modern plate tectonics and proposed a model in which oceanic plates were destroyed along Benioff zones at the margins of Wilson's proto-Atlantic Ocean. Thus the Ballantrae volcanics were erupted along the northwestern side of the ocean and the Borrowdale and Welsh volcanics along the southeastern side.

In recent years a great deal of attention has been paid to the petrochemistry of island arc volcanoes and the lateral variations in magma type across such arcs is now well known. In a review of this subject Kuno [4]

states: If volcanoes are scattered over a zone more than 50 kilometres wide, there is a systematic variation of basalt magma type from the ocean to the continental sides. In the British Ordovician, volcanoes were erupting contemporaneously in the Lake District and in Wales in a volcanic belt now 300 km wide. This is a conservative estimate of the original width because of subsequent tectonic contraction. Consequently a petrochemical study of these volcanic rocks should provide a critical test for the hypotheses of Wilson and Dewey. A discussion of currently available chemical data on these rocks is the purpose of this paper.

### 2. Lake district

The oldest rocks exposed in the Lake District are a sequence of grits, sandstones and shales forming the Skiddaw Group. These are overlain by a considerable thickness of lavas and tuffs (the Borrowdale volcanic group) which are in turn unconformably overlain by limestone and shales of Caradocian age. The nature of the Skiddaw/Borrowdale junction is still in dispute although graptolitic faunas in the uppermost shales of the Skiddaw Group indicate an Upper Llan-

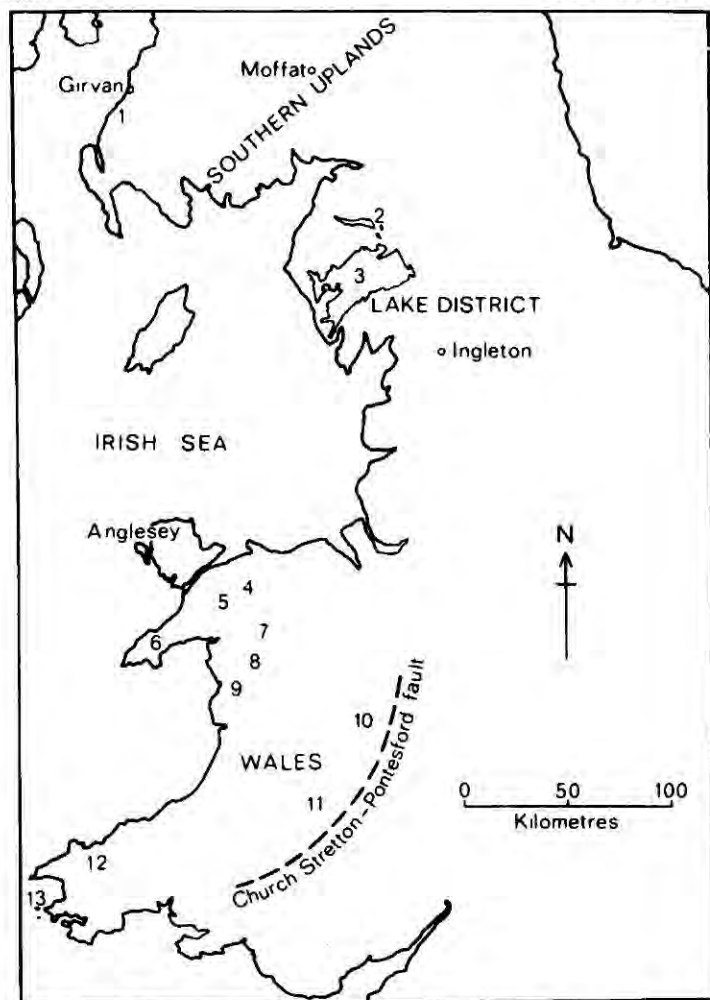


Fig. 1. Locality map. Numbers refer to volcanic areas cited in the text: 1, Ballantrae. 2, northern and 3, southern outcrops of Borrowdale volcanics. 4, Capel Curig. 5, Snowdonia. 6, Lleyn Peninsula. 7, Arenig Mountains. 8, Rhobell Fawr. 9, Cader Idris. 10, shelve area (west Shropshire). 11, Builth Wells. 12, north Pembrokeshire. 13, Skomer Island. Outcrop of Borrowdale volcanics shown stippled. The Church Stretton-Pontesford fault system forms the southeastern margin of the Welsh Basin. Based on Crown Copyright Institute of Geological Sciences map. Reproduced by permission of the Director.

virnian age. The Borrowdale volcanics were thus erupted at some time between the Upper Llanvirnian and the Caradocian. The stratigraphy of the Lake District has been summarised by Mitchell [5].

The Borrowdale volcanics occur in two main outcrops flanking the Skiddaw Anticline (fig. 1). Correlation between these two groups is highly problematical [6] although correlations within each group have been proposed [5,6].

Very little chemical data have been published on the Borrowdale volcanics although the calc-alkaline nature of the lavas and tuffs in the Scafell-Honister re-

gion of the southern outcrop has been established by Oliver [7] and Strens [8]. The findings of these workers have been confirmed by one of the authors (J.G.F., unpublished results). These results (obtained by X-ray fluorescence methods) are presented on an A.F.M. diagram in fig. 2. All these analyses plot about a common calc-alkaline trend suggesting that the rocks approximate in composition to the liquids from which they crystallised. The presence of primary almandine-pyrope garnet as a near-liquidus phase [9] suggests that crystallisation began at depths corresponding to the lower crust or upper mantle [10].

The difficulties involved in correlation northwards across the Skiddaw Anticline have been mentioned above. Eastwood et al. [6] have described the northern outcrop (Binsey-Eycott region) in detail and suggest that the lavas and tuffs in this area were erupted from vents situated to the north of the present outcrop.

Chemical analyses of these rocks (J.G.F., unpublished results) reveal that they differ significantly from those of the Scafell region. Whereas in the

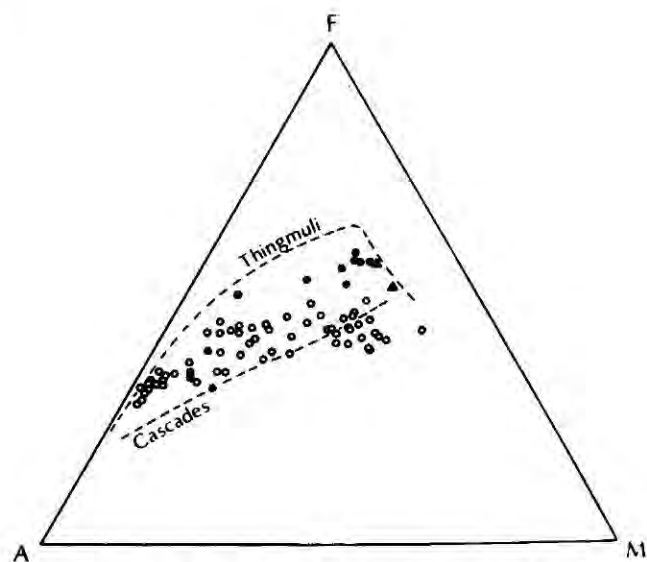


Fig. 2. A.F.M. (weight %) plot of analysed samples from the Borrowdale volcanics. Open circles: lavas and tuffs from the southern outcrop (Scafell area). Closed circles: acid rocks and aphyric basic lavas from the northern outcrop (Binsey-Eycott region). Closed triangles: mechanically separated groundmasses from porphyritic (Eycott-type) lavas from the northern outcrop. A =  $\text{Na}_2\text{O} + \text{K}_2\text{O}$ ; F = total iron (expressed as FeO); M = MgO. Typical calc-alkaline (Cascades) and tholeiitic (Thingmuli) trends, both from Carmichael [32], are shown for comparison.

latter region rocks of andesitic and dacitic composition predominate, in the Binsey-Eycott region these are rare. Instead, basalts and basaltic andesites are abundant with a very minor development of rhyolites.

The basic lavas are often highly porphyritic (Eycott-type lavas) with large phenocrysts of calcic plagioclase. The abundance of these phenocrysts suggests that they are of cumulate origin. This is supported by chemical analyses of the rocks which, when plotted on variation diagrams, give a very wide scatter of points. Good differentiation trends, however, are obtained when only analyses of aphyric basic rocks are plotted together with the analyses of acid rocks from the area. Analyses of groundmasses, mechanically separated from the porphyritic lavas, fall on these same differentiation trends.

When compared with the Scafell rocks the Binsey-Eycott lavas are richer in iron and titanium and poorer in alkalis. On an A.F.M. diagram they show a pronounced trend towards iron enrichment (fig. 2) and may, therefore, be regarded as transitional between calc-alkaline and tholeiitic.

### 3. Wales

The Ordovician igneous rocks of Wales present a complex array of rock types derived from several major centres.

In the extensive Caradocian centres of the Snowdonian range [11–15] the chief products of volcanism are acid potassic and sodic ignimbrites; these are associated with fine-grained, epizonal intrusions almost exclusively of potassic granite [16]. The dominance of the acidic rocks, such features as the abundance of zircon and allanite, and the thoroughly potassic nature of the granites all point to an origin by partial crustal fusion for these rocks. Simple crustal melting does not, however, appear to be sufficient to account for all the features seen. For example, what appear to be primary magmatic garnets occur in the ignimbrites of the Capel Curig suite [17], olivine tholeiite lavas occur in the Devil's Kitchen in Snowdonia and late stage mildly alkaline dolerites are ubiquitous in Snowdonia, as in other centres in Wales.

The Cader Idris centre of Llandeilian age has many affinities with the Snowdonian Caradocian centres, but the central Cader Idris granophyre is adamellitic in

composition with associated diorite [18], suggesting closer affinities with a more normal calc-alkaline suite.

Unequivocal calc-alkaline suites are present, as for example in the Lley Peninsula where Fitch [19] described the sequence: basaltic andesite-andesite-dacite-rhyodacite-rhyolite with complementary intrusive rocks, all of Caradocian age. At the base of the Ordovician a large andesite volcano developed at Rhobell Fawr in Merioneth [20]. Andesites also occur in the Arenig Mountains, at Builth Wells and in west Shropshire.

Tholeiitic rocks are rare in the Welsh Ordovician. A major composite sill of tholeiitic affinities in north Pembrokeshire has been described by Roach [21]. This intrusion is of Arenig age.

Truly alkaline rocks occur at several centres in Wales. A large differentiated alkaline sill at Mynydd Rhiw in the Lley Peninsula has recently been described [22]. As mentioned above, mildly alkaline dolerites occur as late stage intrusions throughout the Ordovician igneous centres in Wales.

Many of the volcanic centres are characterized by a high content of alkalis, often with strikingly variable Na:K ratios. Extensive spilitization is reported [23] but there is no regional alkali metasomatism, and in any one sequence the process affects only certain flows [20]. Characteristic spilitic suites and associations of the Steinmann Trinity type are not present. A high initial alkali content of many of the Welsh Ordovician magmas is indicated.

The final Ordovician volcanic episode in Wales was the eruption of the Skomer volcanic series in Pembrokeshire, recently redated by Ziegler et al. [24] to fall on or about the Ordovician-Silurian boundary. This appears to be a perfectly good alkaline differentiation sequence along the line: alkali olivine basalt-hawaiite-mugearite-benmoreite-trachyte-alkali rhyolite.

### 4. Discussion

From the data presented above a pattern of variation of magma types emerges. In the Lake District, lavas transitional between tholeiitic and calc-alkaline give way southwards to true calc-alkaline lavas. In Wales, the picture is complicated somewhat by the

strong possibility of crustal contamination. Nevertheless calc-alkaline magmas appear to have been replaced by more alkalic types during the course of the Ordovician.

This variation of magma type is essentially similar to that observed in modern island arc or continental margin environments [4] where oceanic lithosphere is being actively destroyed along Benioff zones [25]. The petrochemistry of the British Ordovician volcanics, therefore, provides support for the hypotheses of Wilson [2] and Dewey [3].

Recently, Isacks and Molnar [26] have demonstrated that the descent of lithosphere plates may not be a continuous process. At about 700 km depth the plate would come into contact with the rigid mesosphere and its motion may cease. A new Benioff zone may then develop on the oceanward side of the old one. In Wales, volcanicity occurred in sporadic outbursts throughout the Ordovician whereas in the Lake District it was virtually confined to a single, albeit large, episode. A single Benioff zone can explain variation in magma type in the post-Llanvirnian volcanics of the Lake District and Wales but Welsh volcanics of Arenigian and Llanvirnian age present a problem. It is possible, therefore, that these older volcanics were re-

lated to movement along an earlier, more southerly Benioff zone which ceased to be active in the Llanvirnian (cf. Dewey [3] fig. 2).

The palaeogeographic implications of this ancient island arc system must now be considered. An island arc usually has a deep ocean trench running parallel to it on the oceanic side. Consequently one would expect to find evidence of an Ordovician trench to the north of the Lake District. Such evidence is provided by the Moffat geosyncline in the Southern Uplands of Scotland. The structural similarities between this geosyncline and a modern ocean trench are striking. In this context it is interesting to compare Williams' palaeogeographic section across the northern margin of the Moffat geosyncline ([27] fig. 5) with the seismic sections across the Japan trench published by Ludwig et al. ([28] fig. 2). If this analogy is valid then the spilites which form the 'basement' in the southern Uplands represent remnants of oceanic crust.

As the proto-Atlantic Ocean closed, deformation, in the Lower Ordovician, of Moine and Dalradian sediments gave rise to the Scottish Highlands [3]. Dewey's suggestion [3] that the Ballantrae volcanics were erupted in an ocean trench prior to this defor-

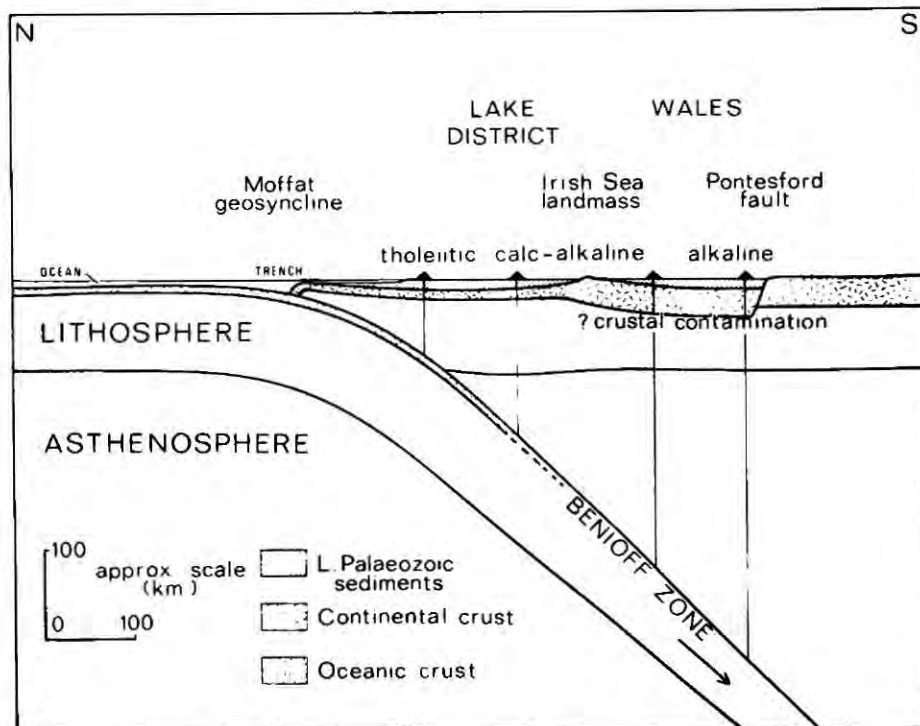


Fig. 3. Diagrammatic section through England and Wales in mid-Ordovician times to illustrate the distribution, and proposed origin of contemporaneous volcanism. The plate tectonic scheme is adapted from the work of Isacks et al. [25].

mation is unrealistic since volcanism is notably absent from modern ocean trenches. As an alternative we would suggest that these spilitic lavas and their associated serpentinites, cherts and shales formed part of the early Ordovician oceanic crust. The development of glaucophane in the spilites and their association with eclogite [29] is consistent with their having been depressed to great depth along a Benioff zone and subsequently returned to the surface, possibly during the deformation giving rise to the Scottish Highlands.

By Caradocian times the two sides of the proto-Atlantic Ocean were close enough for flysch wedges from the eroding Scottish Highlands to reach across the remnants of the ocean to the southeastern side. Thus the active trench of the Lake District arc (Moffat geosyncline) was filled with conglomerates and greywackes yielding shelly faunas of American affinities [27]. The final closure of the ocean in the Upper Ordovician brought movements along the Benioff zone beneath England and Wales to an end and volcanic activity ceased.

One final question remains, that of the crustal structure of England and Wales in the Ordovician. Precambrian rocks occur in the Midlands, Welsh Borders, Anglesey and possibly at Ingleton. Bott [30], using geophysical data, has postulated the presence of Precambrian basement beneath Wensleydale in the northern Pennines. Further north and west, evidence for the existence of Precambrian basement is lacking. It is thus possible, though by no means certain, that the northwesterly limit of sialic crust in the Ordovician lay to the south of the Lake District along the line of the postulated Irish Sea Landmass [31].

The conclusions reached here are summarised in fig. 3, a hypothetical section through England and Wales in the Llandeilian. In detail these conclusions differ from those of Dewey [3] although the underlying principle of oceanic contraction is supported. The possibility of locating ancient plate boundaries from petrochemical studies of contemporaneous igneous rocks has been demonstrated. The results of research on recent volcanic rocks may thus find wide application in the field of palaeogeography.

#### Acknowledgements

The work currently in progress in the Lake District and Wales is supported by grants from the Natural En-

vironment Research Council of Great Britain. We are grateful to Prof. G.M. Brown, Prof. M.H.P. Bott, Dr. W.J. Wadsworth and Dr. G.A.L. Johnson for critically reading the manuscript.

#### References

- [1] G.H. Mitchell, Ordovician Volcanoes, *Advanc. Sci.* 14 (1957) 34–47.
- [2] J.T. Wilson, Did the Atlantic close and then re-open?, *Nature* 211 (1966) 676–681.
- [3] J.F. Dewey, Evolution of the Appalachian/Caledonian orogen, *Nature* 222 (1969) 124–129.
- [4] H. Kuno, Lateral variation in basalt magma type across continental margins and island arcs, *Can. Geol. Surv. Paper* 66–15 (1966) 317–336.
- [5] G.H. Mitchell, The geological history of the Lake District, *Proc. Yorks. Geol. Soc.* 30 (1956) 407–463.
- [6] T. Eastwood, S.E. Hollingworth, W.C.C. Rose and F.M. Trotter, *Geology of the country around Cocker-mouth and Caldbeck*, *Mem. Geol. Surv. Great Britain* (1968).
- [7] R.L. Oliver, The Borrowdale Volcanic and associated rocks of the Scafell area, English Lake District, *Quart. J. Geol. Soc. London* 117 (1961) 377–417.
- [8] R.G.J. Strens, The geology of the Borrowdale-Honister district (Cumberland), with special reference to the mineralisation, *Unpubl. Ph. D. Thesis, Univ. of Nottingham* (1962).
- [9] R.L. Oliver, The origin of garnets in the Borrowdale Volcanic Series and associated rocks, English Lake District, *Geol. Mag.* 93 (1956) 121–139.
- [10] T.H. Green and A.E. Ringwood, Origin of garnet phenocrysts in calc-alkaline rocks, *Contr. Mineral. Petrol.* 18 (1968) 163–174.
- [11] H. Williams, The geology of Snowdon (North Wales), *Quart. J. Geol. Soc. London* 83 (1927) 346–431.
- [12] D. Williams, The geology of the country between Nant Peris and Nant Ffrancon (Snowdonia), *Quart. J. Geol. Soc. London* 86 (1930) 191–233.
- [13] B. Roberts, The Llwyd Mawr ignimbrite and its associated volcanic rocks, in: *The Pre-Cambrian and Lower Palaeozoic rocks of Wales*, ed. A. Wood (Univ. of Wales Press, Cardiff, 1969).
- [14] R.V. Beavon, The succession and structure east of the Glaslyn River, North Wales, *Quart. J. Geol. Soc. London* 119 (1963) 479–512.
- [15] R.M. Shackleton, The stratigraphy of the Moel Hebog district between Snowdon and Tremadoc, *Lpool. Manchr. Geol. J.* 2 (1959) 216–252.
- [16] A.V. Bromley, Acid plutonic igneous activity in the Ordovician of North Wales, in: *The Pre-Cambrian and Lower Palaeozoic rocks of Wales*, ed. A. Wood (Univ. of Wales Press, Cardiff, 1969).

- [17] H.Williams, The igneous rocks of the Capel Curig district (North Wales), *Proc. Lpool. Geol. Soc.* 13 (1922) 166–206.
- [18] R.G.Davies, The Cader Idris granophyre and its associated rocks, *Quart. J. Geol. Soc. London* 115 (1959) 189–216.
- [19] F.J.Fitch, Ignimbrite volcanism in North Wales, *Bull. Volcanol.* 30 (1967) 199–219.
- [20] A.K.Wells, The geology of the Rhobell Fawr district (Merioneth), *Quart. J. Geol. Soc. London* 81 (1925) 463–538.
- [21] R.A.Roach, The composite nature of the St. David's Head and Carn Llidi intrusions of North Pembrokeshire, in: *The Pre-Cambrian and Lower Palaeozoic rocks of Wales*, ed. A. Wood (Univ. of Wales Press, Cardiff, 1969).
- [22] P.Cattermole, A preliminary geochemical study of the Mynydd Penarfynydd intrusions, Rhiw igneous complex, southwest Lleyn, in: *The Pre-Cambrian and Lower Palaeozoic rocks of Wales*, ed. A. Wood (Univ. of Wales Press, Cardiff, 1969).
- [23] G.D.Nicholls, Autometasomatism in the lower spilites of the Builth Volcanic Series, *Quart. J. Geol. Soc. London* 114 (1958) 137–162.
- [24] A.M.Ziegler, W.S.McKerrow, R.V.Burne and P.E.Baker, Correlation and environmental setting of the Skomer Volcanic Group, Pembrokeshire, *Proc. Geol. Assn.* 80 (1969) 409–439.
- [25] B.Isacks, J.Oliver and L.R.Sykes, Seismology and the new global tectonics, *J. Geophys. Res.* 73 (1968) 5855–5899.
- [26] B.Isacks and P.Molnar, Mantle earthquake mechanisms and the sinking of the lithosphere, *Nature* 223 (1969) 1121–1124.
- [27] A.Williams, The Barr and Ardmillan series (Caradoc) of the Girvan district, south-west Ayrshire, with descriptions of the Brachiopoda, *Mem. Geol. Soc. London* 3 (1962).
- [28] W.J.Ludwig, J.I.Ewing, M.Ewing, S.Murauchi, N.Den, S.Asano, H.Hotta, M.Hayakawa, T.Asanuma, K.Ichikawa and I.Noguchi, Sediments and structure of the Japan trench, *J. Geophys. Res.* 71 (1966) 2122–2137.
- [29] T.W.Bloxam and J.B.Allen, Glaucofane-schist, eclogite, and associated rocks from Knockormal in the Girvan-Ballantrae complex, South Ayrshire, *Trans. Roy. Soc. Edin.* 64 (1960) 1–27.
- [30] M.H.P.Bott, Geophysical investigations of the northern Pennine basement rocks, *Proc. Yorks. Geol. Soc.* 36 (1967) 139–168.
- [31] T.N.George, Palaeozoic growth of the British Caledonides, in: *The British Caledonides*, eds. M.R.W.Johnson and F.H.Stewart (Oliver and Boyd, Edinburgh, 1963).
- [32] I.S.E.Carmichael, The petrology of Thingmuli, a Tertiary volcano in eastern Iceland, *J. Petrol.* 5 (1964) 435–460.

(ii) Genesis of island arc magmas

So far, little has been said about the genesis of the Borrowdale Volcanics magma. We have proposed that this magma was generated in an island arc environment and was probably produced by some partial melting process. The petrochemical and mineralogical evidence points to an origin for the whole range of southern outcrop magma compositions (i.e. basalt to rhyolite) somewhere below the crust/mantle boundary. Crystal fractionation of the observed phenocryst phases could not have played an important part in the development of these magmas. The rocks of the northern outcrop were probably produced by a similar partial melting process although in this case the magma was modified to a great extent by crystal fractionation at a fairly high level in the crust.

This partial melting process may be common to all island arc magmas and so deserves special attention here. Two questions in particular need to be answered ; what is the parent material which undergoes partial melting and why do the resulting magmas show continuous variation from tholeiitic to calc-alkaline types across island arcs in a direction away from the ocean? These questions have been considered by the writer (Fitton, 1971) who suggests that the partial melting of oceanic crust along a

Benioff zone can account for the observed features of island arc magmas. At relatively shallow depths, the partial melting of amphibolite could produce magmas of the island arc tholeiitic suite. Calc-alkaline magmas may be generated at greater depths by the partial melting of eclogite. This paper is presented here as a conclusion to the thesis.

## THE GENERATION OF MAGMAS IN ISLAND ARCS

J. G. FITTON

*Department of Geology, University of Durham, England*

Received 16 January 1971

The partial melting, along appropriate geotherms, of a descending slab of oceanic crust is examined in the light of recent experimental studies. The predicted compositions of magmas generated by this model are concurrent with those observed in island arcs. It is suggested that magmas of the island arc tholeiitic series are produced by reactions involving the breakdown of amphibole at shallow depths. At greater depths partial melting of eclogite will generate calc-alkaline magmas. Between these two extreme types a continuum of transitional magmas could be generated.

### 1. Introduction

Lateral variation in magma type across island arcs is a well documented phenomenon [1]. A strong correlation exists between the chemical composition of erupted lavas (notably the  $K_2O$  content) and the depth of earthquakes beneath the volcano [2], suggesting that island arc magmas may be generated at the inclined seismic (Benioff) zone.

In Japan, Sugimura et al. [3] have shown that the volume of Quaternary lavas decreases sharply westwards away from the volcanic front (i.e. with increasing depth to the Benioff zone). Lavas of tholeiitic affinities are therefore more abundant than calc-alkaline rocks. Alkali basalts and their derivatives are volumetrically insignificant.

Recently, Jakeš and Gill [4] have suggested that the dominance of tholeiitic lavas in Japan may be typical of island arcs in general and propose the term "island arc tholeiitic series" to describe these rocks. As defined by Jakeš and Gill in [4], they differ from members of the calc-alkaline suite in many important respects. They are predominantly basaltic whereas in the calc-alkaline suite, andesites predominate. They show varying degrees of iron enrichment, have low potassium contents with high K/Rb ratios and have flat chondrite-normalised rare-earth distribution patterns. In these features the island arc tholeiites resemble the ocean tholeiites but

have low Ni and Cr contents and are, in this respect, similar to calc-alkaline andesites.

The geochemistry of andesites [5] and the results of high pressure experimental work [6] suggest that calc-alkaline magmas are produced by the partial melting of ocean crust (or its high pressure equivalents) carried to great depths on descending lithosphere plates [7]. For this hypothesis to be valid it must also account for the gradual transition of magma type, with increasing depth, from tholeiitic to calc-alkaline. An examination of the partial melting of oceanic crust along appropriate geotherms should, therefore, be a means of testing this hypothesis.

### 2. Partial melting of oceanic crust

The composition and structure of oceanic crust are not known in detail but for the present purposes we will accept the model proposed by Cann [8]. In this model, layer 2 is composed of basaltic pillow lavas metamorphosed to greenschist facies at the base. Layer 3 comprises hornblende-bearing dykes giving way downwards to layered gabbros. As this crust begins its descent beneath an ocean trench the superficial sediments of layer 1 are probably scraped off [9] and the wet basalt of layer 2 will be transformed, through progressive metamorphism, to "dry" amphibolite. This discussion will be concerned,

therefore, with the fate of a 5 km-thick slab composed, in its upper layers, of amphibolite grading downwards into gabbro.

The melting relations of such a system are represented in fig. 1. The water-saturated solidus and liquidus curves for olivine tholeiite together with the stability field of hornblende in this rock are from Lambert and Wyllie [10, 11]. The dry tholeiite solidus was determined by Green and Ringwood [6]. There is some uncertainty as to the exact extent of the hornblende stability field [12] although the curves used are considered adequate for the present semi-quantitative model. Geotherms for the upper surface of the slab (Benioff zone) and for planes situated 1, 2 and 5 km below this surface have been calculated by Oxburgh and Turcotte [13] for a lithosphere plate descending at a rate of 9 cm per year. These geotherms are included in fig. 1 and are labelled 0, 1 km, 2 km and 5 km respectively.

From fig. 1 it is apparent that partial melting will

be confined to the top of the descending plate (i.e. within our 5 km slab of oceanic crust). It should also be noted that the potential for partial melting decreases with increasing depth down the Benioff zone. Geotherms for the upper levels of the slab pass rapidly through the wet melting interval at relatively shallow depths. The degree of melting here will be controlled by the water content of the amphibolite. At greater depths magmas will be generated from the lower layers of the crust where the geotherms tend to run parallel to the wet solidus. Magma generation will thus be slower in these regions. These theoretical considerations are supported by the observations of Sugimura et al. [3] that in Japan the volume of volcanic products decreases away from the volcanic front.

In addition to this downward decline in magma production the mechanisms governing partial melting will also vary. It is likely that all the water in the original ocean crust will be incorporated in amphibolite to give a "dry" assemblage. Consequently,

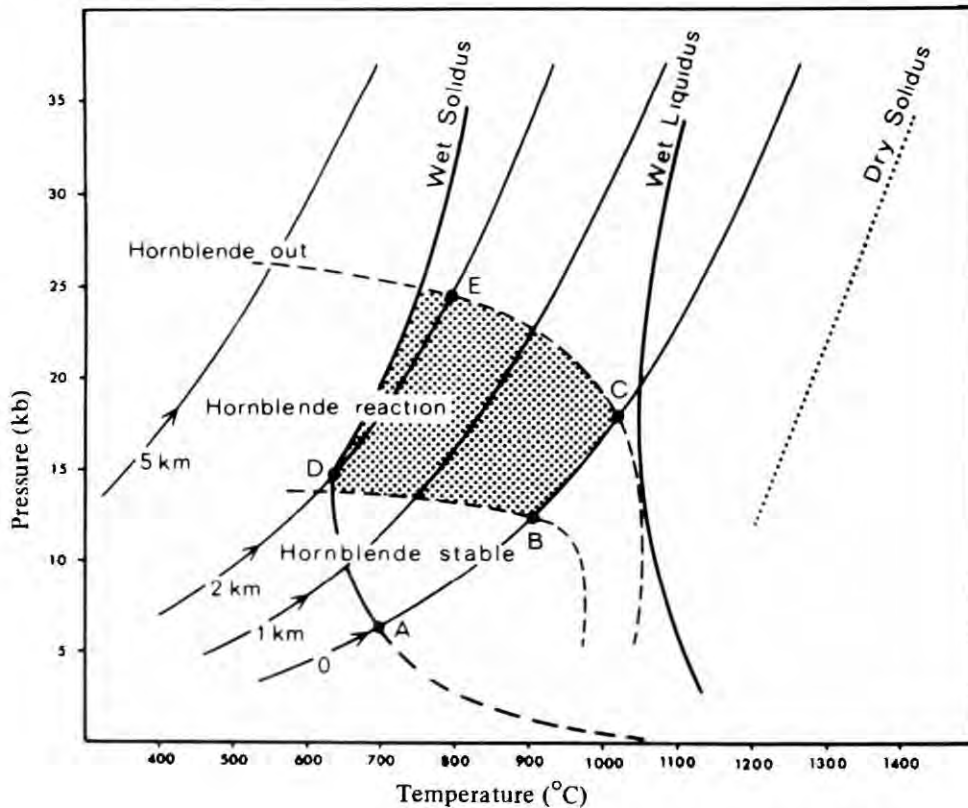


Fig. 1. Partial melting model for a descending slab of oceanic crust. Calculated geotherms [13] for the upper surface of the slab (0) and for points within the slab located 1, 2 and 5 km below this surface are shown. The stippled area represents the field in which magmas are generated by reactions involving amphibole breakdown. See text for further details.

melting of the surface layers of the slab will not occur at the wet solidus (point A on fig. 1) but will be postponed until the amphibole begins to break down (at B) releasing water. This retardation of melting has been observed experimentally by Brown [14] in granitic systems containing amphibole. Between B and C, amphibole will break down to give a water-saturated melt and a granulite residuum.

At deeper levels in the slab, melting will be less influenced by amphibole breakdown. Along the 2 km geotherm, for example, melting will begin at point D. From D to E, dehydration of amphibole will generate a water-rich fluid phase and a small volume of water-saturated silicate melt. Beyond E, the aqueous phase will be used up in the generation of more silicate melt. At still deeper levels amphibolite will transform to a garnet-pyroxene-water assemblage before melting begins [15].

The P–T field in which magmas will be produced by reactions involving amphibole breakdown is shown stippled in fig. 1 and in the diagrammatic section in fig. 2. With increasing depth this field gradually gives way to one in which magmas are generated by partial melting of wet eclogite. This will probably be accompanied by a progressive change in composition of the resulting magmas.

### 3. Composition of partial melts

Green and Ringwood [6] have demonstrated experimentally that partial fusion of wet or dry quartz eclogite will generate calc-alkaline magmas. In the model depicted in fig. 2 these magmas will be formed at depths greater than about 75 km. At shallower depths than this, melting will take place to a greater degree, especially in the upper layers of the slab. Since partial melting is essentially the reverse of fractional crystallisation, the magmas produced here will tend to be more basaltic than those produced lower down the Benioff zone.

Experimental data bearing on the composition of these basaltic magmas are lacking. The experiments of Yoder and Tilley [16] and Green and Ringwood (model II) [6] are not applicable since they were carried out at 10 kb or less and were thus largely within the field of amphibole stability (fig. 1). Wet partial melting under these conditions would leave an

amphibole-rich residuum whereas the liquids considered here would be produced by amphibole breakdown reactions. Nevertheless, it is possible to make a qualitative assessment of the composition of these magmas from a knowledge of the phases present in equilibrium with them.

Carmichael [17] has shown that the oxygen fugacity of liquids in equilibrium with amphibole will be buffered along a temperature– $f_{O_2}$  curve running parallel to, but at higher  $f_{O_2}$  than, the fayalite-magnetite-quartz buffer. The experimental data of Osborn [18] suggest that under these conditions fractional crystallisation (and presumably partial melting) of a basaltic parent will give rise to a magma suite showing iron enrichment. In this respect these magmas are analogous to the island arc tholeiitic series. At greater depth the increasing dominance of iron-rich garnet in the residuum will prevent marked iron enrichment in calc-alkaline magmas [6].

As the descending slab of ocean crust transforms to amphibolite the trace element geochemistry of the original ocean tholeiite will be inherited by the resulting amphibole. Consequently the trace element distribution in partial melts produced by the breakdown of this mineral will be partly governed by amphibole-liquid partition coefficients. Schnetzler and Philpotts [19] have determined these partition coefficients for the rare-earth elements and have shown that for amphiboles, the values for the individual members of the group are fairly constant and slightly less than unity. Consequently a liquid produced in equilibrium with amphibole in the descending slab will have a similar rare-earth distribution pattern (though slightly enriched) to the original tholeiite of the ocean crust.

At greater depths amphiboles will be replaced by an eclogite assemblage and the distribution pattern of partial melts will be controlled by equilibrium with garnet and pyroxene. The garnet molecule will incorporate heavy lanthanides (Gd–Lu) more readily than the lighter ones (La–Eu) [19] and so liquids in equilibrium with garnet will tend to be relatively enriched in the light rare-earths. This type of pattern is characteristic of calc-alkaline rocks. The rare-earth distribution patterns predicted by the present model are thus consistent with those observed in island arc magmas.

A similar argument has been used by Jakeš and

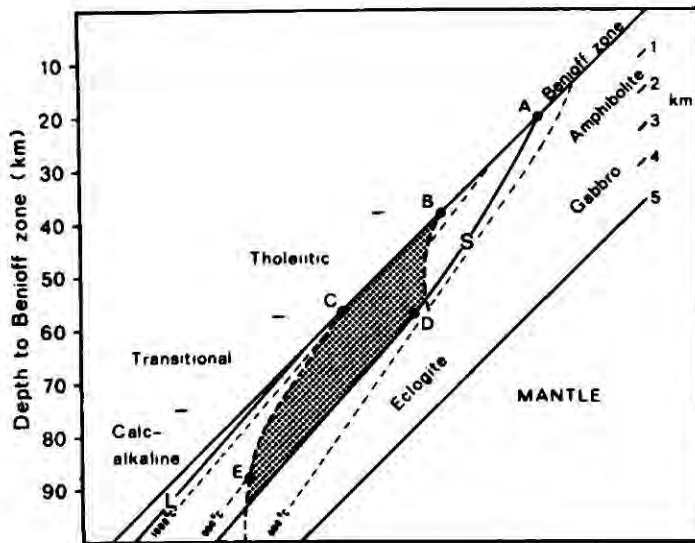


Fig. 2. Diagrammatic section through the descending slab to illustrate the melting relations. Curves S and L are the water-saturated solidus and liquidus curves (fig. 1) for olivine tholeiite [10, 11]. The stippled area and the labelled points are the same as in fig. 1. For clarity, the thickness of the slab has been exaggerated five times.

White [20] to explain variations in K/Rb ratio in island arcs. As noted earlier this ratio decreases with increasing depth to the Benioff zone. These authors suggest that, since K and Rb will not enter readily into garnet or pyroxene, the K/Rb ratio of a melt will reflect that of the phase undergoing partial melting. Thus rapid melting of amphibole (with high K/Rb) in the upper layers of the slab will give magmas with a similar ratio. At greater depths K and Rb will no longer be accommodated in amphibole, and phlogopite (with low K/Rb) may occur as a separate phase. Partial melting involving this phase will produce liquids with low K/Rb ratios. The decreasing ratio of melt to residuum with increasing depth, together with the inability of potassium to enter garnet and pyroxene, accounts for the observation that the  $K_2O$  content of magmas increases with increasing depth to the Benioff zone [2].

Finally, the low abundance of Ni and Cr in island arc tholeiites is consistent with their derivation from a mafic source, such as oceanic crust rather than an ultramafic source. Hypotheses involving a mantle origin for these rocks require extensive fractionation of olivine to reduce the abundance of these elements [4].

#### 4. Conclusions

The broad geochemical features of island arc volcanic rocks as outlined above are consistent with the hypothesis that they are derived by the partial melting of oceanic crust. Alternative mechanisms such as the derivation of island arc tholeiites by the reaction of these partial melts with mantle material above the Benioff zone [4], however, cannot be ruled out. Indeed, some equilibration with overlying mantle material would be expected in the early stages of island arc development. An assessment of the importance of this mechanism is, however, beyond the scope of the present paper.

The theoretical melting relations in a slab of oceanic crust are shown in fig. 2. As in fig. 1, the stippled area represents the field in which magmas are derived by amphibole breakdown reactions. In this model tholeiitic magmas are produced at depths of 40–60 km. From 60 to 75 km transitional magmas are developed and below 75 km the magmas are calc-alkaline.

These values are in general agreement with observed seismic zone depths in some island arcs. Thus in New Britain, tholeiitic volcanoes are associated with a concentration of earthquake foci at depths of 40 to 60 km [21]. In other arcs, however, tholeiitic magmas are associated with deeper seismicity. In Japan, for example, they occur in areas where the seismic zone is located at depths of about 100 km [1]. These discrepancies are not surprising in view of the uncertainties in the positions of some of the curves in fig. 1. Thus an increase in the upper stability limit of amphibole would extend the zone of tholeiitic magma generation to greater depths. There is some evidence to suggest that amphibole is more stable under water-deficient conditions [22] or in systems in which the activity of water is lowered by the presence of other volatiles [23]. Furthermore, magmas are not likely to be released from the slab as soon as they are generated but may well be carried to greater depths before they can escape to the surface.

So far, little mention has been made of the alkali basalt suite in island arcs. Unfortunately, phase relations at depths appropriate to the generation of these magmas (greater than 200 km) are not known.

It is, therefore, not possible to predict the behaviour of our model at these depths.

Finally, it must be emphasised that the model presented above involves a plate descending at a rate of 9 cm per year. Different rates of motion will still produce the same magmas but in different proportions. When more petrochemical data have been accumulated from island arc volcanics it may be possible to test the model further by correlating the volumes of the different magma types with the rate of sea-floor spreading.

#### Acknowledgements

The author is indebted to Prof. G.M. Brown, Dr. D.L. Hamilton and Dr. G.C. Brown for critically reading the manuscript. The financial support of N.E.R.C. is also gratefully acknowledged.

#### References

- [1] H. Kuno, Lateral variation in basalt magma type across continental margins and island arcs, *Can. Geol. Surv. Paper* 66-15 (1966) 317.
- [2] T. Hatherton and W.R. Dickinson, The relationship between andesitic volcanism and seismicity in Indonesia, the Lesser Antilles, and other island arcs, *J. Geophys. Res.* 74 (1969) 5301.
- [3] A. Sugimura, T. Matsuda, K. Chimzei and K. Nakamura, Quantitative distribution of late Cenozoic volcanic materials in Japan, *Bull. Volcanol.* 26 (1963) 125.
- [4] P. Jakeš and J. Gill, Rare earth elements and the island arc tholeiitic series, *Earth Planet. Sci. Letters* 9 (1970) 17.
- [5] S.R. Taylor, A.C. Capp, A.L. Graham and D.H. Blake, Trace element abundances in andesites II. Saipan, Bougainville and Fiji, *Contr. Mineral. Petrol.* 23 (1969) 1.
- [6] T.H. Green and A.E. Ringwood, Genesis of the calc-alkaline igneous rock suite, *Contr. Mineral. Petrol.* 18 (1968) 105.
- [7] B. Isacks, J. Oliver and L.R. Sykes, Seismology and the new global tectonics, *J. Geophys. Res.* 73 (1968) 5855.
- [8] J.R. Cann, New model for the structure of the ocean crust, *Nature* 226 (1970) 928.
- [9] J.F. Dewey and J.M. Bird, Mountain belts and the new global tectonics, *J. Geophys. Res.* 75 (1970) 2625.
- [10] I.B. Lambert and P.J. Wyllie, Stability of hornblende and a model for the low velocity zone, *Nature* 219 (1968) 1240.
- [11] I.B. Lambert and P.J. Wyllie, Melting in the deep crust and upper mantle and the nature of the low velocity layer, *Phys. Earth Planet. Interiors* 3 (1970) 316.
- [12] E.J. Essene, B.J. Hensen and D.H. Green, Experimental study of amphibolite and eclogite stability, *Phys. Earth Planet. Interiors* 3 (1970) 378.
- [13] E.R. Oxburgh and D.L. Turcotte, Thermal structure of island arcs, *Geol. Spc. Am. Bull.* 81 (1970) 1665.
- [14] G.C. Brown, A comment on the role of water in the partial fusion of crustal rocks, *Earth Planet. Sci. Letters* 9 (1970) 355.
- [15] N. Fry and W.S. Fyfe, Eclogites and water pressure, *Contr. Mineral. Petrol.* 24 (1969) 1.
- [16] H.S. Yoder and C.E. Tilley, Origin of basalt magmas: An experimental study of natural and synthetic rock systems, *J. Petrol.* 3 (1962) 342.
- [17] I.S.E. Carmichael, The iron-titanium oxides of salic volcanic rocks and their associated ferromagnesian silicates, *Contr. Mineral. Petrol.* 14 (1967) 36.
- [18] E.F. Osborn, Experimental aspects of calc-alkaline differentiation, in: *Proceedings of the Andesite Conference, Oregon, Dep. Geol. Mineral. Ind. Bull.* 65 (1969) 33.
- [19] C.C. Schnetzler and J.A. Philpotts, Partition coefficients of rare-earth elements between igneous matrix material and rock-forming mineral phenocrysts-II, *Geochim. Cosmochim. Acta* 34 (1970) 331.
- [20] P. Jakeš and A.J.R. White, K/Rb ratios of rocks from island arcs, *Geochim. Cosmochim. Acta* 34 (1970) 849.
- [21] G.G. Lowder, The volcanoes and caldera of Talasea, New Britain: Mineralogy, *Contr. Mineral. Petrol.* 26 (1970) 324.
- [22] R.W. Nesbitt and D.L. Hamilton, Crystallisation of an alkali-olivine basalt under controlled  $P_{O_2}$ ,  $P_{H_2O}$  conditions, *Phys. Earth Planet. Interiors* 3 (1970) 309.
- [23] R.E.T. Hill and A.L. Boettcher, Water in the earth's mantle: Melting curves of basalt-water and basalt-water-carbon dioxide, *Science* 167 (1970) 980.

REFERENCES CITED

- ANDERMANN, G. and KEMP, J.W. 1958. Scattered x-rays as internal standards in x-ray emission spectroscopy. *Analyt. Chem.* 30, 1306-1309.
- BAKER, P.E. 1968a. Comparative volcanology and petrology of the Atlantic island-arcs. *Bull. volcan.* 32, 189-209.
- \_\_\_\_ 1968b. Petrology of Mt. Misery Volcano, St. Kitt's, West Indies. *Lithos* 1, 124-150.
- BONNEY, T.G. 1885. On the so-called diorite of Little Knott (Cumberland), with further remarks on the occurrence of picrites in Wales. *Q. Jl geol. Soc. Lond.* 41, 511-522.
- BOYD, F.R. and ENGLAND, J.L. 1959. Pyrope. *Yb. Carnegie Instn. Wash.* 58, 83-89.
- BROWN, G.M. and SCHAIRER, J.F. 1968. Melting relations of some calc-alkaline volcanic rocks. *Ibid.* 66, 460-467.
- \_\_\_\_ and VINCENT, E.A. 1963. Pyroxenes from the late stages of fractionation of the Skaergaard intrusion, East Greenland. *J. Petrology* 4, 175-197.
- \_\_\_\_ EMELEUS, C.H., HOLLAND, J.G. and PHILLIPS, R. 1970. Petrographic, mineralogic, and x-ray fluorescence analysis of lunar igneous-type rocks and spherules. *Science* 167, 599-601.
- BROWN, P.E., MILLER, J.A. and SOPER, N.J. 1964. Age of the principal intrusions of the Lake District. *Proc. Yorks. geol. Soc.* 34, 311-342.
- BURNS, R.G. and FYFE, W.S. 1964. Site preference energy and selective uptake of transition metal ions from a magma. *Science* 144, 1001-1003.

- CARMICHAEL, I.S.E. 1964. The petrology of Thingmuli, a Tertiary volcano in eastern Iceland. *J. Petrology* 5, 435-460.
- \_\_\_\_ 1967. The iron-titanium oxides of salic volcanic rocks, and their associated ferromagnesian silicates. *Contr. Miner. Petrol.* 14, 36-64.
- \_\_\_\_ and NICHOLLS, J. 1967. Iron-titanium oxides and oxygen fugacities in volcanic rocks. *J. geophys. Res.* 72, 4665-4687.
- CHAYES, F. 1963. Relative abundance of intermediate members of the oceanic basalt-trachyte association. *Ibid.* 68, 1519-1534.
- \_\_\_\_ 1969a Experimentation in the electronic storage and manipulation of large numbers of rock analyses.  
*Yb. Carnegie Instn. Wash.* 68, 174-186.
- \_\_\_\_ 1968b. The chemical composition of Cenozoic andesites. In McBirney, A.R. (Ed.): *Proceedings of the Andesite Conference.* Oregon Dept. Geol. Mineral Ind. Bull. 65, 1-11.
- DEAN, W.T. 1963. The Stile End Beds and Drygill Shales (Ordovician) in the east and north of the English Lake District.  
*Bull. Br. Mus. nat. Hist. Geol.* 9, 49-65.
- DICKINSON, W.R. and HATHERTON, T. 1967. Andesite volcanism and seismicity around the Pacific. *Science* 157, 801-803.
- EASTWOOD, T., HOLLINGWORTH, S.E., ROSE, W.C.C. and TROTTER, F.M. 1968. *Geology of the country around Cockermouth and Caldbeck.* Mem. geol. Surv. U.K.
- FIRMAN, R.J. 1956. Garnets in the Borrowdale Volcanic Series. *Geol. Mag.* 93, 435-436.

- FITTON, J.G. 1971. The generation of magmas in island arcs. *Earth planet. Sci. Lett.* 11, 63-67.
- \_\_\_\_\_ and GILL, R.C.O. 1970. The oxidation of ferrous iron in rocks during mechanical grinding. *Geochim. cosmochim. Acta.* 34, 518-524.
- \_\_\_\_\_ and HUGHES, D.J. 1970. Volcanism and plate tectonics in the British Ordovician. *Earth planet. Sci. Lett.* 8, 223-228.
- FLANAGAN, F.J. 1969. U.S. Geological Survey standards - II. First compilation of data for the new U.S.G.S. rocks. *Geochim. cosmochim. Acta.* 33, 81-120.
- FLEISCHER, M. 1969. U.S. Geological Survey standards - I. Additional data on rocks G-1 and W-1, 1965-1967. *Ibid.* 33, 65-79.
- FRONDEL, C. 1971. Scandium-rich minerals from rhyolite in the Thomas Range, Utah. *Am. Miner.* 55, 1058-1060.
- GEORGE, T.N. 1963. Palaeozoic growth of the British Caledonides. In Johnson, M.R.W. and Stewart, F.H. (Eds.): *The British Caledonides*. Edinburgh: Oliver and Boyd. 1-33.
- GILL, J.B. 1970. Geochemistry of Viti Levu, Fiji, and its evolution as an island arc. *Contr. Miner. Petrol.* 27, 179-203.
- GOLDSCHMIDT, V.M. 1954. *Geochemistry*. Oxford Univ. Press. 730 pp.
- GREEN, J.F.N. 1915. The garnets and streaky rocks of the English Lake District. *Mineralog. Mag.* 17, 207-217.
- GREEN, T.H. and RINGWOOD, A.E. 1968a. Origin of garnet phenocrysts in calc-alkaline rocks. *Contr. Miner. Petrol.* 18, 163-174.
- \_\_\_\_\_ 1968b. Genesis of the calc-alkaline igneous rock suite. *Ibid.* 18, 105-162.

- HADFIELD, G.S. and WHITESIDE, H.G.M. 1936. The Borrowdale Volcanic Series of High Rigg and the adjoining Low Rigg Microgranite. Proc. Geol. Ass. 47, 42-64.
- HÄKLI, T.A. and WRIGHT, T.L. 1967. The fractionation of nickel between olivine and augite as a geothermometer. Geochim. cosmochim. Acta 31, 877-884.
- HAMILTON, D.L. BURNHAM, C.W. and OSBORN, E.F. 1964. The solubility of water and effects of oxygen fugacity and water content on crystallisation in mafic magmas. J. Petrology 5, 21-39.
- HANCOX, E.G. 1934. The Haweswater Dolerite, Westmorland. Proc. Lpool geol. Soc. 16, 173-197.
- HARKER, A. 1895. Carrock Fell. A study in the variation of igneous rock masses. Part II The Carrock Fell Granophyre. Part III The Grainsgill Greisen. Q. J. geol. Soc. Lond. 51, 125-148.
- HARTLEY, J.J. 1925. The succession and structure of the Borrowdale Volcanic Series as developed in the area lying between the Lakes of Grasmere, Windermere and Coniston. Proc. Geol. Ass. 36, 203-226.
- \_\_\_\_ 1932. The volcanic and other igneous rocks of Great and Little Langdale, Westmorland. Ibid. 43, 32-69.
- \_\_\_\_ 1942. The geology of Helvellyn and the southern part of Thirlmere. Q. J. geol. Soc. Lond. 97, 129-162.
- HATHERTON, T. and DICKINSON, W.R. 1969. The relationship between andesitic volcanism and seismicity in Indonesia, the Lesser Antilles, and other island arcs. J. geophys. Res. 74, 5301-5310.

- HEDGE, C.E. 1971. Nickel in high-alumina basalts.  
*Geochim. cosmochim. Acta* 35, 522-524.
- HEINRICH, K.F.J. 1966. X-ray absorption uncertainty.  
 In McKinley, T.D., Heinrich, K.F.J. and Wittry, D.B. (Eds.):  
*The Electron Microprobe*. New York: John Wiley. 296-377.
- HESS, H.H. 1962. History of ocean basins. In Engel, A.E.J.,  
 James, H.L. and Leonard, B.F. (Eds.): *Petrologic studies:*  
 a volume in honor of A.F. Buddington. *Geol. Soc. Am.*, 599-620.
- HSU, L.C. 1968. Selected phase relationships in the system  
 Al-Mn-Fe-Si-O-H: a model for garnet equilibria.  
*J. Petrology* 9, 40-83.
- ISACKS, B., OLIVER, J. and SYKES, L.R. 1968. Seismology and the  
 new global tectonics. *J. geophys. Res.* 73, 5855-5899.
- JEFFREYS, H. 1929. *The Earth: its origin, history and physical  
 constitution*. Cambridge Univ. Press. 420 pp.
- JAKEŠ, P. and GILL, J. 1970. Rare earth elements and the island  
 arc tholeiitic series. *Earth planet. Sci. Lett.* 9, 17-28.
- \_\_\_\_\_ and WHITE, A.J.R. 1970. K/Rb ratios of rocks from island arcs.  
*Geochim. cosmochim. Acta* 34, 849-856.
- KANAMORI, H. 1963. Study on the crust-mantle structure in Japan,  
 part 2, Interpretation of the results obtained by seismic  
 refraction studies in connection with the study of gravity  
 and laboratory experiments. *Earthquake Res. Inst. Bull.* 41,  
 761-779.
- KEESMANN, I., MATTHES, S., SCHREYER, W. and SEIFERT, F. 1971.  
 Stability of Almandine in the system  $\text{FeO}-(\text{Fe}_2\text{O}_3)-\text{Al}_2\text{O}_3-\text{SiO}_2-(\text{H}_2\text{O})$

- at elevated pressures. *Contr. Miner. Petrol.* 31, 132-144.
- KUNO, H. 1966. Lateral variation of basalt magma across continental margins and island arcs. *Bull. volcan.* 29, 195-222.
- \_\_\_\_ 1968. Differentiation of basaltic magmas. In Hess, H.H. and Poldervaart, A. (Eds.): *Basalts*, 2. New York: Interscience Publishers. 623-688.
- KUSHIRO, I. 1969. The system forsterite-diopside-silica with and without water at high pressures. *Am. J. Sci.* 267-A (Schairer Vol.), 269-294.
- LAMBERT, I.B. and WYLLIE, P.J. 1970. Melting in the deep crust and upper mantle and the nature of the low velocity layer. *Phys. Earth planet. Inter.* 3, 316-322.
- LOWDER, G.G. 1970. The volcanics and caldera of Talasea, New Britain: Mineralogy. *Contr. Miner. Petrol.* 26, 324-340.
- \_\_\_\_ and CARMICHAEL, I.S.E. 1970. The volcanoes and caldera of Talasea, New Britain: Geology and Petrology. *Bull. geol. Soc. Am.* 81, 17-38.
- MILLER, A.J. 1962. The potassium-argon ages of the Skiddaw and Eskdale granites. *Geophys. J. R. astro. Soc.* 6, 391-393.
- MINEAR, J.W. and TOKSÖZ, M.N. 1970. Thermal regime of a downgoing slab and new global tectonics. *J. geophys. Res.* 75, 1397-1419.
- MITCHELL, G.H. 1929. The succession and structure of the Borrowdale Volcanic Series of Troutbeck, Kentmere, and the western part of Long Sleddale. *Q. J. geol. Soc. Lond.* 85, 9-44.
- \_\_\_\_ 1934. The Borrowdale Volcanic Series of the country between Long Sleddale and Shap. *Ibid.* 90, 418-444.

- \_\_\_\_ 1940. The Borrowdale Volcanic Series of Coniston, Lancashire.  
Ibid. 96, 301-319.
- \_\_\_\_ 1956a. The geological history of the Lake District.  
Proc. Yorks. geol. Soc. 30, 407-463.
- \_\_\_\_ 1956b. The Borrowdale Volcanic Series of the Dunnerdale Fells,  
Lancashire. Lpool Manchr geol. J. 1, 428-449.
- \_\_\_\_ 1957. Ordovician volcanoes. Advmt. Sci. 14, 34-47.
- \_\_\_\_ 1963. The Borrowdale Volcanic rocks of the Seathwaite Fells,  
Lancashire. Lpool Manchr geol. J. 3, 289-300.
- MIYASHIRO, A. 1955. Pyralspite garnets in volcanic rocks.  
J. geol. Soc. Japan 61, 463-470.
- MOSELEY, F. 1960. The succession and structure of the Borrowdale  
Volcanic rocks south-east of Ullswater. Q. Jl geol. Soc. Lond.  
116, 55-84.
- \_\_\_\_ 1964. The succession and structure of the Borrowdale Volcanic  
rocks north-west of Ullswater. Geol. J. 4, 127-142.
- NAGASAWA, H. 1970. Rare earth concentrations in zircons and apatites  
and their host dacites and granites. Earth planet. Sci. Lett. 9,  
359-364.
- NORMAN, J.C. and HASKIN, L.A. 1968. The geochemistry of Sc: a  
comparison to the rare earths and Fe. Geochim. cosmochim. Acta  
32, 93-108.
- NORRISH, K. and CHAPPELL, B.W. 1967. X-ray fluorescence spectrography.  
In Zussman, J. (Ed.): Physical Methods of Determinative Mineralogy.  
London: Academic Press. 161-214.

- NUTT, M.J.C. 1970. The Borrowdale Volcanic Series and associated rocks around Haweswater, Westmorland. Unpubl. Ph.D. Thesis, Queen Mary College. Univ. of London.
- OLIVER, R.L. 1954. Welded tuffs in the Borrowdale Volcanic Series, English Lake District, with a note on similar rocks in Wales. *Geol. Mag.* 91, 473-485.
- \_\_\_\_ 1956. The origin of garnets in the Borrowdale Volcanic Series and associated rocks, English Lake District. *Ibid.* 93, 121-139.
- \_\_\_\_ 1961. The Borrowdale Volcanic and associated rocks of the Scafell area. English Lake District. *Q. Jl geol. Soc. Lond.* 117, 377-417.
- OSBORN, E.F. 1959. Role of oxygen pressure in the crystallisation and differentiation of basaltic magma. *Am. J. Sci.* 257, 609-647.
- \_\_\_\_ 1969. Genetic significance of V and Ni content of andesites: comments on a paper by Taylor, Kaye, White, Duncan and Ewart. *Geochim. cosmochim. Acta* 33, 1553-1554.
- PHILPOTTS, J.A. and SCHNETZLER, C.C. 1970. Phenocryst-matrix partition coefficients for K, Rb, Sr and Ba with applications to anorthosite and basalt genesis. *Ibid.* 34, 307-322.
- PIWINSKII, A.J. 1968. Experimental studies on igneous rock series: Central Sierra Nevada Batholith, California. *J. Geol.* 76, 548-570.
- REEVES, M.J. 1971. A statistical approach to matrix corrections in X-ray fluorescence. *Proc. 7th X-ray Analytical Conference*, Durham, 1970. (in press).

- RICKWOOD, P.C. 1968. On recasting analyses of garnets into end-member molecules. *Contr. Miner. Petrol.* 18, 175-198.
- SCHNETZLER, C.C. and PHILPOTTS, J.A. 1970. Partition coefficients of rare-earth elements between igneous matrix material and rock-forming mineral phenocrysts - II. *Geochim. cosmochim. Acta* 34, 331-340.
- SHAW, D.M. 1968. A review of K-Rb fractionation trends by covariance analysis. *Ibid.* 32, 573-601.
- SORBY, H.C. 1880. On the structure and origin of non-calcareous stratified rocks. *Q. Jl geol. Soc. Lond.* 36, Proc. 46-92.
- STRENS, R.G.J. 1962. The geology of the Borrowdale-Honister district (Cumberland), with special reference to the mineralization. Unpubl. Ph. D. Thesis, Univ. of Nottingham.
- SWEATMAN, T.R. and LONG, J.V.P. 1969. Quantitative electron-probe microanalysis of rock-forming minerals. *J. Petrology* 10, 332-380.
- THOMAS, H.H. 1911. The Skomer Volcanic Series (Pembrokeshire). *Q. Jl geol. Soc. Lond.* 67, 175-214.
- TAYLOR, S.R. and WHITE, A.J.R. 1965. Geochemistry of andesites and the growth of continents. *Nature* 208, 271-273.
- \_\_\_\_ CAPP, A.C., GRAHAM, A.L. and BLAKE, D.H. 1969a. Trace element abundances in andesites II. Saipan, Bougainville and Fiji. *Contr. Miner. Petrol.* 23, 1-26.
- \_\_\_\_ KAYE, M., WHITE, A.J.R., DUNCAN, A.R. and EWART, A. 1969b. Genetic significance of Co, Cr, Ni, Sc and V content of andesites. *Geochim. cosmochim. Acta* 33, 275-286.

- WADGE, A.J., NUTT, M.J.C., LISTER, T.R. and SKEVINGTON, D. 1969.  
A probable Didymograptus murchisoni zone fauna from the Lake District. *Geol. Mag.* 106, 595-598.
- WAGER, L.R. 1962. Igneous cumulates from the 1902 eruption of Soufrière, St. Vincent. *Bull. volcan.* 24, 93-99.
- \_\_\_\_\_ and BROWN, G.M. 1967. Layered Igneous Rocks. London: Oliver and Boyd. 588 pp.
- WARD, J.C. 1876. The geology of the northern part of the English Lake District. *Mem. geol. Surv. U.K.*
- WYLLIE, P.J. 1963. Effects of the changes in slope occurring on liquidus and solidus paths in the system  $\text{di}^{\text{c}}\text{pside-anorthite-albite}$ . *Spec. Pap. mineralog. Soc. Am* 1, 204-212.
- YODER, H.S., Jr. 1955. Role of water in metamorphism. *Spec. Pap. geol. Soc. Am.* 62, 505-524.
- \_\_\_\_\_ 1971. Contemporaneous rhyolite and basalt. *Yb. Carnegie Instn. Wash.* 69, 141-145.
- \_\_\_\_\_ and CHINNER, C.A. 1960. Almandine-pyrope-water system at 10,000 bars. *Ibid.* 59, 81-84.
- \_\_\_\_\_ and TILLEY, C.E. 1962. Origin of basaltic magmas: an experimental study of natural and synthetic rock systems. *J. Petrology* 3, 342-532.
- ZIEGLER, A.M., MCKERROW, W.S., BURNE, R.V. and BAKER, P.E. 1969. Correlation and environmental setting of the Skomer Volcanic Group, Pembrokeshire. *Proc. Geol. Ass.* 80, 409-439.

APPENDICESAPPENDIX 1.

The oxidation of ferrous iron in rocks during mechanical grinding.

(Fitton and Gill, 1970).

*Reprinted from*

Geochimica et Cosmochimica Acta, 1970, Vol. 34, pp. 518 to 524. Pergamon Press. Printed in Northern Ireland

**The oxidation of ferrous iron in rocks during mechanical grinding**

J. G. FITTON and R. C. O. GILL

Department of Geology, University of Durham, Durham, England

*(Received 3 November 1969; accepted 3 December 1969)*



**PERGAMON PRESS**  
OXFORD NEW YORK LONDON PARIS

## The oxidation of ferrous iron in rocks during mechanical grinding

J. G. FITTON and R. C. O. GILL

Department of Geology, University of Durham, Durham, England

(Received 3 November 1969; accepted 3 December 1969)

**Abstract**—Experiments are described which demonstrate considerable atmospheric oxidation of ferrous iron in hydrous igneous rocks during routine grinding in a disc mill prior to chemical analysis. The causes and implications of this oxidation are discussed.

### INTRODUCTION

THE SUSCEPTIBILITY of ferrous iron in rocks and minerals to non-quantitative oxidation during analysis is well established, and has received much attention from analysts over many years. The diversity of techniques by which this tendency can be suppressed has been covered in a recent review by SCHAFER (1966). In contrast, awareness among authors of the effects of sample preparation on the apparent oxidation status seems to be limited, and on the rare occasions when mention is made the reference is usually to practices accepted before mechanical methods of sample reduction became widespread.

The effect of the various methods of sample preparation on ferrous iron content is twofold:

(i) Contamination can arise from particles of metallic iron derived from milling equipment. This has only recently been examined by RITCHIE (1968). Errors become significant when comparisons are made between different laboratories and various methods, but otherwise the effect is relatively trivial.

(ii) Atmospheric oxidation of ferrous iron is possible during milling, particularly in the last stages when the powder is fine and local temperatures are high. This can be far more severe with some rocks than is commonly accepted, and the evaluation of such errors is the primary object of this note.

It has long been the practice among reputable analysts to carry out determinations of the oxidation status of a rock only on a coarsely ground (but representative) batch of fragments set aside for the purpose. This precaution can be traced back to the observation by MAUZELIUS (1907) that significant oxidation of most rocks could be brought about by very fine milling. It is interesting to note that up to this time the use of extremely fine powders had been advocated by such authorities as HILLEBRAND and WASHINGTON in the interests of the rapid solution of the material. In later publications, however, both authors adopt the cautionary tone set by MAUZELIUS (HILLEBRAND, 1908; WASHINGTON, 1919), although their recommendations differ in detail.

From the accounts given by these authors, it is clear that significant oxidation occurred only after crushing or grinding for long periods, usually much greater than half an hour. It is important to recognise that these times are not directly comparable

with milling times in modern mechanical equipment. In view of the high efficiency of modern methods, and the demand for fine powder imposed by rapid instrumental methods of analysis, there are good grounds for a review of the situation.

### TECHNIQUE

The mill used in these experiments was a Tema Laboratory Disc Mill model T 100 with a tungsten carbide Widia grinding barrel. The barrel was sealed with a smooth rubber gasket. The conditions were those routinely used in these laboratories, except for the method of repeated sampling described below.

All experiments were carried out on  $100.0 \pm 0.5$  g of rock chips (less than 1 cm in size) produced by a mechanical jaw crusher. Two sampling methods were adopted. The first consisted of grinding separate 100-g samples of the same rock continuously for three and six minutes respectively. The results of this method define the broken line of Fig. 1.

The continuous line of Fig. 1 and all the data of Fig. 2 were derived by the alternative method which was designed to allow effectively free access of air and frequent sampling. In this method, the grinding process was interrupted at the intervals shown in Fig. 2 to permit the abstraction of a representative sample of approximately 1 g. The time axis of the graphs records the grinding times exclusive of sampling intervals.

All the ferrous iron measurements were obtained by the oxidising-decomposition method of WILSON (1955). The water determinations were carried out by the RILEY (1958) method. For this purpose, the sample extracted after three minutes of grinding was chosen to represent each specimen, and all such samples were dried for several hours at  $110^{\circ}\text{C}$  prior to water determination.

### RESULTS

Figure 1 shows the results of experiments carried out on one rock, No. 12 in Table 1. The continuous line is the outcome of grinding interrupted at the times shown to allow sampling and the admission of fresh air. The line therefore approximates closely to the oxidation pattern in an abundant excess of air. The point

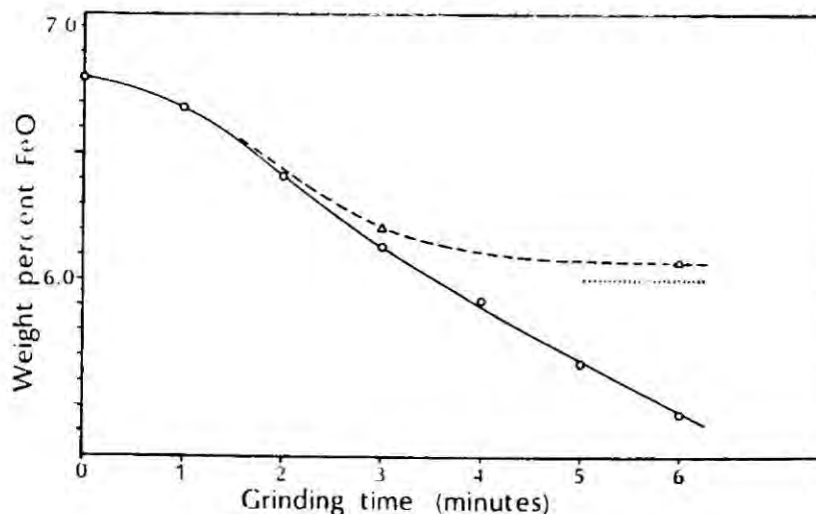


Fig. 1. The variation in FeO content with time of grinding for specimen No. 12.

The unbroken line shows the result of repeated sampling as described in the text. The broken line represents experiments in which samples were ground continuously in the sealed mill for the times shown. The theoretical limit of oxidation under the latter conditions is shown by the dotted line.

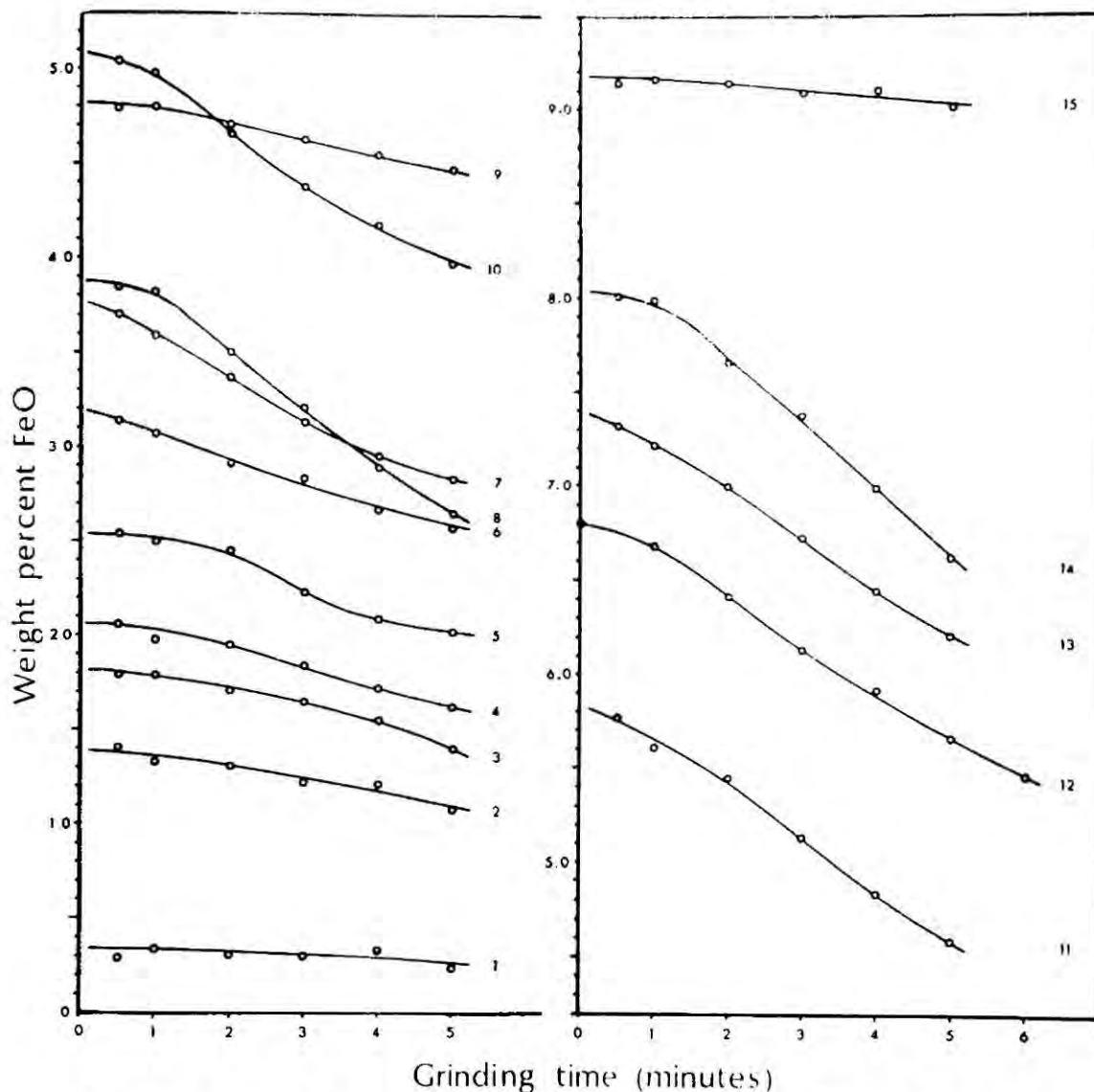


Fig. 2. "Loss curves" for the rocks described in the table. Open circles denote grinding with effectively free access of air (see text). The dark circle (rock No. 12 only) represents brief hand grinding under acetone.

appearing at zero grinding time was obtained from fragments ground briefly by hand under acetone in an agate pestle and mortar, and therefore represents the best possible estimate of the true FeO value.

Besides illustrating the degree of oxidation which can occur in circumstances which favour it, the curve has two features which are notable. The slight initial slope, which probably represents the rapid-breaking first phase of grinding during which little heat is generated, steepens into a region of maximum slope. This appears to be the upper part of a hyperbolic decay curve; the asymptotic character is more pronounced in other specimens studied.

The points shown by triangles identify two runs of continuous grinding for the times shown without admission of air beyond the amount present in the mill at the

Table 1

Specimen	Rock type	Locality	FeO-bearing mineral assemblage*	Initial % FeO (extrapolated)	% H <sub>2</sub> O <sup>+</sup>
1	Trachyte	S.W. Greenland	Bi	0.34	4.65
2	Granite	Aberdeen	Bi(-O)	1.39	0.70
3	Rhyodacite	Lake District	Chl-Am-O(-Gt)	1.82	1.55
4	Microsyenite	S.W. Greenland	Bi	2.06	0.80
5	Dacite tuff	Lake District	Chl-Am-O(-Gt)	2.54	1.60
6	Dacite tuff	Lake District	Chl-Am-O(-Gt)	3.20	1.95
7	Andesite tuff	Lake District	Chl-O	3.78	2.20
8	Dacite pitchstone	Lake District	Chl-O†	3.88	2.00
9	Eucrite	Ardnamurchan	Ol-Cpx-Bi	4.82	1.10
10	Andesite	Lake District	Chl-O	5.08	3.38
11	Foyaite	S.W. Greenland	Bi-Am	5.84	1.27
12	Basalt	Lake District	Chl-Cpx-O	6.80	2.90
13	Basalt tuff	Lake District	Chl-Cpx-O	7.40	3.80
14	Trachyte	S.W. Greenland	Bi-Chl-O	8.04	2.00
15	Olivine basalt	Iceland	Cpx-Ol-O	9.18	0.20

\* Am = amphibole, Bi = biotite, Chl = chlorite, Cpx = clinopyroxene, Gt = garnet, O = opaque oxides, Ol = olivine.

Minerals arranged in order of abundance with minor phases in parenthesis.

† FeO is also present in the brown devitrified groundmass.

outset. Clearly the one-minute open circle also represents the result of an experiment of this type, and one can therefore draw through these three points a line (shown broken), comparable with the unbroken one, which describes the oxidation characteristic when the only air available is that defined by the volume of the milling vessel.

The divergence between the broken and unbroken curves demonstrates the limiting effect imposed by the quantity of oxygen available in the sealed milling vessel. A theoretical limit can be calculated from the known volume of the mill and this is represented by the dotted line in Fig. 1. The agreement with the declining rate of oxidation is obvious, and the oxidation is therefore undoubtedly atmospheric.

In the experiments described below, which provide the data for Fig. 2, the repeated admission of air to the mill when samples are being extracted is assumed to correspond, to all intents and purposes, to the ideal situation in which oxygen is freely available at all times. The data of Fig. 1 demonstrate that the assumption holds good for nearly all the curves. On the other hand, limitation of the oxidation in this manner can be significant at the continuous grinding times used in routine work with this equipment. This fact may find application as a means of correcting for ferrous iron loss when it is known to be large and long grinding times are used. A simple correction can be derived from the volume of the mill, the weight of rock used and the measured FeO content.

Figure 2 summarises the results of comparative experiments on fifteen rocks of widely varying composition, carried out with repeated admission of air. Comparison immediately shows a broad correlation between the amount of FeO lost and the initial ferrous iron content. This is difficult to evaluate because the loss curves are by no means linear and vary with a number of uncontrollable factors. Nevertheless some representation of susceptibility to oxidation has been attempted, and its relationship to the initial FeO content is shown in Fig. 3.

The function used is the area bounded by the loss curve in question, a horizontal line intercepting it at the five-minute stage, and the vertical axis. This area function has been found suitable on an empirical basis for the following reasons:

(i) The initial plateau present on some curves is given a low weighting in the final value. This is appropriate because it is regarded as a function only of rock hardness.

(ii) Cases of rapid but short-lived oxidation are distinguished from those in which oxidation begins late or proceeds slowly, but shows no sign of abating at five minutes. Taking simple differences in FeO values does not achieve this distinction.

(iii) Taking some slope function would only emphasise differences in the rate of reaction, which in itself is not the object of the present investigation.

Three distinct groups emerge from Fig. 3. Most of the rocks fall on a common trend running from No. 1 to No. 14. It is significant that all such rocks have chlorite or biotite as the principal ferrous iron-bearing phase. Accordingly they all contain significant amounts of combined water, but no correlation emerges beyond this qualitative one.

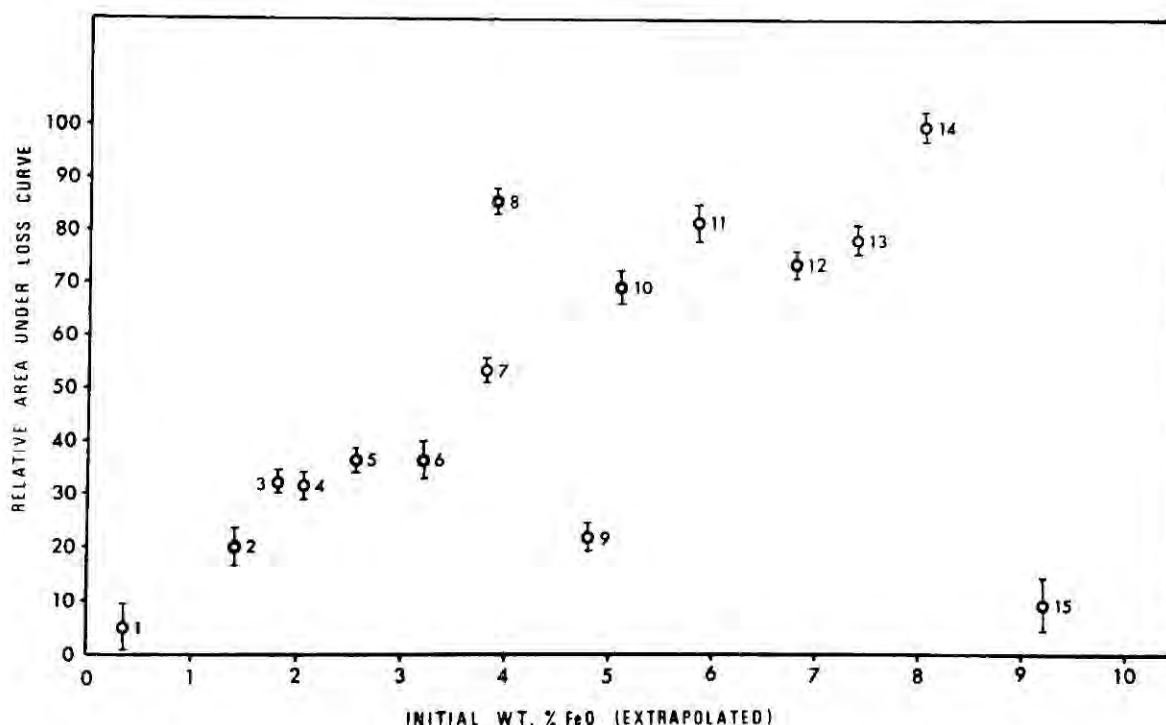


Fig. 3. Relative area under each loss curve, expressed as a percentage of the greatest (No. 14), plotted against initial weight percent FeO (extrapolated).

Statistical uncertainty is shown by the vertical lines through the data points. The vertical extent is equal to twice the area of a hypothetical rectangle in Fig. 2 whose base is five minutes, and whose height is equal to the standard deviation of data points about the loss curve or the estimated analytical standard deviation, whichever is the larger.

Two rocks appear to have the power to resist oxidation on the scale shown by the main trend. This power is almost total in No. 15, an olivine basalt having no microscopically visible trace of any hydrous mineral phase. Specimen 9 is more readily oxidised but nevertheless stands apart from the main trend. In this rock, a eucrite, the ferrous iron resides mainly in fresh olivine and pyroxene, but minor biotite is also present. The intermediate position of this rock in Fig. 3 lends some weight to the influence of biotite (and, by analogy, chlorite) in determining susceptibility to oxidation.

Specimen 8, a porphyritic pitchstone containing a few small chlorite pseudomorphs after pyroxene, shows higher loss relative to initial FeO than any other rock in the experiment. In this rock, however, it is probable that a major part of the ferrous iron resides in the devitrified groundmass, conceivably in incipient chlorite. It is not unreasonable to ascribe the anomalous rate of oxidation to the extremely fine state of division of the groundmass iron-bearing phases.

The relationship between these three groups points to a pattern of oxidation strongly dependent on mineralogical constitution. This is supported by the forms of some of the loss curves which (Fig. 2, Nos. 5, 7, 10) show exponential decline towards asymptotes situated at fairly high levels of ferrous iron content. It is reasonable to suppose that such limits are determined by the proportion of minerals resistant to oxidation. It appears from the limited experiments described here that certain hydrous silicates are very susceptible to oxidation, while other minerals maintain considerable resistance to it.

Since the emphasis of this work is petrological, tests on individual minerals have not been attempted. It is nevertheless clear that a very large proportion of the ferrous iron in biotite and chlorite (and possibly some amphiboles) can become oxidised by the atmosphere during rock grinding. TZVETKOV and VALYASHIKHINA (1956) have observed oxidation in biotite with extended grinding which is brought about by structural water, but this is not the dominant mechanism for the effects described here. Simple surface oxidation is a much more likely explanation, since the potential for the generation of new surface area with grinding is clearly very great with the layer silicates. Such a model does, however, require that the sheets are reduced to an extraordinary degree of fineness in order to account for the amount of oxidation observed in these experiments. In fact a simple calculation shows that the average thickness of such sheets after a few minutes of grinding can be only one order of magnitude greater than the depth of penetration of oxidation. Very fine division of these minerals brought about by the abrasive effect of the hard silicates present can be expected in the rocks studied. Nevertheless some mechanism may exist, possibly involving exchange with hydroxyl ions, whereby oxidation can penetrate to considerable depths below the surface.

The evidence presented here clearly precludes the use of powders produced by routine disc-milling for ferrous oxide determination in a large number of cases. When ferrous oxide must be determined very accurately (for example, for the evaluation of oxidation ratios) it is essential that a sample of the rock be ground very carefully by hand, preferably in a non-oxidising medium such as acetone. During the course of these experiments it has been found that rock samples removed from the disc mill after only 30 sec of grinding are usually fine enough for complete

solution in cold hydrofluoric acid, although oxide minerals sometimes present a problem. Such samples show only slight oxidation (Fig. 2) and could well be used for routine ferrous oxide determinations on most rocks.

*Acknowledgements*—We are indebted to Dr. C. H. EMELEUS for providing some of the rocks used in this work, and we should like to thank Prof. G. M. BROWN for critically reading the manuscript.

#### REFERENCES

- HILLEBRAND W. F. (1908) The influence of fine grinding on the water and ferrous-iron content of minerals and rocks. *J. Amer. Chem. Soc.* **30**, 1120–1131.
- MAUZELIUS R. (1907) On the determination of ferrous iron in rock analysis. *Sverig. Geol. Unders. Arsbok.* **1**, 11 pp.
- RILEY J. P. (1958) Simultaneous determination of water and carbon dioxide in rocks and minerals. *Analyst* **83**, 42–49.
- RITCHIE J. A. (1968) Effect of metallic iron from grinding on ferrous iron determinations. *Geochim. Cosmochim. Acta* **32**, 1363–1366.
- SCHAFFER H. N. S. (1966) The determination of iron(II) oxide in silicate and refractory materials. Part I. A review. *Analyst* **91**, 755–762.
- TZVETKOV A. I. and VALYASHIKHINA E. P. (1956) On the hydration and oxidation of micas. *Bull. Acad. Sci. URSS, Sér. Géol.* **5**, 74–83. (M.A. 13–396).
- WASHINGTON H. S. (1919) *Manual of the Chemical Analysis of Rocks*, 3rd edition, pp. 183–184. John Wiley.
- WILSON A. D. (1955) A new method for the determination of ferrous iron in rocks and minerals. *Bull. Geol. Surv. G.B.* **9**, 56–58.

APPENDIX 2

Trace-element concentrations (p.p.m.) in U.S.G.S. Standards determined for inter-laboratory comparison

	Ba	Nb	Zr	Y	Sr	Rb	Zn	Cu	Ni	Cr	V*	La*
W-1	-	9	95	23	195	26	99	118	84	138	240	10
G-1	-	18	177	13	255	228	71	14	3	14	16	97
AGV-1	-	11	257	21	745	80	90	57	19	-	121	33
GSP-1	1260	12	597	41	263	249	123	29	8	-	52	174
BCR-1	647	10	199	38	367	59	127	14	12	-	384	23
G-2	-	8	335	15	570	198	101	4	3	-	37	82
Detection limit (p.p.m.) **	10	3	3	3	3	3	2	3	2	5	5	2
Counting time (secs.)	20	40	40	40	40	40	100	100	100	40	100	100

- Not determined

\* Values used for calibration from Flanagan (1969); Fleischer (1969)

\*\* Calculated from background counting statistics (Norrish and Chappell, 1967)

APPENDIX 3.

Chemical analyses of rock samples.

Major-element analyses are expressed on a water- and carbon dioxide-free basis, normalised to 100% total.

(a) Southern outcrop.

\* Ignimbrites.

C Castle Head dolerite.

H Haweswater Complex.

M Minor intrusions.

	LD2	LD3	LD4	LD6	LD7	LD8	LD9	LD11	LD12	LD13
	*	*	*	*	*	*	*	*	*	*
PERCENT										
SI02	54.43	57.65	55.59	68.94	68.12	67.72	66.87	68.05	67.41	68.01
AL203	17.12	18.76	17.27	16.48	16.70	16.92	17.10	16.36	17.06	16.93
FE203	10.53	7.78	9.40	4.01	4.13	4.51	4.72	4.40	4.50	4.52
MGO	6.08	3.74	6.45	0.16	0.29	0.55	0.37	0.29	0.63	0.54
CAO	6.32	5.62	5.71	1.93	2.34	1.87	2.52	2.34	1.53	1.69
NA2O	2.14	2.70	2.16	2.81	2.76	2.82	2.57	2.84	2.63	3.05
K2O	1.67	2.36	1.83	4.88	4.80	4.79	5.01	4.96	5.35	4.43
TIO2	1.13	0.94	1.12	0.34	0.37	0.37	0.36	0.33	0.43	0.37
MNO	0.36	0.22	0.25	0.14	0.14	0.13	0.15	0.14	0.16	0.16
S	0.02	0.02	0.01	0.02	0.05	0.03	0.02	0.01	0.01	0.01
P205	0.20	0.19	0.20	0.29	0.29	0.27	0.30	0.27	0.28	0.28
PPM										
BA	194	594	495	879	896	863	1094	1120	1274	774
NB	11	17	12	25	22	23	20	18	20	22
ZR	164	217	177	360	367	377	374	351	354	366
Y	31	41	35	75	74	78	71	74	72	72
SR	150	302	432	117	110	109	126	121	129	111
RB	76	92	78	240	255	245	222	245	246	251
ZN	107	97	104	87	32	53	34	93	78	84
CU	3	13	32	3	0	14	3	0	8	0
NI	36	18	41	2	1	1	0	0	2	3
CR	149	63	160	0	1	2	1	0	5	5
V	164	116	172	4	7	8	4	4	12	13
LA	25			58	60	68	61	54	61	51

	LD14 *	LD24 M	LD34	LD37 *	LC38 *	LD39 *	LD40 *	LD49	LD50	LD54
PERCENT										
SI02	69.93	57.06	57.57	68.43	67.38	65.96	62.57	58.33	57.00	58.16
AL203	16.20	16.18	18.69	16.44	16.39	17.19	17.78	18.87	18.68	18.80
FE203	4.07	9.27	6.77	4.41	4.42	4.21	6.92	6.69	7.15	7.25
MGO	0.30	5.48	2.49	0.48	0.31	0.34	1.03	1.38	2.13	4.01
CAU	1.35	4.92	7.36	1.52	2.43	2.19	3.00	6.31	7.17	3.83
NA2O	4.75	2.96	2.78	2.76	2.62	4.79	3.23	3.24	3.69	4.04
K2O	2.70	2.55	2.82	5.17	5.55	4.50	4.13	3.62	2.54	2.46
TI02	0.27	1.09	1.08	0.34	0.38	0.37	0.70	1.12	1.11	1.01
MNO	0.13	0.24	0.21	0.15	0.14	0.13	0.24	0.19	0.20	0.23
S	0.01	0.01	0.02	0.03	0.04	0.01	0.01	0.02	0.08	0.01
P205	0.27	0.24	0.19	0.26	0.32	0.29	0.39	0.23	0.26	0.20
PPM										
BA	537	602	594	984	559	823	894	1004	862	662
NB	20	12	11	21	19	20	22	16	17	14
ZR	330	185	193	372	332	364	325	227	217	223
Y	70	39	39	71	66	66	71	44	40	42
SR	121	323	340	133	117	124	205	341	432	335
RB	143	77	122	251	263	220	195	144	86	146
ZN	29	106	73	74	70	64	39	74	77	91
CU	5	15	13	7	3	4	0	8	24	0
NI	2	8	11	1	1	3	3	8	6	22
CR	1	83	13	0	1	3	6	12	8	65
V	6	158	109	5	7	3	24	104	107	114
LA	60			59	63	62	47			

	LD56	LD57	LD58	LD59	LD60	LD61 #	LD62 #	LD65 M	LD67	LD68 #
PERCENT										
SI02	55.54	54.41	55.90	53.54	56.37	66.51	68.59	69.48	54.08	65.55
AL203	16.77	15.88	16.46	17.35	16.17	16.28	16.51	17.26	18.20	16.39
FE203	8.88	9.24	9.18	9.36	9.55	4.94	4.27	3.16	9.43	6.48
MGO	6.08	6.89	5.46	7.95	5.74	0.77	0.38	0.45	7.56	0.65
CAO	5.50	7.18	7.21	5.03	6.17	2.77	1.31	1.42	4.97	2.22
NA2O	1.79	1.38	1.71	2.74	1.51	2.44	2.27	2.40	1.47	2.14
K2O	3.98	3.48	2.55	2.43	2.74	5.34	5.92	5.12	2.84	5.32
TI02	1.07	1.07	1.09	1.04	1.13	0.45	0.32	0.29	1.09	0.67
MNO	0.22	0.27	0.23	0.34	0.40	0.18	0.15	0.10	0.21	0.22
S	0.01	0.02	0.04	0.01	0.02	0.03	0.02	0.01	0.01	0.02
P205	0.16	0.18	0.15	0.20	0.18	0.28	0.28	0.29	0.14	0.33
PPM										
BA	769	765	538	520	883	1046	1358	1137	643	1819
NB	12	13	13	10	10	17	20	20	13	20
ZR	176	178	174	182	172	319	360	229	180	304
Y	40	34	37	38	38	66	71	66	34	67
SR	257	271	257	273	240	132	133	103	272	220
RB	205	127	120	100	126	261	278	257	114	189
ZN	97	98	94	163	165	82	92	40	119	105
CU	30	100	32	3	87	7	9	2	44	1
NI	41	37	41	41	44	5	2	4	47	0
CR	149	155	136	158	148	11	0	8	154	55
V	167	154	159	162	175	23	4	8	176	9
LA						49	59	48		42

	LD69	LC70	LD126	LD128	LC129	LD130	LD131	LD132	LD133	LD135
PERCENT										
SI02	48.08	51.23	50.36	52.26	60.76	63.21	53.46	58.53	59.06	57.34
AL203	11.25	14.44	18.00	20.63	18.13	17.26	16.84	17.18	16.71	17.78
FE203	12.95	11.67	10.03	9.81	6.92	8.01	10.17	7.67	8.01	8.46
MGO	11.20	11.41	3.78	7.05	1.31	2.01	3.83	3.73	4.06	4.34
CAO	12.09	7.10	11.34	4.42	5.38	4.40	9.46	6.24	4.80	6.85
NA2O	0.83	1.22	1.62	3.11	3.69	2.80	1.77	1.71	2.19	2.09
K2O	1.41	0.60	3.08	1.09	2.65	1.15	2.69	3.32	3.53	1.67
TIO2	1.58	1.76	1.23	1.16	0.65	0.65	1.22	1.12	1.12	1.03
MNO	0.23	0.17	0.24	0.20	0.24	0.26	0.28	0.18	0.16	0.15
S	0.11	0.10	0.04	0.06	0.04	0.05	0.05	0.08	0.10	0.09
P205	0.28	0.31	0.23	0.15	0.17	0.13	0.19	0.19	0.20	0.15
PPM										
BA	221	0	236	380	475	444	745	723	676	408
NB	12	16	11	13	14	20	14	17	14	13
ZR	144	174	158	163	192	195	152	241	245	152
Y	21	24	33	31	44	42	30	40	45	27
SR	560	144	133	335	207	459	263	235	241	191
RB	44	9	112	38	124	47	104	140	148	66
ZN	83	91	103	142	121	109	96	90	94	101
CU	63	2	1	9	7	35	37	89	70	30
NI	242	220	128	69	0	0	170	55	59	49
CR	634	737	357	162	2	4	407	105	106	113
V	206	245	247	183	38	40	234	163	160	178
LA				26	33	32	25	38	38	24

	LD136	LD137	LD139	LD140	LD141	LD142	LD143	LD144	LD146	LD147
PERCENT										
SI02	59.58	57.68	54.25	62.37	57.83	58.25	58.58	59.52	62.21	48.41
AL203	16.18	20.89	22.06	18.14	20.16	19.65	19.77	19.51	18.71	15.50
FE203	7.89	6.62	7.23	5.97	7.26	8.11	7.47	6.90	4.53	13.62
MGO	5.52	1.77	3.20	2.49	3.20	3.04	2.46	1.82	1.87	7.81
CAO	5.65	6.00	3.99	3.63	2.96	5.71	3.30	2.76	3.25	11.12
NA2O	2.70	1.36	4.13	2.72	3.93	2.10	3.57	5.04	2.66	1.27
K2O	1.13	4.35	3.74	3.47	3.32	1.85	3.55	3.19	5.43	0.22
TIO2	0.87	0.92	0.86	0.69	0.88	0.75	0.82	0.80	0.88	1.14
MNO	0.18	0.14	0.21	0.18	0.15	0.21	0.19	0.17	0.15	0.52
S	0.10	0.07	0.09	0.12	0.10	0.09	0.08	0.08	0.10	0.15
P205	0.13	0.16	0.18	0.16	0.14	0.18	0.15	0.16	0.16	0.18
PPM										
BA	343	614	725	935	671	811	1040	745	2290	109
NB	12	12	14	13	13	13	15	10	14	7
ZR	143	221	263	204	189	226	213	211	220	98
Y	26	45	55	38	40	41	38	42	46	24
SR	252	166	263	255	288	266	288	279	224	224
RB	45	202	176	145	140	59	141	136	197	3
ZN	77	81	108	74	87	118	90	85	82	107
CU	45	13	6	6	25	11	14	9	2	74
NI	44	16	18	11	16	15	15	18	18	360
CR	93	31	46	31	55	38	46	46	32	916
V	150	106	121	96	132	105	114	113	73	276
LA				31				32		

	LC148	LC150*	LC152 <sup>M</sup>	LD153 <sup>M</sup>	LD155	LD156	LD158	LD159	LD160	LD162
PERCENT										
SI02	50.61	74.57	66.93	51.21	54.40	54.88	61.13	52.42	55.42	58.87
AL203	16.16	13.60	17.42	14.78	19.51	18.81	18.34	17.50	18.07	17.55
FE203	11.00	2.23	4.34	11.74	9.15	9.30	6.15	9.86	9.18	7.56
MGO	10.13	0.38	0.67	9.69	4.35	4.91	3.06	3.54	3.21	5.17
CAO	7.73	0.35	4.63	8.75	7.27	6.34	5.05	9.90	7.53	3.53
NA2O	1.26	1.13	2.03	1.97	1.92	1.99	2.85	2.55	2.56	2.35
K2O	1.58	7.07	3.19	0.20	1.75	2.12	1.87	2.36	2.48	3.36
TI02	0.94	0.35	0.36	0.99	1.10	1.11	1.05	1.17	0.95	1.01
MNO	0.26	0.05	0.13	0.26	0.21	0.19	0.16	0.26	0.25	0.19
S	0.12	0.06	0.05	0.18	0.13	0.14	0.14	0.17	0.13	0.19
P205	0.15	0.16	0.21	0.17	0.14	0.15	0.16	0.19	0.17	0.16
PPM										
BA	373	1321	294	228	361	448	1053	775	547	845
NB	6	14	14	6	13	15	10	11	10	13
ZR	90	234	260	98	141	146	220	167	161	183
Y	20	59	58	22	28	29	41	34	35	37
SR	210	80	134	183	271	253	386	168	252	238
RB	57	270	158	12	66	80	70	102	100	141
ZN	89	30	65	84	106	102	79	92	125	93
CU	59	11	3	70	49	19	119	108	6	23
NI	337	2	4	136	34	36	45	37	24	42
CR	863	2	6	601	76	71	125	123	118	157
V	224	12	26	237	201	190	154	173	176	159
LA	16	47		15						

	LD163	LD164	LD167	LD168 *	LD169 *	LD170 *	LD171	LD172	LD173	LD174
PERCENT										
SI02	58.45	52.40	60.47	72.17	72.59	73.21	58.71	57.09	54.75	63.15
AL203	18.19	17.66	16.92	13.42	14.83	14.84	19.74	17.25	16.49	16.43
FE203	7.75	11.43	6.91	3.85	2.71	3.15	7.07	8.77	9.93	7.64
MGO	4.25	5.99	1.60	1.21	0.53	1.01	2.20	5.79	5.73	1.75
CAO	3.36	8.63	6.38	1.33	0.53	0.16	5.56	4.48	6.89	3.15
NA2O	2.10	1.50	2.39	2.50	1.46	1.90	2.86	3.12	2.29	2.56
K2O	4.29	0.71	3.76	4.74	6.80	5.38	2.48	2.01	2.21	3.74
TIO2	1.01	0.99	1.01	0.37	0.27	0.25	0.80	0.88	0.92	0.79
MNO	0.21	0.28	0.16	0.09	0.04	0.02	0.17	0.23	0.35	0.20
S	0.20	0.21	0.11	0.09	0.06	0.07	0.17	0.16	0.22	0.17
P205	0.15	0.16	0.23	0.18	0.12	0.12	0.20	0.17	0.18	0.37
PPM										
BA	848	311	685	1077	1335	963	647	575	501	1044
NB	10	6	15	12	16	16	14	7	12	18
ZR	190	86	271	201	251	254	237	163	173	263
Y	41	22	43	42	74	76	43	30	32	48
SR	223	349	209	169	51	34	498	253	232	249
RB	189	32	152	201	261	221	103	88	100	149
ZN	91	111	82	74	56	72	94	95	109	99
CU	24	1	8	10	0	1	11	24	32	37
NI	33	4	6	4	2	1	17	51	71	23
CR	155	51	6	9	0	2	38	257	403	43
V	158	259	110	25	8	7	105	157	168	79
LA		17	37	41	41	45				38

	LD175*	LD176	LD178*	LD179*	LD180	LD191A	LD192	LD194	LD195	LD196
PERCENT										
SI02	66.63	58.52	69.94	69.56	59.99	59.11	58.14	58.54	58.91	57.68
AL203	17.45	20.98	18.07	15.64	19.82	17.02	18.97	15.39	15.69	16.23
FE203	4.00	8.82	2.68	3.99	9.19	8.24	7.07	8.74	8.45	8.23
MGO	0.92	2.02	0.54	0.86	3.92	2.61	2.01	3.60	3.11	2.93
CAO	3.80	3.00	0.33	1.44	0.24	6.32	6.18	7.74	7.97	8.11
NA2O	2.08	1.18	3.33	3.40	2.17	2.29	1.38	2.57	1.92	2.69
K2O	4.21	4.04	4.41	4.18	3.26	2.73	4.59	1.49	2.06	2.27
TI02	0.28	0.85	0.35	0.33	0.93	1.04	1.11	1.04	1.06	1.05
MNO	0.18	0.19	0.04	0.15	0.12	0.18	0.21	0.27	0.27	0.28
S	0.15	0.17	0.06	0.15	0.16	0.17	0.13	0.35	0.30	0.26
P205	0.25	0.17	0.25	0.24	0.13	0.23	0.16	0.21	0.22	0.21
PPM										
BA	328	682	651	846	446	746	1060	518	628	567
NB	17	18	21	20	13	13	15	12	13	12
ZR	372	271	392	365	233	219	226	226	230	236
Y	91	45	84	77	54	39	40	36	39	45
SR	92	115	72	137	70	249	132	328	299	225
RB	218	177	207	188	151	90	214	42	66	66
ZN	42	120	48	69	86	88	85	97	95	95
CU	11	31	9	2	33	34	24	16	18	19
NI	3	29	2	4	39	42	45	20	21	20
CR	0	46	5	3	140	103	106	139	133	131
V	5	81	8	7	156	140	148	170	167	156
LA	55	49	62	56		32				

	LD197	LD200	LD201	LD202	LD207	LD208	LD209	LD210	LD211	LD212
PERCENT				*						
SI02	59.73	59.30	52.01	67.58	58.98	49.63	59.60	54.61	60.01	58.22
AL203	17.45	16.90	15.54	16.97	18.24	19.70	16.59	17.90	19.31	18.83
FE203	8.38	7.55	10.67	4.85	8.53	9.15	8.63	9.23	6.89	8.14
MGO	5.14	2.10	7.54	0.60	2.08	3.09	4.79	3.53	4.21	2.19
CAO	2.56	7.41	8.27	2.29	5.05	11.56	4.22	8.79	3.02	6.78
NA2O	3.30	2.87	2.42	2.57	2.54	1.69	2.37	2.06	2.15	3.50
K2O	1.69	2.11	1.67	4.44	3.15	3.30	2.37	1.90	2.96	3.84
TIO2	1.08	1.04	1.25	0.42	0.91	1.16	0.77	1.31	0.67	0.95
MNO	0.22	0.22	0.23	0.11	0.18	0.22	0.19	0.16	0.22	0.15
S	0.21	0.22	0.14	0.11	0.12	0.25	0.24	0.22	0.33	0.15
P2O5	0.18	0.22	0.20	0.01	0.16	0.20	0.18	0.23	0.16	0.20
PPM										
BA	267	730	470	746	716	526	818	629	417	237
NB	13	12	11	19	15	13	16	16	11	17
ZR	245	246	132	288	195	157	232	220	200	171
Y	32	38	26	70	33	34	36	30	38	30
SR	138	275	402	96	253	130	482	605	305	211
RB	88	73	56	203	118	142	65	70	152	36
ZN	94	93	108	89	107	88	86	89	100	123
CU	15	11	117	2	22	54	72	124	10	6
NI	23	16	100	1	11	39	58	55	14	0
CR	136	97	307	2	24	151	97	71	42	0
V	164	150	261	13	99	199	118	224	95	128
LA			18	38	32					

	LD213	LD214	LD215	LD216	LD217	LD219	LD220	LD221	LD222	LD223 H
PERCENT										
SI02	57.67	59.65	61.08	60.25	59.40	56.52	62.11	53.25	56.97	58.30
AL203	18.73	18.80	17.41	17.47	19.46	20.65	17.26	15.84	18.18	18.50
FE203	8.64	6.54	8.19	8.81	6.45	6.61	7.75	9.91	9.50	6.98
MGO	2.16	2.00	1.40	1.59	2.20	3.21	1.95	7.24	2.28	2.96
CAO	6.88	6.21	4.10	3.03	3.89	5.36	3.69	8.11	6.18	3.92
NA2O	3.78	2.19	3.19	3.71	3.48	2.39	2.87	1.89	3.08	3.99
K2O	0.58	3.28	3.05	3.42	3.50	3.60	2.80	1.83	2.33	3.51
TIO2	0.96	0.79	0.63	0.77	0.77	0.77	0.76	1.04	0.67	0.98
MNO	0.21	0.13	0.22	0.23	0.17	0.14	0.21	0.21	0.31	0.25
S	0.12	0.16	0.36	0.36	0.44	0.55	0.32	0.48	0.27	0.33
P205	0.22	0.18	0.29	0.29	0.18	0.15	0.22	0.16	0.18	0.24
PPM										
BA	218	685	771	764	642	804	905	515	595	816
NB	16	11	20	16	14	12	17	9	16	15
ZR	167	230	356	320	237	198	279	142	186	254
Y	31	45	61	61	47	39	50	27	46	43
SR	299	257	262	221	289	285	441	309	193	247
RE	18	144	127	160	198	156	133	61	107	125
ZN	120	81	116	128	76	75	111	91	132	183
CU	15	16	8	13	21	13	37	74	10	24
NI	2	16	6	13	19	20	27	192	1	27
CR	2	34	11	39	43	47	46	446	1	41
V	125	94	33	46	101	108	77	233	48	125
LA		32			50			22		

	LD224 H	LD226	LD227 *	LD228	LD229	LD230	LD231	LD232	LD233 H	LD234
PERCENT										
SI02	50.86	58.28	68.49	59.69	61.78	61.16	54.07	54.09	55.59	55.17
AL203	15.63	16.28	18.06	15.29	15.96	16.43	18.74	19.40	17.84	17.21
FE203	9.71	8.95	3.14	9.02	6.72	6.59	9.47	8.27	9.63	8.40
MGO	10.93	3.01	0.72	2.84	3.39	3.56	5.33	4.82	5.32	6.22
CAO	7.35	6.11	2.26	6.47	5.95	6.24	5.85	7.83	6.95	7.63
NA2O	1.24	3.82	2.19	3.05	2.47	2.53	1.03	2.11	1.82	1.30
K2O	2.25	1.64	4.34	1.73	2.46	2.26	3.68	1.92	0.75	2.50
TI02	1.06	1.46	0.31	1.34	0.83	0.78	1.09	1.07	1.37	1.02
MNO	0.23	0.18	0.15	0.26	0.17	0.17	0.38	0.20	0.34	0.25
S	0.40	0.04	0.03	0.03	0.06	0.08	0.12	0.06	0.14	0.06
P205	0.27	0.19	0.25	0.22	0.16	0.15	0.18	0.19	0.20	0.19
PPM										
BA	326	440	605	623	472	375	677	350	158	505
NB	7	11	25	15	13	11	16	11	12	7
ZR	120	221	375	216	226	193	174	168	178	172
Y	23	38	69	36	35	27	33	28	32	31
SR	535	268	94	369	213	197	162	250	283	285
RB	96	61	219	61	100	93	152	81	17	84
ZN	79	99	52	111	78	86	104	81	112	87
CU	118	34	0	11	23	37	15	31	4	20
NI	306	13	3	2	25	43	14	24	2	91
CR	642	30	2	12	62	86	113	106	27	263
V	201	213	7	212	108	125	145	191	226	188
LA		23	51							



	LD247 H	LD248	LD249 *	LD250	LD251	CF253 *	CF256 *	CF259 *	CF261	LD269
PERCENT										
SI02	56.03	57.95	63.79	54.31	57.00	69.35	63.59	66.96	53.36	51.24
AL203	16.06	17.17	19.89	20.71	15.65	14.60	17.00	16.54	14.65	12.74
FE203	10.35	8.23	5.07	6.58	10.22	4.13	8.04	4.45	10.33	11.33
MGO	4.86	3.15	0.98	2.89	4.20	0.90	1.40	1.12	8.59	10.99
CAU	4.67	5.37	3.44	9.29	6.29	0.91	0.97	0.40	7.97	8.60
NA2O	2.48	3.80	1.76	1.93	3.20	3.42	6.83	3.02	1.08	2.83
K2O	2.19	2.50	4.26	2.73	1.60	5.67	0.92	6.79	2.12	0.00
TIO2	1.29	1.34	0.31	1.07	1.32	0.40	0.78	0.43	1.07	1.57
MNO	0.23	0.20	0.13	0.20	0.23	0.22	0.10	0.04	0.24	0.15
S	1.63	0.04	0.03	0.04	0.05	0.33	0.20	0.18	0.39	0.26
P 205	0.17	0.19	0.27	0.18	0.19	0.07	0.17	0.08	0.20	0.31
PPM										
BA	530	575	722	573	580	1610	102	1368	692	54
NB	12	14	20	12	11	24	22	25	13	17
ZR	171	226	460	183	166	467	325	503	173	193
Y	36	39	86	29	30	49	45	58	22	24
SR	261	323	200	360	430	77	197	54	595	820
RB	74	100	177	84	34	248	43	252	51	1
ZN	111	89	75	78	105	93	133	36	92	109
CU	30	9	7	21	31	10	0	1	63	99
NI	9	9	4	32	9	2	13	2	173	306
CR	27	21	3	100	24	0	12	0	485	742
V	267	201	6	148	257	8	42	7	196	210
LA			130		20	39	38	50	20	

	LD270	LD274	LD275	LD278	LD279	LD280	LD281	LD282	LD283 <sub>C</sub>	LD286 <sub>*</sub>
PERCENT										
SI02	51.23	64.17	52.93	57.95	55.98	61.65	55.28	50.81	48.00	68.74
AL203	11.80	17.80	16.71	18.08	17.37	18.89	19.09	17.17	14.36	14.76
FE203	12.62	5.83	10.74	8.95	10.19	6.00	8.92	10.79	12.54	5.84
MGO	12.67	0.92	5.07	2.96	3.79	2.59	4.53	7.47	12.59	0.91
CAO	9.16	3.31	8.72	5.78	7.12	4.31	6.55	8.14	9.19	2.24
NA2O	0.00	2.23	1.70	3.28	2.56	2.55	1.23	1.94	1.08	3.45
K2O	0.13	4.54	2.02	1.38	0.92	2.70	2.67	1.81	0.65	2.69
TI02	1.61	0.66	1.35	0.84	1.40	0.67	1.00	1.23	0.84	0.62
MNO	0.19	0.14	0.21	0.23	0.25	0.18	0.24	0.21	0.24	0.30
S	0.30	0.19	0.38	0.31	0.27	0.23	0.33	0.22	0.32	0.26
P205	0.29	0.21	0.18	0.22	0.16	0.22	0.15	0.22	0.18	0.18
PPM										
BA	28	794	562	403	446	747	840	680	251	874
NB	16	16	11	16	17	14	12	14	5	17
ZR	159	246	136	167	145	227	180	169	90	283
Y	20	32	26	33	37	42	35	29	18	42
SR	735	147	307	282	377	254	472	413	260	239
RB	11	236	63	49	32	115	85	43	32	119
ZN	98	103	109	117	104	96	100	112	81	81
CU	10	11	45	1	1	2	43	83	83	0
NI	304	20	63	0	0	14	44	110	250	1
CR	722	32	166	2	1	38	140	227	547	3
V	213	54	241	82	165	84	183	227	199	24
LA	18	42	20					19		36

	LD287	LD288	LD289 M	LD291	LD292	LD293	LD294 *	LD296 *	LD298	LD299
PERCENT										
SI02	55.28	48.27	67.32	58.17	58.30	57.70	66.62	67.59	52.70	53.39
AL203	15.87	18.46	14.81	15.83	15.77	16.19	15.06	14.89	18.62	17.88
FE203	9.36	11.17	4.64	8.70	8.71	8.88	5.06	5.03	10.06	10.86
MGO	5.25	7.25	1.65	3.46	3.41	3.02	1.19	0.65	6.63	6.29
CAO	9.30	8.03	3.07	6.92	7.24	7.05	2.16	1.96	4.35	4.27
NA2O	1.90	3.11	1.00	2.04	1.71	1.57	2.79	2.82	3.75	2.31
K2O	0.72	1.28	6.37	2.99	3.08	3.81	6.03	6.02	2.06	2.59
TIO2	1.44	1.60	0.62	1.14	1.14	1.21	0.74	0.70	1.21	1.61
MNO	0.31	0.29	0.11	0.26	0.25	0.27	0.10	0.10	0.23	0.30
S	0.30	0.24	0.26	0.27	0.13	0.10	0.10	0.10	0.25	0.19
P2O5	0.27	0.30	0.15	0.20	0.25	0.20	0.15	0.14	0.14	0.30
PPM										
BA	338	449	612	682	714	805	1018	1035	568	1256
NB	9	12	16	15	14	13	34	31	9	11
ZR	151	156	256	190	186	192	415	407	127	174
Y	28	31	38	33	32	34	42	43	32	35
SR	510	352	78	348	339	388	164	232	213	293
RB	46	53	233	111	100	126	211	202	97	145
ZN	80	124	72	99	105	105	93	90	103	118
CU	6	14	1	0	3	1	3	12	0	13
NI	36	71	1	2	0	8	0	0	5	45
CR	168	335	2	26	28	25	52	0	72	193
V	243	271	39	192	199	198	18	16	232	255
LA	19		29	26	25		40	41		

	LD300	LD301	LD302	LD303	LD304	LD305	LD306	LD307	LD308	LD309
PERCENT									*	
SI02	65.05	67.52	58.60	70.31	66.66	70.62	62.74	63.66	68.50	56.94
AL203	17.78	16.53	16.98	15.47	15.21	15.58	18.55	17.39	13.25	16.59
FE2O3	4.70	4.02	8.23	3.78	4.52	3.19	6.69	6.62	5.92	9.24
MGO	0.80	0.58	5.17	1.05	1.21	0.46	1.74	1.59	1.12	5.01
CAO	2.77	2.76	4.67	0.67	2.28	0.59	2.46	0.89	0.33	4.56
NA2O	4.09	4.17	1.61	4.50	3.81	1.63	2.63	2.84	2.37	2.41
K2O	3.56	3.09	3.35	3.42	5.35	7.16	3.77	5.73	6.63	3.34
TI02	0.75	0.73	0.78	0.35	0.61	0.29	0.88	0.83	0.58	1.17
MNO	0.13	0.19	0.19	0.05	0.08	0.07	0.23	0.14	0.39	0.29
S	0.18	0.22	0.22	0.12	0.11	0.11	0.08	0.11	0.77	0.24
P2O5	0.19	0.18	0.18	0.29	0.17	0.30	0.23	0.18	0.15	0.19
PPM										
BA	278	859	648	725	1696	1596	1377	1186	1342	890
NB	24	21	12	24	22	21	21	17	19	10
ZR	343	320	166	376	359	305	290	260	272	156
Y	50	47	33	68	50	68	48	41	41	28
SR	141	322	269	88	226	106	296	227	78	382
RB	182	133	129	165	171	316	152	239	228	93
ZN	81	129	112	22	8	21	57	23	45	102
CU	0	0	3	0	0	0	16	1	0	3
NI	0	1	22	1	5	1	25	25	0	2
CR	1	11	116	6	7	0	39	38	0	56
V	35	30	140	6	36	1	66	67	9	203
LA	57	38		59	37	49	47			

	LD310	LD312	LD313 *	LD314	LD315
PERCENT					
SI02	56.50	53.50	72.01	56.56	52.97
AL203	16.04	18.36	15.31	18.18	16.07
FE203	9.12	7.70	3.31	8.36	11.41
MGO	4.87	6.30	0.58	3.53	7.80
CAU	7.15	6.76	0.42	6.65	8.26
NA2O	2.60	2.88	3.39	2.02	1.06
K2O	1.80	2.65	4.27	2.63	0.35
TI02	1.17	1.11	0.27	1.07	1.33
MNO	0.28	0.23	0.07	0.21	0.25
S	0.28	0.36	0.08	0.55	0.34
P205	0.20	0.15	0.29	0.24	0.16
PPM					
BA	371	563	655	610	304
NB	12	6	19	13	11
ZR	157	86	356	218	134
Y	26	27	69	42	27
SR	455	304	65	261	557
RB	50	127	228	109	15
ZN	103	60	26	98	110
CL	3	0	13	16	60
NI	4	5	0	17	86
CR	57	45	2	35	215
V	202	263	0	126	260
LA					18

(b) Northern outcrop.

\* Ignimbrites.

A Aphyric lavas.

CF Carrock Fell Complex.

E Embleton intrusion.

GC Great Cockup 'picrite'

Specimen numbers with the suffix 'G' are groundmasses separated from Eycott type lavas.

	LD73	LD73A	LD73AG	LD75	LD76	LD77	LD78	LD80 A	LD81	LD82
PERCENT										
SI02	53.19	54.63	56.18	55.05	54.49	54.85	54.15	57.26	54.31	54.03
AL203	17.48	19.13	14.97	15.85	15.70	16.83	16.56	15.48	16.71	17.23
FE203	9.14	8.27	10.53	9.66	10.20	9.78	8.89	12.58	8.94	9.86
MGO	6.22	3.76	4.67	6.26	7.05	7.09	5.97	3.55	5.52	5.66
CAO	7.51	8.90	7.25	8.94	7.97	5.59	8.73	3.58	9.30	7.57
NA2O	2.62	2.03	2.74	1.67	1.87	1.97	1.99	2.67	1.76	1.98
K2O	2.15	1.18	1.32	1.31	1.44	2.22	2.06	2.45	1.77	1.84
TIO2	1.20	1.07	1.44	0.89	0.91	1.25	1.24	2.00	1.22	1.37
MNO	0.18	0.13	0.17	0.18	0.21	0.21	0.15	0.16	0.15	0.19
S	0.15	0.75	0.56	0.04	0.04	0.05	0.04	0.06	0.09	0.10
P2O5	0.16	0.14	0.17	0.13	0.12	0.17	0.23	0.21	0.23	0.19
PPM										
BA	387	348	398	256	256	444	273	413	263	360
NB	10	12	18	11	9	11	18	15	16	19
ZR	138	156	199	106	106	162	175	228	176	177
Y	27	30	41	22	22	29	30	50	29	30
SR	286	221	178	171	237	256	319	215	329	262
RR	80	41	44	47	62	89	68	106	56	59
ZN	75	79	109	80	87	116	80	110	83	92
CU	144	131	183	87	108	105	106	20	102	102
NI	78	75	104	60	51	46	80	7	81	32
CR	172	178	291	182	178	95	141	4	141	47
V	210	197	261	218	214	218	196	303	191	221
LA	16	16	22	12	12	18	19	29	18	18

	LD83	LD85	LD86	LD87	LD88 A	LD91	LD92	LD93	LD94	LD95
PERCENT										
SIJ2	55.71	55.51	55.08	54.22	55.51	52.77	54.64	54.00	53.16	54.86
AL203	17.60	17.39	17.12	16.44	15.66	15.85	19.30	17.90	17.98	19.41
FE203	8.96	9.45	8.16	9.53	11.19	9.60	10.07	9.73	10.09	7.71
MGO	2.86	3.82	5.08	7.30	5.20	8.37	8.79	6.73	9.18	5.52
CAO	8.77	8.41	9.59	7.33	5.56	9.63	1.31	4.89	4.53	6.79
NA2O	2.18	2.51	1.96	2.00	2.40	1.79	3.04	3.36	2.91	3.27
K2O	1.88	0.90	1.27	1.54	1.75	0.44	1.56	1.51	0.84	0.94
TIO2	1.64	1.65	1.35	1.22	2.32	1.18	1.00	1.49	0.93	1.16
MNO	0.17	0.15	0.15	0.17	0.11	0.19	0.17	0.19	0.16	0.13
S	0.03	0.01	0.01	0.02	0.02	0.05	0.04	0.03	0.04	0.03
P205	0.19	0.20	0.23	0.22	0.28	0.14	0.09	0.19	0.17	0.17
PPM										
BA	380	408	284	362	423	203	190	344	355	355
NR	16	14	17	16	22	8	9	11	11	9
ZR	196	195	183	187	279	122	123	155	137	136
Y	38	34	27	28	47	29	27	34	28	27
SR	263	296	280	309	190	202	111	230	356	437
RB	59	23	36	49	48	13	90	40	31	34
ZN	79	91	75	90	140	96	99	89	106	69
CU	146	75	42	85	60	96	23	103	93	98
NI	20	15	44	64	28	110	43	51	93	28
CR	3	6	104	113	18	256	117	95	179	68
V	244	253	208	199	404	233	179	246	176	204
LA	21	20	20	21	29	14	14	19	13	16

	LD95G	LD96	LD97	LD98	LD99	LD100	LD101 A	LD102 *	LD103	LD104
PERCENT										
SI02	52.60	70.32	53.86	54.00	54.99	53.56	53.58	65.34	53.74	53.84
AL203	15.81	15.28	16.81	16.68	16.82	18.49	15.38	14.30	17.19	17.88
FE203	13.36	4.80	9.24	9.60	9.09	9.03	11.95	7.37	10.02	8.89
MGO	8.19	1.09	0.00	5.88	5.73	5.14	5.04	1.09	5.47	6.94
CAJ	4.45	0.61	8.91	8.10	8.53	8.10	5.89	2.37	8.17	7.74
NA2O	2.82	4.82	2.16	2.06	2.24	1.91	3.24	4.21	2.05	2.24
K2O	0.44	2.40	1.30	2.07	0.96	1.42	1.74	3.79	1.57	0.80
TI02	1.88	0.47	1.33	1.24	1.18	1.22	2.34	0.89	1.39	1.33
MNO	0.21	0.12	0.15	0.17	0.26	0.25	0.26	0.20	0.18	0.14
S	0.00	0.00	0.02	0.02	0.02	0.71	0.33	0.13	0.02	0.05
P205	0.23	0.06	0.23	0.19	0.17	0.17	0.25	0.26	0.20	0.15
PPM										
BA	147	332	344	378	241	304	472	810	334	171
NB	16	21	18	17	10	12	19	26	12	9
ZR	246	480	177	188	154	157	236	403	147	137
Y	47	82	30	31	33	32	45	71	30	29
SR	329	84	307	278	413	372	431	162	280	298
RB	16	82	41	69	31	52	53	160	65	36
ZN	126	104	84	96	89	85	116	126	91	88
CU	183	5	100	99	65	73	82	21	53	96
NI	57	3	53	69	21	26	40	4	71	65
CR	140	6	124	134	88	97	48	5	129	100
V	380	10	209	206	206	215	411	16	235	232
LA	28	46	20	20	17	18	25	37	18	17

	LD105	LD106	LD107	LD108	LC109	LD111	LD112	LD114	LD115	LD116
PERCENT										
SI02	55.46	53.64	52.67	54.93	54.61	57.19	58.26	51.84	51.46	52.41
AL203	14.78	18.22	18.89	16.50	17.09	14.09	14.20	18.07	15.50	16.24
FE2O3	12.04	8.65	8.62	9.80	8.41	11.23	12.24	9.77	12.76	11.11
MGO	4.63	5.97	6.41	6.46	4.69	2.71	4.81	5.90	6.41	7.42
CAO	7.57	9.64	8.79	5.08	11.05	6.65	3.97	7.28	7.28	7.23
NA2O	1.95	2.06	2.27	3.18	2.12	2.56	3.23	3.71	3.70	2.26
K2O	1.19	0.26	0.72	1.59	0.43	2.55	0.96	1.83	0.64	1.58
TI02	1.95	1.22	1.24	1.65	1.23	1.99	1.71	1.21	1.78	1.36
MNO	0.18	0.13	0.16	0.16	0.18	0.23	0.25	0.21	0.20	0.18
S	0.03	0.05	0.07	0.41	0.03	0.40	0.02	0.04	0.02	0.04
P205	0.22	0.16	0.16	0.23	0.16	0.40	0.35	0.15	0.26	0.17
PPM										
BA	455	124	250	290	310	530	285	375	414	908
NR	14	10	8	10	10	18	16	8	9	8
ZR	208	119	124	197	132	287	248	124	169	133
Y	33	24	25	33	28	62	56	27	41	32
SR	284	254	300	247	262	209	189	421	380	337
RB	39	8	25	50	8	95	55	59	29	63
ZN	109	86	79	90	77	120	125	78	110	95
CU	65	61	63	54	22	147	34	122	192	79
NI	28	44	45	44	6	3	0	60	78	70
CR	27	71	67	27	10	0	6	71	120	137
V	341	200	211	215	221	196	148	252	349	255
LA	24	15	16	17	18	34	31	14	13	13

	LD117	LD118*	LD119	LD119G	LC121*	LD122	CF252	CF252G	CN-7 CF	CN-10 CF
PERCENT										
SI02	53.62	71.59	54.66	54.85	73.57	53.08	53.22	54.66	50.04	72.94
AL203	16.97	15.34	18.14	13.28	12.63	16.21	20.99	16.69	18.36	12.88
FE2O3	12.51	3.77	8.23	12.30	4.49	11.01	7.73	10.37	10.18	4.00
MGO	4.10	1.48	4.31	5.87	1.08	7.66	4.67	6.05	4.43	0.51
CAO	3.89	0.96	8.95	8.78	0.58	7.05	8.05	6.23	8.99	0.68
NA2O	3.18	0.85	2.32	1.73	2.07	2.53	2.99	3.36	3.16	4.78
K2O	2.79	5.10	1.88	1.05	4.95	0.95	0.26	0.13	0.72	3.72
TI02	2.34	0.45	1.18	1.70	0.39	1.14	1.36	2.10	3.51	0.27
MNO	0.26	0.09	0.14	0.20	0.13	0.17	0.14	0.19	0.20	0.13
S	0.07	0.32	0.04	0.00	0.06	0.06	0.42	0.01	0.16	0.03
P205	0.27	0.05	0.14	0.23	0.05	0.13	0.16	0.22	0.18	0.01
PPM										
BA	418	581	470	303	801	485	161	155	129	591
NB	15	24	8	15	21	8	11	17	10	28
ZR	240	475	135	216	421	104	166	265	107	505
Y	49	82	29	39	77	24	36	52	22	120
SR	76	17	435	181	45	276	285	206	236	69
RB	115	211	58	29	158	44	9	3	31	162
ZN	106	64	72	105	79	100	86	134	74	161
CU	112	4	128	173	1	92	133	218	25	1
NI	13	0	40	72	4	114	67	97	21	6
CR	17	0	111	197	0	353	94	116	49	6
V	376	8	213	332	16	230	211	318	520	0
LA	27	46	15	24	43	9	19	29	14	55

	CN-11	CN-14	CN-16	CN-17	CN-49	CN-64	CN-71	LD285	LD266	LD267
	CF	CF	CF	CF	CF	CF	CF	CF	E	E
PERCENT										
SI02	46.37	71.64	54.15	54.11	71.04	51.85	72.93	63.69	56.09	52.46
AL203	20.40	13.12	26.73	21.14	12.65	17.75	12.69	21.70	14.50	14.10
FE203	9.34	5.41	2.15	7.11	5.44	11.16	5.07	2.72	11.91	14.53
MGO	7.76	1.11	0.67	2.46	0.66	4.69	0.78	3.89	3.58	4.91
CAD	11.33	0.03	8.88	8.98	2.41	7.43	0.06	0.18	5.80	6.27
NA2O	2.04	4.49	4.35	3.24	4.23	3.09	4.60	2.35	3.85	3.97
K2O	1.35	3.66	2.35	1.06	2.88	1.34	3.28	5.15	1.29	0.22
TI02	0.98	0.41	0.46	1.40	0.39	2.11	0.40	0.02	2.00	2.58
MND	0.16	0.09	0.03	0.13	0.14	0.26	0.10	0.02	0.23	0.24
S	0.08	0.01	0.08	0.01	0.06	0.02	0.01	0.20	0.37	0.37
P205	0.16	0.03	0.10	0.29	0.04	0.25	0.02	0.08	0.37	0.34
PPM										
BA	154	458	234	195	490	326	574	334	231	122
NB	4	26	2	6	28	10	26	21	15	12
ZR	76	540	25	212	535	134	597	71	345	254
Y	8	92	9	28	97	35	111	25	62	50
SR	480	46	578	268	75	294	59	75	38	152
RB	65	161	81	43	143	51	123	292	36	13
ZN	68	199	19	67	110	103	167	0	176	170
CU	141	1	13	24	2	14	12	0	7	31
NI	63	6	6	16	4	19	4	0	18	16
CR	272	4	0	31	4	74	7	0	0	26
V	236	2	208	222	2	299	4	5	163	366
LA	7	49	11	18	45	18	47	5	23	18

LD72  
GC

47.56  
7.99  
13.03  
18.67  
9.73  
1.25  
0.28  
0.94  
0.21  
0.16  
0.17

PERCENT  
SiO2  
AL2O3  
FE2O3  
MGO  
CAO  
NA2O  
K2O  
TiO2  
MNO  
S  
P2O5

PPM

BA 127  
NB 5  
ZR 69  
Y 17  
SR 194  
RB 4  
ZN 90  
CU 95  
NI 625  
CR 975  
V 232  
LA 9

(c) Analyses of garnet-bearing samples referred to in the text but not plotted on the variation diagrams.

LD 21 Tuff from Lincomb Tarns Formation.

LD 204 Threlkeld microgranite.

LD 277 Armboth dyke.

	LD 21	LD204	LD277
PERCENT			
SI02	62.81	69.81	74.22
AL203	17.58	15.99	13.85
FE203	7.16	3.38	1.92
MGO	1.64	1.36	0.37
CAO	2.76	0.82	2.23
NA2O	3.15	4.53	2.66
K2O	3.75	3.43	3.93
TI02	0.60	0.31	0.13
MNO	0.21	0.07	0.10
S	0.02	0.09	0.42
P205	0.30	0.15	0.17
PPM			
BA	731	324	210
NB	21	11	12
ZR	333	149	100
Y	66	22	24
SR	188	103	39
RB	178	192	227
ZN	109	34	40
CU	14	43	0
NI	5	22	0
CR	19	25	0
V	29	39	40

APPENDIX 4.

C.I.P.W. Norms.

$\text{Fe}_2\text{O}_3$  / FeO taken as 0.808 (by weight).

(a) Southern outcrop.

BORRCWDALE VOLCANIC GROUP - SOUTHERN OUTCRCP

NORMCAL .. R.C.O.GILL

SUMMARY NORM TABLE

	LD 2	LC 3	LC 4	LD 6	LD 7	LD 8	LD 9	LD 11	LD 12	LD 13	LD 14	LD 24
QUARTZ	11.2	14.2	12.8	29.4	28.2	27.9	26.5	26.8	27.2	28.6	28.4	10.1
CORUNDUM	0.8	2.0	1.8	3.8	3.4	4.4	3.6	2.7	4.8	4.7	3.7	0.2
CRTHCCLEASE	9.9	14.0	10.9	28.9	28.4	28.4	29.7	29.4	31.7	26.3	16.0	15.1
ALBITE	18.3	23.0	18.4	23.9	23.4	24.0	21.8	24.1	22.3	25.9	40.3	25.2
ANORTHITE	30.2	26.7	27.1	7.7	9.7	7.5	10.6	9.9	5.8	6.6	4.9	23.0
HYPERSTHENE	20.5	12.9	20.5	2.5	2.8	3.7	3.5	3.1	3.9	3.8	3.0	18.0
MAGNETITE	6.5	4.8	5.8	2.5	2.5	2.8	2.9	2.7	2.8	2.8	2.5	5.7
ILMENITE	2.2	1.8	2.1	6.6	0.7	0.7	1.7	0.6	0.8	0.7	0.5	2.1
APATITE	0.5	0.5	0.5	0.7	0.7	0.6	0.7	0.6	0.7	0.7	0.6	0.6
PYRITE	0.0	0.0	0.0	0.0	0.1	0.1	0.1	0.0	0.0	0.0	0.0	0.0
DIFF. INDEX	39.4	51.3	42.1	82.2	80.4	80.2	78.0	80.3	81.2	80.8	84.7	50.5
NA/(NA+K)	0.66	0.63	0.64	0.47	0.47	0.47	0.44	0.47	0.43	0.51	0.73	0.64
(NA+K)/AL	3.31	3.37	0.32	0.60	0.58	1.58	0.56	0.61	0.59	0.58	0.66	0.47
F3/(F2+F3)	0.42	0.42	0.42	0.42	0.42	0.42	0.42	0.42	0.42	0.42	0.42	0.42



BORROWDALE VOLCANIC GROUP - SOUTHERN CUTCRCP

NORMCAL .. R.C.O.GILL

SUMMARY NORM TABLE

	LD 60	LD 61	LD 62	LD 65	LD 67	LD 68	LD 69	LD70	126	128	129	130
QUARTZ	13.8	24.5	29.2	32.4	11.2	26.6	1.2	8.8	2.6	8.5	14.7	28.7
CCRUNDUM	0.0	2.1	4.7	5.9	4.0	3.9	0.0	0.0	0.0	6.7	0.0	3.7
CRTHCCCLASE	16.3	31.6	35.1	30.3	16.9	31.5	8.4	3.6	18.3	6.5	15.7	6.8
ALBITE	12.9	20.7	19.2	21.4	12.5	18.1	7.1	10.4	13.8	26.5	31.4	23.8
ANORTHITE	29.4	11.9	4.7	5.1	23.9	8.9	23.0	32.4	33.0	21.1	25.2	21.1
DIOPSIDE	0.1	0.0	0.0	0.0	0.0	0.0	28.2	0.8	17.9	0.0	0.4	0.0
HYPERSTHENE	19.0	4.5	3.3	2.7	23.3	4.9	20.3	32.6	5.3	22.0	6.6	9.3
MAGNETITE	5.9	3.0	2.6	1.9	5.8	4.0	8.1	7.2	6.2	6.0	4.2	4.9
ILMENITE	2.2	0.8	0.6	0.6	2.1	1.3	3.0	3.4	2.4	2.2	1.2	1.2
APATITE	0.4	0.7	0.7	0.7	0.3	0.8	0.7	0.7	0.5	0.4	0.4	0.3
PYRITE	0.0	0.1	0.0	0.0	0.0	0.0	0.2	0.2	0.1	0.1	0.1	0.1
DIFF. INDEX	43.0	76.8	83.5	83.0	40.6	76.3	16.6	22.8	34.7	41.5	61.8	59.3
NA/(NA+K)	0.46	0.41	0.37	0.42	0.44	0.38	0.47	0.76	0.44	0.81	0.68	0.79
(NA+K)/AL	0.34	0.6	0.61	0.55	0.30	0.57	0.26	0.18	0.33	0.31	0.49	0.34
F3/(F2+F3)	0.42	0.42	0.42	0.42	0.42	0.42	0.42	0.42	0.42	0.42	0.42	0.42

BORROWDALE VOLCANIC GROUP - SOUTHERN CUTCRCP

NCRMAL .. R.C.O.GILL

SUMMARY NCRM TABLE

	131	132	133	135	136	137	139	140	141	142	143	144
QUARTZ	8.7	16.2	15.7	16.5	18.1	16.9	1.6	21.1	10.2	21.0	12.4	8.5
CGRUNDUM	0.0	0.0	1.0	0.4	0.6	3.4	4.4	3.7	5.1	4.3	4.4	3.1
ORTHOCLASE	16.0	19.7	21.0	9.9	6.7	25.8	22.2	20.6	19.7	11.0	21.1	18.9
ALBITE	15.1	14.5	18.6	17.8	23.0	11.6	35.1	23.1	33.4	17.9	30.4	42.8
ANORTHITE	30.2	29.5	22.6	33.2	27.3	28.8	18.7	17.0	13.8	27.3	15.5	12.7
DIOPSIDE	12.7	0.3	0.1	0.0	0.0	0.0	0.0	0.0	0.0	0.0	0.0	0.0
HYPERSTHENE	8.1	12.3	13.3	14.5	17.4	7.1	11.3	8.9	11.1	11.6	9.6	7.6
MAGNETITE	6.2	4.7	4.9	5.2	4.8	4.1	4.4	3.7	4.5	5.0	4.6	4.2
ILMENITE	2.3	2.1	2.1	2.0	1.7	1.8	1.6	1.3	1.7	1.4	1.6	1.5
APATITE	5.5	0.5	0.5	0.4	0.3	0.4	0.4	0.4	0.3	0.4	0.4	0.4
PYRITE	0.1	0.2	0.2	0.2	0.2	0.1	0.2	0.2	0.2	0.2	0.2	0.2
DIFF. INDEX	39.8	50.5	55.3	44.2	47.7	54.3	59.0	64.8	63.3	49.9	63.9	70.2
NA/(NA+K)	0.50	0.44	0.49	0.66	0.78	0.32	0.63	0.54	0.64	0.63	0.60	0.71
(NA+K)/AL	0.35	0.37	0.44	0.30	0.35	0.33	0.49	0.45	0.50	0.28	0.49	0.60
F3/(F2+F3)	0.42	0.42	0.42	0.42	0.42	0.42	0.42	0.42	0.42	0.42	0.42	0.42











BORROWDALE VOLCANIC GROUP - SOUTHERN OUTCROP

NORMCAL .. R.C.O.GILL

SUMMARY NORM TABLE

	233	234	235	236	237	238	239	240	243	244	245	246
QUARTZ	18.2	11.9	19.9	19.5	3.4	1.7	2.7	3.2	16.4	12.4	12.5	19.3
CORUNDUM	1.5	0.0	5.0	0.0	2.3	0.5	0.0	0.0	0.0	2.6	0.0	4.7
CRT HCCLASE	4.5	14.9	9.9	10.9	14.6	11.9	17.3	7.3	11.4	12.3	13.2	21.1
ALBITE	15.5	11.1	22.0	22.1	15.5	13.3	18.1	12.7	20.8	26.9	16.0	14.2
ANORTHITE	33.4	33.9	19.8	25.1	28.5	38.6	28.3	42.6	28.2	28.9	31.8	19.6
CIOPSIDE	0.0	2.3	0.0	4.7	0.0	0.0	2.6	2.0	2.1	0.0	2.6	0.0
FYPERSTHENE	17.4	18.3	15.2	8.7	27.5	27.3	22.7	25.6	10.1	10.5	16.2	10.9
MAGNETITE	5.9	5.2	6.0	5.7	5.6	4.8	5.3	4.8	6.5	4.2	5.1	5.0
ILMENITE	2.6	1.9	2.7	2.7	1.9	1.4	2.2	1.3	2.7	1.9	2.0	2.5
APATITE	0.5	0.5	0.4	0.5	0.5	0.5	0.7	0.4	0.4	0.3	0.4	0.4
PYRITE	0.3	0.1	0.1	0.2	0.1	0.1	0.1	0.2	1.5	0.1	0.2	2.4
DIFF. INDEX	38.1	37.8	50.9	52.5	33.5	26.9	38.1	23.1	48.6	51.6	41.7	54.6
NA/(NA+K)	0.79	0.44	0.70	0.68	0.53	0.54	0.53	0.65	0.66	0.70	0.56	0.42
(NA+K)/AL	0.21	0.28	0.33	0.41	0.31	0.25	0.39	0.29	0.37	0.36	0.32	0.36
F3/(F2+F3)	0.42	0.42	0.42	0.42	0.42	0.42	0.42	0.42	0.42	0.42	0.42	0.42









(b) Northern outcrop.



BORROWDALE VOLCANIC GROUP - NORTHERN OUTCROP

NORMCAL .. R.C.O.GILL

SUMMARY NORM TABLE

	LD86	LD87	LD88	LD91	LC92	LC93	LD94	LD95	LD95G	LD96	LD97	LD98
QUARTZ	12.6	5.7	14.6	8.9	13.3	7.0	8.0	8.6	11.0	29.3	9.5	8.6
CORUNDUM	0.0	0.0	0.4	0.0	0.5	2.3	4.5	1.1	3.2	3.8	0.0	0.0
ORTHOCLASE	7.5	9.2	10.4	2.6	9.3	9.0	5.0	5.6	2.6	14.2	7.7	12.3
ALBITE	16.7	17.0	23.4	15.2	25.9	28.6	24.8	27.8	24.0	40.9	18.4	17.5
ANORTHITE	34.3	31.5	25.0	34.1	5.5	23.1	21.5	32.7	20.7	2.6	32.5	30.3
DIOPSIDE	9.5	2.9	0.0	10.3	0.0	0.0	0.0	0.0	0.0	0.0	8.3	7.1
HYPERSTHENE	11.2	21.0	16.2	20.3	26.8	21.6	27.0	16.8	26.0	5.1	14.8	15.5
MAGNETITE	5.0	5.8	6.9	5.5	6.2	6.0	6.2	4.7	8.2	2.9	5.7	5.9
ILMENITE	2.6	2.3	4.4	2.3	1.9	2.8	1.8	2.2	3.6	0.9	2.5	2.4
APATITE	0.5	0.5	0.7	0.3	0.2	0.5	0.4	0.4	0.5	0.1	0.5	0.5
PYRITE	0.0	0.0	0.0	0.1	0.1	0.1	0.1	0.1	0.0	0.0	0.0	0.0
DIFF. INDEX	36.8	35.9	45.5	26.7	48.4	44.6	37.7	42.0	37.7	84.5	35.6	38.4
NA/(NA+K)	0.70	0.66	0.68	0.86	0.75	0.77	0.84	0.84	0.91	0.75	0.72	0.60
(NA+K)/AL	0.27	0.33	0.37	0.22	0.35	0.40	0.32	0.33	0.32	0.69	0.30	0.34
F3/(F2+F3)	0.42	0.42	0.42	0.42	0.42	0.42	0.42	0.42	0.42	0.42	0.42	0.42

BORROWDALE VOLCANIC GROUP - NORTHERN CUTCRCP

NORMCAL .. R.C.O.GILL

SUMMARY NORM TABLE

	LD99	100	101	102	LC103	LC104	LD105	LD106	LD107	LD108	LD109	LD111
QUARTZ	11.9	11.6	8.3	19.3	15.2	10.0	16.9	11.6	8.1	9.2	12.8	16.3
CGRUNDUM	0.0	0.0	0.0	0.0	0.0	0.0	0.0	0.0	0.0	0.9	0.0	0.0
ORTHOCLASE	5.7	8.4	13.4	22.5	9.3	4.8	7.1	1.5	4.3	9.4	2.6	15.2
ALBITE	19.1	16.2	27.6	35.8	17.4	19.1	16.6	17.5	19.3	27.1	18.1	21.8
ANORTHITE	33.2	37.9	22.4	9.0	33.3	36.6	28.3	39.9	39.4	23.8	36.0	19.5
DIOPSIDE	6.6	1.1	4.3	0.9	5.0	0.8	6.5	5.7	2.7	0.1	14.4	8.9
HYPERSTHENE	15.3	15.2	14.0	5.5	15.5	20.4	12.9	15.7	18.2	19.1	8.3	5.8
MAGNETITE	5.6	5.5	7.3	4.5	6.2	5.5	7.4	5.3	5.3	6.0	5.2	6.9
ILMENITE	2.3	2.3	4.5	1.7	2.7	2.5	3.7	2.3	2.4	3.2	2.3	3.8
APATITE	0.4	0.4	0.6	0.6	0.5	0.4	0.5	0.4	0.4	0.5	0.4	1.0
PYRITE	0.0	1.3	0.6	0.2	0.0	0.1	0.1	0.1	0.1	0.8	0.1	0.8
DIFF. INDEX	36.7	36.2	46.3	77.6	37.0	33.8	40.6	30.7	31.6	45.7	33.4	53.3
NA/(NA+K)	0.78	0.67	0.74	0.63	0.66	0.81	0.71	0.92	0.83	0.75	0.88	0.61
(NA+K)/AL	0.28	0.25	0.47	0.77	0.30	0.25	0.30	0.20	0.24	0.42	0.23	0.49
F3/(F2+F3)	0.42	0.42	0.42	0.42	0.42	0.42	0.42	0.42	0.42	0.42	0.42	0.42

BORROWDALE VOLCANIC GROUP - NORTHERN OUTCROP

NCRMAL .. R.C.D.GILL

SUMMARY NCRM TABLE

	LD112	LD114	LD115	LD116	LD117	LD118	LD119	LD119G	LD121	LD122	252	252G
QUARTZ	18.9	0.0	3.0	6.1	8.9	42.5	9.5	15.3	38.9	7.2	10.2	11.5
CORUNDUM	1.5	0.0	0.0	0.0	2.3	6.8	0.0	0.0	2.9	0.0	1.5	0.2
ORTHOCLASE	5.7	1.9	3.8	5.4	16.6	30.2	11.2	6.2	29.3	5.7	1.5	7.8
ALBITE	27.5	31.6	31.5	19.2	27.1	7.2	19.7	14.7	17.6	21.5	25.4	28.6
ANORTHITE	17.5	27.4	24.0	29.7	17.7	4.4	33.7	25.6	2.6	3.3	39.1	29.6
DIOPSIDE	2.0	6.3	8.6	4.2	0.0	0.0	8.0	13.5	0.0	3.3	0.0	0.0
HYPERSTHENE	17.2	12.6	17.2	21.4	14.4	4.9	17.2	13.3	4.9	22.7	13.7	18.4
CLIVINE	0.0	2.4	0.0	0.0	0.0	0.0	0.0	0.0	0.0	0.0	0.0	0.0
MAGNETITE	7.5	6.0	7.8	6.8	7.7	2.3	5.0	7.6	2.7	6.8	4.7	6.4
ILMENITE	3.3	2.3	3.4	2.6	4.5	0.9	2.3	3.3	0.7	2.2	2.6	4.7
APATITE	0.8	0.4	0.6	0.4	0.6	0.1	0.3	0.5	0.1	0.3	0.4	0.5
PYRITE	0.0	0.1	0.0	0.1	0.1	0.6	0.1	0.0	0.1	0.1	0.8	0.0
DIFF. INDEX	52.2	42.4	38.4	34.8	52.6	80.0	40.4	36.3	85.8	34.4	37.1	47.9
NA/(NA+K)	0.84	0.75	0.00	0.68	0.63	0.20	0.65	0.71	0.35	0.80	0.95	0.98
(NA+K)/AL	1.45	0.45	0.44	0.33	0.49	0.45	1.32	0.31	0.69	0.32	0.25	0.34
F3/(F2+F3)	0.42	0.42	0.42	0.42	0.42	0.42	0.42	0.42	0.42	0.42	0.42	0.42

BORROWDALE VOLCANIC GROUP - NORTHERN OUTCROP

NORMCAL .. R.C.C.D.GILL

SUMMARY NORM TABLE

	CN-7	CN-10	CN-11	CN-14	CN-16	CN-17	CN-49	CN-64	CN-71	LD285	LD266	LD267
QUARTZ	5.4	27.9	0.0	28.7	0.0	8.7	29.2	5.9	31.3	23.8	12.1	8.7
CORUNDUM	0.0	0.0	0.0	1.8	1.1	0.0	0.0	0.0	1.5	12.1	0.0	0.0
ORTHOCLASE	4.3	22.0	8.0	21.7	13.9	6.3	17.1	8.0	19.5	30.5	7.7	1.3
ALBITE	26.9	40.6	17.4	38.1	36.9	27.5	35.9	26.3	39.1	19.9	32.8	33.9
ANORTHITE	34.0	2.7	42.8	0.1	43.5	40.2	7.1	30.8	0.2	0.4	18.6	20.2
DIOPSIDE	7.6	0.5	10.1	0.0	0.0	2.1	4.0	3.7	0.0	0.0	6.4	7.2
HYPERSTHENE	8.1	3.2	0.4	5.5	1.8	7.4	2.5	13.8	4.6	11.0	9.7	13.4
OLIVINE	0.0	0.0	13.2	0.0	0.3	0.0	0.0	0.0	0.0	0.0	0.0	0.0
MAGNETITE	6.3	2.4	5.7	3.3	1.3	4.4	3.3	6.9	3.1	1.7	7.3	8.9
ILMENITE	6.7	0.5	1.9	0.8	0.9	2.7	0.7	4.0	0.8	0.0	3.8	4.9
APATITE	0.4	0.0	0.4	0.1	0.2	0.7	0.1	0.6	0.0	0.2	0.3	0.8
PYRITE	0.3	0.1	0.2	0.0	0.2	0.0	0.1	0.0	0.0	0.4	0.7	0.7
DIFF. INDEX	36.6	90.5	25.4	88.5	50.8	42.5	82.2	40.2	89.8	74.2	52.6	43.9
NA/(NA+K)	0.87	0.66	0.70	0.65	0.74	0.82	0.69	0.78	0.68	0.41	0.82	0.96
(NA+K)/AL	0.33	0.92	0.24	0.86	0.36	0.31	0.80	0.37	0.88	0.44	0.53	0.48
F3/(F2+F3)	0.42	0.42	0.42	0.42	0.42	0.42	0.42	0.42	0.42	0.42	0.42	0.42

BORROWDALE VOLCANIC GROUP - NORTHERN OUTCROP

NORMCAL .. R.C.O.GILL

SUMMARY NORM TABLE

LD 72

ORTHOCLASE	1.7
ALBITE	10.7
ANORTHITE	15.5
DIOPSIDE	25.3
HYPERSTHENE	23.9
OLIVINE	12.5
MAGNETITE	8.0
ILMENITE	1.8
APATITE	0.4
PYRITE	0.3
DIFF. INDEX	12.3
NA/(NA+K)	0.87
(NA+K)/AL	0.30
F3/(F2+F3)	0.42

APPENDIX 5.

Electron microprobe analyses.

(a) Clinopyroxenes.

CLINOPYROXENE ANALYSES

PX-148/1 PX-148/2 PX-148/3 PX-148/4 PX-221/1 PX-221/2 PX-221/3 PX-221/4 PX-221/5

OXIDE WEIGHT PERCENTAGE

SiO2	50.75	50.49	50.55	50.43	51.97	52.45	51.21	52.27	51.63
Al2O3	3.74	3.78	3.45	3.58	1.54	1.97	2.95	2.26	2.39
TiO2	0.78	0.84	0.90	1.12	0.55	0.53	0.71	0.44	0.66
FeO	8.28	9.30	9.02	9.13	8.83	7.95	9.92	7.29	9.26
MnO	0.38	0.39	0.35	0.32	0.43	0.35	0.38	0.31	0.32
MgO	14.95	14.52	14.35	14.38	16.20	16.94	15.77	16.98	16.02
CaO	20.29	20.07	20.07	20.09	18.71	18.55	18.12	19.14	18.47
Cr2O3	0.29	0.18	0.13	0.22	0.31	0.50	0.18	0.58	0.34
TOTAL	99.46	99.57	98.82	99.27	98.54	99.24	99.24	99.27	99.09

ATOMIC PROPORTIONS ON THE BASIS OF 6 OXYGENS

Si	1.892	1.888	1.902	1.891	1.951	1.944	1.914	1.935	1.929
Al	0.164	0.167	0.153	0.158	0.068	0.086	0.130	0.099	0.105
Ti	0.022	0.024	0.025	0.032	0.016	0.015	0.020	0.012	0.019
Fe	0.258	0.291	0.284	0.286	0.277	0.246	0.310	0.226	0.289
Mn	0.012	0.012	0.011	0.010	0.014	0.011	0.012	0.010	0.010
Mg	0.831	0.809	0.805	0.803	0.906	0.936	0.879	0.937	0.892
Ca	0.811	0.804	0.809	0.807	0.753	0.737	0.726	0.759	0.739
Cr	0.009	0.005	0.004	0.007	0.009	0.015	0.005	0.017	0.010

END MEMBER COMPOSITIONS

WC	42.41	41.96	42.39	42.32	38.60	38.18	37.68	39.31	38.30
EN	43.46	42.22	42.15	42.13	46.48	48.48	45.60	48.50	46.19
FS	14.14	15.82	15.45	15.55	14.92	13.34	16.72	12.19	15.51

CLINOPYROXENE ANALYSES

PX-309/1 PX-309/2 PX-309/3 PX-309/4 PX-309/5 PX-115/1 PX-115/2 PX-115/3 PX-115/4 PX-115/5

OXIDE WEIGHT PERCENTAGE

SI02	52.10	53.27	52.58	51.85	52.11	51.39	51.54	51.00	51.14	51.20
AL2O3	2.28	1.60	1.58	2.33	2.52	2.45	2.23	2.46	2.35	2.40
TI02	0.47	0.30	0.34	0.49	0.48	0.74	0.62	0.70	0.70	0.73
FEO	7.08	7.62	7.29	7.90	7.34	10.48	10.91	10.98	10.76	10.93
MNO	0.37	0.35	0.44	0.43	0.36	0.27	0.28	0.25	0.24	0.26
MGO	16.64	15.56	16.14	15.73	15.46	16.02	15.85	15.54	15.73	15.73
CAO	20.57	20.35	20.44	20.46	20.68	17.73	17.62	17.69	17.77	17.77
CR2O3	0.31	0.39	0.26	0.31	0.40	0.14	0.16	0.07	0.13	0.10
TCTAL	99.82	99.44	99.07	99.50	99.35	99.22	99.21	98.69	98.82	99.12

ATOMIC PROPORTIONS ON THE BASIS OF 6 OXYGENS

SI	1.925	1.973	1.957	1.929	1.935	1.923	1.932	1.924	1.925	1.923
AL	0.099	0.070	0.069	0.102	0.110	0.108	0.099	0.109	0.104	0.106
TI	0.013	0.008	0.010	0.014	0.013	0.021	0.017	0.020	0.020	0.021
FE2	0.219	0.236	0.227	0.246	0.228	0.328	0.342	0.346	0.339	0.343
MN	0.012	0.011	0.014	0.014	0.011	0.009	0.009	0.008	0.008	0.008
MG	0.916	0.859	0.895	0.872	0.856	0.894	0.886	0.874	0.883	0.880
CA	0.814	0.808	0.815	0.816	0.823	0.711	0.708	0.715	0.717	0.715
CR	0.009	0.011	0.008	0.009	0.012	0.004	0.005	0.002	0.004	0.003

END MEMBER COMPOSITIONS

WO	41.53	42.21	41.78	41.89	42.91	36.63	36.41	36.80	36.84	36.73
EN	46.72	44.88	45.88	44.79	44.61	46.03	45.54	44.96	45.35	45.21
FS	11.75	12.91	12.34	13.32	12.48	17.34	18.05	18.24	17.80	18.06

CLINOPYROXENE ANALYSES

PX-86/1 PX-86/2 PX-86/3 PX-86/4 PX-86/5 PX-111/1 PX-111/2 PX-111/3 PX-111/4 PX-111/5

OXIDE WEIGHT PERCENTAGE

SI02	51.43	51.16	50.42	50.18	52.20	51.41	51.23	51.23	50.64	51.18
AL2O3	2.93	3.61	4.32	3.76	2.73	1.91	1.59	1.84	2.16	1.93
TIO2	0.41	0.53	0.59	0.79	0.49	0.87	0.71	0.78	0.95	0.84
FEO	6.45	6.79	6.78	8.15	6.60	11.88	13.21	13.18	14.39	11.53
MNO	0.20	0.20	0.20	0.22	0.17	0.41	0.50	0.51	0.54	0.43
MGO	16.32	16.06	15.77	15.16	16.17	14.68	13.88	14.03	13.82	14.82
CAD	20.13	20.24	20.38	20.49	20.95	18.75	18.20	18.19	17.48	18.55
CR2O3	0.28	0.57	0.49	0.20	0.39	0.02	0.0	0.01	0.01	0.0
TCTAL	98.15	99.16	98.95	98.95	99.70	99.93	99.32	99.77	99.99	99.28

ATOMIC PROPORTIONS ON THE BASIS OF 6 OXYGENS

SI	1.923	1.898	1.877	1.881	1.925	1.930	1.945	1.936	1.918	1.931
AL	0.129	0.158	0.190	0.166	0.119	0.085	0.071	0.082	0.096	0.086
TI	0.012	0.015	0.017	0.022	0.014	0.025	0.020	0.022	0.027	0.024
FE2	0.202	0.211	0.211	0.256	0.204	0.373	0.419	0.417	0.456	0.364
MN	0.006	0.006	0.006	0.007	0.005	0.013	0.016	0.016	0.017	0.014
MG	0.909	0.888	0.875	0.847	0.889	0.821	0.785	0.790	0.780	0.833
CA	0.807	0.805	0.813	0.823	0.828	0.754	0.740	0.737	0.710	0.750
CR	0.008	0.017	0.014	0.006	0.011	0.001	0.000	0.000	0.000	0.000

END MEMBER COMPOSITIONS

WC	41.92	42.14	42.67	42.59	43.00	38.45	37.75	37.59	36.15	38.25
EN	47.27	46.50	45.92	43.82	46.15	41.87	40.04	40.32	39.74	42.50
FS	10.81	11.36	11.41	13.58	10.85	19.68	22.21	22.09	24.11	19.26

(b) Garnets.

	G-65/1	G-65/2	G-65/3	G-65/4
SV1.02.	38.02	38.00	37.66	37.66
AL2.03.	20.70	20.90	20.58	20.61
FE1.01.	34.66	35.52	35.87	35.41
MN1.01.	3.67	3.29	3.55	3.67
MC1.01.	2.79	3.29	3.15	3.19
CA1.01.	1.05	1.06	1.04	1.08
TOTAL	100.89	102.06	101.85	101.62

## UNIT FORMULA

ST	6.082	6.020	6.005	6.010
Al	3.903	3.903	3.868	3.877
FE	4.637	4.706	4.783	4.726
MN	0.497	0.442	0.479	0.496
MC	0.665	0.777	0.749	0.759
CA	0.180	0.180	0.178	0.185
D	24.000	24.000	24.000	24.000

## GARNET MOLECULES (RICKWOOD(1968))

PYROPE	11.36	13.27	12.91	13.05
SPESSART	8.49	7.54	8.26	8.53
GROSSULA	3.07	3.07	3.06	3.18
ALMANDIN	77.07	76.11	75.77	75.24

## PERCENTAGE CATIONS ASSIGNED

97.79	97.40	96.32	96.60
-------	-------	-------	-------

	G-174/1	G-174/2	G-174/3	G-174/4	G-174/5	G-174/6
SYL.C2.	38.16	38.30	38.42	38.02	38.22	38.43
AL2.O3.	21.13	21.17	21.33	21.18	21.13	21.07
FR1.O1.	33.00	32.42	32.92	32.56	32.31	32.68
MN1.Cl.	2.11	2.01	2.04	2.07	1.96	2.31
MC1.O1.	5.90	6.26	5.92	6.20	5.99	5.76
CA1.O1.	1.62	1.54	1.50	1.47	1.81	1.47
TOTAL	101.92	101.70	102.13	101.50	101.42	101.72

## UNIT FORMULA

ST	5.963	5.976	5.978	5.953	5.982	6.006
AL	3.892	3.893	3.912	3.909	3.898	3.881
FR	4.312	4.230	4.284	4.263	4.229	4.272
MN	0.279	0.266	0.269	0.275	0.260	0.306
MC	1.374	1.456	1.373	1.447	1.397	1.342
CA	0.271	0.257	0.250	0.247	0.304	0.246
O	24.000	24.000	24.000	24.000	24.000	24.000

## GARNET MOLECULES (RICKWOOD(1968))

PYROPE	23.54	24.93	23.40	24.68	23.90	23.05
SPESSART	4.78	4.55	4.58	4.68	4.44	5.25
GROSSULA	4.65	4.41	4.26	4.21	5.19	4.23
ALMANDIN	67.03	66.11	67.76	66.43	66.46	67.47

## PERCENTAGE CATIONS ASSIGNED

96.74	96.86	97.40	97.15	97.03	96.72
-------	-------	-------	-------	-------	-------

	G-175/1	G-175/2	G-175/3	G-175/4
STL.02.	36.88	37.03	37.09	36.87
AL2.03.	21.41	21.37	21.48	21.48
FFL.01.	34.86	34.74	35.12	34.48
MNL.01.	2.82	3.05	2.99	3.01
MFL.01.	3.12	3.26	3.18	3.32
CL.01.	1.26	1.27	1.27	1.23
TOTAL	100.35	100.72	101.13	100.39

UNIT FORMULA				
ST	5.934	5.937	5.928	5.924
AL	4.061	4.038	4.047	4.068
FF	4.691	4.658	4.694	4.633
MN	0.384	0.414	0.405	0.410
MC	0.748	0.779	0.758	0.795
CA	0.217	0.218	0.217	0.212
O	24.000	24.000	24.000	24.000

GARNET MOLECULES (RICKWOOD(1968))				
PYRUPE	12.61	13.12	12.78	13.42
SPESSART	6.48	6.98	6.83	6.92
GROSSULA	3.66	3.67	3.67	3.57
AMANDIN	77.25	76.22	76.72	76.09

PERCENTAGE CATIONS ASSIGNED				
	98.68	98.67	98.50	98.48

	G-176/1	G-176/2	G-176/3	G-176/4	G-176/5	G-176/6	G-176/7	G-176/8
S <sup>1</sup> .C2.	38.28	38.11	37.59	37.76	38.14	38.66	38.68	38.21
A <sup>1</sup> 2.C3.	21.94	21.67	21.48	21.66	21.75	22.14	21.87	21.79
F <sup>1</sup> 1.C1.	30.93	30.75	33.73	34.14	32.14	31.79	32.31	32.49
M <sup>1</sup> 1.C1.	2.00	2.07	2.36	1.87	1.93	1.28	1.84	2.28
M <sup>1</sup> 1.C1.	5.51	5.84	3.64	4.32	5.04	6.45	5.88	5.26
C <sup>1</sup> 1.C1.	2.61	2.57	3.08	1.84	2.54	1.64	1.46	1.52
TOTAL	101.27	101.01	101.88	101.59	101.54	101.96	102.04	101.55
UNIT FORMULA								
S <sup>1</sup>	5.969	5.960	5.932	5.948	5.964	5.967	5.992	5.973
A <sup>1</sup>	4.032	3.995	3.595	4.022	4.009	4.028	3.993	4.015
F <sup>1</sup>	4.033	4.022	4.451	4.497	4.203	4.103	4.186	4.248
M <sup>1</sup>	0.264	0.274	0.315	0.250	0.256	0.167	0.241	0.302
M <sup>2</sup>	1.281	1.361	0.856	1.014	1.175	1.484	1.358	1.226
C <sup>1</sup>	0.436	0.431	0.521	0.311	0.426	0.271	0.242	0.255
O	24.000	24.000	24.000	24.000	24.000	24.000	24.000	24.000
GARNET MOLECULES (RICKWOOD(1968))								
PYROPE	21.46	22.84	14.44	17.05	19.70	24.87	22.67	20.52
SPIESSART	4.43	4.60	5.32	4.19	4.29	2.80	4.03	5.05
GROSSULA	7.31	7.23	8.78	5.22	7.14	4.55	4.05	4.26
ALMANDIN	66.81	65.33	71.47	73.53	68.88	67.78	69.25	70.16
PERCENTAGE CATIONS ASSIGNED								
	99.38	99.07	98.43	98.88	99.20	99.32	99.75	99.44

G-220/1      G-220/2      G-220/3      G-220/4

SV1.02.	38.72	38.60	38.54	38.62
AL2.03.	20.90	21.15	20.99	21.23
FF1.01.	32.10	31.86	31.40	31.77
MN1.01.	1.66	2.09	2.00	2.00
MC1.01.	6.53	6.29	6.30	6.33
CA1.01.	1.49	1.43	1.79	1.62
TOTAL	101.40	101.42	101.02	101.57

UNIT FORMULA

SY	6.035	6.019	6.028	6.010
AI	3.840	3.887	3.869	3.894
FE	4.184	4.155	4.107	4.135
MN	0.219	0.276	0.265	0.264
MC	1.517	1.462	1.469	1.469
CA	0.249	0.239	0.300	0.270
C	24.000	24.000	24.000	24.000

GARNET MOLECULES (RICKWOOD(1968))

P"RCPE	26.34	25.07	25.31	25.14
SP"SSART	3.81	4.73	4.56	4.51
GPOSSULA	4.32	4.10	5.17	4.62
AI MANDIN	65.53	66.09	64.96	65.72

PERCENTAGE CATIONS ASSIGNED

95.73	96.95	96.51	97.10
-------	-------	-------	-------

	G-249/1	G-249/2	G-249/3	G-249/4
ST1.02.	37.65	37.58	37.68	37.58
AV2.03.	21.64	21.82	21.88	21.60
FF1.01.	35.26	35.44	35.50	35.62
MV1.01.	2.82	3.03	3.02	2.82
MC1.01.	3.45	3.37	3.45	3.39
CA1.01.	1.54	1.17	1.20	1.34
TOTAL	102.36	102.41	102.73	102.35

UNIT FORMULA				
ST	5.936	5.925	5.921	5.933
AV	4.021	4.055	4.053	4.020
FF	4.649	4.673	4.666	4.703
MV	0.377	0.405	0.402	0.377
MC	0.811	0.792	0.808	0.798
CA	0.260	0.198	0.202	0.227
O	24.000	24.000	24.000	24.000

GARNET MOLECULES (RICKWOOD(1968))				
PYROPE	13.66	13.37	13.65	13.45
SPESSART	6.34	6.83	6.79	6.36
GROSSULA	4.38	3.34	3.41	3.82
ALMANDIN	75.61	76.47	76.15	76.38

PERCENTAGE CATIONS ASSIGNED				
	98.60	98.46	98.37	98.53

	G-274/1	G-274/2	G-274/3	G-274/4	G-274/5	G-274/6	G-274/7	G-274/8
STL.C2.	38.21	38.14	38.35	38.43	38.70	39.03	38.45	38.35
AL2.O3.	20.90	20.95	20.99	20.81	20.94	21.25	20.94	21.12
FR1.O1.	31.46	31.82	31.11	32.01	31.29	30.88	31.27	32.06
MN1.O1.	1.35	1.72	1.34	2.03	1.34	1.02	1.52	1.75
MR1.O1.	6.89	6.39	7.30	6.28	6.88	7.62	6.96	6.11
CA1.O1.	1.62	1.50	1.85	1.48	1.83	1.61	1.51	1.48
TOTAL	100.43	100.52	100.54	101.04	100.98	101.41	100.65	100.87
UNIT FORMULA								
ST	6.000	6.001	5.983	6.025	6.033	6.028	6.017	6.015
AL	3.868	3.886	3.860	3.845	3.848	3.868	3.863	3.904
FR	4.132	4.187	4.059	4.197	4.080	3.988	4.093	4.205
MN	0.180	0.229	0.177	0.270	0.177	0.133	0.201	0.232
MR	1.613	1.499	1.698	1.468	1.599	1.754	1.624	1.428
CA	0.273	0.253	0.309	0.249	0.306	0.266	0.253	0.249
O	24.000	24.000	24.000	24.000	24.000	24.000	24.000	24.000
GARNET MOLECULES (RICKWOOD(1968))								
PYROPE	27.80	25.72	29.32	25.44	27.70	30.23	28.02	24.39
STESSART	3.09	3.93	3.06	4.67	3.07	2.30	3.48	3.97
GROSSULA	4.70	4.34	5.34	4.31	5.30	4.59	4.37	4.25
ALMANDIN	64.41	66.01	62.28	65.57	63.94	62.87	64.13	67.39
PERCENTAGE CATIONS ASSIGNED								
	96.32	96.80	95.98	95.82	95.94	96.47	96.26	97.40

	G-302/1	G-302/2	G-302/3	G-302/4	G-302/5	G-302/6	G-302/7	G-302/8
SYL.02.	37.34	38.25	37.47	37.46	37.22	37.33	37.55	38.27
AL2.03.	21.65	20.71	21.27	20.15	21.21	20.07	20.10	20.76
FL.01.	30.47	31.62	33.92	32.35	35.66	35.90	32.07	31.92
M.01.	2.90	3.13	4.00	4.47	3.91	3.29	4.40	2.80
M.01.	5.82	4.91	3.28	3.46	2.21	2.18	3.48	5.06
CA.01.	1.91	1.58	1.62	1.56	1.17	0.99	1.58	1.49
TOTAL	100.09	100.20	101.56	99.45	101.38	99.76	99.18	100.30
UNIT FORMULA								
ST	5.911	6.070	5.958	6.066	5.970	6.084	6.086	6.065
AL	4.039	3.874	3.987	3.846	4.010	3.855	3.840	3.878
FL	4.034	4.197	4.511	4.381	4.784	4.893	4.347	4.230
M.	0.389	0.421	0.539	0.613	0.531	0.454	0.604	0.376
MC	1.373	1.162	0.778	0.835	0.528	0.530	0.841	1.195
CA	0.324	0.265	0.276	0.271	0.201	0.173	0.274	0.253
O	24.000	24.000	24.000	24.000	24.000	24.000	24.000	24.000
GARNET MOLECULES (RICKWOOD (1968))								
PYRUPE	23.23	19.99	13.05	14.48	8.85	9.16	14.60	20.55
STESSART	6.58	7.24	9.04	10.63	8.90	7.85	10.49	6.46
GROSSULA	5.48	4.62	4.63	4.69	3.37	2.99	4.76	4.35
ALMANDIN	64.71	68.15	73.28	70.20	78.88	80.00	70.15	68.64
PERCENTAGE CATIONS ASSIGNED								
	98.08	96.90	99.01	96.08	99.35	96.45	96.04	96.96

	G-306/1	G-306/2	G-306/3	G-306/4	G-306/5	G-306/6
STL.02.	38.84	38.88	38.15	39.14	39.04	38.39
AL2.03.	22.30	22.40	22.20	22.26	22.39	22.06
FL1.01.	30.90	31.16	31.68	30.46	31.03	31.95
ML1.01.	1.12	1.15	1.87	1.00	1.26	1.69
MC1.01.	7.49	7.46	6.86	8.14	7.73	6.56
CA1.01.	2.00	1.70	1.49	1.66	1.60	1.46
TOTAL	102.65	102.75	102.25	102.66	103.05	102.11
UNIT FORMULA						
ST	5.930	5.931	5.890	5.950	5.933	5.934
AL	4.013	4.027	4.040	3.989	4.011	4.019
FL	3.945	3.975	4.090	3.873	3.944	4.130
ML	0.145	0.149	0.245	0.129	0.162	0.221
MC	1.705	1.696	1.579	1.845	1.751	1.511
CA	0.327	0.278	0.246	0.270	0.261	0.242
C	24.000	24.000	24.000	24.000	24.000	24.000
GARNET MOLECULES (RICKWOOD(1968))						
PYRCP	28.75	28.60	26.81	31.00	29.52	25.47
SPSSART	2.44	2.51	4.15	2.16	2.73	3.73
GROSSULA	5.52	4.69	4.18	4.54	4.39	4.08
ALMANDIN	63.29	64.21	64.86	62.29	63.36	66.72
PERCENTAGE CATIONS ASSIGNED	98.43	98.50	97.62	98.83	98.50	98.54

	G-316/1	G-316/2	G-316/3	G-316/4
ST1.02.	36.78	36.49	36.31	36.22
Al2.03.	20.62	20.44	20.34	20.27
Fe1.01.	36.82	36.85	35.08	36.62
Mn1.01.	5.86	5.91	8.14	6.52
Mg1.01.	0.79	0.77	0.60	0.83
Ca1.01.	0.62	0.47	0.26	0.42
TOTAL	101.49	100.93	100.73	100.88

UNIT FORMULA				
ST	5.980	5.974	5.969	5.949
Al	3.952	3.944	3.941	3.924
Fe	5.007	5.046	4.823	5.031
Mn	0.807	0.820	1.134	0.907
Mg	0.191	0.188	0.147	0.203
Ca	0.108	0.082	0.046	0.074
O	24.000	24.000	24.000	24.000

## GARNET MOLECULES (RICKWOOD(1968))

PYROPE	3.23	3.18	2.49	3.45
SPESSART	13.62	13.85	19.17	15.41
GROSSULA	1.82	1.39	0.77	1.26
ALMANDIN	81.33	81.58	77.57	79.88

PERCENTAGE CATIONS ASSIGNED	98.52	98.28	98.17	97.57
-----------------------------	-------	-------	-------	-------

	G-317/1	G-317/2	G-317/3	G-317/4	G-317/5	G-317/6	G-317/7	G-317/8	G-317/9	G-317/
ST1.O2.	37.83	37.63	37.55	37.23	37.10	37.50	37.51	37.58	37.69	37.5
AT2.O3.	21.66	21.39	21.32	21.28	21.33	21.61	21.66	21.54	21.74	21.5
FT1.O1.	33.71	34.61	35.74	35.94	36.08	34.60	33.93	34.16	34.03	34.5
MM1.O1.	3.36	3.90	3.06	3.86	3.83	3.90	3.53	3.49	3.48	3.5
ML1.O1.	3.70	2.60	2.75	2.25	2.27	2.83	3.44	3.44	3.48	3.5
CA1.O1.	1.54	1.39	1.21	1.20	1.10	1.36	1.52	1.42	1.45	1.5
TOTAL	101.80	101.52	101.63	101.76	101.71	101.80	101.59	101.63	101.87	101.87

UNIT FORMULA

ST	5.967	5.993	5.981	5.955	5.940	5.955	5.945	5.956	5.952	5.9
AT	4.027	4.015	4.003	4.012	4.026	4.045	4.046	4.024	4.047	4.0
FT	4.447	4.610	4.761	4.808	4.831	4.595	4.497	4.528	4.495	4.4
MM	0.449	0.526	0.413	0.523	0.519	0.525	0.474	0.469	0.466	0.4
ML	0.870	0.617	0.653	0.536	0.542	0.670	0.813	0.813	0.819	0.8
CA	0.260	0.237	0.207	0.206	0.189	0.231	0.258	0.241	0.245	0.2
D	24.000	24.000	24.000	24.000	24.000	24.000	24.000	24.000	24.000	24.000

GARNET MOLECULES (RICKWGD(1968))

Pyrope	14.58	10.30	10.92	9.01	9.12	11.25	13.67	13.65	13.76	14.0
Saessart	7.52	8.78	6.90	8.78	8.74	8.81	7.97	7.87	7.82	7.0
Grossula	4.36	3.96	3.45	3.45	3.18	3.89	4.34	4.05	4.12	4.0
Almandin	73.53	76.95	78.73	78.76	78.96	76.05	74.02	74.44	74.29	73.0

PERCENTAGE CATIONS ASSIGNED

	99.33	99.85	99.58	99.00	98.71	99.12	98.88	99.08	99.06	98.9
--	-------	-------	-------	-------	-------	-------	-------	-------	-------	------

	G-21	G-204	G-277
STL.C2.	36.79	38.09	37.05
AL2.O3.	21.48	21.65	21.15
FL.O1.	33.58	33.05	37.08
MNI.O1.	3.27	2.24	3.16
MCL.O1.	3.46	4.92	2.03
CAL.O1.	1.46	1.47	0.86
TOTAL	100.04	101.42	101.33

UNIT FORMULA			
ST	5.921	5.975	5.963
AL	4.074	4.005	4.012
FF	4.520	4.338	4.991
MM	0.446	0.298	0.431
MC	0.830	1.151	0.487
CA	0.252	0.247	0.148
C	24.000	24.000	24.000

GARNET MOLECULES (RICKWOOD(1968))			
PERCPE	14.02	19.25	8.17
SPESSART	7.53	4.98	7.22
GOSSULA	4.25	4.14	2.49
AMANDIN	74.20	71.63	82.12

PERCENTAGE CATIONS ASSIGNED			
	98.42	99.53	99.18

**APPENDIX 6.**

Eight-figure National Grid references of sample localities.  
The samples are listed by area and stratigraphic unit (Fig. 3).  
Within each unit they are listed numerically.

EYCOTT HILL AND RIVER CALDEW

HIGH IREBY GROUP

LD 75 NY 3600 3435, LD 76 NY 3606 3436, LD 77 NY 3605 3445, LD 78 NY 3612 3484,  
LD 80 NY 3631 3537, LD 82 NY 3630 3438, LD 85 NY 3838 3014, LD 86 NY 3840 3016,  
LD 87 NY 3843 3015, LD 88 NY 3847 3013, LD 91 NY 3863 3019, LD 92 NY 3866 3021,  
LD 93 NY 3871 3019, LD 96 NY 3839 2963, LD 97 NY 3849 2959, LD 98 NY 3854 2956,  
LD 99 NY 3857 2954, LD 100 NY 3860 2951, LD 101 NY 3863 2947, LD 102 NY 3870 2940,  
LD 103 NY 3874 2940, LD 104 NY 3884 2944, LD 105 NY 3895 2946, LD 106 NY 3903 2947,  
LD 107 NY 3905 2964, LD 108 NY 3906 2975, LD 109 NY 3915 2976,

MIDDLE EYCOTT LAVAS

LD 73 NY 3601 3425, LD 73A NY 3601 3425, LD 81 NY 3625 3441, LD 95 NY 3825 2970,

BINSEY GROUP

LD 83 NY 3832 3042, LD 94 NY 3820 2967,

BINSEY

HIGH IREBY GROUP

LD 117 NY 2215 3730, LD 118 NY 2215 3726, LD 121 NY 2213 3712,

MIDDLE EYCOTT LAVAS

LD 119 NY 2271 3638,

BINSEY GROUP

LD 111 NY 2251 3551, LD 112 NY 2240 3545, LD 114 NY 2230 3527,

LOWER EYCOTT LAVAS

LD 115 NY 2223 3515, LD 116 NY 2358 3488, LD 122 NY 2292 3605,

BORROWDALE AND SCAFELL

ESK PIKE HORNSTONE

LD 17 NY 2350 840, LD 18 NY 2367 853,

LINCOMB TARNs FORMATION

LD 16 NY 2323 857, LD 20 NY 2395 904, LD 21 NY 2407 931, LD 22 NY 2429 981,  
 LD 26 NY 2296 886, LD 27 NY 2302 903,

SEATHWAITE FELL TUFFS

LD 10 NY 2474 1097, LD 15 NY 2534 1104, LD 23 NY 2462 1044, LD 25 NY 2282 918,  
 LD 28 NY 2299 906, LD 29 NY 2312 921, LD 30 NY 2321 947, LD 31 NY 2326 956,  
 LD 32 NY 2326 956, LD 33 NY 2334 974, LD 45 NY 2225 959, LD 46 NY 2240 954,  
 LD 47 NY 2277 952, LD 48 NY 2343 992,

AIRYS BRIDGE GROUP

LD 5 NY 2472 1247, LD 6 NY 2468 1240, LD 7 NY 2463 1222, LD 8 NY 2456 1185,  
 LD 9 NY 2461 1138, LD 11 NY 2522 1241, LD 12 NY 2554 1238, LD 13 NY 2584 1249,  
 LD 14 NY 2570 1174, LD 37 NY 2341 1088, LD 38 NY 2265 1064, LD 39 NY 2244 1042,  
 LD 40 NY 2225 1013, LD 41 NY 2225 1006, LD 42 NY 2223 995, LD 43 NY 2225 989,  
 LD 61 NY 2717 1264, LD 62 NY 2727 1280, LD 63 NY 2734 1288, LD 66 NY 2771 1358,  
 LD 68 NY 2133 1050, LD 317 NY 2346 1039,

GREY KNOTTs GROUP

LD 1 NY 2528 1341, LD 2 NY 2522 1323, LD 3 NY 2520 1306, LD 4 NY 2515 1281,  
 LD 34 NY 2235 1243, LD 35 NY 2244 1212, LD 36 NY 2288 1222, LD 49 NY 2008 1248,  
 LD 50 NY 2016 1240, LD 51 NY 2023 1237, LD 52 NY 2040 1239, LD 53 NY 2081 1240,  
 LD 54 NY 2090 1227, LD 55 NY 2092 1225, LD 56 NY 2094 1226, LD 57 NY 2094 1223,  
 LD 58 NY 2153 1197, LD 59 NY 2188 1258, LD 60 NY 2208 1286, LD 67 NY 2713 1353,  
 LD 274 NY 2794 1525, LD 275 NY 2915 1469,

BORROWDALE AND SCAFELL (CONTINUED)

LAVA FROM SEATOLLER TUFF GROUP

LD 280 NY 2343 1373,

LAVA FROM HONISTER TUFF GROUP

LD 281 NY 2244 1381,

LOWER ANDESITES

LD 278 NY 2539 1725, LD 279 NY 2532 1648, LD 282 NY 2165 1450,

CONISTON AND DUNNERDALE

WRENGILL ANDESITE

LD 309 SD 2928 9829, LD 310 NY 3093 87,

PADDY END RHYOLITE

LD 308 SD 2830 9882,

LANGDALE, GRASMERE AND HELVELLYN

UPPER ANDESITE

LD 312 NY 3490 698,

HELVELLYN ANDESITE

LD 302 NY 3245 566,

LANGDALE-THIRLMERE RHYOLITE

LD 202 NY 3568 1644, LD 303 NY 2921 678, LD 304 NY 2910 511, LD 305 NY 2893 322,  
LD 313 NY 3244 1375,

LAVAS IN BEDDED TUFFS

LD 201 NY 3603 1715, LD 215 NY 3648 1995, LD 216 NY 3590 1971, LD 217 NY 3531 1875,  
LD 219 NY 3624 2090, LD 220 NY 3672 2105, LD 221 NY 3680 2103, LD 222 NY 3705 2093,  
LD 314 NY 3200 1553, LD 315 NY 3162 1629,

MOSEDALE ANDESITE

LD 306 NY 2466 171, LD 307 NY 2550 191,

HIGH RIGG

MIDDLE HIGH RIGG ANDESITE

LD 209 NY 3047 2166, LD 210 NY 3064 2151, LD 211 NY 3093 2138, LD 214 NY 3077 2044,

FINE-GRAINED LAVAS AND TUFFS

LD 208 NY 3042 2177,

PYROXENE ANDESITE

LD 207 NY 3050 2211, LD 212 NY 3069 2234, LD 213 NY 3068 2243,

ULLSWATER

ANGLE TARN ANDESITE

LD 162 NY 4184 1568, LD 163 NY 4196 1572,

PLACE FELL GROUP

LD 161 NY 4174 1573, LD 164 NY 4101 1611,  
LD 167 NY 4156 1836,

LD 165 NY 4051 1693, LD 166 NY 4139 1809,

BIRK FELL GROUP

LD 150 NY 4130 2230, LD 151 NY 4118 2169,  
LD 170 NY 4103 1869, LD 175 NY 4141 2185,

LD 168 NY 4135 1840, LD 169 NY 4115 1854,  
LD 178 NY 4725 2151, LD 179 NY 4715 2135,

UPPER ULLSWATER GROUP

LD 137 NY 4055 2050, LD 138 NY 4059 2059,  
LD 141 NY 4090 2085, LD 142 NY 4095 2115,  
LD 145 NY 4074 2196, LD 146 NY 4067 2200,  
LD 160 NY 4362 1951, LD 171 NY 4111 1894,  
LD 177 NY 4606 2123, LD 180 NY 4735 2178,  
LD 192 NY 4841 2187, LD 193 NY 4847 2181,  
LD 196 NY 4860 2167, LD 197 NY 4866 2161,

LD 139 NY 4059 2059, LD 140 NY 4074 2072,  
LD 143 NY 4091 2156, LD 144 NY 4077 2177,  
LD 147 NY 3966 2109, LD 148 NY 3923 2241,  
LD 172 NY 4097 1914, LD 176 NY 4590 2116,  
LD 191 NY 4836 2191, LD 191A NY 4839 2189,  
LD 194 NY 4851 2176, LD 195 NY 4856 2171,  
LD 200 NY 4892 2134,

LOWER ULLSWATER GROUP

LD 126 NY 4242 2330, LD 128 NY 4251 2269,  
LD 131 NY 4281 2305, LD 132 NY 4286 2307,  
LD 136 NY 4301 2169, LD 155 NY 4293 2018,  
LD 159 NY 4335 1982, LD 173 NY 4093 1923,

LD 129 NY 4273 2281, LD 130 NY 4276 2296,  
LD 133 NY 4275 2318, LD 135 NY 4305 2168,  
LD 156 NY 4310 2028, LD 158 NY 4349 2017,  
LD 174 NY 4096 1935,

S.E. HAWESWATER

HAWESWATER DAM ANDESITE

LD 226 NY 5040 1560, LD 235 NY 5020 1550,

SCALEBARROW ANDESITE

LD 229 NY 5200 1450, LD 230 NY 5110 1600,

LAVAS IN BEDDED TUFFS

LD 231 NY 5140 1330, LD 234 NY 5100 1330,

THORNY KNCTT ANDESITE

LD 245 NY 5030 1290, LD 251 NY 5090 1350,

NAN BIELD ANDESITE

LD 228 NY 4790 1260, LD 248 NY 4880 1430,

HAWESWATER IGNIMBRITE GROUP

LD 227 NY 4800 1290, LD 249 NY 5030 1360,

HIGH NADDLE ANDESITE

LD 232 NY 5030 1390, LD 250 NY 4950 1330,

KENTMERE AND SHAP

UPPER RHYOLITE

LD 286 NY 4536 487, LD 300 NY 4470 450, LD 301 NY 4496 448,

UPPER ANDESITE

LD 287 NY 4557 502, LD 288 NY 4590 513, LD 299 NY 4415 472,

WRENGILL ANDESITE

LD 291 NY 4772 844, LD 292 NY 4779 830, LD 293 NY 4775 794,

KENTMERE PIKE RHYOLITE

LD 294 NY 4775 775, LD 296 NY 4799 636,

NAN BIELD ANDESITE

LD 298 NY 4429 874,

GREENSCOE

LAVAS

LD 69 SD 2233 7608, LD 70 SD 2233 7608, LD 269 SD 2217 7581, LD 270 SD 2206 7571,

CROSS FELL INLIER

IGNIMBRITES

CF 253 NY 6870 2852, CF 256 NY 6885 2778, CF 259 NY 6942 2669,

LAVA

CF 261 NY 7466 2062,

EYCOTT TYPE LAVA

CF 252 NY 6251 3736,

CARROCK FELL COMPLEX

GABBRO

CN-7 NY 3560 3270, CN-16 NY 3332 3405, CN-17 NY 3488 3297, CN-64 NY 3536 3281,

DIABASE

CN-11 NY 3347 3372,

GRANOPHYRE

CN-10 NY 3363 3374, CN-14 NY 3335 3421, CN-49 NY 3505 3410, CN-71 NY 3141 3430,

HARESTONES FELSITE

LD 285 NY 3147 3473,

HAWESWATER COMPLEX

LD 223 NY 4947 1519, LD 224 NY 4871 1550, LD 233 NY 5090 1410, LD 236 NY 4970 1500,  
LD 237 NY 4970 1500, LD 238 NY 4970 1490, LD 239 NY 4970 1490, LD 240 NY 4950 1530,  
LD 243 NY 5050 1410, LD 244 NY 5070 1430, LD 246 NY 4930 1430, LD 247 NY 4930 1430,

OTHER INTRUSIVE ROCKS MENTIONED IN TEXT

EMBLETON

LD 266 NY 1752 3091, LD 267 NY 1747 3080,

GREAT COCKUP

LD 72 NY 2670 3270,

CASTLE HEAD DOLERITE

LD 283 NY 2705 2266,

BORROWDALE

LD 24 NY 2278 918, LD 65 NY 2774 1365,

ULLSWATER

LD 152 NY 3837 1871, LD 153 NY 4020 2006,

KENTMERE

LD 289 NY 4564 510,

THRELKELD MICROGRANITE

LD 204 NY 3211 2327,

ARMBOTH DYKE

LD 277 NY 2986 1693,